The Effects of SUMO modification of the Tumour Suppressor p53

Thesis submitted for the degree of

Doctor of Philosophy

at the University of Leicester

by

Diana Mota Marouco

Department of Molecular and Cell Biology

University of Leicester

August 2015

I. Abstract

The Effects of SUMO modification of the Tumour Suppressor p53

Diana Mota Marouco

p53 is a major tumour suppressor protein implicated in many cellular processes, regulating cell cycle arrest, apoptosis and DNA repair. The regulation of p53 can be achieved by post-translational modifications (PTMs), which alter the function of the protein in the cell. Among such PTMs, p53 can be modified via sumoylation – the covalent binding of SUMO (Small Ubiquitin MOdifier) protein – on lysine 386. This work aimed to define the role of sumoylation in regulation of p53 activity. By implementing a MS-proteomics approach, I identified a number of potential binding partners of sumoylated p53, and immunoprecipitation confirmed the transcriptional repressor lysine specific demethylase 1 (LSD1) as a specific interactor of SUMO-modified p53. The overexpression of wild type p53 protein fused with the sumoylation conjugating enzyme ubc9 (p53-ubc9) in p53-null cells H1299 shows a reduced ability to activate p53-target genes, when compared to the sumoylation deficient mutant ($p53_{K386R}$-ubc9). Furthermore, sumoylation of p53 with both SUMO-1 and SUMO-2 significantly decreases the transcriptional activity of p53 towards its target genes p21 and PUMA, in both U2OS and HCT116 cell lines. Interestingly, ChIP analysis indicate that rather than preventing p53 from binding, sumoylation leads to the stabilization of p53 to these promoters. Moreover, p53 sumoylation led to the recruitment of HDAC2 to target-promoters, which correlated with an increase in H3K9me and a decrease in H3 acetylation, suggesting that p53 sumoylation leads to the recruitment of co-repressor complexes to the nearby chromatin. In addition, *in vitro* assays showed that p53 acetylation by CBP/p300, as well as the methylation of lysine 372 by SET7/9, is affected by the presence of sumoylation of lysine 386. Lastly, immunofluorescence microscopy showed increased localization of SUMO-p53, but not K386R mutant, to the nuclear membrane and cytoplasm, implicating SUMO on p53 nuclear export. These results highlight the importance of sumoylation as a modulator of p53 activity, and the point to existence of interplay between post-translational modifications in p53 protein to regulate its activity.

II. Acknowledgements

Firstly I would like to express my gratitude to my supervisor, Dr Nick Barlev. The completion of this work would have not been possible without his insight and guidance. I would also like to thank Dr Shaun Cowley, for accepting to take me on as his research student almost at the end of my journey. His invaluable input, firstly as a member of my thesis committee and later as my supervisor, were determinant to help me reach the finish line. To Dr Salvador Macip, I have to thank for his kind comments and support during committee meetings. I would also like to thank my fellow lab members, Larissa, Sheree and Miran. Thank you for your help and words of advice, patience and support, in and outside the lab.

To my friends, for their encouragement and support, I cannot thank enough. Mariana, Jesvin, Ana, Rob, Li, Matt, Vítor, Sandra, you made my journey in Leicester an incredible one. A special thanks to Marion and Virgínia, for their patience and company at home. To the friends I left at home, Marta, Sara, Leonor, Inês, thank you for always having time for a coffee. And to my *rebanho*, Susana, Rui, Joana, Neuza and Manel, thank you for being there, in spite of the distance. Your encouragement and friendship led me to where I am today. Obrigada.

I would like to thank my family, who has always encouraged me to pursue my dreams and never doubted my abilities. Mãe e pai, obrigada pelo vosso apoio em todas as decisões que tomei. Esta tese é, em parte, vossa. Sem vocês, não seria possível. Aos meus avós, tia, David, Tito e Marco, obrigada pelo carinho e palavras de incentivo.

For last I reserve my deepest expression of gratitude to my partner, Ghazi. Thank you for your love and companionship; you are my rock. Your blind faith in my abilities gave me the confidence and determination to go through the rough times. Without your encouragement this wouldn't be possible.

III. Contents

IV. Figures and Tables

Abbreviations

%	Percentage
Δ	Delta
°C	Degrees Celsius
µg	microgram
µl	microlitre
µM	micromolar
^{3}H	Tritium
6His	Hexa-histidine
aa	amino acid
Ac	Acetylated
ATP	Adenosine triphosphate
BAX	Bcl-2-associated X protein
bp	base pairs
BSA	Bovine Serum Albumin
C-	Carboxy-
CBP	CREB-binding protein
Cdc	Cell division cycle
CDK	Cyclin-dependent kinase
cDNA	Complimentary deoxyribonucleic acid
ChIP	Chromatin Immunoprecipitation
CO_2	Carbon dioxide
DAPI	4,6-diamidino-2-phenylindole
DBD	DNA-binding domain
DMEM	Dulbecco's Modified Eagle Medium
DMSO	Dimethyl sulfoxide
DNA	Deoxyribonucleic acid
DNase	Deoxyribonuclease
dNTP	Deoxyribonucleic triphosphate
DTT	Dithiothreitol
e.g.	*exemplī grātiā*
ECL	Enhanced chemiluminescence

EDTA	Ethylenediaminetetraacetic acid
EGTA	Ethyleneglycoltetraacetic acid
et al.	*et alii* (and others)
EtBr	Ethidium bromide
FACS	Fluorescence-activated cell sorting
FBS	Foetal Bovine Serum
FITC	Fluorescein isothiocyanate
g	gram
GAPDH	Glyceraldehyde 3-phosphate dehydrogenase
GST	Glutathione-S-Transferase
H3K9me3	Trimethylation of Lys9 of Histone H3
H3ac	Acetylation of Histone H3
i.e.	*id est* (it is)
Ig	Immunoglobulin
IP	Immunoprecipitation
IPTG	Isopropyl-β-D-thiogalactopyranoside
K	Lysine
Kb	kilo base
kDa	kilo Daltons
LB	Luria broth
LC-MS/MS	Liquid chromatography-mass spectrometry/mass spectrometry
M	Molar
MDM2	Mouse double minute 2 homolog
MDMX/MDM4	Mouse double minute X homolog/Mouse double minute 4 homolog
Me	Methylated
mRNA	messenger ribonucleic acid
MS	Mass Spectrometry
N-	amino-
NE	Nuclear protein Extract
NES	Nuclear export signal
ng	nanogram
NLS	nuclear localisation signal

nM	nanomolar
nm	nanometer
NP-40	Nonident P-40
OD_{600}	optical density (absorbance) at 600 nm
PBS	Phosphate Buffered Saline
PCR	Polymerase Chain Reaction
PFA	Paraformaldehyde
pH	Potential of Hydrogen
PI	Propidium Iodide
PML	Promyelocytic Leukemia
PMSF	Phenylmethylsulfonyl Fluoride
PNACL	Protein Nucleic Acid Chemistry Laboratory
PROTEX	Protein Expression laboratory
PTMs	Post-translational modifications
PUMA	p53 upregulated modulator of apoptosis
qRT-PCR	Quantitative reverse transcription polymerase chain reaction
R	Arginine
RING	Really Interesting New Gene
RNA	Ribonucleic Acid
rpm	revolutions per minute
ROS	Reactive Oxygen Species
RT	Room Temperature
SAM	S-Adenosyl Methionine
SDS	Sodium Dodecyl Sulphate
SDS-PAGE	Sodium Dodecyl Sulphate Polyacrilamide Gel Electrophoresis
SENP	SUMO/Sentrin Specific peptidase
shRNA	Short hairpin RNA
siRNA	Small interfering RNA
SIM	SUMO Interacting Motif
STUbLs	SUMO-targeted ubiquitin ligases
SUMO	Small-ubiquitin Modifier
TEMED	N,N,N',N'-tetramethylethylethylenediamine

TEV	Tobacco Etch Virus
UV	Ultraviolet
Ubc9	Ubiquitin-conjugating enzyme 9
Ubl	Ubiquitin-like protein
WCE	Whole cell protein extract
WT	Wild-Type

CHAPTER 1

Introduction

Chapter 1. Introduction

1.1 Overview

The regulation of protein expression and activity is critical to establish the correct function of the cell, and relies on a very complex network of signals that provides control at many levels. One of the ways that this refined control can be achieved is by the modification of proteins at a post-translational stage.

Post-translational modifications occur in almost all proteins, and provide a very sophisticated mechanism that allows the cell to tightly control the functions of regulatory proteins within the cell. This is mainly achieved as a result of the high reversibility of post-translational modifications (PTMs), allowing the refined control of protein function in space and time (Kim & Baek 2006). Whether these modifications occur as a result of the addition of a functional group, such as methylation, acetylation or phosphorylation, or by the binding of specific proteins, such as ubiquitination, sumoylation and neddylation, the modification of proteins can have significant effects in their localization, stability or function.

The covalent modification of proteins by small ubiquitin modifier protein – SUMO – has become a matter of intense research in recent years, and among its targets is the well-known tumour suppressor p53. Here, I focus on SUMO modification of p53, and explore the consequences of p53 sumoylation, particularly regarding p53's transcriptional activity.

1.2 The tumour suppressor p53

Cancer is a group of pathologies that arises from aberrant growth and uncontrolled invasion of abnormal cells to surrounding tissues. This is caused by the accumulation of mutations that impair the mechanisms that control cell proliferation, survival and migration. Consequently, these cells become transformed. Cells, however, have developed mechanisms to impede cancer cell transformation. The so-called tumour suppressor genes act as a break to the spread of tumourigenic cells, by stopping or slowing down cell division and limiting cell migration and survival (Junttila & Evan 2009).

Amongst the numerous proteins that orchestrate tumour suppression, p53 is one of the most well-known, yet arguably the most controversial. Firstly discovered in 1979 and described as an oncogene (Lane & Crawford 1979; Linzer & Levine 1979; DeLeo et al. 1979; Jenkins et al. 1984), p53 has come a long way to become one of the most studied tumour suppressor genes.

p53 is responsible for the activation of numerous metabolic pathways triggered in response to stress signals, leading to different cellular outcomes that ultimately attempt to avoid tumour cell growth and proliferation. p53 exerts its role primarily as a sequence-specific transcription factor, binding to p53-responsive elements (p53 RE) within the promoter region of target genes (el-Deiry et al. 1992; Beckerman & Prives 2010). Its transcriptional regulator functions are also reliant on its ability to recruit transcriptional co-regulators (Laptenko & Prives 2006), which allow p53 to both activate or repress the transcription of specific genes. From those, the first identified was the cyclin-dependent kinase inhibitor p21/WAF/CIP (CDKN1a) gene, whose product binds to and obstructs the activity of cyclinE-CDK2, cyclinA-CDK1, and cyclinD-CDK4/6 complexes, thus restraining cell-cycle progression and arresting cells in G1 phase (Bieging & Attardi 2012). Other p53-activated genes involved in cell cycle arrest include GADD45 (Growth Arrest and DNA Damage inducible 45) and 14-3-3σ, which activation prevents cell cycle progression from G2 to M phase (Bieging & Attardi 2012; Hermeking & Benzinger 2006). p53 can also induce the repression of genes involved in cell cycle progression, as is the case with CDC25c or Cyclin B2, essential components of the cell cycle machinery for G2-M transition (Beckerman & Prives 2010). Another major tumour suppressor function of p53 is inducing apoptosis of damaged cells. p53 is able to promote the activation of several pro-apoptotic genes, including BAX (Bcl-2–associated X protein), PUMA (p53 upregulated modulator of apoptosis) and PIGs (p53-inducible genes) (GPI (glycosylphosphatidylinositol) transamidase components) (Beckerman & Prives 2010), as well as repress anti-apoptotic genes such as Survivin (Böhlig & Rother 2011).

Many stimuli contribute to the activation of p53; these can range from cellular stimuli, such as oxidative stress (Sermeus & Michiels 2011; Gogna et al. 2012), nutritional deprivation (Maddocks et al. 2013), ribosomal stress (Bhat et al. 2004), ribonucleotide depletion (Linke et al. 1996) and Nitric Oxide (NO) (Hussain et al. 2003), to oncogenic stresses, including DNA damage (Sakaguchi et al. 1998), oncogene activation (Lowe 1999) or telomere shortening

(Artandi & DePinho 2010). In a general way, these insults stabilize p53 by impeding its degradation, thereby increasing p53 cellular levels. Once stabilized, p53 can bind to p53 RE and function as a transcriptional regulator (Zilfou & Lowe 2009).

Depending on the extent of the stress, p53 can activate different pathways, resulting in disparate responses: mild or physiological stresses lead to metabolic homeostasis, antioxidant defence or DNA repair, whereas more severe insults can result in temporary cell cycle arrest, senescence or even apoptosis (Chen et al. 1996) [**Figure 1.1**].

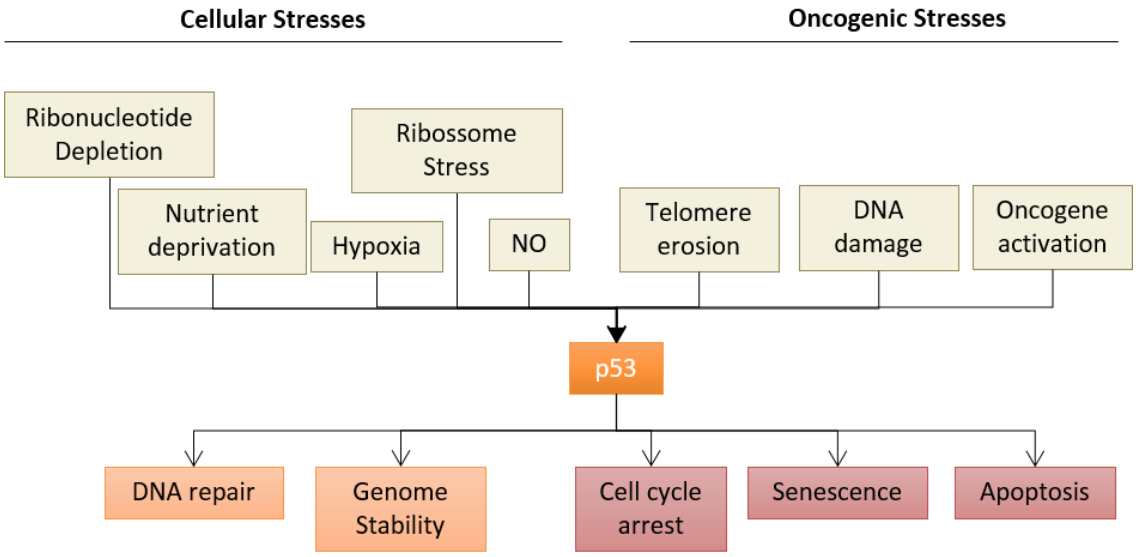

Figure 1.1. Activation of p53 by multiple stresses and resultant physiological responses

Following stress, p53 protein becomes stabilized and activates or represses the transcription of a number of genes that ultimately lead to the appropriate cellular outcome.

Being such a powerful tumour-suppressor, it is not surprising that the gene that encodes p53, TP53, is mutated in virtually half of all cancers, with the other half harbouring mutations that inactivate some part of the p53 pathway (Toledo & Wahl 2006). A germline mutation in the TP53 gene is the cause of Li-Fraumeni syndrome, a rare hereditary condition that predisposes patients to many types of cancer at an early age (Malkin et al. 1990; Srivastava et al. 1990). Consequently, p53 is often described as the guardian of the genome, due to its potent tumour suppressor capabilities upon genotoxic insult combined with the severe genomic instability shown by several p53 deficient cell lines (Junttila & Evan 2009; Efeyan & Serrano 2007).

1.2.1 p53 Structure

p53 is active as a tetramer, and each monomer consists of 393 amino acids, organized in 4 distinct structural and functional domains [**Figure 1.2a**]. The N-terminal region contains the Transactivation domain (TAD), which is sometimes subdivided into 2 sub-domains – TAD1 and TAD2, and a Proline-rich region. The transactivation domain, responsible for the transcriptional activity of p53, is an important region for protein interactions, recruiting components of the transcription machinery and transcriptional co-activators CBP/p300 (Gu et al. 1997; Teufel et al. 2007). In addition, it provides a binding site for the p53-negative regulators MDM2 and MDM4 (also known as MDMX), influencing p53 stability (Kussie et al. 1996). The transactivation domain is also a hub for post-translational modifications, specifically phosphorylation of threonine and serine residues, which correlate with transcriptional activation of p53 (DeHart et al. 2014).

The core domain of p53 is the DNA-binding domain. This region allows p53 to specifically bind to p53-responsive elements on the promoter region of p53-target genes. It is in the central DNA binding domain that most cancer-related mutations occur, causing defective DNA binding and thus resulting in altered p53 response (Toledo & Wahl 2006). The oligomerization domain (OD) follows the central DNA binding domain and allows the formation of p53 dimers and tetramers. The tetramerization state of p53 allows p53 to stably bind to DNA and activate transcription (Weinberg et al. 2004). The oligomerization domain also contains a nuclear localization signal (NLS), which together with the nuclear export signal

(NES) located in the Carboxyl-terminus, allow p53 to shuttle between the cytoplasm and the nucleus.

Finally, the C-terminal region of p53 harbours the so-called regulatory domain. Rich in basic lysine residues, this domain is target to many post-translational modifications, including ubiquitylation, acetylation, sumoylation, neddylation and methylation, which work together to regulate p53 function [**Figure 1.2b**].

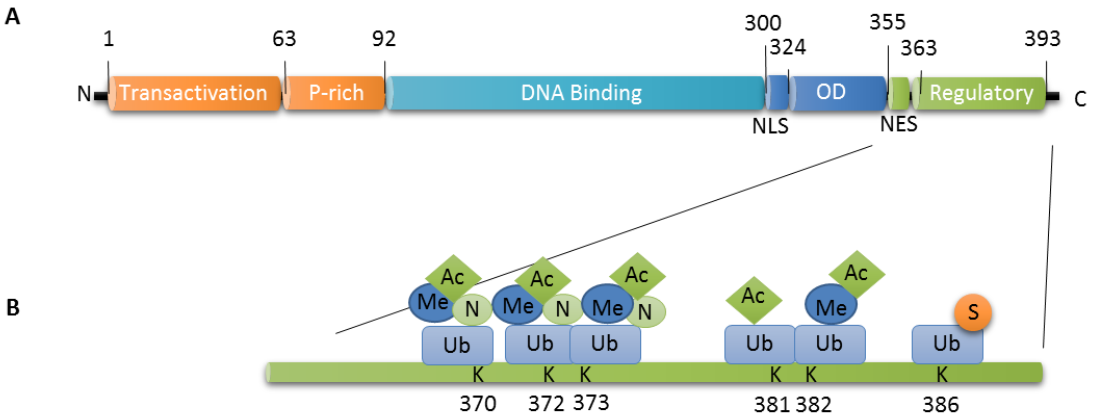

Figure 1.2. p53 Structure

(A) p53 contains 4 major domains: the transactivation domain in the N-terminal region, followed by a proline-rich region, a DNA binding domain, an oligomerization domain (OD), and a C-terminal regulatory domain, where most of post-translational modifications occur. NLS – Nuclear Localization Signal, NES – Nuclear Export Signal.

(B) The lysines enclosed in the C-terminal regulatory domain are heavily modified by a number of PTMs, which fine-tune and regulate p53 function. Ub – ubiquitylation, Me – Methylation, Ac – Acetylation, N – Neddylation, S – Sumoylation.

1.2.2 Mechanism of p53 activation

The activation of p53 following stress is mainly achieved by the disruption of the interaction of p53 with its negative regulator MDM2. DNA damage, induced for example by ionizing radiation or UV light, activates a number of kinases - including ATM (Ataxia–Telangiectasia Mutated), ATR (Ataxia-Telangiectasia and Rad3-related), DNA-PK (DNA-dependent protein kinase), Chk1 and Chk2 (Checkpoint Kinase 1 and 2) - that phosphorylate N-terminal Serines and Threonines in the transactivation domain of p53. These phosphorylation events, particularly phosphorylation of Serine 15 and 20, block the interaction between p53 and MDM2 thereby leading to p53 stabilization (Appella & Anderson 2001). Further, this results in an increased affinity of p53 to co-activators such as histone acetyl-transferases (HATs) p300 and CREB-binding protein (CBP), which acetylate p53 and enable its transactivation functions (Toledo & Wahl 2006).

Another way of triggering p53 activation is by aberrant expression of oncogenes such as Myc and Ras. This pathway of activation seems to be independent of DNA damage, and involves the up-regulation and stabilization of p14ARF protein, a tumour suppressor protein that blocks MDM2 interaction with p53 (Eischen & Lozano 2014). As a result, p53 is able to avoid MDM2-mediated degradation and becomes stabilized [**Figure 1.3**].

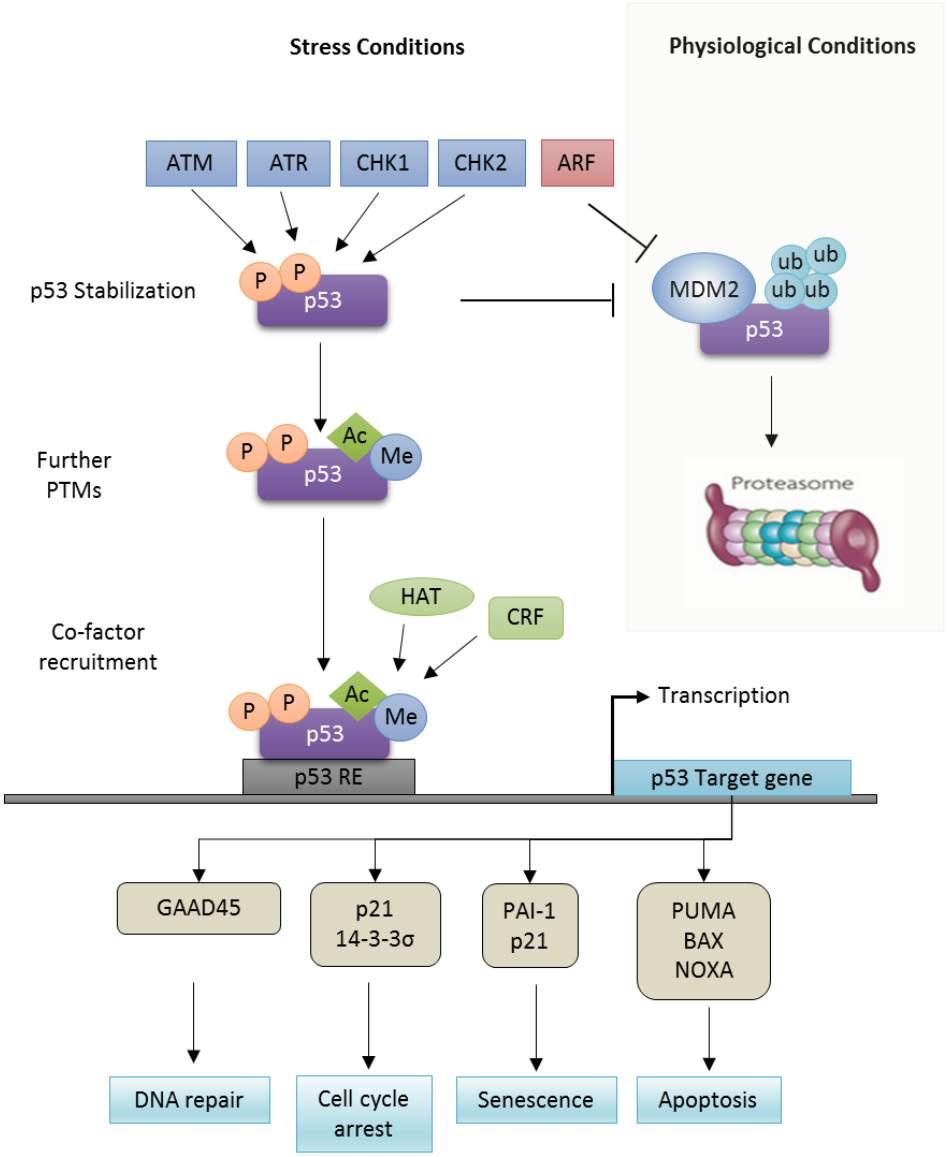

Figure 1.3. p53 Activation and Outcomes

Under normal conditions, p53 levels are kept low by MDM2-mediated ubiquitination and degradation. Under stress conditions, p53 stabilization occurs via activation of several kinases that promote p53 phosphorylation. Stabilization can also occur via stabilization and activation of ARF, which binds MDM2 and prevents MDM2-targeted degradation of p53. Upon stabilization, p53 is modified by additional post-translational modifications (PTMs), such as acetylation and methylation, which further enhance p53 stability and DNA-binding activity. p53 binds DNA recognizing specific p53 Responsive Elements (p53 RE) and promotes the recruitment of co-activators such as Histone Acetyl-Transferases (HAT) and Chromatin Remodelling Factors (CRF), which facilitate p53-mediated transcription of target genes. p53-responsive genes are involved in many pathways crucial for impeding tumour progression, the most important of which are DNA repair, cell cycle arrest, senescence and apoptosis. Adapted from (Riley et al. 2008).

1.2.3 Functional Outcomes of p53 Activation

In broad terms, p53 response to stress falls into one of these categories: cell cycle arrest, apoptosis or senescence.

The primary mechanism by which p53 was though to suppress tumour growth was by mediating the apoptotic response of tumourigenic cells. This was supported by the fact that mice expressing a mutant p53 incapable of inducing cell cycle arrest but retaining the ability to promote apoptosis were able to efficiently evade tumourigenic transformation (Toledo et al. 2006). In fact, p53 is able to promote apoptosis via two distinct mechanisms: firstly, as a transcription factor, p53 specifically promotes the expression of pro-apoptotic genes (e.g. BAX, PUMA, NOXA), as well as the repression of anti-apoptotic genes (Survivin), and secondly, p53 is able to interact with proteins involved in the apoptotic pathway in the cytosol and mitochondria, promoting apoptosis in a transcriptional-independent manner (Pflaum et al. 2014). Although apoptosis clearly presents an effective tumour suppressive mechanism, p53 possesses other equally important functions to avoid cancer progression. For example, knockout mice where the PUMA gene has been deleted are not prone to developing cancer, despite having a deficient p53-mediated apoptotic response (Michalak et al. 2008). Furthermore, mice harbouring a particular hot-spot mutation in the DNA binding domain (R172P, correspondent to R175 in humans), which prevents p53 from inducing apoptosis but retains its ability to arrest cell cycle, were able to escape early onset thymic lymphomas characteristic of p53-null mice (Liu et al. 2004).

Another mechanism to evade tumour progression is by arresting cell growth. p53 is able to mediate the expression of several genes known to be involved in cell cycle arrest, such as p21, 14-3-3σ and GADD45 (El-Deiry 1998). The observation that the induction of p21 expression is triggered by even small amounts of p53 lead to the idea that temporarily stopping cell division might be advantageous under mild stress conditions, in order to allow the cell to repair the DNA damage and prevent the spread of genetic alterations (Vousden & Lane 2007). While a temporary cell cycle arrest might be sometimes beneficial, it might carry risks if the damage is not appropriately repaired and allowed to prevail and spread as the cell resumes normal divisions. To prevent this, another mechanism can be activated by p53 – senescence. Cellular senescence is the permanent arrest of cell growth, conveying an efficient

way to prevent oncogenic propagation without cell death. In response to DNA damage, p53 is able to initiate the transcription of pro-senescent genes, such as p21 and PAI-1 (plasminogen activator inhibitor type-1) (Kortlever et al. 2006). A mouse model for liver carcinoma with conditional knockout of p53 showed that upon p53 re-expression, the primary response was not apoptosis, but instead the triggering of senescence program (Xue et al. 2007). Although this might seem more like a delay of the problem, rather than its eradication, as *in vitro* p53 re-activation results in cell cycle arrest, *in vivo* senescence is able to trigger an innate immune response that targets the tumour cells (Xue et al. 2007). Hence, senescence delivers an effective mechanism to avoid tumour progression.

1.2.4 Regulation of p53-response

The adequate response of p53 to each situation depends on a number of factors, including the severity and duration of the stress (Vousden & Lane 2007), promoter binding affinity (Inga et al. 2002; Menendez et al. 2007), the interaction with specific regulators and co-factors and post-translational modifications (Olsson et al. 2007; Carvajal & Manfredi 2013).

As mentioned earlier, it is known that the activation of p21 expression is extremely sensitive to changes in p53 levels. It is, therefore, likely that in cells that experience mild stresses, p53 will trigger survival responses, temporarily arresting cell growth and promoting DNA repair. Conversely, severe, concomitant stress that results in irreparable damage to cells, leads to the activation of apoptotic or senescence programs by p53 (Vousden & Prives 2009). In line with this, it has been suggested that the specificity of p53 response depends largely on the affinity to different target-promoters. Hence, low levels of p53 would associate more easily with high affinity promoters, such as those for genes involved in cell cycle arrest, whereas only high levels of p53 (occurring upon severe stress) would bind to low-affinity promoters, generally associated with apoptotic response (Chen et al. 1996; Weinberg et al. 2005).

The picture gets further complicated when placing it in a cellular context, where many co-factor proteins bind p53, directly or indirectly, and thus influence the cellular outcome. For example, members of ASPP (Apoptosis Stimulating Protein of p53) family, ASPP1 and ASPP2,

directly bind to the DNA binding domain of p53 and enhance p53-mediated apoptosis (Samuels-Lev et al. 2001). Haematopoietic zinc finger (Hzf) protein also directly binds p53, but rather than stimulating apoptosis, Hzf binding promotes cell cycle arrest (Das et al. 2007). The specificity of promoter selectivity by p53 upon stress is further defined by post-translational modifications (PTMs). The phosphorylation of Serine 46, in the transactivation domain, leads to the specific induction of pro-apoptotic gene p53AIP1 (Oda et al. 2000). Similarly, acetylation of Lysine 120 in the DNA binding domain promotes the apoptotic response by inducing PUMA and BAX expression (Tang et al. 2006; Sykes et al. 2006).

These examples demonstrate that the modification of a single residue of p53 is enough to target p53 to specific promoters. However, p53 modifications can also affect co-factor binding by either generating new or blocking protein-protein interactions. Adding to that, the ability of p53 to induce a determined cellular response also relies on certain regulators and/or accessory factors, which are expressed in a cell-type/tissue specific way. In fact, different studies have compared the responses to γ-irradiation in both WT and p53-deficient mice, and verified a differential response dependent on the murine body tissue (MacCallum et al. 1996; Midgley et al. 1995). After exposure to γ-irradiation different tissues either: a) exhibit an increase in p53 concentration and the induction of apoptosis (e.g. spleen, thymus); b) showed an increase in p53 expression, but no induction of apoptosis (e.g. Kidney, adrenal glands); or c) showed no alteration of p53 levels and failure to induce apoptosis (e.g. Skeletal muscle, liver).

Other studies revealed the importance of tissue and cell-type specificity for the induction of apoptosis, by investigating the expression of apoptosis-inducing p53 target genes after γ-irradiation (Bouvard et al. 2000). One explanation for this differential behaviour could rely on the rate of cellular proliferation in different tissues (Jackson et al. 2011). For example, while the rapidly proliferating cells of the central nervous system of the mouse embryo undergo apoptosis, in the adult mouse, where cells are mainly in post-mitotic phase, cells are mostly apoptosis-resistant (Lee et al. 2001). A possible mechanism underlying this phenomenon could be that in actively proliferating cells the volume of DNA damage overwhelms the capacity of the DNA repair system thus triggering a continuous and robust activation of the ATM/ATR pathway. The latter leads to the stabilization and activation of p53, which would in turn switch on transcription of the target pro-apoptotic genes. In non-

proliferating cells, however, the amount of DNA damage is rather small and the DNA repair machinery is able to cope with it in a timely manner, thus hindering the apoptotic response. Another example of differential responses dependent on the tissue type is the expression of the E3 ubiquitin ligase MDM2, responsible for the degradation of p53. The loss of MDM2 triggers apoptosis in several cell-types such as cardiomyocytes, intestinal epithelium and neural progenitor cells, but otherwise induces senescence in mouse embryonic fibroblasts (Jackson et al. 2011).

1.2.5 Regulation of the p53 protein

The intricate signalling network of responses that p53 is able to coordinate turns p53 into one of the most powerful tumour suppressor proteins. Therefore, the negative regulation of p53 is utterly important to prevent cell cycle arrest or apoptosis in normal, unstressed cells and assure the maintenance of the appropriate cellular homeostasis. Indeed, p53 is regulated by a multitude of factors at the transcriptional, post-transcriptional, translational and post-translational levels. Starting at the transcriptional/translational level, the TP53 gene can be transcribed into up to 10 different p53 isoforms, using alternative splicing, different promoters and alternative translation initiation sites (Hollstein & Hainaut 2010). At the protein level, p53 is regulated by diverse mechanisms, which operate by directly promoting p53 degradation, alter its cellular localization or silence its transcriptional functions. These mechanisms, whether they operate via protein-protein interactions or structural changes in the p53 protein, are frequently driven by a complex code of post-translational modifications (PTMs). Broadly speaking, PTMs can stimulate two discerned effects on the functional activity of p53: on the one hand, PTMs can have a positive effect, activating p53 (as is the case for phosphorylation, acetylation and methylation of Lysine 372), or, on the other hand, promote p53 inactivation and degradation (such as ubiquitylation and other ubiquitin-like modifications, and methylation of certain lysines) (Marouco et al. 2013).

Thus, PTMs convey a refined way to control and fine-tune p53's function and levels. Arguably, the additional layer of regulation provided by PTMs could explain how a single protein can discern such a range of different stresses and activate cellular responses accordingly.

1.2.5.1 MDM2 feedback

In normal, unstressed cells, p53 protein levels are kept low through the ubiquitin-proteasome pathway. One of the key regulators of p53 cellular levels is the E3 Ubiquitin-ligase MDM2 (Murine Double Minute 2) and its homologue MDM4. MDM2 and MDM4 interact with an N-terminal α-helix of p53, concealing the transactivation domain and thus hindering p53 transcriptional activity. Furthermore, the E3 ligase activity of MDM2, conferred by the C-terminal RING domain, allows it to directly target the conjugation of ubiquitin to lysine residues within the regulatory domain of p53. Low levels of MDM2 promote mono-ubiquitylation of p53, linked with its nuclear export and cytoplasmic accumulation; on the contrary, high levels of MDM2 stimulate poly-ubiquitylation of p53 C-terminal lysines, leading to its rapid proteasomal degradation by the 26S proteasome (Dai & Gu 2010; Wade et al. 2010). The discovery of MDM2 and MDM4 function as p53 regulators came from observations in knockout mice. MDM2 knockout mice display early embryonic lethality caused by aberrant p53-mediated apoptosis, a phenotype that can be rescued by the ablation of p53 expression (Jones et al. 1995)(Montes de Oca Luna et al. 1995). Similar phenotypes were observed in MDM4-knockout mice, which could also be rescued by deletion of p53 (Parant et al. 2001).

It is thought that MDM2-mediated p53 degradation is primarily driven by p53 mono-ubiquitylation and nuclear export. The re-localization of p53 to the cytoplasm prevents its activities as a transcription factor, where it will be target for further ubiquitylation by MDM2 (Wade et al. 2010). Even though MDM4 is a homologue of MDM2 and also contains a catalytic RING domain, MDM4 does not display E3 ligase activity towards p53. However, it can form heterodimers with MDM2, and actually enhance MDM2 E3 ligase activity this way (Linares et al. 2003). The formation of MDM2/MDM4 heterodimers occurs through their respective RING domains, and seems to be critical for p53 inactivation. In fact, mice expressing a mutant version of MDM2 with no ligase activity exhibited the same phenotype as MDM2 knockout mice (Itahana et al. 2007). Similarly, conditional knockout mice expressing a mutant form of MDM4 with impaired ability to bind to MDM2 display p53-dependent embryonic lethality (Huang et al. 2011), although MDM4 seems to be dispensable in adult mice (Pant et al. 2011). These studies emphasize the importance of both MDM2 and MDM4 in the regulation of p53 in early embryogenesis.

Interestingly, MDM2 is itself a product of p53-mediated transcription, creating an auto-regulatory loop where p53 regulates its regulator. MDM2 is also regulated by the tumour suppressor p14ARF (Alternative Reading Frame) protein, an alternative reading frame product of the Ink4a/CDKN2A human locus. In response to cell stress, ARF is able to actively associate MDM2 and sequester it to either the nucleus or the nucleolus, preventing MDM2 from associating with p53. In turn, p53 is able to avoid MDM2-mediated degradation, leading to an increase in its cellular levels and transcriptional function (Eischen & Lozano 2014). Another way of regulating p53 stability is by counterbalancing MDM2-mediated ubiquitylation, which can be achieved by de-ubiquitylases. An example of such enzymes is HAUSP (Herpesvirus-Associated Ubiquitin-Specific Protease Hausp, also known as USP7). HAUSP was firstly identified as a p53 interacting protein and thought to operate by removing ubiquitin conjugates from p53, thereby preventing its degradation (Li, Chen, et al. 2002). However, later observations using HAUSP deficient cell lines showed a complete stabilization of p53, indicating a more complex role for HAUSP in the regulation of p53 (Cummins et al. 2004; Li et al. 2004). In fact, HAUSP operates mainly by de-ubiquitylating MDM2, which allows the later to maintain low levels of p53. Loss of HAUSP promotes MDM2 de-stabilization, and thus results in increased p53 cellular levels [**Figure 1.3**].

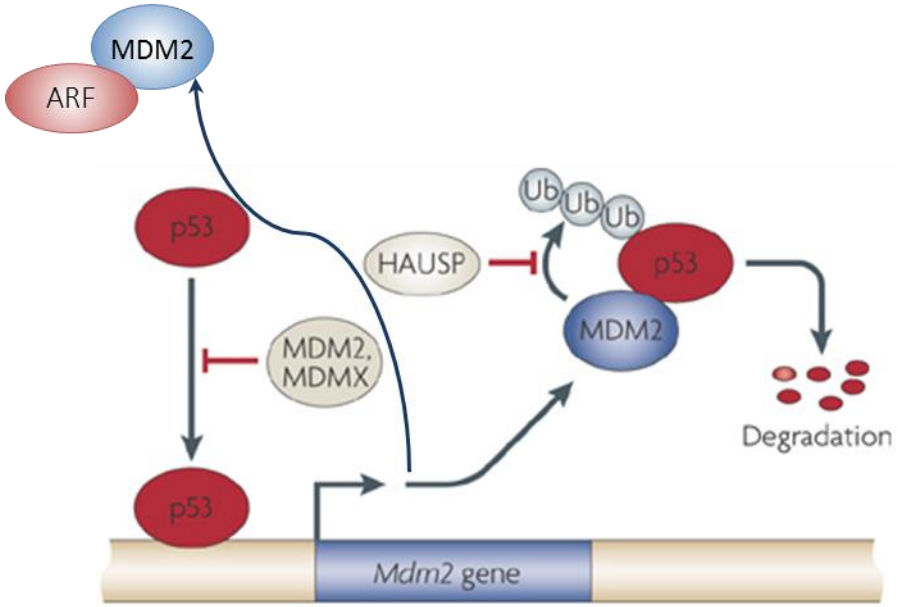

Figure 1.4. MDM2-p53 feedback loop

MDM2, a transcriptional product of p53, is responsible for the maintenance of low levels of p53's activity in the cell. Together with MDMX, MDM2 binds to the TAD domain of p53 and restrains its transcription activity. MDM2 also acts as an E3 ubiquitin ligase, promoting p53 ubiquitylation, and marking it for proteasomal degradation. De-ubiquitylation by HAUSP is able to stabilize p53 and MDM2 functions can be inactivated by ARF, which impedes its association with p53. Adapted from (Murray-Zmijewski et al. 2008).

1.2.5.2 Regulation by PTMs

The p53 protein encloses two major regions that are target to intensive PTMs: the N-terminal Transactivation domain, rich in Serine/Threonine residues, which phosphorylation is critical for the stabilization and activation of p53; and the lysine-rich C-terminal Regulatory domain, hub for diverse PTMs, including acetylation, methylation, ubiquitylation, neddylation and sumoylation. For the purpose of this thesis, I will explore PTMs occurring only in C-terminal lysines of p53.

Acetylation

p53 was the first non-histone protein found to be regulated via acetylation, which, like phosphorylation, is linked with increased levels of p53 activation (Luo et al. 2000; Gu & Roeder 1997; Tang et al. 2008). Acetylation of p53 regulates protein activity in three ways: firstly, it counteracts p53 ubiquitylation by acetylating the same target-lysines, thereby promoting p53 stabilization; secondly, acetylation prevents the interaction of repressor complexes with p53; and thirdly it promotes the association of co-activator complexes, thus enabling p53 transcriptional activity (Dai & Gu 2010).

p53 contains at least 8 lysine residues, distributed between the C-terminal regulatory domain and the DNA binding domain, that are subject to acetylation by a number of Histone Acetyl Transferases (HATs). These include co-activators p300/CBP (CREB-binding protein), responsible for the acetylation of multiple residues in the C-terminus of p53 (Gu & Roeder 1997), PCAF (p300/CBP-Associated Factor), and the MYST family of HATs comprising TIP60 (Tat-Inter-active Protein of 60 kDa), MOZ (Monocytic leukemia zinc finger) and MOF (Males absent On the First) (Dai & Gu 2010). Two knockin studies in mice, where all C-terminal lysines were mutated to arginine residues (6KR and 7KR mutants), showed only mild effects in overall p53 response to induce cell growth arrest and apoptosis, with defects in p53-dependent transcription being cell-type specific (Feng et al. 2005; Krummel et al. 2005). However, the abolishment of all C-terminal acetylation sites in conjunction with a newly discovered site for CBP/p300-mediated acetylation at lysine 164 (8KR mutant), completely abolished p53 capacity to induce cell cycle arrest and apoptosis (Tang et al. 2008). Importantly, loss of acetylation of any of the individual sites has no effect in p53 transactivation activity, indicating that

acetylation in p53 is highly redundant, and can be compensated by acetylation of nearby residues. Although the 8KR mutant was still able to function as a DNA-binding transcription factor and activate the transcription of MDM2, this study showed that acetylation is crucial for the tumour suppressor abilities of p53 in response to stress.

Conversely, deacetylation of p53 by Histone Deacetylase complexes (HDAC) leads to decreased levels of p53 transcriptional activation, and repression of growth arrest and apoptosis (Luo et al. 2000; Luo et al. 2001). Deacetylation may, in part, inactivate p53 by enabling ubiquitylation of the same residues. That way, deacetylation could convey a quick mechanism to re-establish normal levels of p53 and avoid cell growth arrest and apoptosis when no longer needed (Li, Luo, et al. 2002).

Methylation

Methylation of p53 C-terminal lysines can result in different outcomes, depending on the lysine targeted, and the extent of the modification (mono-, di-, or tri-methylation). For example, mono-methylation of K372 by SET7/9 leads to stabilization of DNA-associated fraction of p53 and promotes activation of p53-dependent transcription (Chuikov et al. 2004). All other known lysine methylation events on p53 result in repression of p53 activity. Lysine methyltransferase SMYD2 is responsible for the mono-methylation of K370, leading to a decrease in p53-mediated transcription of target genes p21 and MDM2 due to the decreased ability of p53 to bind to these promoters (Huang et al. 2006). Moreover, the levels of K370 methylation were reduced upon genotoxic stress, and correlated with increased levels of Set9-mediated methylation. This indicates that methylation of K372 inhibits methylation of the nearby site K370, by preventing the interaction between p53 and SMYD2 (Huang et al. 2006). The methylation output of K370 seems to become even more complicated, as another yet unknown methyltransferase is able to di-methylate this lysine residue. In contrast to mono-methylation, it appears that di-methylation of K370 leads to an increased ability of p53 to promote gene-expression, by enhancing p53 interaction with coactivator 53BP1 (Huang et al. 2007). The di-methyl mark in K370 can be removed by the histone lysine-specific demethylase LSD1, which results in repression of p53-mediated apoptosis (Huang et al. 2007). Another lysine-specific methyltransferase, SET8, was discovered to mono-methylate another C-terminal Lysine in p53 – K382. This event results in the suppression of p53-mediated cell

growth arrest and apoptosis, and the levels of K382 mono-methylation decline upon DNA damage (Shi et al. 2007). Finally, two homologue methyltransferases, G9a and G9a-like protein (Glp), were reported to catalyse the di-methylation of K373, which correlated with the inactivation of p53-mediated apoptosis (Huang et al. 2010).

Ubiquitin and ubiquitin-like modifications

The C-terminal lysines of p53 can also be modified by ubiquitin and other ubiquitin-like proteins. Poly-ubiquitylation, as described above, has profound effects in the stability of p53 (See section **1.2.5.1**). Mono-ubiquitylation of p53, on the other hand, is thought to play a major role in the cytoplasmatic localization of p53 (Brooks & Gu 2006). This re-location of p53 to the cytoplasm has two effects: on the one hand, it prevents p53 from operating as a nuclear transcription factor, and thus disables its tumour suppressor abilities; on the other hand, it allows p53 to perform transcription-independent functions, promoting apoptosis and inhibiting autophagy (Green & Kroemer 2009).

Although the best-known function of MDM2 is acting as an ubiquitin E3 ligase, the RING domain of MDM2 also allows it to operate as a ligase for other ubiquitin-like proteins. The covalent conjugation of NEDD8 (Neural precursor cell Expressed Developmentally Downregulated protein 8) to p53 can be catalysed by MDM2, occurring in 3 lysines (K370, K372, K373) that are also target for ubiquitylation. Neddylation of these lysines does not affect p53 stability or subcellular localization, but strongly inhibits p53's transcriptional abilities (Xirodimas et al. 2004). MDM2 can also enhance and catalyse sumoylation of p53, on Lysine 386 (Chen & Chen 2003; Stindt et al. 2011). Intriguingly, more than 15 years after it was discovered (Gostissa et al. 1999; Rodriguez et al. 1999), the role of p53 sumoylation is not yet defined. Contradictory reports show that sumoylation can increase (Rodriguez et al. 1999) or dampen (Wu & Chiang 2009a; Stindt et al. 2011) p53 transcriptional activities. There is also evidence that sumoylation is involved in the nuclear export of p53 (Carter et al. 2007; Takabe et al. 2011; Santiago et al. 2013), and that it may play a role in inducing premature senescence (Li et al. 2006; Yates et al. 2008).

Interplay among PTMs in p53's C-terminus

Although particular PTMs can have a significant impact in the regulation of p53, it is the interplay among these that allows the fine-tuning of p53 responses upon stress. As mentioned briefly above, acetylation and ubiquitylation compete for the same C-terminal lysines, leading to opposite functional outcomes. Under normal conditions, low levels of p53 are maintained thanks to MDM2 association with p53, which targets it for proteasomal degradation. Genotoxic insult causes MDM2 dissociation and reduces p53 lysine ubiquitylation; these lysines can then be targeted for acetylation by CBP/p300, extending p53 half-life significantly (Meek & Anderson 2009). Another example is the crosstalk between methylation of K372 by Set9, which promotes the acetylation of nearby residues and thus increases p53 stability and transactivation function (Ivanov et al. 2007)(Kurash et al. 2008). The same modification also prevents SMYD2 mono-methylation of the nearby residue K370, which has an antagonistic effect to K372 mono-methylation (Huang et al. 2006). On another study, Wu and Chiang show that p53 sumoylation on K386 hinders acetylation of nearby lysines, even though the ability to interact with p300 is unaltered (Wu & Chiang 2009a).

Collectively these observations demonstrate that PTMs are not static processes in proteins, but rather dynamic. This dynamic nature allows the intricate interplay between PTMs, which ultimately results in a controlled coordination of protein functions. In that way, PTMs represent a complex code, which changes in accordance to cellular stimuli, and confers a high degree of specificity to p53 responses.

1.3 Small Ubiquitin Modifier (SUMO) proteins

Small Ubiquitin MOdifier (SUMO) proteins are part of the Ubiquitin-like modifier (UbL) family of proteins, which share similarities in the protein sequence and tri-dimensional structure with ubiquitin (van der Veen & Ploegh 2012). Ubls have a characteristic C-terminal di-glycine motif, which becomes exposed upon maturation, and that is essential for conjugation to the target protein (Flotho & Melchior 2013; Jentsch & Psakhye 2013). The conjugation of Ubls to the target protein occurs in a process that resembles the ubiquitin pathway, through an enzymatic cascade that involves E1 activating and E2 conjugating enzymes and E3 ligases.

Sumoylation is a covalent post-translational modification defined by the addition of a Small Ubiquitin Modifier (SUMO) protein to the target protein. Numerous proteins have been shown to be modified by SUMO, contributing to the modulation of many cellular processes, including mitosis (Klein et al. 2009; Ban et al. 2011), cell growth and differentiation (Yang & Paschen 2009; Taylor & Labonne 2005), senescence (Bischof & Dejean 2007) and apoptosis (He et al. 2015). The covalent binding of SUMO to proteins may alter their localization, stability or function. Yet, it is as a regulator of transcription that SUMO plays its major role, being able to modify many proteins involved in the regulation of gene expression, including transcription factors, co-factors and regulators of chromatin structure (Gill 2003).

1.3.1 SUMO Isoforms

Yeast and lower eukaryotes present one single SUMO isoform, known as Smt3 in *Saccharomyces cerevisiae* and Pmt3 in *Schizosaccharomyces pombe* (Wilkinson & Henley 2010; Andrews et al. 2005), whereas in mammals there is evidence of four different isoforms of SUMO: SUMO-1, SUMO-2, SUMO-3 and SUMO-4 (Wilkinson & Henley 2010).

SUMO isoforms comprise approximately 100 amino acid in length and all contain an essential di-glycine motif (GG) in the C-terminal region, which becomes exposed upon maturation. SUMO-1 was firstly identified as an interacting protein of RAD51/52 nucleoprotein filament proteins (Shen et al. 1996) and PML (promyelocytic leukaemia) (Boddy et al. 1996), and soon were re-discovered as a covalent protein modifier of RanGAP1 (Ran-

GTPase-activating protein 1) (Matunis et al. 1996; Mahajan et al. 1997). Since then, SUMO-1 has been the most studied isoform, promoting mono-sumoylation of target lysines.

Sharing 96% similarity, SUMO-2 and 3 differ only in 3 N-terminal residues upon maturation, and are thus commonly referred to as SUMO-2/3 (van der Veen & Ploegh 2012). While SUMO-2/3 are nearly identical, they only share about 50% homology with SUMO-1 [**Figure 1.5**]. In addition, SUMO-2/3 were shown to be able to form poly-SUMO chains *in vivo* on their substrates, in contrast with SUMO-1 (M H Tatham et al. 2001). These mixed multi-SUMO chains are formed due to an internal SUMO consensus site (ΨKXE (where Ψ is isoleucine, valine or lysine)), located in the N-terminus of SUMO-2 and 3, which allows the conjugation of other SUMO molecules (Michael H. Tatham et al. 2001). Thus, although lacking this internal consensus site, SUMO-1 is able to recognize the consensus region of other SUMO molecules, and hence terminate poly-SUMO chains (Hay 2013) [**Figure 1.6**].

This distinction in the ability to form chains seems to be the reason for the different functional outcomes mediated by SUMO-1 and SUMO-2/3. For example, microtubule motor protein CENP-E was found to specifically recognize and bind to SUMO2/3 polymeric chains. CENP-E is a key regulator for the chromosomal alignment during metaphase, and its correct localization to the kinetochore was dependent on non-covalent interactions between CENP-E and SUMO-2/3 polymeric chains, revealing a paralogue-specific role for SUMO-2/3 in prometaphase progression (X.-D. Zhang et al. 2008). It has also been proposed that poly-SUMO chains may function as an anchorage point for specific E3 ubiquitin ligases, targeting sumoylated proteins for subsequent proteasomal degradation. This newly discovered family of ubiquitin ligases – known as SUMO-targeted ubiquitin ligases or STUbLs – is characterized for having multiple SIMs (SUMO Interacting Motifs) which enables them to recognize and bind to polymeric SUMO chains. One such protein is RNF4, a RING finger containing E3 ligase, harbours 4 SIMs in its N-terminus. RNF4 was shown to be recruited to sumoylated PML via these N-terminal SIMs, and promote its poly-ubiquitylation as its RING domain drives the transfer of ubiquitin (Lallemand-Breitenbach et al. 2008; Tatham et al. 2008). Poly-ubiquitylated proteins are then send to the 26S proteasome and targeted for degradation.

A

```
Smt3p     msdsevnqeakpevkp  ...  eqigga ty
SUMO-1    msd    qeakpsted  ...  eqtgghstv
SUMO-2    mad    ekpkegvk   ...  qqtggvy
SUMO-3    mse    ekpkegvk   ...  qqtggvpesslaghsf
SUMO-4    man    ekpteevk   ...  qptggvy
aa        1                      90
```

B

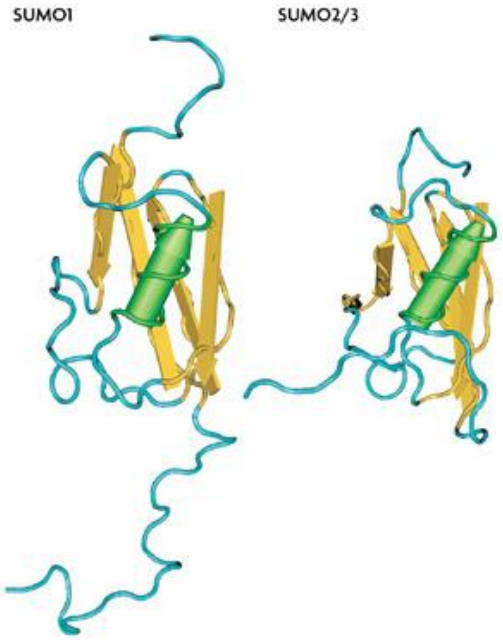

Figure 1.5. SUMO isoforms

(A) Part of the amino acid sequence of the different isoforms of SUMO proteins in mammals (SUMO-1, SUMO-2, SUMO-3 and SUMO-4) and yeast (Smt3p). An essential di-glycine motif (red) is exposed after maturation, by removal of C-terminal residues (blue). All isoforms except mammalian SUMO-1 contain an internal SUMO target lysine at the N-terminus (purple), which allows them to form poly-SUMO chains. SUMO-4 contains a proline residue (green) in position 90 that prevents its normal maturation. Adapted from (Mukhopadhyay & Dasso 2007).

(B) Comparison of the three-dimensional NMR structures of SUMO-1 and SUMO-2/3. SUMO-2 and SUMO-3 have identical structures, as they only differ by 3 residues in their active sequence. Adapted from (Martin, K. a Wilkinson, et al. 2007).

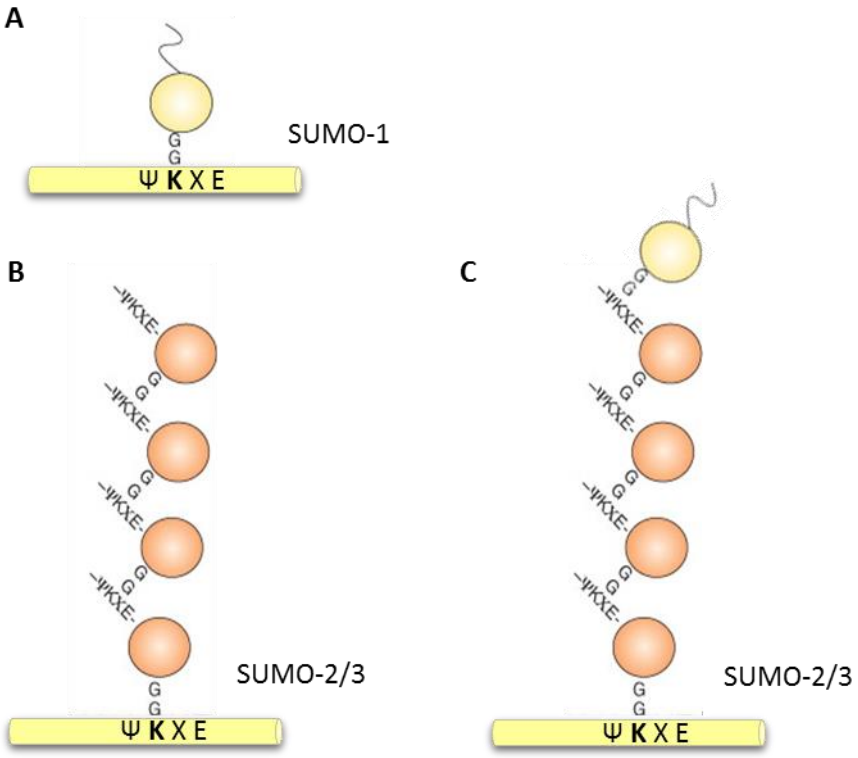

Figure 1.6 SUMO chains

The presence of an internal SUMO consensus site (ΨKXE) within the N-terminus of SUMO-2 and SUMO-3, allows the formation of poly-SUMO chains (**B**). Lacking this sequence, SUMO-1 can only promote mono-sumoylation of target proteins (**A**) or terminate poly-SUMO chains (**C**). Adapted from (Hay 2007).

Although some substrates display SUMO-paralogue specificity, such as RanGAP1, modified solely by SUMO-1 (Saitoh & Hinchey 2000), most SUMO targets can be modified by both isoforms (Vertegaal et al. 2006), suggesting some level of redundancy of SUMO paralogues. This redundancy was also evidenced *in vivo*, where mice that lacked SUMO-1 were still viable, as SUMO-1 functions were compensated by SUMO-2/3 (Evdokimov et al. 2008)(F.-P. Zhang et al. 2008). In another study, the observation that the pool of free, non-conjugated SUMO-2/3 proteins is greater than that of free SUMO-1, together with the fact that SUMO-2/3 conjugation is enhanced by cellular stresses like acute temperature fluctuation, indicates that

SUMO-2/3 may act as a supply source of SUMO in the event of physiological stress (Saitoh & Hinchey 2000).

SUMO-1 and SUMO-2/3 also differ in their cellular distribution. While SUMO-1 has an overlapping distribution with SUMO-2 and SUMO-3 in the nucleoplasm and PML bodies, SUMO-1 localizes uniquely to the nucleolus, nuclear envelope and cytoplasmic foci (Ayaydin & Dasso 2004). During mitosis, SUMO-1 localizes to the mitotic spindle, whereas SUMO-2/3 localize to centromeres and condensed chromosomes (X.-D. Zhang et al. 2008; Ayaydin & Dasso 2004). This differential pattern of localization might explain the paralogue preference/specificity of target proteins. Notably, SUMO-1 and SUMO-2/3 conjugated proteins also have differential dynamics. The rate of conjugation/de-conjugation of SUMO-2/3 proteins is much higher than SUMO-1 conjugates (Ayaydin & Dasso 2004), in agreement with the notion that the percentage of free SUMO-2/3 is higher that the percentage of non-conjugated SUMO-1 (Saitoh & Hinchey 2000).

There is evidence pointing towards the existence of a fourth member of the SUMO family in mammals. SUMO-4 shows close similarity to SUMO-2/3, albeit with a clear amino acid distinction in position 90. Instead of a Glutamine, SUMO-4 contains a Proline in this position, which prevents the interaction with SENP proteases responsible for SUMO-4 maturation (*i.e.* exposure of the di-glycine motif). As a result, SUMO-4 isn't processed or conjugated under normal conditions, and is therefore rapidly degraded (Owerbach et al. 2005). However, under stressful conditions like starvation, SUMO-4 becomes stable and can be processed by endogenous hydrolases. Under such conditions, SUMO-4 is able to be covalently conjugated to its substrates, indicating a critical role for SUMO-4 in the regulation of stress response (Wei et al. 2008).

Additionally, a common polymorphism in SUMO-4 gene (M55V) which is associated with lower SUMO-4 activity, has also been associated with a prevalent susceptibility to type I diabetes mellitus (Bohren et al. 2004; Guo et al. 2004; Wang & She 2008; Wang et al. 2006). In contrast with other SUMO isoforms, SUMO-4 expression occurs predominantly in the kidney,

immune tissues and pancreatic islets (Bohren et al. 2004)(Wang et al. 2006). These observations suggest a role for SUMO-4 as a regulator of the immune response.

1.3.2 Mechanism of action

Sumoylation, much like the ubiquitin system, occurs as a cascade of enzymatic reactions that lead to the covalent attachment of SUMO to a target protein. The process starts with the cleavage of SUMO precursor by Sentrin/SUMO-specific proteases (SENPs), exposing a C-terminus di-glycine motif essential for its further conjugation to target proteins. After its maturation, SUMO can be activated in an ATP-dependent manner by the heterodimer SAE1/2 (SUMO-activating enzyme E1), through the formation of a thioester bond between the C-terminal glycine residue of SUMO and a cysteine residue in the active-site of SAE2. The activated SUMO is then transferred to the active-site cysteine of E2 conjugating enzyme Ubc9 (Ubiquitin conjugating 9), which catalyses the binding of SUMO to the target protein. The covalent conjugation of SUMO occurs through an isopeptide bond formed between the C-terminus glycine residue (G) of SUMO and the ε-amino group of a lysine residue (K) in the target protein. The acceptor lysines can often be found within a consensus sequence ΨKxE (where Ψ defines a large hydrophobic residue), although not all sumoylation consensus regions are sumoylated, and in some cases sumoylation can occur in non-consensus regions (Xu et al. 2008). Even though Ubc9 is able to recognize and directly bind to the sumoylation consensus motif of the target protein, *in vivo* sumoylation generally requires the presence of E3 ligases. These enzymes enhance the conjugation of SUMO to their substrates, either by promoting the direct contact of SUMO-ubc9 to the target protein, by re-orientating the acceptor lysine or by stabilizing the thioester bond between SUMO and ubc9 (Wilkinson & Henley 2010; Melchior 2003) [**Figure 1.7**].

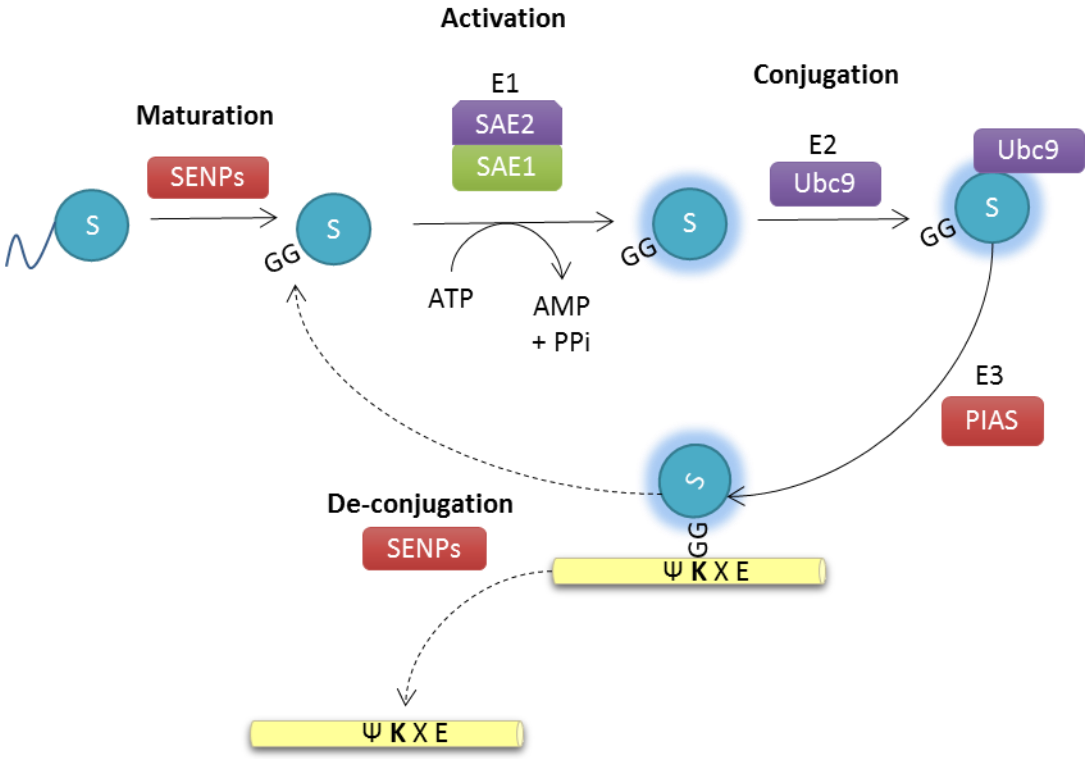

Figure 1.7. Sumoylation Pathway

Sumoylation, involves 3 steps of enzymatic reactions: Maturation of SUMO, carried out by SUMO Specific Peptidases (SENP) to expose the di-glycine motif; Activation of SUMO by the E1 SUMO activating enzyme, SAE2/1 heterodimer; and Conjugation: activated SUMO can be directly conjugated to the target protein by E2 conjugating enzyme ubc9, or a E3 SUMO ligase (such as PIAS) can facilitate the process. Sumoylation is also a reversible modification, due to the presence of SENPs, which cleave the covalent bound between the target lysine and SUMO.

1.3.2.1 SUMO E3 Ligases

The first E3 ligases to be described as being involved in SUMO modification are members of the PIAS family (protein inhibitor of activated STAT): PIAS1, PIAS3, PIASxα, PIASxβ and PIASy (Kahyo et al. 2001; Schmidt & Müller 2002; Nishida & Yasuda 2002). These proteins contain a SP (Siz/PIAS)-RING (Really Interesting New Gene) domain analogous to ubiquitin E3 ligases, and are able to bind to Ubc9, SUMO and their target proteins, thus enhancing the SUMO transfer. Another SP-RING containing E3 ligase is Nse2, a component of the SMC5/6

complex, which is involved in DNA repair and maintenance of genomic stability (Andrews et al. 2005; Potts & Yu 2005)[**Table 1.1**].

Table 1.1: SUMO E3 Ligases

SUMO E3 Ligase		Target (e.g.)	SUMO ligase Domain	Ref
PIAS Family	PIAS 1	p53, c-Jun AR, Sp3, GRIP1, CtBP1	SP-RING	(Chu & Yang 2011) (Melchior 2003).
	PIAS 3	IRF-1		
	PIASxα	AR, c-Jun, STAT1, Smad4		
	PIASxβ	p53, c-Jun, CtBP1		
	PIASγ	LEF1, Tcf-4, cMyb, C/EBPα, Smad4		
Nse2		hSMC6, TRAX	SP-RING	(Potts & Yu 2005)
MDM2		p53	?	(Chen & Chen 2003; Stindt et al. 2011)
TRIM Family	TRIM28	IRF7	TRIM motif of RING domain and B box	(Chu & Yang 2011; Liang et al. 2011; Li et al. 2014)
	PML (TRIM19)	p53, MDM2, c-Jun		
	TRIM27	MDM2		
	TRIM32	MDM2		
RanBP2		Sp100, HDAC4, PML	other	(Pichler et al. 2002; Hay 2005)
Pc2		CtBP, Dnmt3a, SIP1, HIPK2	other	(Kagey, T. A. Melhuish, et al. 2003) (B. Li et al. 2007)(Long et al. 2005)(Roscic et al. 2006).
Class II HDACs	HDAC4	MEF2, LXRα, and HIC1	other	(Ghisletti et al. 2007) (Stankovic-Valentin et al. 2007)
	HDAC7	PML		(Gao et al. 2008)
TOPORS		p53, Sin3A, Topoisomerase I	other	(Weger et al. 2005; Pungaliya et al. 2007; Hammer et al. 2007)
E1B 55-Kd		p53	other	(Muller & Dobner 2008; Pennella et al. 2010)
Fus		Ebp1	other	(Oh et al. 2010)
UHRF2		ZNF131	other	(Oh & Chung 2013).

Another group of SUMO ligases that does not contain the canonical RING type domain has been described. Within this group, the nucleoporin RanBP2 (Ran-binding protein 2) is able to catalyse the transfer of SUMO by interacting only with ubc9, and not with the target proteins (Pichler et al. 2002; Reverter & Lima 2005). Therefore, RanBP2 is very distinct from ubiquitin E3 ligases, promoting sumoylation in what seems to be a substrate-independent way (Ulrich 2009). Polycomb protein Pc2 is another SUMO ligase shown to promote the sumoylation of co-repressors CtBP (Kagey, T. a Melhuish, et al. 2003), as well as other proteins involved in chromatin regulation (Wotton & Merrill 2007). Histone Deacetylases HDAC4 (Grégoire et al. 2005) and HDAC7 (Gao et al. 2008) have also shown E3 ligase activities, independently of the lack of a RING-domain. Also the Adenovirus E1B 55-Kd protein has been observed to promote p53 sumoylation and contribute to its localization to PML nuclear bodies (Pennella et al. 2010; Muller & Dobner 2008).

The E3 ubiquitin ligase TOPORS (topoisomerase I-binding, arginine/serine-rich) was the first protein to be discovered to also function as a SUMO E3 ligase. Interestingly, the sumoylation activity of TOPORS does not depend on its N-terminal RING finger motif, despite this motif being essential for its ubiquitination activity (Weger et al. 2005). Other ubiquitin ligases were also reported to function as SUMO ligases: MDM2, is able to sumoylate p53 in conjunction with p14ARF (Chen & Chen 2003; Stindt et al. 2011); and UHRF2 acts as a SUMO ligase for ZNF131 (Zinc Finger Protein 131). Similarly to TOPORS, the SUMO ligase activity of UHRF2 does not depend on the RING domain, but rather on the presence of SET and RING finger-associated (SAR) and NLS containing Region (NCR) domains (Oh & Chung 2013). However, whether the SUMO ligase activity of MDM2 relies on its RING domain remains unclear.

More recently, a new class of proteins containing a TRIM (Tripartite motif-containing) motif have been described as novel E3 SUMO ligases (Chu & Yang 2011). TRIM proteins are characterized by having a tripartite motif composed of a RING domain, one or two B-box motifs and a coiled-coil region. Many TRIM proteins are E3 ubiquitin ligases (Meroni & Diez-Roux 2005), and some can also function as SUMO ligases (Chu & Yang 2011). Some examples are TRIM28, which stimulates IRF7 sumoylation (Liang et al. 2011); and TRIM19 (also known as PML), TRIM27 and TRIM32, all been shown to stimulate MDM2 SUMO modification (Chu & Yang 2011). In Chu and Yang's study, out of the 15 TRIM proteins (belonging to different

classes) screened, 8 were able to promote MDM2 sumoylation, showing a certain prevalence for TRIM proteins to harbour SUMO E3 ligase activity. TRIM proteins are able to bind both ubc9 and the target proteins, bridging them together, and thus enhance SUMO transfer. The SUMO ligase activity of TRIM proteins requires both RING and B-box domains, suggesting that the TRIM motif could be the first discovered canonical SUMO E3 motif (Chu & Yang 2011).

1.3.2.2 SUMO-Targeted Ubiquitin Ligases (STUbLs)

The existence of E3 ligases that can simultaneously act as both ubiquitin and SUMO ligases further reinforces the similarities between the ubiquitin and SUMO pathways. The discovery of SUMO-targeted ubiquitin ligases (STUbLs) brings these two pathways to close interplay. As described briefly before, STUbLs are characterized by having multiple SIMs, which recognize and bind to poly-sumoylated proteins and trigger their poly-ubiquitination and consequent degradation (Prudden et al. 2007). SIMs are typically short peptide sequences, comprising 3 hydrophobic amino acids (I, L or V) arranged as V/I-V/I-X-V/I/L or V/I-X-V/I-V/I (Song et al. 2004), which provide an anchorage site for SUMO to bind non-covalently to target proteins (Perry et al. 2008). STUbLs are evolutionary conserved proteins in eukaryotes. One of the first identified STUbL was the Slx8-Rfp complex in *S. pombe*. In mammals, so far, only 2 STUbLs have been identified: RNF4 (Lallemand-Breitenbach et al. 2008; Tatham et al. 2008) and RNF111/Arkadia (Poulsen et al. 2013). Yeast lacking Slx8-Rfp show an accumulation of sumoylated proteins and genomic instability (Sun et al. 2007). Despite the differences in size and structure, these phenotypes could be reversed with the expression of the human homologue RNF4, evidencing the functional conservation of STUbLs (Prudden et al. 2007).

PML was the first physiological substrate identified for RNF4 (Tatham et al. 2008; Weisshaar et al. 2008). Acute promyelocytic leukaemia (APL) occurs when PML is fused to the retinoic acid receptor α (RAR), and can be treated with arsenic, which leads to proteolytic degradation of PML. Arsenic induces poly-sumoylation of PML, which acts as a substrate for RNF4-mediated ubiquitylation and leads to PML proteasomal degradation (Tatham et al. 2008). Kinetochore protein CENP-1 seems to be regulated in a similar manner, as depletion of

RNF4 leads to accumulation of poly-SUMO2/3 CENP-1; on the other hand, depletion of SUMO-chain depolymerizing enzyme SENP6 restores CENP-1 degradation mediated by RNF4, indicating that RNF4 targets poly-sumoylated CENP-1 for degradation (Mukhopadhyay et al. 2010). Similarly, several transcription factors seem to be regulated by a poly-sumoylation and subsequent RNF4-mediated poly-ubiquitylation mechanism: Hypoxia Inducible Factor HIF2α (van Hagen et al. 2010); transcription factor PEA3 (Guo & Sharrocks 2009); and PARP-1 (poly(ADP-ribose) polymerase 1) transcriptional activity is also regulated by PIASy sumoylation and consequent poly-ubiquitylation by RNF4 (Martin et al. 2009).

Interestingly, the RNF4 and PML interaction seems to be more extensive than what is described above, as it has been recently suggested that they co-operate in the degradation of misfolded proteins (Guo et al. 2014). As a member of the TRIM family, PML has E3 SUMO ligase activity and it seems to preferentially select misfolded proteins as SUMO-targets. The accumulation of terminally misfolded proteins leads to the formation of toxic protein aggregates, linked with several neurodegenerative disorders such as Alzheimer's, Parkinson's or Huntington's disease. The pathway proposed involves selective targeting and PML-driven poly-sumoylation of misfolded proteins. The poly-SUMO2/3 chains are recognized as an anchorage site for RNF4, which catalyzes poly-ubiquitination of the misfolded proteins and leads to their consequent degradation (Guo et al. 2014; Gärtner & Muller 2014).

The other known member of STUbLs in mammals is RNF111/Arkadia (Erker et al. 2013; Poulsen et al. 2013). RNF111 has 3 functional SIMs, and similarly to RNF4, functions as a homodimer, although it cannot form heterodimers with RNF4 (Erker et al. 2013). RNF111 is able to recognize poly-SUMO-2/3 chains and promote further poly-ubiquitylation. However, while studies on RNF111-mediated degradation of sumoylated PML show an analogy with RNF4 (Erker et al. 2013), another study using Xeroderma Pigmentosum C (XPC) protein has revealed that although RNF111 is able to ubiquitylate poly-sumoylated XPC, it does not lead to its proteolytic degradation (Poulsen et al. 2013).

1.3.2.3 De-Conjugation of SUMO

Like most post-translational modifications, sumoylation is a highly dynamic process, and thus can be reversible. De-sumoylation is caused by SENPs, which, along with their participation in the maturation of SUMO, also catalyse the cleavage of the isopeptide bond between the target protein and SUMO. The SENP family includes six isoforms (SENP1-3, SENP5-7) that differ in their specificity to the SUMO isoform, cellular localization and function in either the maturation of SUMO proteins or de-sumoylation (Wilkinson & Henley 2010) [**Table 1.2**].

SENP enzymes localize mostly in the nucleus region, with SENP1 and SENP2 localizing to specific sub-nuclear structures such as nuclear pore complex and nuclear foci (Chow et al. 2014). Both contain NLS (Nuclear Localization Signal) and NES (Nuclear Export Signal), which allows them to shuttle between the nucleus and the cytoplasm and contribute to their substrate specificity (Goeres et al. 2011). SENP3 and SENP5 localize to the nucleolus (Chow et al. 2014), whereas SENP6 and SENP7 are found mostly throughout the nucleoplasm (Kolli et al. 2010).

Regarding their functional activity, SENP proteins are very different. SENP1 and SENP2 can have both de-conjugating activities and contribute to the exposure of the di-glycine motif in SUMO maturation. While they can both target SUMO-1 and SUMO-2/3 isoforms, SENP2 tends to have a preference in hydrolising SUMO-2/3 conjugates. All other SENP enzymes have preference towards de-conjugation of SUMO-2/3 isoforms. In addition to de-conjugating roles, SENP5 can also process SUMO precursors by cleaving and exposing the di-glycine motif (Kolli et al. 2010). SENP6 and SENP7 function in chain editing of SUMO-2/3 conjugates, i.e. are capable of removing SUMO moieties, without cleaving the entire SUMO chain (Hickey et al. 2012; Guo & Henley 2014).

Table 1.2: Mammalian SUMO proteases.

Adapted from (Wilkinson & Henley 2010) and (Hickey et al. 2012).

SUMO Protease	Target isoform	Function	Cellular Localization
SENP1	SUMO-1 & SUMO-2/3	Maturation, Deconjugation	Nuclear Pore and nuclear foci
SENP2	SUMO-2/3>SUMO-1	Maturation, Deconjugation	Nuclear Pore, nuclear foci and cytoplasm*
SENP3	SUMO2/3	Deconjugation	Nucleolus
SENP5	SUMO2/3	Maturation, Deconjugation	Nucleolus and mitochondria
SENP6	SUMO2/3	Deconjugation, Chain Editing	Nucleoplasm
SENP7	SUMO2/3	Deconjugation, Chain Editing	Nucleoplasm
DESI1	SUMO-1 & SUMO-2/3	Deconjugation	Cytoplasm and Nucleus
DESI2	?	?	Cytoplasm
USPL1	SUMO-2/3>SUMO-1	Deconjugation, Chain Editing	Cajal Bodies**

*SENP2 has 3 splicing variants, which localize differently in different cells, but the most common splice variant localizes in the nuclear pore.

**Cajal Bodies are subnuclear organelles involved in the metabolism of spliceosomal small nuclear ribonucleoprotein particles (snRNPs).

More recently, two additional classes of mammalian SUMO proteases were discovered: desumoylating isopeptidase (DESI) (Shin et al. 2012), which includes two members, DESI1 and DESI2; and ubiquitin-specific protease-like 1 (USPL1) (Schulz et al. 2012). DESI1 is found dispersed in the nucleus and cytoplasm and has specificity towards both SUMO-1 and SUMO-2/3. Interestingly though, DESI1 seems to specifically de-sumoylate one substrate, the transcriptional repressor BZEL (BTB-ZF protein expressed in effector lymphocytes) (Shin et al. 2012). DESI1 also displays weak chain editing activities for the same substrate. The closely related DESI2 locates in the cytoplasm but its functions as a SUMO protease remain unknown. USPL1 was identified as the latest SUMO protease and localizes to specific organelles within the nucleus denominated Cajal bodies (Schulz et al. 2012). It has

broad specificity towards SUMO isoforms, but preferentially de-sumoylates substrates conjugated to SUMO-2/3 isoforms. USPL1 has some C-terminal hydrolase activity towards SUMO precursors, although not comparable to SENP1, and is able to edit SUMO chains (Schulz et al. 2012).

Regulation of sumoylation/de-sumoylation of substrates is an important feature for cell homeostasis. The different localization of SUMO proteases to specific compartments within the nucleus suggests a role for these enzymes in the de-sumoylation of selected substrates. Moreover, the relative abundance of DESI proteins in the cytoplasm compared to SENPs, combined with the ability of some SENPs to traffic between the nucleus and the cytoplasm, may indicate a role in de-sumoylation of extra-nuclear SUMO substrates (Guo & Henley 2014).

1.3.3 Regulation of Sumoylation

A variety of stresses has been shown to modulate levels of protein sumoylation in the cell (Wilkinson & Henley 2010). Early studies on this matter show that a global increase in SUMO-2/3 (but not SUMO-1) protein conjugation occurs when mammalian cells are subject to external stresses, such as heat shock, oxidative stress, ethanol and, to a lesser extent, osmotic shock (Saitoh & Hinchey 2000). Heat shock leads to a rapid cellular increase in SUMO-2/3 conjugation of substrates involved in a variety of cellular functions, and contributes to increased cell survival (Golebiowski et al. 2009). A global decrease in SUMO conjugation was found when cells were exposed to oxidative stress with nitric oxide (NO) (Qu et al. 2007), and low to moderate doses of Hydrogen peroxide (H_2O_2) in mammalian cells (Bossis & Melchior 2006a), although high H_2O_2 dosages actually result in increased global sumoylation (Saitoh & Hinchey 2000). This can be explained by the fact that low dosages of H_2O_2 temporarily inactivate SUMO-E1 and E2 enzymes (Bossis & Melchior 2006a), and stabilize SENP3 at the same time (Yan et al. 2010), whereas higher dosages of H_2O_2 result in the inactivation of SUMO proteases (Flotho & Melchior 2013).

Sumoylation has been shown to play an important role in response to metabolic stresses such as hypoxia. Mammalian cells exposed to hypoxia showed increased levels of protein sumoylation, which correlated with a significant increase in SUMO-1 expression (Comerford et al. 2003; Shao et al. 2004). Moreover, induction of ischemia (restriction of

blood flow that causes a shortage in oxygen and glucose supply) in mice resulted in a relevant increase in overall sumoylation levels (Cimarosti et al. 2008). A rapid increase in SUMO conjugation is also visible in neurons, following hypothermic stress (Martin, K. A. Wilkinson, et al. 2007).

The response of the sumoylation machinery to genotoxic stress seems to rely more on individual substrates, rather than being a global phenomenon. For example, UV irradiation increased sumoylation of transcriptional regulator DJ1 (Shinbo et al. 2006), DNA repair protein XPC (Q.-E. Wang et al. 2005) and acetyl-transferase Tip60 (Cheng et al. 2008), but reduced the levels of hRIPβ (human RPA (replication protein A)-interacting protein β) sumoylation, also involved in DNA repair mechanisms (Park et al. 2005). Treatment with camptothecin, an anti-cancer drug that targets topoisomerase I, causes an increase in sumoylation levels of Topoisomerase I, and doxorubicin treatment leads to decreased levels of KAP-1 (kinesin-associated protein-1) sumoylation (Tempé et al. 2008).

Although many stresses seem to induce a global change in protein sumoylation, it is more likely that these changes are regulated in a substrate-specific manner, by means of interplay with other PTMs. For example, phosphorylation of substrates can either enhance or block further sumoylation. On that subject, it is worth mentioning the existence of an extended SUMO-acceptor motif – the phosphorylation-dependent sumoylation motif (PDSM) – composed of a regular SUMO consensus site followed by a proline-directed phosphorylation site (Hietakangas et al. 2006). This motif regulates phosphorylation-dependent sumoylation of multiple substrates, such as heat shock factor-1 (HSF1), or myocyte enhancer factor 2 (MEF2). This enhanced sumoylation is presumably a result of an enhanced interaction between the target and ubc9, caused by the additional negative charge of the phosphate group (Hietakangas et al. 2006). On the other hand, phosphorylation of substrates can also hinder their subsequent sumoylation. For example, KAP-1 decreased sumoylation upon doxorubicin treatment is thought to be owned to its previous phosphorylation (X. Li et al. 2007). Similarly, phosphorylation of p53 (Lin et al. 2004) and c-Fos/c-Jun (Bossis et al. 2005) result in a decrease in their sumoylation. Although the mechanism has not been unravelled yet, phosphorylation could lead to a re-localization of the protein, or physically interfere with the SUMO binding site.

Another way that substrate sumoylation could be affected by other PTMs is by competing for the same target-lysines. Acetylation, ubiquitylation and methylation all target lysines, and in some substrates they occur in the same residue as sumoylation. In MEF2A (myocyte enhancer factor 2A) and Sp3 transcription factors, co-activator p300 and tumour suppressor HIC1 (hypermethylated in cancer 1) sumoylation and acetylation compete for the same lysines and result in opposing outcomes for protein function (Bossis & Melchior 2006b). A very recent mass spectrometry approach using global human sumoylated proteome identified an extremely rich cross-talk between sumoylation and other PTMs (Hendriks et al. 2014). In this study, Hendricks and co-workers report that almost one quarter of all sumoylation sites are also targets for ubiquitylation. Acetylation and methylation cross-talk with sumoylation also occur in the same lysine for some substrates, although to a lesser extent. Furthermore, the authors identified 70 substrates with a phosphorylation site in the proximity of the SUMO consensus site, in agreement with the earlier described PDSM motif. Strikingly, acetylation sites for four SUMO substrates were found to be adjacent to the SUMO motif, constituting what could be an acetylation-dependent sumoylation motif. In accordance with this notion, one of these identified substrates was Histone H3, whose sumoylation is regulated in an acetylation-dependent manner (Hendriks et al. 2014). These results contribute to our understanding of the regulation of sumoylation, and emphasize the importance of cross-talk among several modifications to the control of protein function.

1.3.4 Effects of Protein Sumoylation

At the molecular level, the covalent attachment of SUMO alters proteins surfaces and can, therefore, lead to a change in proteome interactions. In that manner, sumoylation of target proteins can provide additional binding sites and thus increase the number of protein-protein interactions [**Figure 1.8**]. A classic example is RanGAP1 which is able to interact with RanBP2 when sumoylated (Matunis et al. 1996; Mahajan et al. 1997); also sumoylation of p300 facilitates its interaction with HDAC6 (Girdwood et al. 2003); and as mentioned before, poly-sumoylation of PML leads to the recruitment of RNF4 (Tatham et al. 2008; Weisshaar et al. 2008). The recruitment of proteins to sumoylated targets can be via the new interaction domain at the SUMO-substrate interface, or an effect of non-covalent interactions with the SUMO moiety via SIMs (Geiss-Friedlander & Melchior 2007). On the contrary, SUMO modification of substrates may conceal the binding site of certain interacting proteins, and in

that way prevent protein-protein interactions. For example, sumoylation of the transcriptional repressor ZNF76 abolishes its interaction with TATA-binding protein (TBP) and relieves its repressive activity (Zheng & Yang 2004). Similarly, sumoylation of ubiquitin conjugating enzyme E2-25K interferes with its interaction with E1 ubiquitin enzyme (Pichler et al. 2005).

Additionally, sumoylation of substrates may result in a consequent conformational change of the protein, creating new binding sites for protein interactions. A well-documented example is covalent modification of Thymine DNA Glycosylase (TDG) with SUMO-1, which causes a conformational change in TGD and leads to its release from the DNA (Hardeland et al. 2002). The change in conformation is due to non-covalent interactions of the SUMO moiety with a nearby SIM (Baba et al. 2005).

As is the case with other modifications, sumoylation also interferes with other PTMs, and hence affect protein localization, stability and enzymatic activity (Wilkinson & Henley 2010; Geiss-Friedlander & Melchior 2007)[**Figure 1.8**]. Ubiquitylation and sumoylation were first described as antagonistic modifications in the NFκB (nuclear factor κB) regulator IκBα (Desterro et al. 1998). Both modifications occur on the same lysine residue and the observation that sumoylated IκBα is protected from proteasomal degradation led to the conclusion that ubiquitylation and sumoylation compete for the same lysine, although competition occurs rather in a phosphorylation-dependent way, as ubiquitylation occurs following phosphorylation of a nearby serine residue (Desterro et al. 1998). Conversely, sumoylation can lead to the subsequent ubiquitylation of substrates. NEMO (NF-κB essential modulator) is sumoylated at two C-terminal lysines. This event results in the accumulation of the protein in the nucleus and promotes phosphorylation-dependent ubiquitylation of the same lysine residues. Ubiquitylation of NEMO leads to its nuclear export and activation of the NF-κB survival pathway (Huang et al. 2003). Another example of cooperation between SUMO and ubiquitin pathways are the recently described STUbLs, which connect the ubiquitin and SUMO in targeted proteasomal degradation (Sriramachandran & Dohmen 2014).

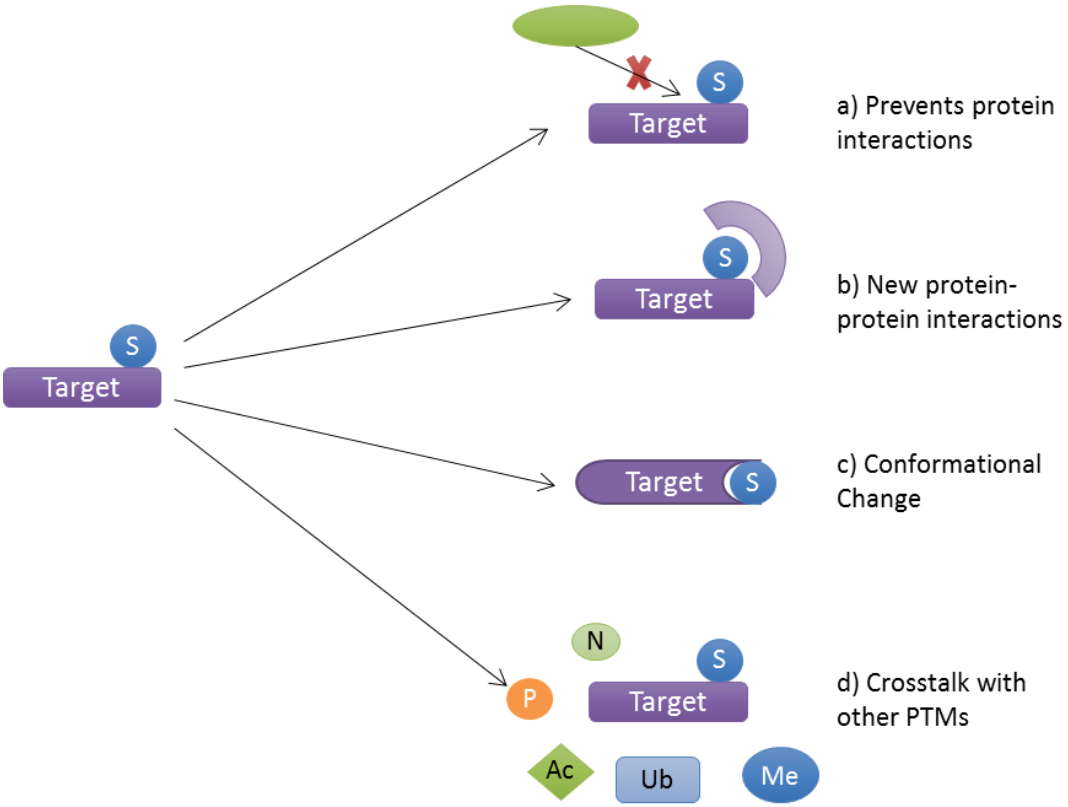

Figure 1.8. Effects of Protein Sumoylation.

Sumoylation of target proteins can prevent the binding of interacting proteins due to the occlusion of a binding site (a), or provide a new recruitment site for novel interactions (b). SUMO modification can also lead to changes in protein conformation (c). Finally, sumoylation can interfere with other PTMs, altering protein function (d).

1.3.5 Physiological Relevance of Protein Sumoylation

The process of sumoylation/de-sumoylation of substrates is crucial for normal cell physiology. Studies in mice show that de-regulation of the sumoylation machinery causes developmental defects in embryos (Kim & Baek 2009; Bawa-Khalfe & Yeh 2010). Depletion of ubc9 conjugating enzyme in knockout mice leads to early embryonic lethality, with blastocysts presenting abnormalities in nuclear architecture and severe defects in chromosome segregation (Nacerddine et al. 2005). SUMO-1 knockout mice seem to have controversial phenotypes: while the first knockout mice generated displayed cleft palate defects and increased rates of late embryonic and early postnatal death (Alkuraya et al. 2006), two other SUMO-1 knockout mice exhibited apparent normal phenotypes, suggesting that loss of SUMO-1 could be compensated by SUMO-2/3 (F.-P. Zhang et al. 2008; Evdokimov et al. 2008). A closer look at these mice, however, revealed congenital heart defects (Wang et al. 2011), irregular adipogenesis and differences in body weight (Mikkonen et al. 2013), indicating paralogue-specific functions of SUMO-1 that could not be compensated by other isoforms.

Knockout of SENP enzymes also results in drastic consequences. SENP1-depleted mice displayed severe foetal anaemia and mid-gestational embryonic lethality (Cheng et al. 2007; Yamaguchi et al. 2005). Moreover, studies in MEFs lacking SENP1 show increased sumoylation of hypoxia-inducible factor 1α (HIF1α), resulting in the down-regulation of hypoxia-induced genes, and HIF1α ubiquitylation and proteasomal degradation (Cheng et al. 2007). Depletion of SENP2 in MEFs results in cell cycle arrest in G1 (Chiu et al. 2008) and increased sumoylation of Polycomb group protein (PcG), resulting in chromatin remodelling and gene silencing (Kang et al. 2010). These observations clearly demonstrate the major role of the sumoylation machinery components to maintain cell homeostasis.

1.3.5.1 Cancer

Under normal physiological conditions, the dynamic nature of sumoylation only permits a small fraction of substrates to be SUMO modified. The maintenance of this balance is achieved with a tight regulation of the sumoylation components. In hepatocellular carcinomas, high levels of SUMO-activating enzyme SAE2/1 are associated with poor survival rates (Lee & Thorgeirsson 2004), and a recent high-throughput RNA interference screening revealed SAE2/1 to be a Myc-synthetic lethal gene, and to contribute to Myc-dependent

oncogenesis (Kessler et al. 2012). Ubc9 overexpression is associated with ovarian tumours (Mo et al. 2005), lung adenocarcinoma (McDoniels-Silvers et al. 2002) and prostate adenocarcinoma (Kim et al. 2006), and ubc9 polymorphisms are associated with tumour grade in breast carcinomas (Dünnebier et al. 2009). Increased expression of SUMO E3 ligase PIAS3 has been detected in a variety of cancers, including lung, breast, prostate, colon-rectum, and brain tumours (Wang & Banerjee 2004). The expression of SUMO proteases, in particular SENPs, has been shown to be de-regulated in several cancers. SENP1 and SENP3 overexpression appears to contribute to prostate cancer development, whereas SENP6 down-regulation seem to influence ovarian cancer development (Bawa-Khalfe & Yeh 2010).

Although the de-regulation of the sumoylation machinery has general effects in the organism, it is at the level of individual substrates that SUMO exerts its role. For example, the introduction of a mutation in the SUMO-accepting site of Sp3 transcription factor leads to dramatic chromatin remodelling, accompanied by silencing of spermatocyte-specific and neuronal genes (Stielow, Sapetschnig, Kru, et al. 2008). Also, knock-in mice expressing sumoylation-deficient of steroidogenic factor 1 (SF-1) displayed severe endocrine abnormalities resultant from ectopic hedgehog signaling (Lee et al. 2011).

Two recent studies have identified a germ-line mutation in the MITF (microphthalmia-associated transcription factor) transcription factor that is associated with predisposition of fair-skinned individuals to familial and sporadic melanoma and renal carcinoma (Yokoyama et al. 2011; Bertolotto et al. 2011). The mutation impairs sumoylation of MITF and affects its transcriptional activity, leading to increased cell growth, proliferation, and inflammation and contributing to oncogenesis.

In a more general way, SUMO has been shown to modify many proteins involved in cell signalling pathways including Wnt (Mabb & Miyamoto 2007), NFκB (Mabb & Miyamoto 2007) and steroid hormone receptor pathways (Faus & Haendler 2006), thus contributing significantly to carcinogenesis. Moreover, SUMO modification even occurs in cell surface receptors, e.g. Insulin-like growth factor 1 receptor IGF-1R (Sehat et al. 2010), type I TGFβ receptor (Kang et al. 2008), Reptin and Pontin (Kim et al. 2006), signifying the involvement of sumoylation in signalling pathways is not restricted to downstream proteins. Adding to that, many tumour suppressor proteins are known to be covalently modified by SUMO, including

p53 and family members p63 and p73, pRB (retinoblastoma protein), as well as oncoproteins c-Myb (myeloblastosis), Mdm2 and others (Sarge & Park-Sarge 2011). Lastly, SUMO has been identified as an important modification for DNA repair systems, such as Nucleotide Excision Repair (NER) and homologous recombination, implicating sumoylation as a crucial regulator of genome integrity and stability (Bartek & Hodny 2010; Silver et al. 2011).

1.4 p53 Sumoylation

The history of p53 sumoylation started over 15 years ago, when Gostissa and colleagues reported the attachment of SUMO-1 to one single lysine residue (K386) in the C-terminal regulatory domain of p53 (Gostissa et al. 1999). However, despite years of research, the effect that sumoylation has on p53 has been a matter of controversy. As many SUMO targets are transcription factors, and this modification occurs mainly in inhibitory or regulatory motifs of these proteins, sumoylation was mostly regarded as having an inhibitory function on transcriptional regulation (Stehmeier & Muller 2009; Gill 2005). Yet, the first studies reported that overexpression of both SUMO-1 and p53 led to an enhanced ability of p53 to activate transcription of a PG13 reporter, suggesting that p53 sumoylation results in increased transcriptional activity of p53 (Gostissa et al. 1999; Rodriguez et al. 1999). Although both studies presented similar conclusions, in one of them the sumoylation-deficient mutant shows a higher transcriptional ability than the WT p53 (Rodriguez et al. 1999), suggesting that disruption of sumoylation at this site might contribute to enhanced p53 transactivation.

Adding to the controversy, a later study using reporter assays on the p53 target-gene p21, showed that sumoylation had no effect on p53 transcriptional activity, as well as no co-relation between p53 localization and its sumoylation status (Kwek et al. 2001). However, another report observed a slight decrease in p53 apoptotic activity in the sumoylation-impaired mutant K386R, when compared to the WT p53, indicating that sumoylation might be important for the full activity of p53 (Müller et al. 2000). Moreover, another gene-reporter assay showed that over-expression of PIAS family of E3 ligases (PIAS1 and PIASxβ) lead to a decrease in p53-dependent transcriptional activity (Schmidt & Müller 2002). Nevertheless, this decrease was also visible when the sumoylation deficient mutant (K386R) was used, indicating that this effect was not sumoylation-dependent. In contrast, Megidish and colleagues demonstrated that ectopic expression of PIAS1 resulted in p53-mediated activation, in particular of p21, and a consequent G1 arrest, although this effect was independent of PIAS1 RING domain (Megidish et al. 2002). In another study, over-expression of PIASγ led to a decrease in DNA-binding activity of p53, accompanied by a reduction of p53-mediated expression of target genes p21 and BAX, but did not interfere with the apoptotic programme (Nelson et al. 2001). Conversely, a different report showed an up-regulation of p53-target

gene p21 upon PIASγ overexpression in human fibroblasts, accompanied by premature senescence. The authors suggested that PIASγ-mediated sumoylation leads to the activation of p53 and Rb to promote the induction of senescence (Bischof et al. 2006).

MDM2 is another E3 ligase reported to promote p53 sumoylation and modulate its transcriptional activity. MDM2 overexpression correlated with an increased sumoylation of p53, which was further stimulated by the ectopic expression of ARF (Chen & Chen 2003). Interestingly, the induction of sumoylation by MDM2 also correlated with p53 localization to the nucleolus, which led to the conclusion that MDM2-ARF complex targets p53 to the nucleolus where the recruitment of sumoylation co-factor stimulates its sumoylation (Chen & Chen 2003). In contrast, although sumoylation has been implicated in protein subcellular localization, MDM2 was shown to be involved in nuclear export of several proteins, by triggering their mono-ubiquitination. In regards to p53, it has been reported that its mono-ubiquitination by MDM2 directly promoted the interaction between p53 and PIASγ, inducing p53 sumoylation and nuclear export (Carter et al. 2007). In fact, abolishment of p53 sumoylation site led to a decrease in its cytoplasmic accumulation and it has been proposed that sumoylation, triggered primarily by mono-ubiquitination, may unmask the NES (Nuclear Export Signal) of p53, and promote its export from the nucleus (Carter et al. 2007). Consistent with this, a later study using a fused p53-SUMO-1 protein showed a distinct localization pattern when compared to p53 alone, with the fused protein partially localizing to the cytoplasm and nuclear envelope (Carter & Vousden 2008). Furthermore, a recent study shows that sumoylation of p53 mediates its nuclear export not by exposure of NES, but rather by its interaction with nuclear export receptor CRM1 (Chromosomal region maintenance 1) (Santiago et al. 2013). The authors propose that nuclear p53 binds CRM1 which targets proteins to the nuclear pore complex. Its further sumoylation then promotes p53 dissociation from the CRM1 complex and its release to the cytoplasm.

As p53 exerts its functions mainly as a transcription factor, it is found in high concentrations within the nucleus. Here, a sub-fraction of p53 resides in multi-protein structures named PML-NBs (Promyelocytic Leukaemia Protein Nuclear Bodies). The PML protein is the key organizer of these structures, and PML modification by SUMO-1 is essential for the formation of PML nuclear bodies (Müller et al. 1998). PML-NBs are small spherical structures associated with the nuclear matrix, which seem to recruit several unrelated

proteins which only common feature seems to be their ability to be sumoylated or harbour a SIM domain (Lallemand-Breitenbach & de Thé 2010). Strikingly, the fused p53-SUMO-1 construct used in Carter and Vousden's study did not co-localize with PML (Carter & Vousden 2008). On the contrary, overexpression of the adenovirus E1B 55-Kilodalton protein induced SUMO-1 modification of p53, leading to the repression of its transcriptional activities via its sequestration to PML-NBs and subsequent nuclear export (Muller & Dobner 2008; Pennella et al. 2010). Similarly, in *Drosophila melanogaster* p53 sumoylation has been shown to be critical for both its transactivation and apoptotic functions, and to promote p53 localization to nuclear structures that can be marked for human PML (Mauri et al. 2008). These observations provide some circumstantial evidence of the involvement of SUMO modification in the trafficking of p53 within the cell and its localization to specialized structures, which directly affect its transcriptional functions.

Despite the similarities between the ubiquitin and SUMO system, it is largely accepted that sumoylation is not involved in mediating proteins for proteolytic degradation. Quite the opposite, it has been proposed that SUMO can in fact prevent protein degradation by competing with ubiquitin for the same lysine residues, and thus acting as a shield for their ubiquitination (Anckar & Sistonen 2007). More recently, however, the discovery of STUbLs (E3 ligases that recognize sumoylated substrates and promote their ubiquitylation) has challenged this concept, re-connecting the SUMO and ubiquitin pathways (see section **1.3.2.2**). In the case of p53, very few data showed a convincing correlation between the conjugation of SUMO and p53's protein stability. Overexpression of E3 ligase TOPORS enhanced SUMO-1 conjugation of p53, which was accompanied by an increase in protein stabilization (Weger et al. 2005). A previous study has also shown that overexpression of TOPORS in mice led to increased p53 stability and transactivation activity (Lin et al. 2005). Interestingly, the SUMO E3 ligase activity of TOPORS does not depend on its RING domain, indicating that the sumoylating and ubiquitylating activities of TOPORS are distinct features (Weger et al. 2005). Moreover, TOPORS phosphorylation by Plk1 (Polo-like kinase 1) promotes its SUMO vs ubiquitin ligase activity, whereby phosphorylation inhibits TOPORS-mediated sumoylation of p53, promoting instead p53 ubiquitylation (Yang et al. 2009). A recent study demonstrated that in response to stress, PACT-PKR (activator of PKR) signalling may regulate p53 stability through a mechanism

dependent on its sumoylation (Bennett et al. 2012). PKR is a Ser/Thr kinase activated in response to stress. The authors observed that the activation of this signalling pathway stimulates p53 sumoylation and phosphorylation of S392, resulting in increased p53 stability (Bennett et al. 2012).

Other roles have been assigned regarding the sumoylation status of p53. It has been proposed that p53 sumoylation is involved in p53-mediated autophagy, via the collaborative effect of PIASγ-mediated K386 sumoylation and Tip60 acetylation of K120 (Naidu et al. 2012). Additionally, p53 sumoylation has been linked with interferon activities, as SUMO modification of p53 occurs in response to type I interferon (IFN) signalling, resulting in the activation of a cellular senescence program, and thus contributing to the antiviral functions of interferon (Marcos-Villar et al. 2013).

Despite intensive research and a large number of publication on this matter, it seems that the role of SUMO in the modulation of p53 functions remains elusive. Perhaps one possible explanation is the minute fraction of SUMO-modified p53 that occurs in the cell (normally less than 5%) when compared to the total population of endogenous p53 (Wu & Chiang 2009b). This discrepancy is attributed to the presence of SUMO proteases, which quickly cleave the covalent bond between SUMO and p53. Additionally, the restricted localization of the sumoylation machinery within the nucleus restrains the sumoylation process to this organelle (Chen & Chen 2003). The low abundancy of sumoylated substrates limits the functional analysis of the role of sumoylation in protein stability, activity and localization. In addition, most of the first studies regarding p53 sumoylation assessed its role in p53 transcriptional activity using artificial reporter systems, which many times do not reflect the real expression of endogenous target-genes.

More recently, sumoylation of p53 has been linked with the inhibition of p53-dependent transcription. Utilizing an ACF (ATP-utilizing chromatin assembly and remodelling factor) based chromatinized template transcription system, Wu and Chiang demonstrate that p53 sumoylation impairs p53's DNA-binding ability, by disrupting its subsequent acetylation by p300 (Wu & Chiang 2009a). Importantly, sumoylated p53 does not lose the capacity to

interact with p300, indicating that SUMO likely prevents p300 to access adjacent lysines in the C-terminal domain. Moreover, the authors show that SUMO modification of DNA-bound p53 triggers the recruitment of transcriptional co-repressors *in vitro*, confirming the role of p53's sumoylation as a negative regulator of transcription activity (Wu & Chiang 2009a; Wu & Chiang 2009b). The picture is further complicated when a later study reported that SUMO-1 could be itself acetylated in its N-terminus, and its acetylation status can modulate p53 activity (Cheema et al. 2010). Indeed, the authors demonstrate that acetylated SUMO-1 conjugated to p53 is unable to activate the expression of the p21 reporter gene, in agreement with the previous findings of Wu and Chiang. Likewise, a SUMO mutant lacking the N-terminal domain but containing the SUMO acetylation domain (SAD) revealed the same result when conjugated to p53. On the other hand, SUMO-1 conjugation to p53 in its non-acetylated form resulted in the activation of the p21 reporter gene. Additionally, sumoylated p53 can result in different physiological responses, depending on the acetylation status of SUMO-1. If acetylated, SUMO-1 conjugation promotes apoptosis, whilst non-acetylable form favours cell-cycle arrest (Cheema et al. 2010).

p53 sumoylation by SUMO-2/3 isoforms was recently described to be enhanced by MDM2 (Stindt et al. 2011). Yet, unlike the previously described model for SUMO-1 modification involving MDM2-ARF complex (Chen & Chen 2003), p53 modification by SUMO-2/3 does not require its nucleolar localization. Further, MDM2 interaction with p53 is essential for MDM2-mediated sumoylation, although the RING domain of MDM2 is dispensable. This report revealed that SUMO-2/3 modification also affects p53 transcriptional activity, leading to the inactivation of p53-mediated transcription of both p53-activated and repressed genes (Stindt et al. 2011).

Overall, sumoylation seems to play an important part in the regulation of many features of p53 regulation. Therefore, the comprehension of this modification and particularly how it affects the transcriptional activity of the tumour suppressor p53 could present a valuable tool in the search to unravel the post-translational code that determines p53 response.

1.5 Research Aims

p53 is a key player in the prevention of tumour formation and growth. Being able to activate numerous metabolic pathways to prevent the spread of tumourigenic cells, the activity of p53 has to be well regulated. Disastrous consequences can derive from its de-regulation, such as apoptosis of healthy cells or tumour progression. One way to keep controlled levels of p53's activity is through post-translational modifications. While some PTMs are well-studied and their roles well-defined, the effect of Small Ubiquitin Modifier proteins on p53 remains somewhat controversial.

The investigation carried out here was directed towards the understanding of how sumoylation affects the functions of the tumour suppressor of p53. Sumoylation of other transcription factors as been proposed to alter the network of protein-interactions, either by promoting novel interactions or abolishing existing ones. As such, the starting point for this investigation was to evaluate changes in the interacting partners of p53, in the context of its sumoylation status.

In brief, the specific objectives of this work were:

- To identify putative interacting proteins of p53-SUMO-1 *in vitro* and to confirm these interactions *in vivo*;
- To characterize the effect of SUMO in p53's transcription activity;
- To explore how sumoylation may interact with other post-translational modifications and thus influence p53 response;
- To investigate the role of p53 sumoylation in the cellular localization of p53.

CHAPTER 2

Materials and Methods

Chapter 2. Materials and Methods

2.1 Molecular Biology Techniques

2.1.1 Plasmid Construction

Plasmids to be used *in vitro* and *in vivo* experiments were generated by molecular cloning and/or site-directed mutagenesis, using the primers specified in **Table 2.1**. **Table 2.2** summarizes the plasmids constructed by myself and other members of the lab (some in collaboration with PROTEX), or kindly given by collaborators.

2.1.1.1 Molecular Cloning

Molecular cloning was used to construct plasmids able to be expressed in either bacteria or mammalian cell lines. For the construction of GST-p53-ubc9 plasmids, p53-ubc9 (WT and K386R) were amplified by Polymerase Chain Reaction (PCR) with primers flanked with restriction sites for BamHI and XbaI. The insert products were digested with BamHI and XbaI, along with the backbone vector pGEX-5x-3. Inserts and vector were then ligated, resulting in bacterial expression vectors GST-p53-ubc9. For TEV cleavage site insertion to create p53-TEV-ubc9 constructs for mammalian expression, ubc9 was amplified with two sets of primers which included a TEV recognition site flanked by EcoRI site on the 5' and XbaI site on 3'. pcDNA3-p53-ubc9 plasmids, kindly given by Dr. Niedenthal, contain an EcoRI site between p53 and ubc9 (Jakobs et al. 2007). The plasmids and PCR products were then digested with EcoRI and XbaI, and then ligated to form p53-TEV-ubc9 constructs. TEV protease was cloned into pCMV2 plasmid within SalI and XbaI restriction sites. Cloning of pLEISC plasmids was conducted by PROTEX facility, and the backbones can be found in **Appendix A**.

2.1.1.2 Site-Directed mutagenesis

Site-directed mutagenesis was used to construct the mutant $p53_{K386R}$ and p53 proteins which lacked the oligomerization domain of p53, GST-$p53_{WT}$Δ324-355/GST-$p53_{K386R}$Δ324-355. Site-directed mutagenesis was performed using the primers specified on **Table 2.1** in a PCR reaction utilizing Pfu Turbo (Agilent Technologies), according to the manufactor's instructions.

Table 2.1: List of primers used for Cloning and Site-directed mutagenesis.

Primer name	Primer sequence 5'-3'
F-pLEISC01-SUMO-1-GG	TAC TTC CAA TCC ATG ATG TCT GAC CAG GAG GCA
R-pLEISC01-SUMO-1-GG	TAT CCA CCT TTA CTG TCA TCA ACC CCC CGT TTG TTC CTG ATA
F-pLEISC01-SUMO-2-GG	TAC TTC CAA TCC ATG GCC GAC GAA AAG CCC AA
R-pLEISC01-SUMO-2-GG	TAT CCA CCT TTA CTG TCA ACC TCC CGT CTG CTG
F-pLEIS01-ubc9	TAC TTC CAA TCC ATG ATG TCG GGG ATC GCC CTC AG
R-pLEIS01-ubc9	TAT CCA CCT TTA CTG TCA TTA TGA GGG GGC AAA CT
F-pLEISC12-SUMO-1	GTA TTT TCA GGG CGC CAT GTC TGA CCA GGA
R-pLEISC12-SUMO-1	GAC GGA GCT CGA ATT TCA AAC TGT TGA ATG ACC C
F-pLEISC12-SUMO-2	GTA TTT TCA GGG CGC CAT GGC CGA CGA AAA G
R-pLEISC12-SUMO-2	GAC GGA GCT CGA ATT TCA GTA GAC ACC TCC CGT CT
F-pGEX-5x-3-p53	GGT CGT GGG ATC CCC ATG GAG GAG CCG CAG T
R-pGEX-5x-3-p53	CCG GGA ATT CCT TCA GTC TGA GTC AGG CCC T
F-p53$_{K386R}$	AAA AAA CTC ATG TTC AGG ACA GAA GGG CCT GAC
R-p53$_{K386R}$	GTC AGG CCC TTC TGT CCT GAA CAT GAG TTT TTT
F-p53Δ 324-355	AAG AAG AAA CCA CTG GGG AAG GAG CCA GGG GG
R-p53Δ 324-355	CCC CCT GGC TCC TTC CCC AGT GGT TTC TTC TT
F1-TEV-ubc9	GAA AAC CTG TAT TTT CAG GGC ATG TCG GGG A
F2-EcoRI-TEV-ubc9	GAG AAT TCG AAA ACC TGT ATT TTC AGG GCG GCT
R-XbaI-TEV-ubc9	CAT CTA GAT TAT GAG GGG GCA AAC TTC TTC G
F-pFLAG-TEV	ACG CGT CGA CAT GGG AGA AAG CTT GTT TAA GGG A
R-pFLAG-TEV	TCT AGA CGA TTC GGG ACG GCG ACG ACG ATT CAT

Table 2.2: List of Plasmids generated by molecular cloning.

Vector name	Application	Tag	Source
GST-p53$_{WT}$	Bacterial Expression	GST	Dr Barlev's lab
GST-p53$_{K386R}$	Bacterial Expression	GST	Dr Barlev's lab
GST-p53$_{WT}$300-393	Bacterial Expression	GST	Dr Barlev's lab
GST-p53$_{K386R}$300-393	Bacterial Expression	GST	Dr Barlev's lab
GST- p53$_{WT}$-ubc9	Bacterial Expression	GST	Dr Barlev's lab
GST - p53$_{K386R}$-ubc9	Bacterial Expression	GST	Dr Barlev's lab
GST - p53Δ 324-355	Bacterial Expression	GST	Dr Barlev's lab
GST - p53$_{K386R}$Δ 324-355	Bacterial Expression	GST	Dr Barlev's lab
pLEISC01-Ubc9	Bacterial Expression	6-HIS	Dr Barlev's lab /PROTEX
pLEISC01-SUMO-1	Bacterial Expression	6-HIS	Dr Barlev's lab /PROTEX
pLEISC01-SUMO-2	Bacterial Expression	6-HIS	Dr Barlev's lab /PROTEX
pcDNA3-p53$_{K386R}$	Mammalian Expression	Na	Dr Barlev's lab
pLEICS12-Sumo-1	Mammalian Expression	FLAG	Dr Barlev's lab /PROTEX
pLEICS12-Sumo-2	Mammalian Expression	FLAG	Dr Barlev's lab /PROTEX
pcDNA3-p53$_{WT}$-TEV-ubc9	Mammalian Expression	Na	Dr Barlev's lab
pcDNA3-p53$_{K386R}$-TEV-ubc9	Mammalian Expression	Na	Dr Barlev's lab
pCMV2-FLAG-TEVpro	Mammalian Expression	FLAG	Dr. Xiaowen Yang

Na: not applicable

2.1.2 Generation of competent bacteria

A small amount of *Escherichia coli* (*E.coli*) Top10 and BL21 Rosetta strains (2µL) was inoculated in 4mL of LB (Luria broth) without antibiotics, and left shaking at 200rpm for 16h at 37°C. The next day, 1mL of the culture was diluted in 100mL of LB (without antibiotic) and grown at 37°C until OD_{600} reached 0.4. The culture was pelleted by centrifugation, and the pellet was resuspended in cold TFB I buffer (30mM KOAc, 50mM $MnCl_2$, 100mM RbCl,10mM $CaCl_2$, 15% glycerol, adjusted to pH 5.8). After an incubation of 20min on ice, the cells were again centrifuged and the pellet was resuspended in 4mL of pre-chilled TFB II buffer (10mM NaMOPS pH 7.0, 7.5mM $CaCl_2$, 10mM RbCl, 15% glycerol, adjusted to pH 7.0). After an incubation of 30min on ice, cells were aliquoted in sterile microtubes, and snap frozen in liquid nitrogen. Competent cells were kept at -80°C until use [**Table 2.3**].

Table 2.3. *E.coli* strains used for plasmid propagation

***E. coli* strain**	**Genotype**
Top 10	F- mcrA Δ(mrr-hsdRMS-mcrBC) ϕ80lacZΔM15 ΔlacX74 nupG recA1 araD139 Δ(ara-leu)7697 galE15 galK16 rpsL(Str^R) endA1 λ^-
BL21 Rosetta	F^- *ompT hsdS*$_B$(r_B^- m_B^-) *gal dcm* pRARE (Cam^R)

2.1.3 Plasmid Preparation

The plasmids used for transfections in mammalian cells were produced in Top 10 competent bacterial cells. Top 10 *E. coli* strain is ideal for high-efficiency cloning and plasmid propagation, allowing the efficient transformation of unmethylated DNA from PCR amplifications. Upon transformation, a single colony was picked from the plate and inoculated in 5mL of LB broth supplemented with 100µg/ml of Ampicillin at 37°C. 8h after inoculation, the bacterial culture was diluted in 100mL of LB broth containing 100µg/ml of Ampicillin and left to grow for 16h at 37°C. The bacterial cells were pelleted and plasmid DNA was purified using Plasmid Midi kit (Qiagen), according to manufacturer's instructions. The plasmid DNA was resuspended in 100µL of Tris-HCl pH 8.5 buffer, and kept at -20°C until use.

2.2 Analysis of Recombinant Proteins

2.2.1 Bacterial Expression and Protein Purification

All recombinant proteins were purified from *E. coli* BL21 Rosetta strain [**Table 2.4**]. This strain designed to enhance the expression of eukaryotic proteins that contain codons rarely used in *E. coli*. Following transformation with plasmids containing GST-tagged or 6his-tagged proteins, 1L of each bacterial culture was grown at 17°C overnight, and induced by the addition of 0.2mM IPTG when OD was approximately 0.4.

For the purification of GST-tagged proteins, 30mL of sonication supernatant from bacterial strain harbouring GST-tagged proteins was incubated for 1h at 4°C with 0.2 mL of glutathione sepharose beads, previously washed with PBS with 0.1% Triton X-100 and 1mM PMSF. After incubation, the beads were washed again three times with the same solution, and the bound proteins were eluted from the beads by incubation with elution buffer pH 7.5 containing 100mM glutathione, 100mM Tris-HCl pH 8.8, 150mM NaCl, 0.2% Triton X-100 and 1 mM PMSF for 30min at 4°C. Sequential elutions were made, decreasing the times of incubation to 20 and 10min, respectively.

For the purification of hexahistidine-tagged protein SUMO-1, bacterial culture containing recombinant 6his-tagged proteins was grown as mentioned before, and 30 ml of sonication supernatant with increased concentration of salt (300mM NaCl) and 10mM Imidazole were incubated with 0.2 ml of Ni^{2+}-NTA agarose beads (Qiagen) at 4°C overnight. The beads were then washed three times with PBS with 0.2% Triton, 500mM NaCl, 20mM Imidazole and 1mM PMSF. To elute the bound protein, beads were incubated with 100mM imidazole-containing buffer for 30min at 4°C. Two additional elutions were performed increasing the concentration of imidazole to 200 and 400mM, respectively.

2.2.2 Column chromatography

Following purification, *in vitro* recombinant proteins were loaded on BioRad Econo-Pac 10DG Desalting Columns, in order to exclude glutathione and exchange the buffer for one containing 20mM Tris pH 8.0, 50mM NaCl, 10% glycerol and 1mM PMSF. Several fractions were collected and analysed by Bradford assay, and the ones containing a higher amount of protein were aliquoted and stored at -80C for later use in *in vitro* assays.

Table 2.4: Recombinant proteins purified to use in *in vitro* assays

Recombinant Proteins	Tag	Cleavage site
GST-p53$_{WT}$	GST	TEV
GST-p53$_{K386R}$	GST	TEV
GST-p53$_{WT}$300-393	GST	TEV
GST-p53$_{K386R}$300-393	GST	TEV
GST- p53$_{WT}$-ubc9	GST	TEV
GST - p53$_{K386R}$-ubc9	GST	TEV
GST - p53$_{WT}$ Δ324-355	GST	TEV
GST - p53$_{K386R}$ Δ324-355	GST	TEV
GST-Set9	GST	n/a
GST-MDM2	GST	n/a
6His-ubc9	6His	TEV
6His-SUMO-1	6His	TEV
6His-SUMO-2	6His	TEV
6His-UbcH5c	6His	n/a
GST-SAE2/1	GST	Thrombin

2.2.3 *In vitro* Sumoylation Assay

The sumoylation reactions were performed in a volume of 20 µL, containing 1µg of GST-p53-ubc9/GST-p53/GST-p53$_{300-393}$ (WT or K386R), 2µg of 6His-SUMO-1, 0.4µg of SAE1/SAE2, 5mM Mg-ATP, and SUMO-buffer containing 1M of Tris-HCl pH 7.5 and 100mM of $MgCl_2$, were incubated at 30°C for 1h. The reaction was stopped by the addition of 7µL of 4x Protein Loading buffer (250mM Tris-Cl pH 6.8, 8% SDS, 40% glycerol, 0.02% Bromophenol and 8% of β-mercaptoethanol) and boiled at 95°C for 5 min. The products were either immediately run in SDS polyacrylamide gel electrophoresis, or kept at 4°C.

2.2.4 Incubation of Nuclear Extract proteins with p53-SUMO

For the incubation of sumoylated p53 with the H1299 nuclear extract proteins, a large-scale sumoylation reaction (400µL, equivalent to 20x 20µL reaction) using 20µg of GST-p53$_{WT}$-ubc9 or GST-p53$_{K386R}$-ubc9, 40 µg of 6his-SUMO-1, 8µg of SAE1/SAE2, 5mM Mg-ATP, and SUMO-buffer containing 1M of Tris-HCl pH 7.5 and 100mM of $MgCl_2$, was performed in the same conditions as before (1hour at 30°C). Both sumoylation reactions were then incubated with 20µL of glutathione sepharose beads for 1h at 4°C. An additional negative control containing 10µg of GST-p53$_{WT}$-ubc9 that was not subject to prior sumoylation was also incubated with 20µL of glutathione sepharose beads for 1h at 4°C.

1mg of nuclear protein extract was split equally into three tubes and incubated with either sumoylation reactions (GST-$p53_{WT}$-ubc9 or GST-$p53_{K386R}$-ubc9), or non-sumoylated GST-$p53_{WT}$-ubc9, with 1mM PMSF, 1% protease inhibitors and 20mM of NEM for 3h at 4°C. The reactions were washed once with PBS with 0.1% Triton X-100 and 1mM PMSF, and proteins were eluted from the beads by incubation with elution buffer pH 7.5 containing 100mM glutathione, 100mM Tris-HCl pH8.8, 150mM NaCl, 0.2% Triton X-100 and 1 mM PMSF for 30min at 4°C. The products were boiled with 4x Laemmli's loading buffer (250mM Tris-HCl pH 6.8, 8% SDS, 40% glycerol, 8% β-mercaptoethanol, 0.02% bromophenol) and resolved in SDS polyacrylamide gel electrophoresis. Proteins in the gel were stained with SYPRO Ruby Protein Gel Stain (Bio-Rad) and visualized under UV light.

2.2.5 Mass Spectrometry (MS) analysis

The proteins of interest were cut from a SDS-PAGE gel stained with SYPRO Ruby protein stain, and placed in fresh eppendorfs. The analysis was performed by PNACL Proteomics facility, utilizing in-gel trypsin digestion and Liquid Chromatography-MS/MS (LTQ-Orbitrap-Velos-ETD-SN03106B). The database search algorithm used was Mascot v2.2.04, MS/MS Ion Search.

2.2.6 *In vitro* Sumoylation-Methylation Assays

To assess the mutual effect of p53 sumoylation on K372 methylation of p53, *in vitro* methylation reactions were performed prior, after or simultaneously to p53 sumoylation.

Methylation reactions prior to sumoylation were performed in a volume of 20 µL, containing 1µg of GST-$p53_{300-393}$ (WT or K386R), 1µg GST-Set9, 1.5µL of radiolabelled ^{3}H-SAM (Perkin Elmer), in a methylation buffer (20mM Tris-HCl pH 8.0, 50mM NaCl, 0.5mM DTT, 5mM $MgCl_2$, 1mM PMSF), and incubated at 30°C for 1h. Once the methylation reaction was completed, components for the sumoylation reaction (2µg of 6His-SUMO-1, 1 µg of 6his-ubc9, 0.4µg of SAE1/SAE2, 5mM Mg-ATP) were added up to a final volume of 30 µL. The reactions were then incubated at 30°C for 1h. Sumoylation reactions prior to methylation were performed as described in **Section 2.2.3**, in methylation buffer. Once the sumoylation reaction was completed, methylation components (1µg of GST-Set9 and 1.5µL of ^{3}H-SAM) were added up to a final volume of 30 µL, and incubated at 30°C for 1h. Simultaneous sumoylation and

methylation reactions were performed including all sumoylation and methylation components (GST-$p53_{300-393}$ (WT or K386R), 1µg of GST-Set9, 1.5µL of ^{3}H-SAM, 2µg of 6His-SUMO-1, 1 µg of 6his-ubc9, 0.4µg of SAE1/SAE2, 5mM Mg-ATP), in acetylation buffer with a total final volume of 30 µL, and incubated at 30°C for 1h.

The reactions were stopped by the addition of 10µL of 4x Protein Loading buffer (250mM Tris-Cl pH 6.8, 8% SDS, 40% glycerol, 0.02% Bromophenol and 8% of β-mercaptoethanol) and boiled at 95°C for 5 min. The reactions were then run on SDS-PAGE and transferred to a nitrocellulose membrane. After two washes with ddH_2O, the membrane was stained with Direct Blue 71 and scanned. Methylated proteins were visualized by spraying the membrane with EN^{3}HANCE (Perkin Elmer) and exposure to autoradiography film overnight at -80°C. The films were developed the next day using a compact X4 x-ray film processor (Xograph imaging system, UK).

2.2.7 *In vitro* Sumoylation-Acetylation Assays

To assess the mutual effect of p53 sumoylation on C-terminal acetylation of p53, *in vitro* acetylation reactions were performed prior, after or simultaneously to p53 sumoylation.

Acetylation reactions prior to sumoylation were performed in a volume of 20 µL, containing 1µg of GST-$p53_{300-393}$ (WT or K386R), 0.5µg of GST-CBP/p300 and 10µM Acetyl-CoA, and acetylation buffer (50mM Tris-HCl pH 8.0, 10% glycerol, 10mM Sodium butyrate, 50mM $MgCl_2$ and 1mM DTT), and incubated at 30°C for 1h. Once the acetylation reaction was completed, components for the sumoylation reaction (2µg of 6His-SUMO-1, 1 µg of 6his-ubc9, 0.4µg of SAE1/SAE2, 5mM Mg-ATP) were added up to a final volume of 30 µL. The reactions were then incubated at 30°C for 1h. Sumoylation reactions prior to acetylation were performed as described in **Section 2.2.3**, in acetylation buffer (50mM Tris-HCl pH 8.0, 10% glycerol, 10mM Sodium butyrate, 50mM $MgCl_2$ and 1mM DTT). Once the sumoylation reaction was completed, acetylation components (0.5µg of GST-CBP/p300 and 10µM Acetyl-Coa) were added up to a final volume of 30 µL. The reactions were then incubated at 30°C for 1h. Simultaneous sumoylation and acetylation reactions were performed including all sumoylation and acetylation components (GST-$p53_{300-393}$ (WT or K386R), 0.5µg of GST-

CBP/p300, 10µM Acetyl-Coa,2µg of 6His-SUMO-1, 1 µg of 6his-ubc9, 0.4µg of SAE1/SAE2, 5mM Mg-ATP), in acetylation buffer with a total final volume of 30 µL, and incubated at 30°C for 1h. The reaction was stopped by the addition of 10µL of 4x Protein Loading buffer (250mM Tris-Cl pH 6.8, 8% SDS, 40% glycerol, 0.02% Bromophenol and 8% of β-mercaptoethanol) and boiled at 95°C for 5 min. The reactions were then run on SDS-PAGE and analysed by western blotting.

2.3 Cell culture

Cell lines from different tissues were cultured in Dulbecco's modified eagle medium GlutaMAX™ (Gibco, Life Technologies) supplemented with 10% FBS and 200U penicillin-streptomicin, at 37°C and 5% CO_2 (**Table 2.5**.)

Table 2.5 Cell lines used for *in vivo* experiments.

Cell line	Source	Characteristics
H1299	Human non-small cell lung carcinoma	p53 null cells
HCT116 p53+/+	Human Colorectal Carcinoma	
HCT116 p53-/-	Human Colorectal Carcinoma	p53 knockout by homologous recombination
U2OS	Human Osteosarcoma	
U2OS pLKO p53	Human Osteosarcoma	Lentivirus shRNA against p53

2.3.1 Cell Maintainance by trypsinization

Cells were maintained by changing the media every 24h until 100% confluent. Once cells reached a confluence of 100%, the media was aspirated and the plates were washed once with sterile PBS (Gibco, life technologies) to remove any residual media. (This washing step was skipped in the case of HEK 293T cells). Cells were detached from the surface of the dish using 0.05% trypsin-EDTA (Gibco, life technologies) and incubated at 37°C in a 5% CO2 atmosphere for 3-5min. Trypsin-EDTA was deactivated by adding an equal or greater volume of growth medium. Cells were then seeded in new plates at an appropriate density.

2.3.2 Long Term Storage

To store cells for longer periods of times, confluent 10cm tissue culture dishes of cells were used. Growth media was removed and cells were washed and collected as described in section 2.2.1. Cells were spun down at 1100rpm for 5min to remove media and resuspended in DMEM containing 10% DMSO. Cells were then aliquoted into 1.5mL cryovials (StarLab) so that each cryovial would contain approximately ¼ of cells present in a 10cm dish. Cells were then stored at -80°C for 24h, and transferred into a liquid nitrogen tank for long term storage.

To recover frozen cells, the cryovials were rapidly thawed in a 37ºC water bath. To remove DMSO, cells were transferred to a 15mL tube and spun down for 5min at 1100rpm. The supernatant was discarded and cells were resuspended in warm growth media and seeded in a 10cm culture dish for incubation at 37°C, 5% CO_2.

2.3.3 Cell counting

Cells were counted using a haemocytometer of 0.0025 mm^2/0.1 mm depth (Neubauer Improved, Marienfeld-Superior). 10µL of suspension cells were placed in the haemocytometer and cells were counted in each 4x1mm^2 corner squares. The number of cells was calculated by taking the average of each square (total number of cells divided by 4) and multiplied by a factor of 10^4, which gives the number of cells per mL of cell suspension.

Trypan Blue stain was used to assess the viability of the cells. In this case, a small portion of suspension cells were mixed in 1:1 ratio with Trypan Blue stain 0.4% (Gibco, Invitrogen) and 10µL of suspension cells were placed in the haemocytometer. The cells were counted as described before, and the total number of cells per mL was calculated using the same method but taking in consideration the dilution factor (Average number of cells per square x 10^4 x 2 (dilution factor)).

2.3.4 Transfections

Transfections in H1299, U2OS (p53+/+ and pLKO p53) and HCT116 (p53+/+ and p53-/-) cells were made using Turbofect Transfection reagent (Thermo Scientific). For transfections, cells were grown up to a confluence of 40-50% in 24 well-plates, 6 well-plates or 10cm dishes. A total of 1µg, 4µg or 10µg of plasmid DNA were diluted in 100µL, 400µL or 1mL of Opti-MEM media, respectively, (Gibco, Invitrogen) and incubated for 20min at RT with appropriate amounts of Turbofect reagent. The mixture was then added drop wise to the cells growing in DMEM media and the plates were placed back in the incubator. After 24h, cells were either collected or split to be treated with doxorubicin or other drugs.

2.3.5 Drug Treatments

2.3.5.1 Doxorubicin

Cells were treated with a final concentration of 0.5µM or 1µM of doxorubicin hydrochloride (Sigma), added directly to the media, 16h upon transfection. Cells were then collected at different time-points, after 0h, 16-18h or 24h upon treatment.

2.3.5.2 Puromycin

In order to induce the expression of p53 shRNA, inducible cell line U2OS pLKO was treated with a final concentration of 0.5 µg/mL of Puromycin (Gibco), for a minimum of 3 days before transfection.

2.3.5.3 Geneticin (G418)

For colony formation assays, H1299 cells transiently transfected with pcDNA3 backbone plasmids were selected by the addition of 500µg/mL of Geneticin (Santa Cruz) to the media, 24h upon transfections.

2.1.1.1. Trichostatin A (TSA)

To measure acetylation levels of p53, H1299 cells transiently transfected with p53-ubc9 plasmids growing in 10cm plates were treated with 100nM of HDAC inhibitor TSA (Sigma) 16h upon transfection for 8h.

2.4 Protein Analysis

2.4.1 Preparation of Cell Extracts

Growing medium was aspirated from cells growing on 10cm dishes or 6 well-plates, and were washed twice with PBS (except in the case of HEK 293T cells). Cells were either collected by scraping (10cm dishes) or trypsinized (6 well-dishes) as described in section 2.3.1. The equivalent of 1:5 of a 6 well-plate was used for cell extracts. Cells were collected to a tube and pelleted by centrifuging at 1200g for 5min. Pellets were resuspended in 100µL of PBS and 4x Laemmli's SDS-sample loading buffer (250mM Tris-HCl pH 6.8, 8% SDS, 40% glycerol, 8% β-

mercaptoethanol, 0.02% bromophenol) and sonicated twice for 5min with a Diagenode Bioruptor 200 sonicator, in a water bath. Samples were boiled for 5min at 95°C and run on SDS-PAGE.

Alternatively, if cells needed to be quantified prior to western blot analysis, cells were collected on ice and resuspended with ice-cold Lysis buffer (50mM Tris-HCl pH 7.5, 150mM NaCl, 1mM EDTA, 1% Triton, 1% protease inhibitor cocktail (Sigma)). Cell debris was collected by centrifugation at 13000 rpm at 4°C and the protein supernatant was transferred to a new tube. The protein concentration was measured by Bradford Assay, and the appropriate volume of sample was loaded in the SDS-PAGE.

2.4.2 Preparation of Nuclear Extracts

H1299 cells were washed with 1xPBS and collected from 12 15cm plates. The cells were spun down at 1200 rpm for 5min and the pellet was washed with PBS. Chilled Buffer A (10mM Tris-HCL pH 8, 1.5mM $MgCL_2$, 10mM KCl, 0.5mM DTT, 0.2mM PMSF, 2mM Na Orthovanadate, 10mM NaF, 1% Protease inhibitor cocktail (Sigma)) was added to the cells and the pellet was homogenized with 15 strokes using a 7mL Dounce homogenizer B pestle. The cells were spun down at 10.000 rpm for 8min, supernatant removed and pellet was kept at -80ºC overnight. The nuclei pellet was resuspended in Buffer C (20mM Tris-HCl pH 8, 1.5mM $MgCL_2$, 420mM NaCl, 0.2mM EDTA, 25% Glycerol, 0.2mM PMSF, 2mM Na Orthovanadate, 10mM NaF, 1% Protease inhibitor cocktail (Sigma)) and homogenized with 15 strokes of a 2mL Dounce homogenizer. The suspension was incubated on a rotator at 4°C for 30 min, and spun down at 14.000 rpm. The supernatant containing the nuclear proteins was kept in a new tube, and the pellet was resuspended once again with Buffer C and sonicated. The sonication supernatant containing the remaining nuclear proteins was kept, and protein concentration was measured by Bradford assay.

2.4.3 Bradford Assay

Total protein concentration was analysed by Bradford Assay. A series of dilutions of Bovine Serum Albumin (BSA) ranging from 0.2mg/mL to 1mg/mL were made and combined with 1:5 Bio-rad protein assay reagent (Bio-Rad). The mixtures were transferred to cuvettes, and the absorbance was measured at 595nm, in a Smart Spec Plus spectrophotometer (Bio-

Rad). The measurements were used to create a standard curve plotting absorbance vs. protein concentration. Proteins of unknown concentration were mixed with diluted Bio-rad protein assay reagent and concentrations were calculated by comparing the absorbance values with the standard curve.

2.4.4 Immunoprecipitation & Co-Immunoprecipitation

Immunoprecipitation and co-immunoprecipitation were used to analyse possible interactions between sumoylated p53 and other cellular proteins. Cells growing in confluent 10cm dishes were washed twice with PBS and collected by scraping. Cells were pelleted by centrifugation at 2000g for 5min, and resuspended in 1mL of ice-cold Lysis buffer (50mM Tris-HCl pH 7.5, 150mM NaCl, 1mM EDTA, 1% Triton, 1% protease inhibitor cocktail (Sigma)). Tubes containing the lysing cells were left rotating for 20min at 4°C. Cell debris was pelleted by centrifugation at 12000g and the supernatant transferred to a new chilled tube. 100µL of lysate was kept for input (10%). The lysates were incubated with 1µg of antibody against the protein of interest at 4°C overnight.

Per IP sample, 20µL of Protein G Magnetic beads (Millipore) were used. Beads were washed 3 times with 1mL of Lysis buffer prior to incubation with the lysate supernatants for 3-4h at 4°C with rotation. Beads were then centrifuged at 2000rpm and the flow through recovered and kept. Beads were then washed 3 times with 1mL of Lysis buffer. 45µL of Lysis buffer and 15µL of 4x Laemmli's loading buffer were added to the beads. Samples were boiled for 5min at 95°C and run on SDS-PAGE.

2.4.5 Protein Analysis by SDS-PAGE

Proteins to be analysed were first separated by SDS-PAGE, and depending on the purpose, the gel was directly stained or the proteins were transferred to a nitrocellulose membrane for further identification by Western blotting.

2.4.5.1 Protein Staining

After running the samples, the gel was washed with destiled water, and proteins were fixed for 5-15min with fixing solution (10% methanol, 7% acetic acid). The gel was washed 2-3

times with destiled water, and stained with either 10mL Instant Blue (Expedeon, Lucerna-Chem) for 15-30min or with 20mL SYPRO Ruby protein stain (Bio-Rad) overnight.

2.4.5.2 Western Blotting

Proteins in the gel were transferred to a nitrocellulose membrane for 1h, according to standard procedures. Membranes were usually blocked with 5% Milk/PBS-T for 1h at room temperature, followed by 3x 10min washes with PBS-T, and incubated for 1h at RT or overnight at 4°C with the appropriate primary antibody, diluted in 5% BSA/PBS-T with 0.02% NaN_3 [**Table 2.6**]. Membranes were again washed 3x 10min and incubated for 1h with secondary antibody, appropriately diluted in 3% milk/PBS-T [**Table 2.7**]. After another 3x10min washes, the membrane was incubated with HRP chemiluminescent reagent (Millipore), according to manufacturer's instructions. The signal was detected developing in a compact X4 x-ray film processor (Xograph imaging system, UK).

Table 2.6. List of Primary Antibodies used in Western Blotting.

List of Primary Antibodies used for WB			
Primary Ab	**Source**	**Dilution**	**Supplier**
Flag M2 tag	Mouse monoclonal	1:2000	Sigma Aldrich (F3165)
Myc tag	Mouse monoclonal	1:5000	Sigma Aldrich (9E10)
6His tag	Mouse monoclonal	1:1000	AnaSpec (61250)
Ab-1 p53 C-Terminus	Mouse monoclonal	1:1000	Calbioch (OP43A)
Ab-6 p53 N-Terminus	Mouse monoclonal	1:1000	Calbioch (OP03)
Ac-p53 (Lys373)	Rabbit Polyclonal	1:1000	Upstate (06-916)
β-Actin	Mouse monoclonal	1:2000	Abcam (ab8226)
Ku-70	Mouse monoclonal	1:2000	Abcam (ab3114)
β-Tubulin	Mouse monoclonal	1:2000	Sigma (T-8535)
GAPDH	Mouse Monoclonal	1:1000	Abcam (ab9484)
p21	Mouse monoclonal	1:200	Santa Cruz (sc-53870)
PUMA	Rabbit Polyclonal	1:1000	Cell signalling (4976)
hLSD1	Rabbit Polyclonal	1:1000	Diagenode (PAb-067-050)
HDAC2	Mouse monoclonal	1:1000	Millipore (05-814)
BAF 155 (H-76)	Rabbit Polyclonal	1:1000	Santa Cruz (sc-10756)
YY1	Rabbit Polyclonal	1:1000	Santa Cruz (sc-1703)

Table 2.7. List of Secondary Antibodies used for Western Blotting.

List of Secondary Antibodies used for WB		
Secondary Ab	**Dilution**	**Supplier**
Goat anti mouse HRP	1:10000	Biorad (170-5046)
Goat anti rabbit HRP	1:10000	Sigma Aldrich

2.5 RNA Isolation and qRT-PCR

2.5.1 RNA extraction

For RNA extraction, cells growing on 6-well plates were harvested by trypsinization and 1/5 of the cell pellet was kept for western blot analysis. Cells were homogenized by the addition of 1mL of TRI Reagent® (Ambion, life technologies) and left at room temperature for 5min. The homogenate was supplemented with 200µL of chloroform, shook and left at room temperature for 10min. The samples were then spun down at 13000rpm (table top centrifuge) for 15min at 4ºC. The aqueous phase containing the RNA was transferred to new, RNase-free tubes, and precipitated by the addition of 500µL of isopropanol for 20min at -20°C. Samples were centrifuged and the RNA pellet was washed twice with 80% ethanol. The pellet was air-dried for 5-10min and dissolved in 30µL of RNase-free water.

2.5.2 cDNA Synthesis

cDNA was synthesised from 1µg of total RNA extracted from cells. Firstly, 1µg of total RNA was incubated with 0.5µg of 1:1 mixture of oligodT (Thermo scientific) and random hexameres (Thermo Scientific) for 5min at 70°C. A reverse transcriptase mixture containing Improm-II 5X reaction buffer (Promega), 3mM $MgCl_2$, 10mM dNTPs and Improm-II reverse transcriptase (Promega) was added to the RNA/primer mixture. The reaction was incubated for 5min at 25°C for annealing, and the first strand was extended at 42°C for 1h. The reverse transcriptase was then heat inactivated by incubating at 70°C for 15min.

2.5.3 qPCR

The cDNA synthesised was used for quantitative real time PCR (qRT-PCR). Each reaction contained 10ng of cDNA and optimized concentrations of the relevant primers, and was performed using the SensiMix SYBR® No-ROX kit (Bioline). Each reaction was performed in triplicates, using a Corbett Life Science Rotor-Gene™ 6000 real-time PCR machine. Reactions were performed under the following conditions: an initial hold of 10min at 95°C, and then 40 cycles of 25 sec at 95°C, 20sec at 61°C with a 4 cycle touch down (61°C-58°C) and 20 sec at 72°C. The specificity of primers was confirmed through the post-PCR melting curve analysis.

The following primers were used to perform the quantitative real time PCR (qPCR):

Table 2.8: List of Primers used for qRT-PCR reactions

Primer name	5'-3' Primer Sequence	Concentration used
F-GAPDH Ex1-Ex2	GGG AGG GTG AAG GTC GGA GT	350nM
R-GAPDH Ex1-Ex2	TTG AGG TCA ATG AAG GGG TCA	
F-p21 p1	GAC ACC ACT GGA GGG TGA CT	200nM
R-p21 p1	CTC TTG GAG AAG ATC AGC CG	
F-PUMA	GAC CTC AAC GCA CAG TAC GA	350nM
R-PUMA	CAC CTA ATT GGG CTC CAT CT	
F-BAX Ex4-5	GGG TTG TCG CCC TTT TCT	350nM
R-BAX Ex4-5	CAG CCC ATG ATG GTT CTG ATC AG	

2.6 Chomatin Immunoprecipitation (ChIP) assay

To examine the mechanism by which sumoylation modulates p53 binding to known target promoters, ChIP assay was performed. For this, H1299/U2OS/HCT116 cells were grown in 10cm dishes, transfected and treated with 0.5µM doxorubicin for 16h. Prior to crosslinking, cells were washed twice with PBS, and a relevant amount of cells (1:6 of 10cm dish) was collected for RNA extraction and western blot analysis.

2.6.1 Cross-linking of DNA-binding proteins

Cells growing in confluent 10cm tissue culture dishes were cross-linked with 1% Formaldehyde (Thermo Scientific) rocking for 13min at RT, and neutralized by the addition of 0.125M Glycine for 13min at RT. Cells were then collected by scrapping and the cell pellet was kept at -80°C until use.

2.6.2 Cell lysis and sonication

Cell pellets were resuspended in 4mL of Lysis buffer 1 (10mM Tris-HCl pH 8.0, 0.25% Triton X-100, 10mM EDTA, 0.5mM EGTA, 1mM PMSF) and incubated for 30min rotating at 4°C. Nuclei were spun down at 2000rcf 10 min 4°C and supernatant discarded, and the pellet was again resuspended in 4mL of Lysis buffer 2 (10mM Tris-HCl pH 8.0, 200mM NaCl, 10mM EDTA, 0.5mM EGTA, 1mM PMSF) and incubated for 15min, rotating at 4°C. Chromatin was again

centrifuged at 2000rcf 15min 4°C and the pellet was resuspended in IP buffer (300µL per 1-3 x 10^6 cells) (20mM Tris-HCl pH 8.0, 200mM NaCl, 0.5% Triton X-100, 0.5% NP-40, 0.05% DOC, 1mM PMSF, 0.05% SDS) and split into 300µL samples for sonication. Sonication was performed in a Diagenode Bioruptor 200, in an icy water-bath. The Bioruptor was set to high and sonication was performed in 3 cycles of 10 min for 30second on/off intervals, keeping the samples in an icy water-bath. After sonication, samples were transferred to new tubes and spun down to pellet debris. The supernatant (sheared DNA) was transferred to another tube and diluted 1:1 with IP buffer containing no SDS, and 50µL were taken for input.

2.6.3 Immunoprecipitation

Per each IP sample, 20 µL of Protein A agarose beads pre-blocked with salmon sperm DNA slurry (Upstate, Millipore) was incubated with 1:1 ratio of 5% BSA rotating overnight at 4°C. At the same time, 1µg of antibody against the protein of interest was incubated with each sonicated sample, and left rotating at 4°C overnight [**Table 2.9**]**.**

Table 2.9: Antibodies used for ChIP assay

Antibody	Source	Supplier
Ab-6 (p53 N-Terminus)	Mouse monoclonal	Calbioch (OP43A)
H3K9me^3	Rabbit Polyclonal	Diagenode (pAB-056-050)
Acetyl-H3	Rabbit Polyclonal IgG	Upstate (06-599)
HDAC2	Mouse monoclonal IgG1	Millipore (05-814)
CBP (A-22)	Mouse Monoclonal	Santa Cruz (sc369)
H3 mono methyl K4	Rabbit polyclonal IgG	Abcam (ab8895-100)
hLSD1	Rabbit Polyclonal	Diagenode (pAB-067-056)

The sonicated samples pre-incubated with antibody were added to the beads and left rotating for 3h at 4°C. Beads were then spun down gently at 2000rpm for 5min and washed once with IP buffer. The beads were then transferred to Spin-X centrifuge tube filter collumns (Corning® Costar®) and washed as follows: once with IP buffer, twice with IP-500 buffer (20mM Tris-HCl pH 8.0, 500mM NaCl, 0.5% Triton X-100, 0.5% NP-40, 0.05% DOC, 1mM PMSF), twice with LiCl buffer (10mM Tris-HCl pH 8.0, 250mM LiCl, 1% Triton X-100, 0.5% NP-

40, 0.05% DOC, 0.5mM EDTA, 1mM PMSF) and twice with TE buffer (10mM Tris-HCl pH 8.0, 0.5mM EDTA). The DNA-protein complexes were then eluted with 100µL of warmed Elution buffer (10mM Tris-HCl pH 8.0, 0.5mM EDTA, 1% SDS) at 65°C for 30min.

2.6.4 Reverse Crosslinking and DNA purification

150 µL of Elution buffer were added to the sonicated inputs, and a final concentration of 200mM NaCl was added to both inputs and IP samples. The samples were left in a 65°C water-bath overnight.

TE buffer was added to the samples at a ratio of 1:1 to dilute the SDS concentration, and 0.1µg/µL of RNase A was added to each sample for incubation at 45°C for 1h. 40µg of proteinase K was then added to the samples and incubated for 3h at 45°C to digest DNA-bound proteins. The DNA was purified using the QIAquick PCR purification kit (Qiagen), according to the manufacturer's instructions.

2.6.5 Analysis by qRT-PCR

The DNA isolated was analysed by qRT-PCR. The input samples were diluted 1:4 and IP samples were undiluted in the reaction. Each reaction contained 2µL of DNA and an appropriate concentration of primers for the promoter region of p53-target genes [**Table 2.10**], and was performed using the SensiMix SYBR® No-ROX kit (Bioline). The PCR reaction was performed as described in section 2.5.3 and the specificity of the primers was confirmed by analysis of the melting curve.

Table 2.10: List of primers used for ChIP assay

Primer name	Primer sequence 5'-3'	Concentration used
F- p21 TM	GTG GCT CTG ATT GGC TTT CTG	200nM
R- p21 TM	CTG AAA ACA GGC AGC CCA AG	
F- Pumab TM	GCG AGA CTG TGG CCT TGT GT	350nM
R- Pumab TM	CGT TCC AGG GTC CAC AAA GT	
F- actin	TGG CTC AGC TTT TTG GAT TC	200nM
R- actin	GGG AGG ATT GGA GAA GCA GT	
F-BAX	ACC CAT GTA AAC ACC ATT CAG	350nM
R-BAX	GGC AGA AAC TAA TCT GTG CTG	

2.7 Immunofluorescence Microscopy

Immunofluorescence microscopy was used to assess the effect of Sumoylation on p53 subcellular compartmentalization. For this, coverslips were placed inside 24-well plates and coated overnight with 1mL of 0.1mg/mL solution of Poly-L-Lysine. Cells were seeded on coverslips and transfected 24h after. Transfected cells were washed twice in PBS and fixed with ice-cold methanol for at least 15min at -20°C.

Fixed cells were washed twice with PBS and then blocked and permeabilized with a solution of 1% BSA+0.1% Triton X-100 for 30min at room temperature. The cells were then incubated with 1:500 dilutions of p53 (DO-1) FITC primary-conjugated antibody (Santa Cruz sc-126-FITC) overnight at 4°C. Cells were washed 3 times for 5min in PBS and stained with 1µg/mL of DAPI for 15min at room temperature. Cells were washed twice with PBS and the coverslips were then inverted and mounted onto glass slides with a small drop of Mowiol (4-88, Calbiochem). The slides were left to dry for a minimum of 2h and kept at 4°C in the dark until use. All slides were analysed using a Nikon TE300 semi-automatic inverted microscope with a Plan Apo VC 60x DIC oil-immersion objective (NA 1.4). Fluorescent images were captured with an ORCA-R2 digital camera (Hamamatsu, Japan) with Volocity® software, version 6.0.1 (Perkin Elmer, UK).

2.8 Colony Formation Assay

Colony formation assay is a cell survival assay that is based on the principle that a single cell in able to form a colony. To evaluate the physiological role of p53 Sumoylation, H1299 cells were seeded in 6-well plates (2000 cells per well) in triplicates, and transfected with either $p53_{WT}$-ubc9 or the sumoylation deficient mutant $p53_{K386R}$-ubc9. 24h upon transfection, cells were treated with 500µg/mL of G418. Cells were allowed to grow for 2-3 weeks, changing the media with G418 every 3days.

After 2-3 weeks, the plates were washed with 1× PBS and fixed with 2 ml of 4% Paraformaldehyde (Sigma-Aldrich). Plates were incubated at room temperature for 15 min. After fixation, the cells were washed twice with 1× PBS and allowed to dry completely. Colonies were stained with 2mL of Giemsa Staining Reagent (64mM PO_4, 4% Giemsa Stain

(Fluka)) for 5 hours. The plates were then washed twice with ddH_2O and allowed to dry. The number of colonies from each plate was then counted and recorded.

CHAPTER 3

p53 Sumoylation alters the Spectrum of Protein Interactions

Chapter 3. p53 Sumoylation alters the Spectrum of Protein Interactions

3.1 Introduction

The modification of p53 by the Small Ubiquitin Modifier (SUMO) protein has been studied for more than 15 years and although some advances have been made, the functional effects of p53 sumoylation remain elusive.

Protein sumoylation is known to alter the substrate surfaces, potentially leading to changes in protein interactions. The covalent attachment of SUMO to a protein can, therefore, modulate the recruitment of protein interactors. In the case of transcription factors, SUMO modification can lead to the recruitment of transcription co-regulators or chromatin-remodeling factors, which ultimately affect gene transcription (Geiss-Friedlander & Melchior 2007). Hence, it is plausible that the changes in transcriptional activity described upon p53 sumoylation are a result of a change in interacting partners caused by the SUMO moiety.

To address this issue, I aimed to investigate whether SUMO modification causes a differential interaction of proteins to p53. Additionally, the identification of regulatory proteins that specifically interact with sumoylated/non-sumoylated p53 would provide clues to their role in p53 dependent transcription and further our understanding of the mechanisms behind the effect on p53 transcription activity triggered by SUMO.

3.2 Results

3.2.1 *In vitro* sumoylation – System Optimization

To explore whether the conjugation of SUMO to p53 affects the hub of protein interactions, I firstly developed an *in vitro* system that would generate a large population of sumoylated p53. *In vitro* sumoylation requires the presence of E1 activating enzyme SAE2/1 and E2 conjugation enzyme ubc9, but the presence of E3 SUMO ligases is dispensable.

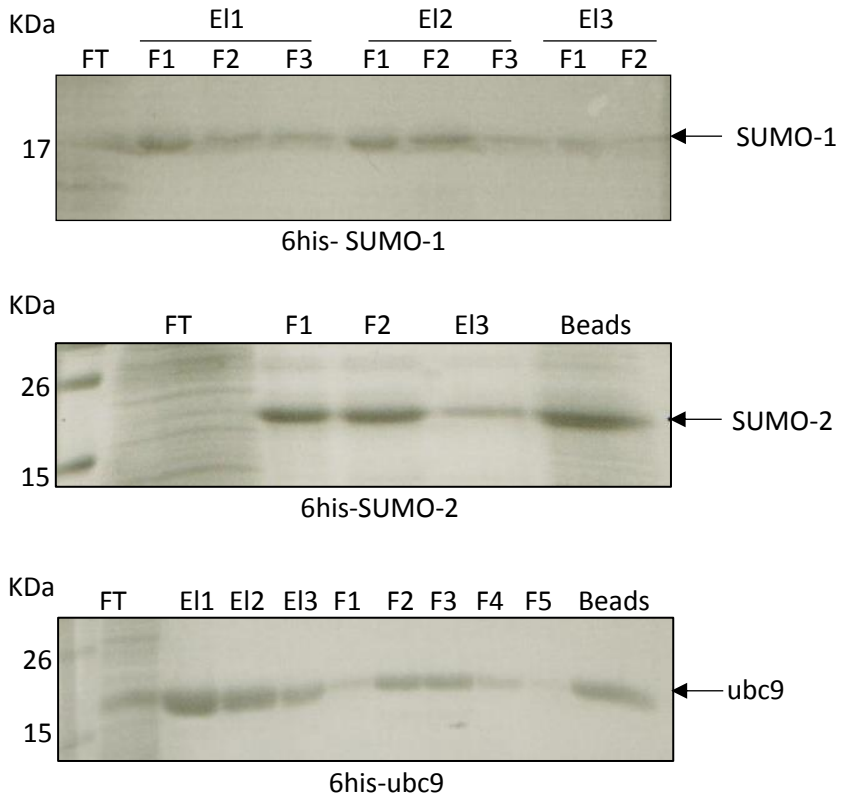

Figure 3.1. Bacterial expression and subsequent steps of purification of Hexa-Histidine-tagged proteins used for in vitro studies.

Bacterial expression plasmids for Hexa-histidine tagged SUMO-1, SUMO-2 and ubc9 proteins were transformed and subsequently induced in *E. coli* (*Rosetta* strain). Bacterial lysates expressing hexa-histidine proteins were incubated with Ni-NTA beads and the flow through (FT) was run on the gel. Sequential elutions (El1, El2, El3) were made and were then passed through a buffer exchanging column, and different fractions were collected (F1-5), as described in sections **2.2.1** and **2.2.2**. Proteins were detected with Instant Blue (Expedeon, Lucerna-Chem). Molecular weights (kDa) are indicated.

I generated bacterial plasmids for the recombinant proteins SAE2/1, ubc9, SUMO-1 and SUMO-2, which were expressed in bacterial cells and subsequently purified. The plasmids containing the recombinant proteins ubc9, SUMO-1 and SUMO-2 were cloned into pLEISC01 plasmid, which contains an N-terminal hexa-histidine tag, and were purified using Ni-NTA agarose beads. The recombinant proteins were then run on SDS-PAGE to evaluate their purity and molecular weight [**Figure 3.1**]. The heterodimer SAE2/1 recombinant protein, a gift from Dr Ronald T. Hay, was N-terminally tagged with Glutathione S-transferase (GST). Following purification with glutathione beads, the GST tag from SAE2/1 had to be removed prior to use, as the protein was not functional with it. Increasing concentrations of thrombin were tested and the optimal amount (2U) was used for the complete cleavage of the GST tag [**Figure 3.2**].

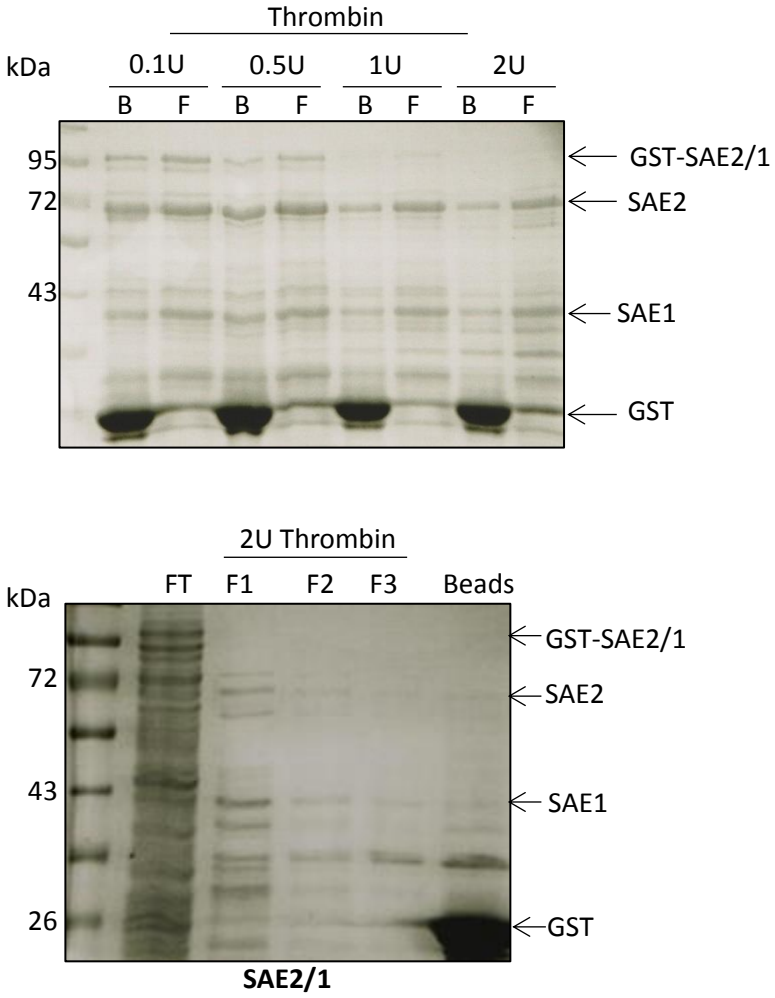

Figure 3.2.Bacterial expression and purification of Glutathione-S-transferase tagged SAE2/1 protein used for in vitro studies.

Bacterial expression plasmid for GST tagged SAE2/1 protein was induced in *E. coli* (*Rosetta* strain). Bacterial lysates expressing GST proteins were incubated with glutathione beads and the flow through (FT) was run on the gel. The GST tag from GST-SAE2/1 was removed by adding 2U of GST-Thrombin to the bacterial lysate bound to glutathione beads. Sequential fractions were collected (F1-3) and used for *in vitro* sumoylation), as described in section **2.2.2**. Proteins were detected with Instant Blue (Expedeon, Lucerna-Chem). Glutathione beads (B) were boiled with loading buffer and the supernatant also loaded on SDS-PAGE. Molecular weights (kDa) are indicated.

As sumoylation occurs at lysine 386 in the C-terminus of p53, I opted to use recombinant proteins which contained the last 93 amino acids of p53. This was also

discouraged by the low expression efficiency of the full length protein. The plasmid containing the C-terminus of p53 was already available in Dr Barlev's lab, and a mutant where lysine 386 was substituted for an arginine was generated by site-directed mutagenesis. Both $p53_{300-393}$ proteins contained an N-terminal GST tag, and were purified by affinity chromatography using glutathione beads [**Figure 3.3a**].

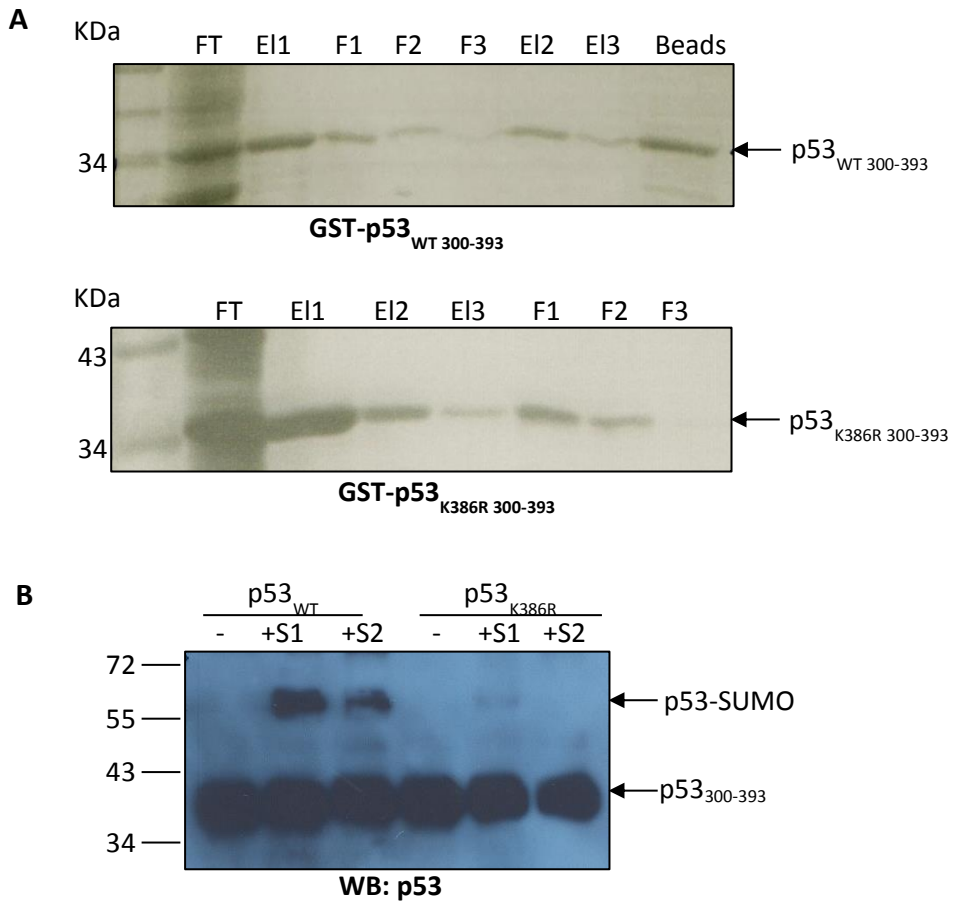

Figure 3.3.Sumoylation of p53 occurs at Lysine 386, in the C-terminus domain of p53.

(A) Purification of C-terminus of human p53 proteins. GST-$p53_{300-393}$ proteins were expressed in bacterial cells and purified with glutathione beads. The flow through (FT) was run on the gel and sequential elutions (El1, El2, El3) were made. The elutions were then passed through a buffer exchanging column, and different fractions were collected (F1-3), as described in sections **2.2.1** and **2.2.2**. Proteins were detected with Instant Blue (Expedeon, Lucerna-Chem). Molecular weights (kDa) are indicated.

(B) *In vitro* Sumoylation of $p53_{300-393}$ proteins was performed as described in section **2.2.3**, in the presence of either 6his-SUMO-1 or 6his-SUMO-2. The reactions were then run on SDS-PAGE and analysed by western blot, using p53 (AB-1) antibody. S1-SUMO-1; S2-SUMO-2.

Once the required enzymes were purified, an *in vitro* sumoylation assay was performed to assess the efficiency of p53 sumoylation. As 6His-SUMO recombinant proteins have an apparent molecular weight of 17kDa, the occurrence of p53 sumoylation was determined by a 17Kda shift on the molecular weight of p53. This was evident for the $p53_{WT}$ protein in the presence of both 6his-SUMO-1 and 6his-SUMO-2, but absent in the reaction where no SUMO proteins were added (-) [**Figure 3.3b**]. The absence of such shift on the sumoylation-deficient mutant $p53_{K386R}$ was expected, and confirmed that p53 sumoylation occurs at lysine 386.

Though with a working system established, we faced the challenge of relatively low amounts of SUMO modified p53. Although not as low as the endogenous <5% reported (Melchior & Hengst 2002), the percentage of SUMO modified p53 was not higher than 10-20% of total p53. Since p53 is active and occurs in solution as a tetramer, it is possible that sumoylation does not occur equally in all subunits. This could be a direct consequence of inaccessibility of the sumoylation machinery to some subunits. In fact, the C-terminal regulatory domain is natively unfolded (Bell et al. 2002), providing an anchorage point for proteins involved in PTMs. The binding of proteins provokes the organization of this region, which can assume different conformations depending on the structural context (Joerger & Fersht 2010). Structural studies on p53 have revealed that the tetrameric form of p53 can hold monomers that present distinct C-termini conformations (Kitayner et al. 2006; Okorokov et al. 2006). Consequently, differential sumoylation of p53 monomers could occur, explaining the low percentage of overall SUMO-modified p53.

In an attempt to raise the efficiency of p53 monomer sumoylation, I constructed plasmids for p53 recombinant proteins lacking the oligomerization domain ($p53_{300\text{-}393}\Delta 324\text{-}335$). The removal of the oligomerization domain (amino acids 324-335) was carried out by site-directed mutagenesis, and the proteins were purified after expression in bacterial cells [**Figure 3.4a** and **b**]. However, sumoylation of these proteins with SUMO-1 did not prove to be more efficient than the C-terminal protein, with only approximately 10% of total p53 being SUMO-modified [**Figure 3.4c**].

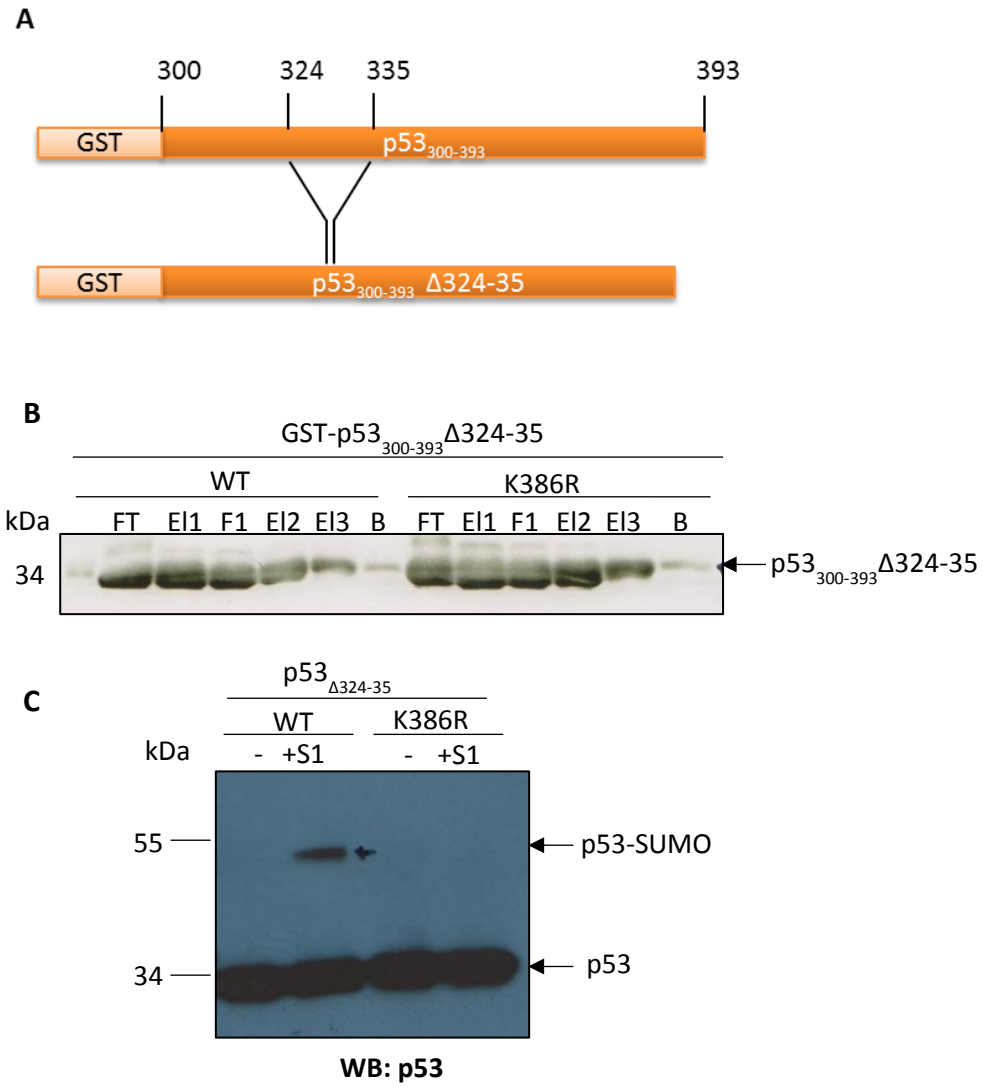

Figure 3.4.Removal of the oligomerization domain of p53 does not increase p53 sumoylation efficiency in vitro.

(A) Schematic representation of the mutant recombinant proteins GST-p53$_{300-393}$Δ324-35 lacking the oligomerization domain of p53.
(B) Purification of human GST-p53$_{300-393}$Δ324-335 proteins. GST-p53$_{300-393}$ Δ324-335 proteins were expressed in bacterial cells and purified with glutathione beads. The flow through (FT) was run on the gel and sequential elutions (El1, El2, El3) were made. The elutions were then passed through a buffer exchanging column, and different fractions were collected (F1-3), as described in sections **2.2.1** and **2.2.2**. Proteins were detected with Instant Blue (Expedeon, Lucerna-Chem). Glutathione beads (B) were boiled with loading buffer and the supernatant also loaded on SDS-PAGE.
(C) *In vitro* Sumoylation of p53$_{300-393}$Δ324-335 proteins was performed as described in section **2.2.3**, in the presence of 6his-SUMO-1. The reactions were then run on SDS-PAGE and analysed by western blot, using p53 (AB-1) antibody. S1-SUMO-1.

An interesting alternative was the use of the Ubc9 fusion-directed sumoylation (UFDS), a system developed in Dr Rainer Niedenthal's lab (Jakobs et al. 2007). In this system, the protein of interest (p53) is fused with the E2 SUMO conjugating enzyme ubc9, greatly enhancing sumoylation efficiency *in vivo*. We then decided to evaluate the efficiency of this system in promoting p53 sumoylation *in vitro*. The mammalian plasmids containing p53-ubc9 constructs, kindly given by Dr Rainer Niedenthal, were cloned into bacterial expressing plasmids with an N-terminal GST tag, and subsequently expressed and purified as described before [**Figure 3.5a** and **b**].

A sumoylation assay performed using the fused proteins and SUMO-1 revealed a great improvement in the efficiency of p53 sumoylation, increasing the sumoylated population to approximately 50% [**Figure 3.5c**]. Interestingly, the molecular weight shift between non-sumoylated and sumoylated p53 is around 35kDa, rather than the estimated 17kDa of SUMO-1. This discrepancy could be just an artifice resultant from the inaccuracy of the pre-stained molecular marker used. Alternatively, the molecular weight difference could be due to the covalent attachment of more than one SUMO molecule to p53-ubc9 proteins. Although this hypothesis seems more plausible at first, the lack of an intermediate form (i.e. a p53 molecule with a shift of 17kD, corresponding to the addition of one SUMO-1 molecule) makes the first possibility more reliable. Irrespectively, the western blotting results confirm that the shift in molecular weight is due to the addition of SUMO to the $p53_{WT}$-ubc9 protein, which does not happen in the sumoylation deficient mutant $p53_{K386R}$-ubc9 [**Figure 3.5c**].

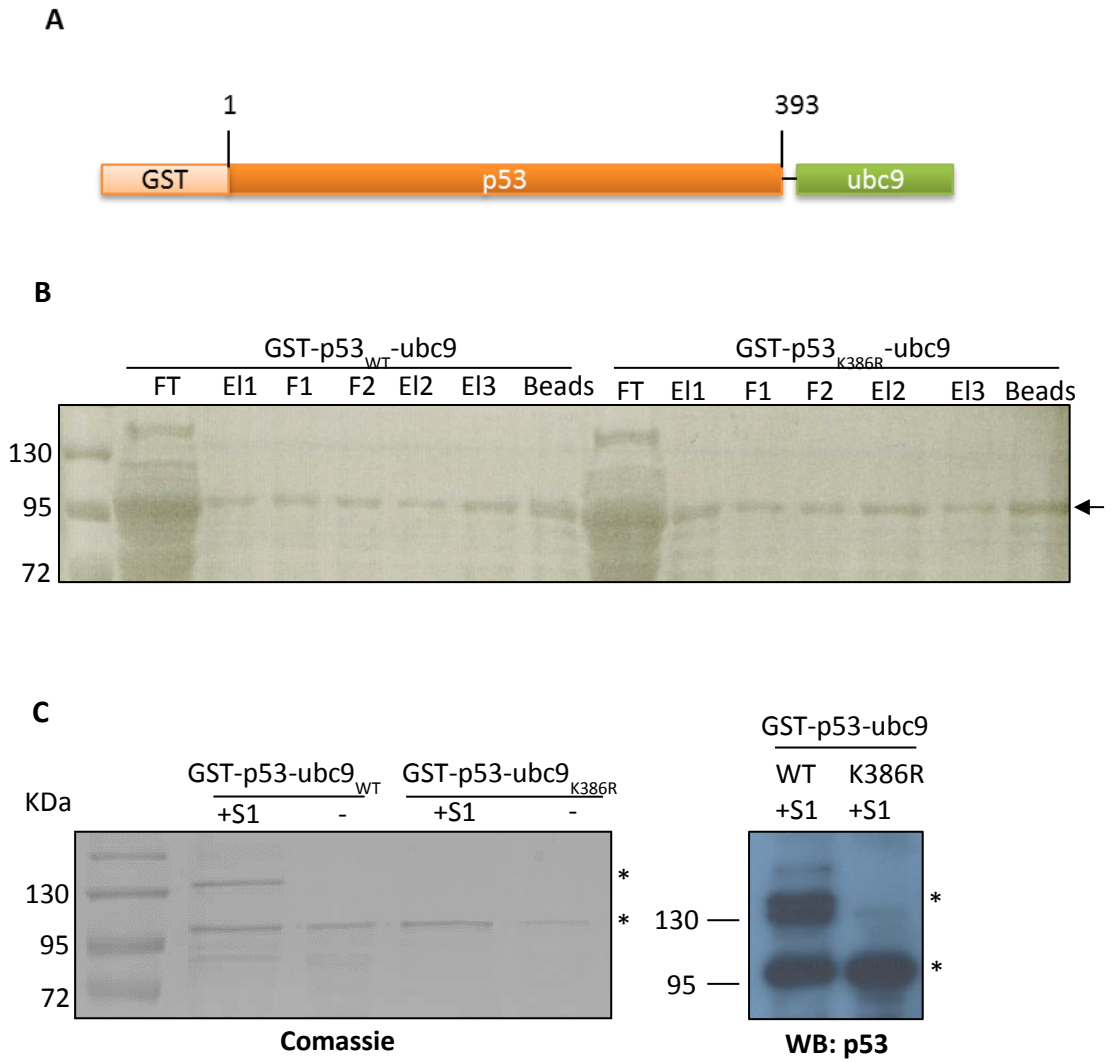

Figure 3.5. UFDS system enhances p53 sumoylation in vitro.

(A) Schematic representation of the fused recombinant proteins GST-p53-ubc9.

(B) Purification of human GST-p53-ubc9 fusion proteins. GST-p53-ubc9 proteins were expressed in bacterial cells and purified with glutathione beads. The flow through (FT) was run on the gel and sequential elutions (El1, El2, El3) were made. The elutions were then passed through a buffer exchanging column, and different fractions were collected (F1-3), as described in sections **2.2.1** and **2.2.2**. Proteins were detected with Instant Blue (Expedeon, Lucerna-Chem). Glutathione beads (B) were boiled with loading buffer and the supernatant also loaded on SDS-PAGE. Molecular weights (kDa) are indicated. Arrow indicates purified proteins.

(C) *In vitro* Sumoylation of GST-p53-ubc9 proteins was performed as described in section **2.2.3**, in the presence of 6his-SUMO-1. The reactions were then run on SDS-PAGE and analysed by Comassie based stain (left panel) and confirmed by western blot using p53 (AB-6) antibody (right panel). S1-SUMO-1. Stars (*) indicate p53-ubc9 proteins.

3.2.2 Identification p53-SUMO-1 binding proteins

To search for potential binding proteins of SUMO-1 modified p53, a non-bias global proteomic mass spectrometry (MS) approach was used. This approach brings the advantage of creating a library of possible binding partners previously unidentified.

The strategy implemented here to identify new binding partners of sumoylated p53 was based on a GST pull down of the fused p53 proteins, previously sumoylated and incubated with nuclear protein extract, followed by MS analysis [**Figure 3.6a**]. Primarily, a large-scale *in vitro* sumoylation reaction with 6His-SUMO-1 was performed, utilizing both fused recombinant proteins GST-p53-ubc9 (WT and K386R) as substrates. Nuclear extracts were prepared from H1299 cells (p53 null), and split into 3 equal parts. After the sumoylation reaction was completed, the nuclear extracts were incubated with either GST-$p53_{WT}$-ubc9 or GST-$p53_{K386R}$-ubc9. To discard the hypothesis that proteins could be bound to p53 by specifically recognizing K386 (or a sequence in which this lysine was enclosed), and not because p53 was sumoylated, an additional sample containing GST-$p53_{WT}$-ubc9 that was not subjected to prior sumoylation was incubated with the nuclear proteins. Given the conditions in which protein incubation was performed (at 4°C), it is improbable that GST-$p53_{WT}$-ubc9 could be sumoylated by endogenous SUMO proteins, and therefore this sample was used as an extra non-sumoylated control. The employment of H1299 cell line (which does not contain endogenous p53) insured that the only p53 present in the extract after incubation was from the recombinant proteins added. The following step was to pull down the p53 proteins from the extract, and for that I took advantage of the presence of the GST tag in the recombinant proteins. A GST pull down with glutathione beads was conducted, and the proteins were then run on SDS-PAGE. The staining method used (Sypro ruby), with increased sensitivity, allowed the visualization of a higher number of distinct bands compared to the standard comassie-based method. In the gel it is possible to discern bright ~100kDa bands corresponding to the fused recombinant proteins, and a distinct higher molecular weight band of approximately ~130kDa in the lane corresponding to the sumoylated version of $p53_{WT}$-ubc9, confirming that sumoylation was successful [**Figure 3.6b**]. The gel was then cut into 3 sections (250KDa-100KDa, 100-35KDa and 35-10KDa) for each sample and these were sent for ESI-LC-MS/MS (Electrospray ionization Liquid chromatography mass spectrometry) analysis.

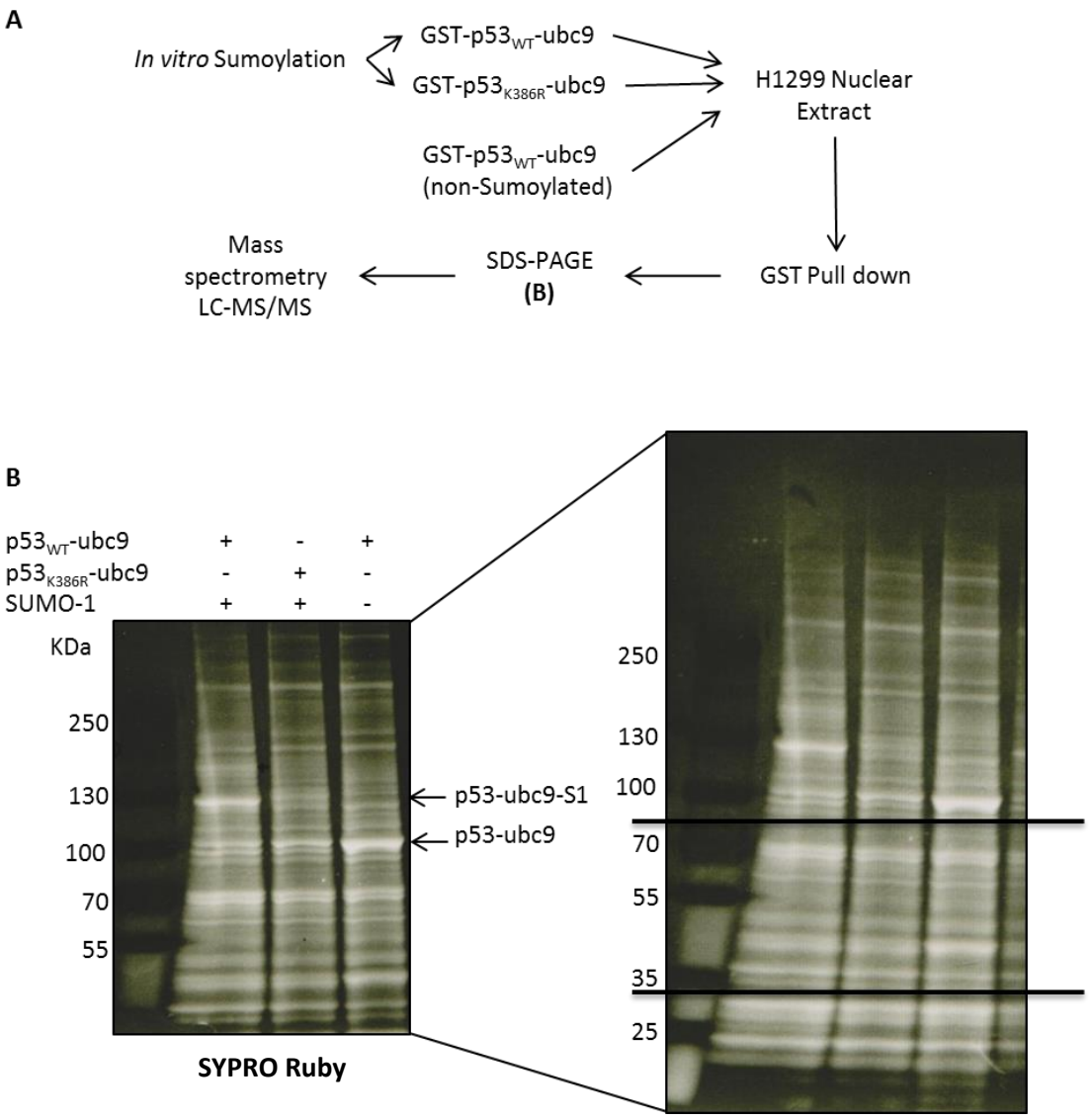

Figure 3.6. Incubation of GST-p53-ubc9-SUMO with nuclear extract proteins from H1299 cells

(A) Diagram representing the incubation procedure of sumoylated/non-sumoylated p53 proteins and the following steps of analysis.

(B) SDS-PAGE gel showing protein pulled-down. Upon performing large scale sumoylation reactions with GST-p53-ubc9 proteins, in the presence ($p53_{WT}$-SUMO1 and $p53_{K386R}$) or absence ($p53_{WT}$) of SUMO-1 protein, the reactions were incubated with nuclear extract proteins from H1299 cells and empty glutathione beads. GST-p53-ubc9 proteins were subsequently eluted from the beads, and the samples were run on SDS-PAGE. The gel was stained with SYPRO Ruby protein stain (Bio-Rad) and proteins were visualized under UV light. The gel was then cut in 3 sections (250KDa-100KDa, 100-35KDa and 35-10KDa) for each sample and sent for mass spectrometry analysis.

The first set of data obtained from MS was analysed with Mascot v2.2.04, and manually set on an excel spread sheet [**Appendix B**]. Results from the second set of MS data were analysed using Scaffold4 software where parameters were set to a minimum of two peptides to confirm presence of each identified protein and false discovery rate (FDR) of 1% [**Appendix D**]. A total of 363 proteins were identified in the first run, whereas the second run revealed a total of 997 proteins. Potential binding partners were sorted from the total amount of identified proteins in each data set by cross-referencing the proteins in each sample ($p53_{WT}$+S1, $p53_{K386R}$+S1 and $p53_{WT}$). Proteins present in all three biological samples were disregarded as non-sumoylation specific partners, and proteins present in only one or two fractions were retained and categorized by function [**Appendix C.1** and **Appendix D.1**]. From these, candidate proteins were selected and compared between both data sets (MS 1 and MS 2), listed on **Table 3.1**.

From the total amount of identified possible partners, a number of detected proteins was discredited based on their cellular localization, such as components of the cytoskeleton, ribosome, ER and Golgi, or function, such as proteins involved in the spliceosome, proteasome and heat-shock proteins. These proteins were regarded as non-specific interactions and therefore not considered for the present study. The remaining proteins were then analysed for their presence in each sample. Proteins present in the fraction containing sumoylated p53 ($p53_{WT}$ +S1) but absent in the non-sumoylated controls ($p53_{K386R}$ +S1 and $p53_{WT}$) were considered as potential true p53-SUMO-1 interactors. Interestingly, a number of proteins was found absent in the sumoylated p53 fraction, but present in at least one non-sumoylated control fraction. This observation suggests that p53 SUMO-1 conjugation may not just promote interactions with new partners, but also disrupt existing protein-protein interactions.

Table 3.1. List of Selected potential binding partners for p53-SUMO-1 from MS analysis.

Bands cut from SDS-PAGE were subjected to MS analysis and their presence was compared between samples containing sumoylated p53 ($p53_{WT}$+S1), or non-sumoylated p53 ($p53_{K386R}$ and $p53_{WT}$). Proteins selected for further confirmation are highlighted in blue.

	Data MS 1			Data MS 2			
Identified Proteins	**$p53_{WT}$ +S1**	**$p53_{K386R}$ +S1**	**$p53_{WT}$**	**$p53_{WT}$ +S1**	**$p53_{K386R}$ +S1**	**$p53_{WT}$**	**Function**
SWI/SNF complex subunit SMARCC1 (BAF155)	+			+			Chromatin Remodelling
SWI/SNF complex subunit SMARCC2	ND			+			
Chromodomain-helicase-DNA-binding protein 1	ND					+	
Heterochromatin protein 1-binding protein 3			+		+		
High mobility group protein 20A	ND			+			
Histone Acetyltransferase HAT1	ND			+			
Histone-arginine methyltransferase CARM1	ND			+		+	
Histone-binding protein RBBP4	ND			+		+	
WD repeat-containing protein 61	ND					+	
WD repeat-containing protein 82	ND				+		
Lysine-specific demethylase KDM1A (LSD1)	ND			+			Transcriptional Regulation
Transcriptional Repressor YY1	ND			+			
Histone Deacetylase HDAC2	ND			+			
Global Transcription Activator SMARCA1	ND				+	+	
PC4 and SFRS1-interacting protein		+	+	+		+	
Bcl-2-associated transcription factor 1			+			+	
Exportin-7	ND			+			Nucleo-cytoplasmatic Transport
Importin alpha-1	ND					+	
Importin alpha-3	ND				+	+	
Importin subunit alpha-2			+	ND			
Nuclear pore complex protein Nup155	ND				+		
Importin-8	ND				+		
Dihydrofolate reductase	ND				+		Metabolism
Glucosamine-6-phosphate isomerase 1	ND			+			
Inositol-3-phosphate synthase 1	ND			+			
Malate dehydrogenase	ND			+			

Glucosamine--fructose-6-phosphate aminotransferase [isomerizing] 1	ND			+			
Guanine nucleotide-binding protein G(I)/G(S)/G(T) subunit beta-2	ND			+			
General transcription factor II-I repeat domain-containing protein 2A			+	ND			Transcription
DNA-directed RNA polymerase I subunit RPA34			+	ND			
Nucleolar RNA helicase 2 DDX21			+		+	+	
UPF0568 protein C14orf166			+			+	
RNA polymerase II subunit A SSU72	ND			+			
RNA-binding protein 39	+		+			+	
RNA-binding protein 4	ND					+	
RNA-binding protein FUS			+	+		+	
RNA-binding protein PNO1	ND					+	
PHD and RING finger domain-containing protein 1		+		ND			mRNA processing
Probable ATP-dependent RNA helicase DDX23			+	+		+	
Probable ATP-dependent RNA helicase DDX46			+			+	
Probable ATP-dependent RNA helicase DDX47			+		+	+	
Probable ATP-dependent RNA helicase DDX6			+		+	+	

ND: Not detected, +: Presence of protein detected

Candidate interacting partners were selected with respect to their cellular function and categorized accordingly. Interestingly, the MS screen identified several proteins involved in chromatin remodelling and transcriptional regulation. Among the candidate proteins found to bind specifically to sumoylated p53, was lysine-specific demethylase KDM1A (LSD1), a modulator of chromatin structure. LSD1 is responsible for the demethylation of Lys-4 (H3K4me) and Lys-9 (H3K9me) of histone H3, thus mediating both activation and repression of specific genes, depending on which mark is targeted for de-methylation (Shi et al. 2004; Metzger et al. 2005). Similarly, components of the SWI/SNF chromatin remodelling complex SMARCC1 and SMARCC2 (also known as BAF155 and BAF170, respectively) were found in the fractions containing sumoylated p53, only. This complex is involved in both transcriptional

activation and repression of selected genes, indicating that sumoylation could influence p53's transcriptional activity.

Other transcriptional co-repressors were found associated with SUMO-1 modified p53, as is the case of transcriptional repressor YY1 and histone deacetylase HDAC2. Both YY1 and HDAC2 have been previously found to directly interact with p53, and act as negative regulators of p53's activity. YY1 is thought to repress p53's activity by both stimulating its interaction with MDM2 (and thus promoting p53's degradation), and by restraining its interactions with co-factor p300 (Grönroos et al. 2004; Sui et al. 2004). On the other hand, HDAC2 interaction can lead to p53's deacetylation and its consequent inactivation. Additionally, HDAC2 recruitment to p53-target genes results in transcriptional repression (Wagner et al. 2014). The association of these repressors specifically with SUMO-1 modified p53, but not with non-sumoylated p53, rises the possibility that these interactions could be sumoylation-dependent.

The presence of proteins with roles in transcriptional initiation (such as global transcription activator SMARCA1) and mRNA processing (a number of RNA helicases) mainly associated with non-sumoylated p53 fractions further suggests that sumoylation might enhance transcriptional repression activities of p53.

A number of proteins involved in nucleo-cytoplasmic traffic were pulled down and identified in the MS screen. Of note was the presence Exportin 7 in the fractions containing p53-SUMO-1 only, and the presence of various Importin subunits in the fractions containing non-sumoylated p53, suggesting a role for p53-sumoylation in nuclear export. The identification of a nuclear pore complex subunit (Nup155) associated with non-sumoylated p53 might also suggest that non-modified p53 localizes mostly to the nucleus and the nuclear envelope.

Other selected binding partners included proteins involved in metabolism and ubiquitylation.

3.2.3 Confirmation of p53-SUMO-1 interacting partners via Immunoprecipitation

The MS screen provided a good indication that sumoylation might indeed cause a change in the protein-protein interactions in p53. Moreover, these data suggest that SUMO modification might not only promote novel interactions, but also disturb existing ones, thus likely influencing p53's activity.

From the potential binding partners of p53-SUMO-1 retrieved by MS analysis, four were selected as the most interesting candidates, due to their role in transcriptional control. These were SMARCC1 (from here forth referred to as BAF155), YY1, LSD1 and HDAC2. In order to verify whether these interactions occurred in cells, H1299 cells were transiently transfected with pcDNA3-p53-ubc9 proteins (or an empty vector as a control), and Immunoprecipitation (IP) experiments were carried out. Transfected cells were lysed and p53 proteins were immunoprecipitated with 1µg of anti-p53 antibody (Ab-6). Soluble lysates and IPs were resolved by SDS-PAGE and immuno-blotted with anti-BAF155, anti-YY1, anti-LSD1 and anti-HDAC2 antibodies [**Figure 3.7**].

To ensure the loading of equal amounts of each sample, a small amount of soluble lysate prior to immunoprecipation (input) was included in all blots. Input lanes also function as positive controls for antibody efficiency in western blot technique. Additionally, a percentage of the flow through (FT) – lysate recovered after Immunoprecipitation – was loaded. This served as an additional indicator of the proportion of protein not bound to p53 after IP.

Perhaps surprisingly, BAF155 protein did not co-precipitate with sumoylated p53 [**Figure 3.7a**]. Moreover, BAF155 did not co-precipitate with either of the p53 proteins, as indicated by the absence of bands in the IP lanes. Although BAF155 was retrieved by MS analysis as specific binders of sumoylated p53, this interaction could not be replicated in human cells. One possible explanation is that this protein was identified as a non-specific binder. However, this possibility seems unlikely as BAF155 was identified in both MS screens, making it a reliable candidate. The inability to detect the interactions was more likely due to the low proportion of protein that interacts with p53; alternatively the interactions could be too transient and weak to be easily detected.

The use of YY1 antibody showed that interactions occurred between YY1 and both WT and sumoylation-deficient p53 proteins, as evidence by the presence of YY1 bands in both IP samples [**Figure 3.7b**]. An additional faint band can be discerned in the pcDNA3 IP negative control sample, indicating that some unspecific binding of YY1 to the p53 antibody occurred, though the strong band visible in the corresponding flow though (pcDNA3 FT) indicates that most protein was not pulled down in the IP. Although these results do not replicate in full the data obtained by MS, as YY1 does not seem to specifically target sumoylated p53, they corroborate previous studies reporting the interaction between YY1 and p53 (Grönroos et al. 2004; Sui et al. 2004).

Probing of immunoprecipitates with HDAC2 and LSD1 showed that these proteins did co-precipitate with p53 proteins [**Figure 3.7c, d**]. In the case of HDAC2, co-precipitation occurred with both $p53_{WT}$-ubc9 and $p53_{K386R}$-ubc9 [**Figure 3.7c**]. A faint band is also visible in the IP lane corresponding to the negative control pcDNA3 (vector only), indicating some unspecific binding of HDAC2 to the p53 antibody. Unexpectedly, HDAC2 co-precipitated more with the sumoylation deficient mutant $p53_{K386R}$-ubc9, as indicated by the slightly stronger band on the corresponding IP sample. However, the input bands suggest that the amount of total protein in each sample varied slightly, with more total protein in the $p53_{K386R}$-ubc9 sample. Taking that in consideration, the amount of HDAC2 that co-precipitated with $p53_{WT}$-ubc9 is comparable to that co-precipitated with $p53_{K386R}$-ubc9. Nevertheless, these results do not replicate those obtained by MS, and suggest that HDAC2 is able to interact with both sumoylated and non-sumoylated p53.

The immunoprecipitates probed with anti-LSD1 antibody revealed a faint band present in the lysate sample where $p53_{WT}$-ubc9 was expressed [**Figure 3.7d**]. The presence of LSD1 in the $p53_{WT}$-ubc9 IP sample, but not in the sumoylation deficient $p53_{K386R}$-ubc9, indicates that LSD1 could be a specific interacting partner of sumoylated p53.

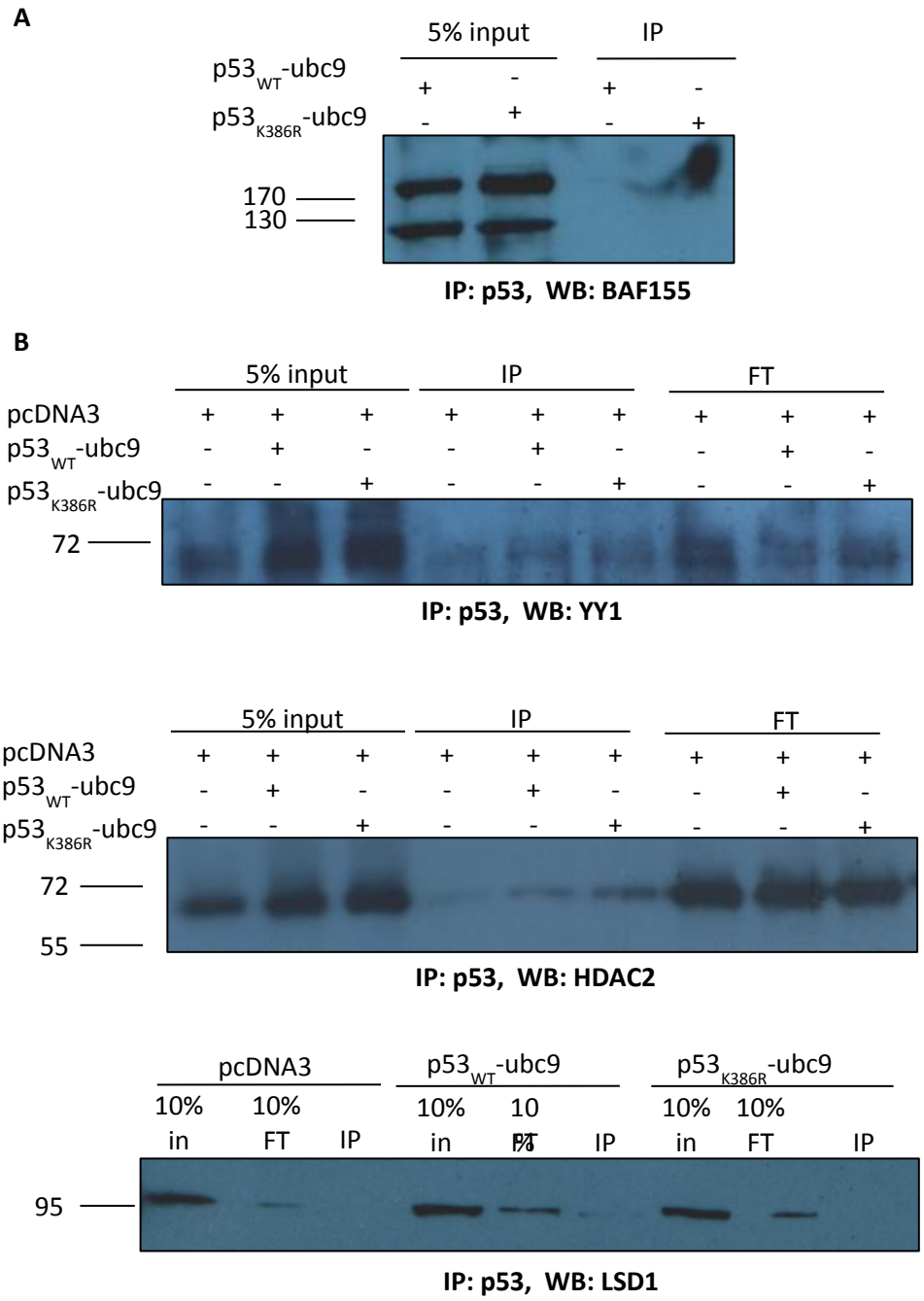

Figure 3.7. Verification of potential protein interactions with p53-SUMO-1 by IP in H1299 cells.

Immunoprecipitates were probed with BAF155 **(A)**, YY1 **(B)**, HDAC2 **(C)** and LSD1 **(D)** antibodies. H1299 cells transiently transfected with either $p53_{WT}$-ubc9 or mutant $p53_{K386R}$-ubc9 plasmids, or with an empty vector (pcDNA3) were lysed and immunoprecipitated with p53 Ab-6 antibody. The immunoprecipitates (IP) were then run on SDS-PAGE, alongside 5% input and 5% Flow through (FT), and analyzed by western blot with antibodies against the proteins of interest BAF155, YY1, HDAC2 and LSD1. Molecular weights (kDa) are indicated.

In an attempt to confirm that LSD1 selectively binds SUMO-1 modified p53, I performed the reciprocal IP, where LSD1 was pulled down by IP and the immunoprecipitates probed with anti-p53 antibody. Since endogenous LSD1 was not highly expressed in H1299 cells, in order to achieve a better yield LSD1 was co-transfected in H1299 cells, in addition to either $p53_{WT}$-ubc9 or $p53_{K386R}$-ubc9, as well as an empty vector pcDNA3. Cells were lysed and proteins were precipitated with 1µg of LSD1 antibody. Cell lysates and IPs were then analyzed by western blots probed with anti-p53 (Ab-6) antibody [**Figure 3.8**].

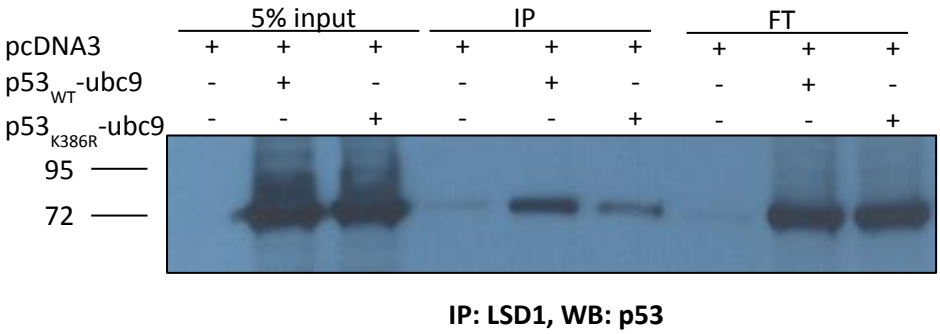

Figure 3.8. LSD1 binds preferably to $p53_{WT}$-ubc9, when compared to the sumoylation deficient mutant $p53_{K386R}$-ubc9.

H1299 cells transiently transfected with either $p53_{WT}$-ubc9 or mutant $p53_{K386R}$-ubc9 plasmids, or with an empty vector (pcDNA3) were lysed and immunoprecipitated with anti-LSD1 antibody. The immunoprecipitates (IP) were then run on SDS-PAGE, alongside 5% input and 5% Flow through (FT), and analyzed by western blot with anti-p53 (Ab-6) antibody. Molecular weights (kDa) are indicated.

Probing of LSD1-immunoprecipitated lysates with anti-p53 antibody confirmed that LSD1 is able to interact with $p53_{WT}$-ubc9. Interestingly, the reverse IP showed that LSD1 is also able to bind the sumoylation mutant $p53_{K386R}$-ubc9, but with a lower binding affinity.

These findings substantiate the pull-down/MS screen data indicating that LSD1 interacts specifically with sumoylated p53. This could be due to the presence of SIMs in LSD1, which provide a preferential binding site for LSD1. To date, no SIMs have been identified for LSD1 in

the literature; nevertheless bioinformatic tools allow the prediction of SUMO interacting motifs (SIMs), such as GPS-SUMO, which predicts sumoylation sites and SIMs (Zhao et al. 2014). This software allows the prediction of 9 different types of consensus SIMs. Using GPS-SUMO, five SUMO-interacting motifs could be identified for LSD1 with a low threshold [**Table 3.2**]. Whether any of the potential SIMs are true remains to be investigated *in vitro*, but these predictions indicate that LSD1 may preferentially interact with sumoylated p53 via non-covalent SIM interactions.

Table 3.2. Prediction of SIMs in LSD1 using GPS-SUMO 1.0

ID	Position	Peptide	Score	Cutoff	Type
LSD1	301 - 305	PTKKTGK **VIIIG** SGVSGLA	57.583	55.31	SIM
LSD1	324 - 328	LQSFGMD **VTLLE** ARDRVGG	57.468	55.31	SIM
LSD1	626 - 630	YTASGCE **VIAVN** TRSTSQT	55.389	55.31	SIM
LSD1	649 - 653	CDAVLCT **LPLGV** LKQQPPA	57.622	55.31	SIM
LSD1	686 - 690	GFGNLNK **VVLCF** DRVFWDP	58.346	55.31	SIM

SUMO interaction Treshold: Low

3.3 Discussion

3.3.1 Methodology for MS approach

This chapter aimed to investigate whether sumoylation of K386 on p53 affected the pool of protein interactions between p53 and other proteins, and thus contribute to a change in p53's activity. To determine whether this hypothesis was valid, I implemented an unbiased GST-pulldown/MS approach. Three biological samples were screened and compared among themselves: two samples were subjected to prior sumoylation *in vitro* ($p53_{WT}$-ubc9+SUMO-1 and $p53_{K386R}$-ubc9+SUMO-1) and one was not ($p53_{WT}$-ubc9). These were incubated with the same nuclear extract from H1299 cells (p53 null) and represented sumoylated ($p53_{WT}$-ubc9+SUMO-1) and non-sumoylated ($p53_{K386R}$-ubc9+SUMO-1 and $p53_{WT}$-ubc9) p53 samples. The use of non-sumoylated $p53_{WT}$-ubc9 as a negative control, even considering the presence of endogenous SUMO-1 in the nuclear protein extract, was justified, since the incubation conditions was improper for sumoylation. Furthermore, an examination of the MS data reveals that SUMO-1 protein is only present in the lower molecular weight section of the gel (in contrast to the samples subjected to prior sumoylation), indicating this was in fact a non sumoylation control [highlighted in grey in **Appendix B** and **Appendix D**].

The possibility that proteins identified in the $p53_{WT}$-ubc9+SUMO-1 fraction could be SUMO-1 partners rather than partners of sumoylated p53 was discarded by the fact that the negative control $p53_{K386R}$-ubc9+SUMO-1 was also sumoylated beforehand, and therefore the presence of exogenous SUMO-1 is present in both biological samples. Because proteins that appeared in both sumoylated and non-sumoylated controls were disregarded for this study, we could assume that proteins identified in the $p53_{WT}$-ubc9+SUMO-1 fraction were indeed potential binding partners of sumoylated p53. Similarly, we could assume that MS results were not conditioned by the presence of GST or ubc9, as all the samples compared contained GST-p53-ubc9 fused proteins and therefore any GST-non-specific binding or ubc9-partners should be ruled out by appearing in all samples.

MS is a comprehensive and useful tool for large-scale proteomics. However, some difficulties can be encountered when using such technique. When examining the list of identified targets obtained by the two MS screens [**Table 3.1**], a great variability has been found, reflecting the biological variance that occurs with different biological samples. In

addition, a direct comparison between the two data sets is most likely unachievable, as both data sets were analysed utilizing different programs. Another relevant issue is that this type of MS approach is not quantitative, meaning that abundant cellular proteins could preclude the identification of low expressing/scarce cellular proteins, and thus prevent the identification of possible interactors. One technique utilized to minimize this effect was the use of sections of the gel to be separately analysed by MS. An alternative method to LC-MS/MS is iTRAQ (isobaric Tag for Relative and Absolute Quantitation), which allows the differential isotop labeling of peptides at the N-terminus, allowing absolute quantification. It is a quantitative technique which allows the detection of changes in protein amounts.

3.3.2 Identification of Novel interaction partners

The MS approach identified numerous new potential binding partners of sumoylated p53. Moreover, several proteins were identified in the fractions containing non-sumoylated p53, which were absent in the p53-SUMO-1 fraction. This observation suggests that sumoylation may in fact alter the protein interactome of p53, not only by creating a new recognition surface for new partners, but also by abolishing existing interactions. Interestingly, many of the proteins identified were involved in transcriptional regulation and chromatin remodeling, suggesting a role for SUMO modification in the transcriptional activity of p53.

3.3.2.1 Chromatin Remodeling and Transcriptional Regulation proteins

The SWI/SNF core components BAF155 and BAF170 were found associated with sumoylated p53. SWI/SNF chromatin remodeling complex is an ATP-dependent multi-subunit complex that alters the position of nucleosomes, changing the accessibility of DNA in promoter regions (Hohmann & Vakoc 2014). Several SWI/SNF subunits have been shown to have tumour suppressor abilities, and are mutated in a variety of cancers (Reisman et al. 2009).

Various subunits of the SWI/SNF complex has been previously shown to interact with p53. For example, the ATPase subunit BGR1 is able to bind to p53 via a unique proline rich region in BGR1, and this interaction results in the inactivation of p53 activity and increased

turnover (Naidu et al. 2009). In another publication, yeast two-hybrid assays revealed that p53 is able to recruit SWI/SNF complex through its direct interaction with BAF60a, which results in the repression of p53-target genes involved in cell cycle arrest and apoptosis (Oh et al. 2008). Other core subunits of SWI/SNF complex seem to promote p53's activation, as is the case of the core subunit SNF5 (BAF47), which directly interacts with p53, stimulating transactivation of cell cycle arrest genes (Lee et al. 2002). Moreover, cells where SNF5 was knockdown had impaired p53-dependent transcription of p21 and MDM2, possibly caused by a decrease in p53 translation (Xu et al. 2010).

Regarding BAF155 and BAF170, no published data exist on possible interactions with p53. My data revealed that these components were identified specifically associated with sumoylated p53. In particular BAF155 was pulled down and identified in both pull-down/MS screens as a potential p53-SUMO-1 partner, making it a strong candidate interactor. Interestingly, BAF155 was shown to directly interact with mSin3A, a component of the transcriptional co-repressor complex Sin3 (Sif et al. 2001). Moreover, Wu and Chiang demonstrated that chromatin bound SUMO-modified p53 was able to recruit mSin3A more efficiently, when compared to non-modified p53 (Wu & Chiang 2009a). The association of sumoylated p53 with transcriptional modulators such as BAF155 and mSin3A could promote chromatin condensation, resulting in the transcriptional repression that has been linked with sumoylation. Nevertheless, mSin3A was not detected in either of the GST-pull-down/MS screens, possibly reflecting the low abundance of the protein in the nuclear extracts used.

Although BAF155 was identified by both MS runs as a specific interactor of sumoylated p53, IPs failed to demonstrate any interactions with p53 irrespective of the presence of sumoylation. This could point to another matter to consider when analysing MS data, as some proteins detected by MS could be unspecific binders. In this case, proteins could unspecifically bind to the glutathione matrix, which with insufficient washes, could appear as possible candidates. As such, the data obtained by MS should not be taken as irrefutable fact, but rather as a starting screening for large-scale proteomics that needs to be further validated.

Alternatively, the inability to detect these interactions in cells could reflect the low amount of BAF155 that interacts with p53. As mentioned above, LC-MS/MS is not a quantitative method, and thus the amount of protein detected is not taken into consideration

in MS analysis. Therefore, the proportion of BAF155 that interacts could be too small to be detectable by IP. Another possibility is that the interactions are too weak and/or transient, and thus not easily reproduced by IP. The exogenous expression of BAF155, or the use of a crosslinking agent such as EGS to crosslink the proteins in the cell should stabilize the interactions and thus facilitate the detection of protein interactions.

YY1 and HDAC2 were two other co-repressor proteins identified as potential interacting partners of sumoylated p53. As mentioned in section **3.2.2**, both these proteins associate with p53 and repress p53 activity, either by suppressing its transactivation functions or promoting its degradation (Grönroos et al. 2004; Sui et al. 2004). HDAC2 is also responsible for chromatin remodeling, actively deacetylating histone proteins in the promoter regions of target genes, and thus promoting transcriptional repression (Wagner et al. 2014). The observation that presence of these proteins was restricted to the fraction containing sumoylated p53 only, prompted me to investigate the possibility that these interactions could be specific and occur only when p53 is modified by SUMO-1. However, p53-immunoprecipitates probed with either YY1 or HDAC2 revealed that interactions of both these proteins with p53 occurred, irrespective of p53's sumoylation. The recruitment of these factors to p53 is, therefore, sumoylation independent.

3.3.2.2 Nucleo-cytoplasmic Transporters

Some reports suggest that p53 sumoylation might contribute to the subcellular localization of p53, arguing that sumoylation of p53 can lead to its nuclear export and cytoplasmic accumulation (Carter et al. 2007; Carter & Vousden 2008). Accordingly, proteins involved in nucleo-cytoplasmic transport were retrieved in the MS screening. The trafficking of proteins within the cell, and in particular in and out of the nucleus, is controlled by the nuclear pore complex (NPC). Importins and exportins permit the import and export of macromolecules and proteins to the nucleus, by recognizing either NLS or NES sequences, respectively, and transporting them via the NPC. The co-precipitation of Importin subunits with non-sumoylated p53 controls, indicates that unmodified p53 could be restricted to the

nucleus and nuclear membrane. On the contrary, Exportin-7 was found associated exclusively with sumoylated p53, indicating that p53 sumoylation could promote its nuclear export.

Although this data only provides circumstantial evidence, it corroborates previous findings that sumoylation of C-terminal K386 on p53 promotes its export from the nucleus and cytoplasmic localization. Nonetheless, these interactions would inevitably have to be confirmed by IP.

3.3.2.3 Metabolism-associated proteins

Interestingly, a number of proteins involved in metabolism were found associated with p53-SUMO-1. The role of p53 in metabolism is an emerging new field of study, and the traditional view of p53 as a tumour suppressor is challenged by accumulated evidence of its role in maintaining cellular homeostasis. It is now evident that p53 is not only able to activate pathways that prevent cell growth and survival, but is also involved in the regulation of numerous other processes, including glycolysis, glutaminolysis, mTOR signaling, mitochondrial oxidation, nucleotide biosynthesis, anti-oxidant response and autophagy (Bensaad & Vousden 2007; Maddocks & Vousden 2011).

With many metabolic proteins associated with sumoylated p53, it is tempting to speculate whether metabolic functions of p53 could in some way be triggered by post-translational modifications, particularly by SUMO-1 modification. Further investigation on this matter should elucidate how p53's function in the regulation of metabolic processes is activated.

3.3.3 SUMO-1 modified p53 recruits LSD1

The Lysine-specific demethylase LSD1 was one of the proteins predicted by the MS screen to be associated specifically with sumoylated p53. LSD1 is mainly responsible for the demethylation of Lys-4 (H3K4me), but in certain conditions it is also able to demethylate Lys-9 (H3K9me) of histone H3 (Metzger et al. 2005). H3K4me1/me2 is a chromatin mark associated with active transcription, whereas H3K9me1/me2 is a heterochromatin mark associated with transcriptional repression. Consequently, depending on the lysine targeted, LSD1 can be associated with transcriptional repression or transcriptional activation. It can act as a

transcriptional co-repressor by removing methyl groups from H3K4, but in association with the androgen receptor, LSD1 specificity shifts towards H3K9, resulting in enhanced target gene transcription (Metzger et al. 2005).

A previous study has shown that sumoylation of the transcriptional co-repressor CtBP is essential for the repression of its transcriptional activity, via the recruitment of CoREST complex, HDACs1/2, G9a and LSD1 (Shi et al. 2003; Garcia-Dominguez & Reyes 2009). In a similar way, sumoylated p53 might recruit LSD1, resulting in the altered transactivation of target-genes. Additionally, LSD1 is responsible for the de-methylation of p53 on K370, leading to the repression of p53 apoptotic activity (Huang et al. 2007). All these lines of evidence led me to investigate whether p53 sumoylation promotes the recruitment of LSD1.

The interactions predicted by MS were confirmed by IP and subsequent reciprocal IP, showing that LSD1 has a strong preference to interact with sumoylated p53, when compared to the sumoylation-deficient mutant. These results validate the ones obtained by MS analysis, and provide the first evidence of a sumoylation-dependent binding partner for p53. Furthermore, these data support the initial hypothesis, in which p53 modification by SUMO-1 alters the pool of protein-protein interactions in p53, both by hindering and promoting novel interactions.

The identification of LSD1 as a specific binding partner of sumoylated p53 presents a novel mechanism by which sumoylation alters p53's function. The recruitment of LSD1 upon p53 sumoylation might alter gene activity in two ways: First, by de-methylation of histone marks in the promoter region of p53-responsive genes. Acting most likely as a co-repressor, LSD1 could catalyse de-methylation of H3K4, thus stimulating gene repression. Secondly, by de-methylating K370me2 on p53 itself. Di-methylation of K370 on p53 as an activating role on p53 transcriptional activity, through the formation of a new interacting surface for co-activator 53BP1 (p53 binding protein 1). By preventing the accumulation of K370me2 mark, LSD1 leads to the loss of p53 association with 53BP1, thus maintaining p53 in an inactive state (Huang et al. 2007). The two mechanisms proposed are not mutually exclusive, as LSD1 could function at both p53 and chromatin level. In either case, the association of p53 with LSD1 seems to be preferential when a SUMO moiety is present, at least in the case of SUMO-1.

The investigation carried out in this chapter begins to unravel the unknown functions of p53 sumoylation. The data shown here presents a novel mechanism by which sumoylation may affect p53 interactions, through both the recruitment of transcriptional regulators as well as by abolishing existing interactions. Further analysis on the changes of interacting partners upon SUMO modification of p53 should provide additional insight into the mechanism by which p53 sumoylation alters its function.

CHAPTER 4

Sumoylation Modulates p53 activity

Chapter 4. Sumoylation Modulates p53 activity

4.1 Introduction

Many post-translational modifications alter the transactivation functions of several transcription factors. As discussed in section **1.2.5.2**, p53 activity is highly influenced by PTMs, which, among other functions, contribute for either the enhancement or attenuation of its transcriptional activity. The modulation of p53's transcriptional activity by SUMO has been proposed since its discovery, in 1999 (Gostissa et al. 1999). However, the role of sumoylation in the transcriptional activity of p53 has been an ongoing matter of debate, with different publications reporting increased (Gostissa et al. 1999; Rodriguez et al. 1999), decreased (Wu & Chiang 2009a; Stindt et al. 2011) and even unchanged transcriptional potential (Kwek et al. 2001).

The previous chapter established that SUMO-1 modification of p53 provides an additional binding interface for the interaction with transcriptional regulators, namely LSD1. Additionally, it provides circumstantial evidence that sumoylation might disrupt potential interactions between p53 and transcriptional co-activators. Since protein sumoylation has been generally linked with transcriptional repression by means of recruitment of transcriptional co-repressors (Gill 2005), it is possible that p53 sumoylation might hamper its transcriptional functions. In this chapter, I aim to elucidate the role of sumoylation on p53's transcriptional activity, and test the proposed hypothesis in which modulation of p53's transactivation functions is achieved through the recruitment and/or removal of transcriptional regulatory proteins.

4.2 Results

4.2.1 Sumoylation affects p53-target gene expression and p53-binding activity in H1299 cells

Investigation of the effect of SUMO on the transcriptional activity of p53 was assessed by measuring endogenous levels of p53-target gene transcripts in p53-null cell line H1299. Three *bona fide* p53-responsive genes were analysed for this matter: p21, PUMA and BAX. Cell cycle arrest gene p21 (CDKN1a) was the first p53-responsive gene to be identified (Bieging & Attardi 2012). p21 is a cyclin-dependent kinase inhibitor, which retrains the activity of cyclin-CDK complexes, and thus inhibit cell cycle progression. p53 is also able to promote the apoptotic response, either via intrinsic or extrinsic signalling pathways. The intrinsic apoptotic pathway is determined by the activation of pro-apoptotic genes, such as PUMA and BAX. BAX belongs to the Bcl-2 pro-apoptotic family of proteins, which are responsible for mitochondrial membrane permeabilization and release of cytochrome c, and further activation of effector caspases. Bcl-2 pro-survival proteins, such as Bcl-2 and Bcl-XL, bind to BAX and thus prevent mitochondrial outer membrane permeabilization. PUMA belongs to the BH3-only (Bcl-2 Homology Domain 3) pro-apoptotic Bcl-2 family, which disturb these interactions and allow BAX to promote apoptosis (Bieging & Attardi 2012).

The highly dynamic nature of protein sumoylation results in an overall low percentage of sumoylated substrates *in vivo* (usually less than 5%), which represents a challenge to study the effects of SUMO modification. Previous attempts to increase the pool of sumoylated proteins in the cell included the fusion of the protein of interest with SUMO-1 (Carter & Vousden 2008). However, this method did not take in consideration that fused p53-SUMO-1 did not necessarily correlate with the covalent attachment of SUMO-1 to p53. This is evidenced by the different results obtained by the use of a p53-SUMO-1ΔGG mutant, in which SUMO-1 lost the ability to covalently attach to target lysines. A different approach, introduced by Jakobs et al. was the use of a UFDS (ubc9-fusion-directed sumoylation) system, where p53 is fused with the E2 conjugating enzyme ubc9 (Jakobs et al. 2007). The use of this system in p53-null H1299 cells proved to be an efficient way to enhance p53 sumoylation *in vivo*.

Thus, H1299 cells were transiently transfected with two versions of the fused p53-ubc9 constructs, one containing WT p53 and one with a lysine to arginine substitution in the

sumoylation residue at position 386 (K386R) [**Figure 4.1**]. Part of the collected cells were used for western blot, to assess the efficiency of transfection. RNA was extracted from the remaining cells, reverse transcribed into cDNA and analysed by quantitative Real time PCR (qRT-PCR). As expected, endogenous expression of p53-target genes p21, PUMA and BAX is elevated by 2 to 4 fold after transfection with p53 constructs, when compared to the empty vector control pcDNA3. The differential activation among the p53-targets reflects previous studies indicating that p53 has differential selectivity for different target-genes. For example, p53 displays higher binding affinity to certain REs of target-genes such as p21, compared to pro-apoptotic genes PUMA or BAX (Weinberg et al. 2005).

Interestingly, wild type p53-ubc9 showed a significantly reduced ability to activate p53-target genes p21 and PUMA, when compared to the sumoylation deficient mutant $p53_{K386R}$-ubc9 [**Figure 4.1b**]. This trend is also visible in the transcript levels of BAX, although with a less evident effect.

The western blots performed with anti-p53 (Ab-6) antibody confirmed the efficiency of the transfection method. p53-ubc9 constructs are visible at a molecular range of 72kDa, with sumoylated p53-ubc9 at 95kDa (indicated with a star *) [**Figure 4.1a**]. Actin was used to normalize the amount of lysate loaded, and assure equal transfection efficiency of both p53 constructs. Additionally, protein levels of target-genes p21 and PUMA were analysed. Although the changes are minimal, protein level of p21 and PUMA seem to follow the same trend as indicated by qRT-PCR, with an increased level of expression in cell expressing K386R mutant, comparing to the wild type p53. These results indicate that p53 sumoylation leads to a decrease in transcriptional potential of p53, leading to reduced transcription of p53-responsive genes p21 and PUMA, and the consequent decrease of the corresponding proteins.

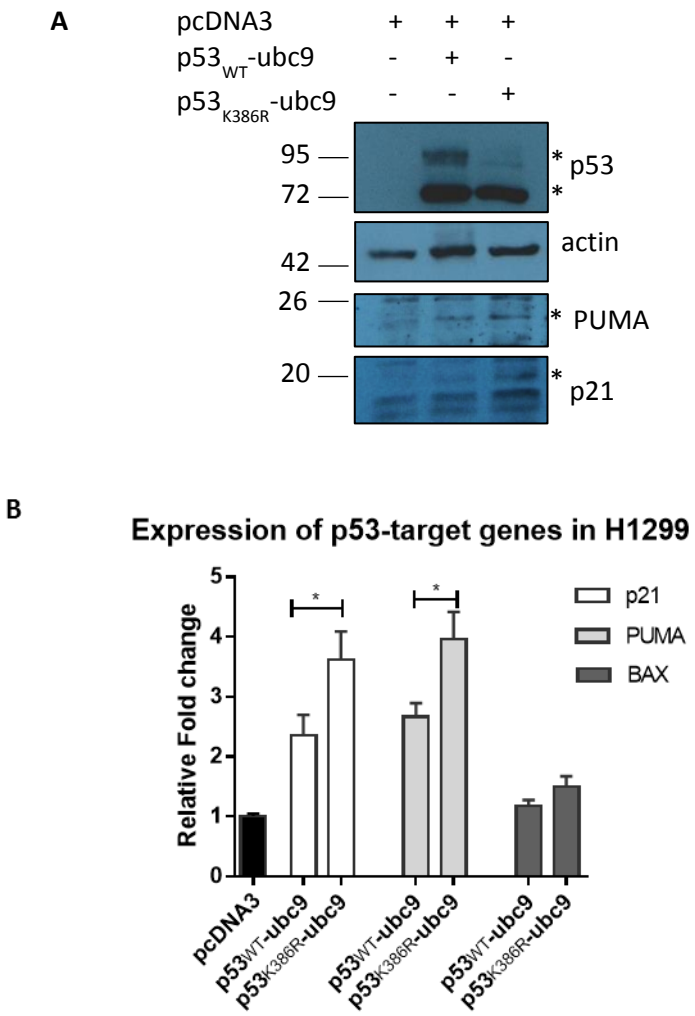

Figure 4.1. p53-target gene expression is affected by p53 Sumoylation in H1299 cells.

H1299 cells were transiently transfected with $p53_{WT}$-ubc9 or mutant $p53_{K386R}$-ubc9 constructs, along with an empty vector (pcDNA3). Cells were collected and 1/5 was analysed by western blot **(A)**, whereas the remaining were used for RNA isolation and cDNA synthesis to be analysed by quantitative real-time PCR (qRT-PCR) **(B)**.

(A) Representative western Blot showing over-expression of p53 constructs to confirm efficiency of transfection, and induction of p53-target genes p21 and Puma. Molecular weights (kDa) are indicated. The bands corresponding to the proteins of interest are indicated with a star (*).

(B) Real-time qPCR showing differential gene expression of p53-target genes upon Sumoylation. Results are displayed as mean of $2^{\Delta\Delta}$Ct values obtained from 3 independent experiments. Error bars represent the standard error of the mean. *p-value<0.05 as calculated by an unpaired student t-test.

To further investigate the effect of SUMO on p53's transactivation function, p53 protein was co-expressed along with SUMO-1 or SUMO-2 and the E3 SUMO ligase PIASx [**Figure 4.2**]. Western blots were performed to confirm successful transfection of the plasmids, and to visualize expression of p53 targets at the protein level. In **Figure 4.2a** over-expression of p53, FLAG-SUMO and myc-PIASx is evident after probing with the appropriate antibodies. p53 is sumoylated when co-transfected with SUMO proteins, evidenced by the higher molecular band of 72kDa present in the blots probed with anti-p53 and also anti-FLAG antibodies. As expected, the presence of E3 SUMO ligase PIASx in cells seems to enhance p53 sumoylation, which is reflected by stronger, darker bands in the samples containing both PIASx and SUMO proteins. p21 and PUMA protein expression was also assessed via western blot. As predicted, transfection of H1299 cells with p53 lead to the increase of p21 and PUMA protein levels. However, over-expression of p53 in conjunction with SUMO proteins significantly decreased the levels of both p21 and PUMA. This decrease was more noticeable when PIASx was co-expressed with p53 and SUMO proteins, indicating a correlation between levels of p53 sumoylation with reduced levels of p53-target gene expression.

Next, to investigate whether the reduced levels of protein related with reduced expression at mRNA level, quantitative real-time PCR was performed [**Figure 4.2b**]. Analysis by qRT-PCR revealed that levels of p21 were significantly reduced after co-expression of SUMO and PIASx proteins. However, levels of PUMA and BAX transcripts did not show the same variation upon SUMO and PIASx transfection.

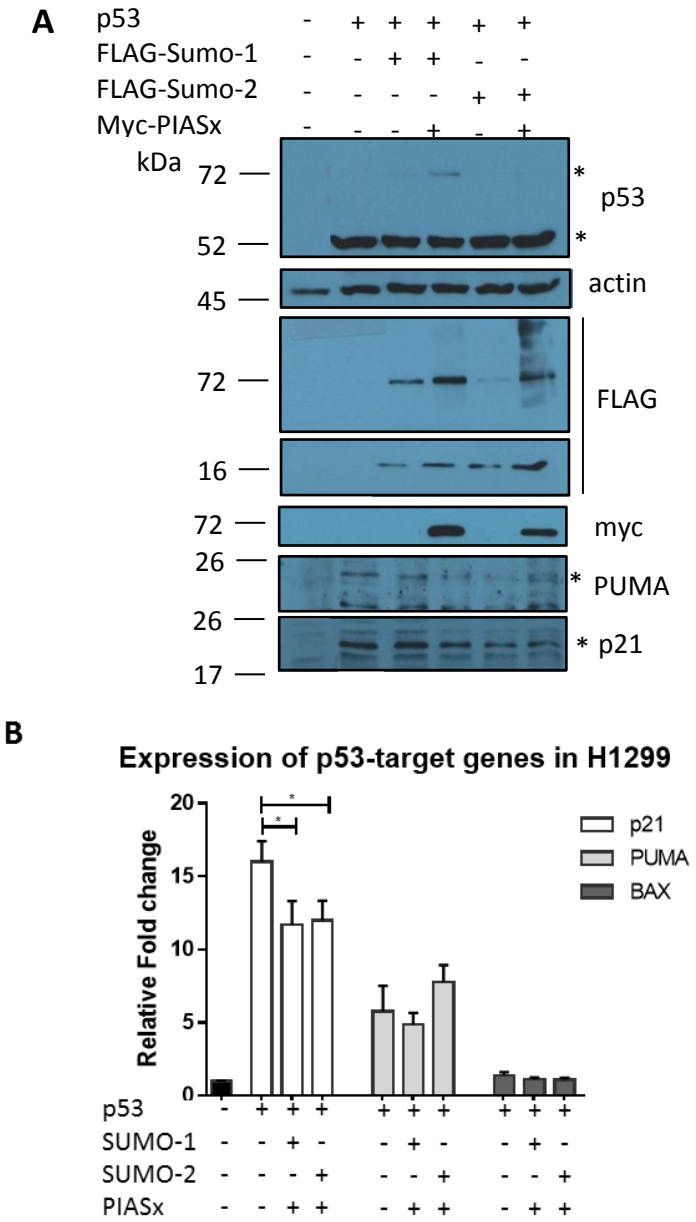

Figure 4.2. SUMO overexpression leads to a decrease in p53-dependent gene expression in H1299 cells. H1299 cells were transiently transfected with $p53_{WT}$, FLAG-SUMO-1, FLAG-SUMO-2 and Myc-PIASx, and analysed by qPCR.

(A) Representative western blot showing over-expression of p53, SUMO-1, SUMO-2 and PIASx proteins and induction of p53-target genes p21 and PUMA. Molecular weights (kDa) are indicated. The bands corresponding to the proteins of interest are indicated with a star (*).

(B) Real-time qPCR showing differential gene expression of p53-target genes upon Sumoylation. Results are displayed as mean of $2^{\Delta\Delta}$Ct values obtained from 3 independent experiments. Error bars represent the standard error of the mean. *p-value<0.05 as calculated by a paired student t-test.

A possible explanation to the diminished capacity of SUMO-p53 to induce transcription is the reduced binding of p53 to the promoter region of these genes. To investigate whether that was true, I performed chromatin Immunoprecipitation assays (ChIP). ChIP is a technique that allows the study of interactions between proteins and DNA, by detecting whether specific proteins are associated with specific regions of chromatin. Firstly, proteins associated with DNA are cross-linked in the cells. The DNA is then shredded into small fragments via sonication, and the protein-DNA complexes are pulled down via immunoprecipitation with the appropriate antibody. Finally, the protein-DNA complexes are dissociated and the DNA amplified via quantitative RT-PCR. Because I wanted to assess p53's ability to bind to the p53-target genes tested, the regions amplified by qRT-PCR were the promoter regions of p21, PUMA and BAX.

Intereatingly, ChIP analysis revealed that rather than preventing p53 from binding to the promoters, sumoylation leads to an enrichment of p53 to these promoters [**Figure 4.3**]. In cells transfected with fused proteins p53-ubc9, there is a significant increase in the binding of $p53_{WT}$-ubc9 to the promoter regions of p21 and PUMA, compared to the sumoylation deficient mutant $p53_{K386R}$-ubc9 [**Figure 4.3a**]. Similarly, cells co-transfected with $p53_{WT}$ together with SUMO proteins and PIASx, display an increased ability to bind to p53-target promoter p21 and PUMA in the case of SUMO-2 co-transfection, when compared to p53 alone [**Figure 4.3b**].

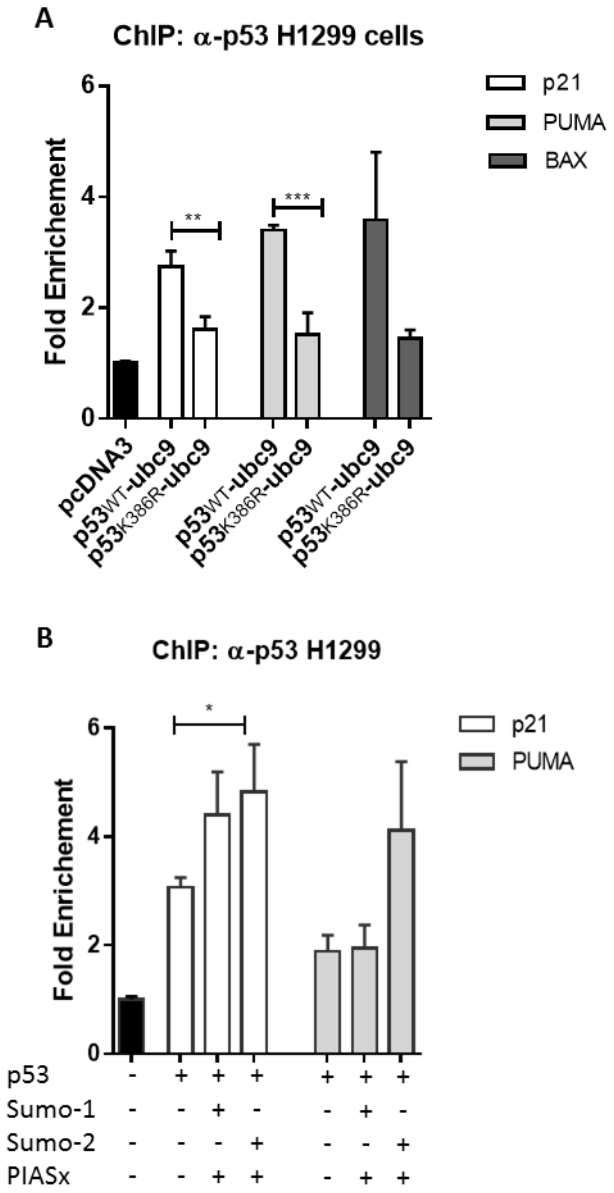

Figure 4.3. Sumoylation of p53 leads to an enrichment of p53 to target-gene promoters p21, PUMA and BAX, in H1299 cells.

H1299 cells were transfected with $p53_{WT}$-ubc9 or mutant $p53_{K386R}$-ubc9 constructs **(A)** or co-transfected with $p53_{WT}$, FLAG-SUMO-1, FLAG-SUMO-2 and Myc-PIASx **(B)**. Cells were then cross-linked and analysed by ChIP with anti-p53 antibody. Representative western blots showing transfection efficiency are shown in **Figure 4.1a** and **Figure 4.2a**.

ChIP was quantified relative to input and the housekeeping gene actin, according to the comparative $^{\Delta\Delta}$Ct-method. Results are displayed as mean of $2^{\Delta\Delta}$Ct values obtained from 3 independent experiments. Error bars represent the standard error of the mean. *pvalue<0.05, **pvalue<0.001, ***p-value<0.0005 as calculated by an unpaired student t-test.

These findings indicate that sumoylation leads to the enrichment of p53 on the target promoters, in particular p21 and PUMA, which correlates with a decreased transcription of these target-genes. Although unexpected, the increased binding of p53 to target promoters upon sumoylation is compatible with the hypothesis stipulated in **Chapter 3**, where the covalent attachment of SUMO to p53 would stimulate interactions with transcriptional co-repressors. When bound to chromatin, sumoylated p53 could promote the recruitment of co-repressor proteins, and thus lead to transcriptional inactivation. To ascertain this possibility, I examined chromatin marks associated with these promoters. Histone H3 acetylation is a chromatin mark commonly associated with active gene expression. In contrast, di- and tri-methylation of Lysine 9 of histone H3 is associated with gene repression and heterochromatin formation (Yan & Boyd 2006). Therefore, regions enriched with H3 acetylation (H3ac) marks should have active gene expression, while regions enriched with H3K9 methylation (H3K9me) indicate gene silencing.

ChIP analysis of chromatin marks was carried out via immunoprecipitation with anti-acetylated H3 and anti-trimethylated H3K9 antibodies, in cells overexpressing either WT or K386R p53-ubc9 fused proteins. Enrichment of histone H3 acetylation (H3ac) is reduced in the presence of $p53_{WT}$-ubc9 in the promoter regions of the target genes tested, when compared to K386R mutant, particularly in the PUMA promoter [**Figure 4.4a**]. Although to a lesser extent, p21 promoter seems to also have enriched H3ac marks when sumoylation-deficient mutant K386R is over-expressed. Conversely, histone H3 lysine 9 methylation (H3K9me) seems to be more abundant in promoters of p21 and PUMA in cells expressing WT p53, compared to cells transfected with K386R mutant [**Figure 4.4b**]. The promoter region of BAX does not show enrichment or reduction of these marks, suggesting that activation/silencing of this gene is not affected by p53 sumoylation. This observation is consistent with results observed by qRT-PCR, where the expression pattern of BAX does not change significantly in the presence of p53 sumoylation [**Figure 4.1b**].

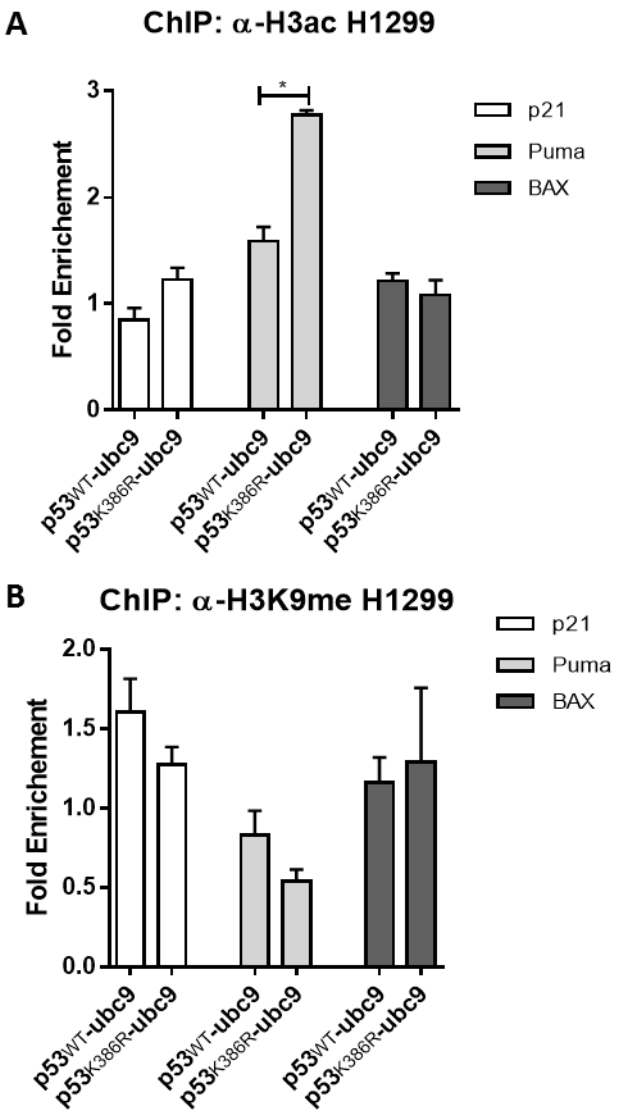

Figure 4.4. Sumoylation of p53 leads to differential enrichment of chromatin marks on Histone H3 on p53-target promoters p21, PUMA and BAX, in H1299 cells.

H1299 cells were transfected with $p53_{WT}$-ubc9 or mutant $p53_{K386R}$-ubc9 constructs. Cells were then cross-linked and analysed by ChIP with anti-H3ac and anti-H3K9me^3 antibodies.

ChIP analysis shows reduced H3 acetylation upon p53 sumoylation **(A)**, whereas H3 Lysine 9 tri-methylation (H3K9me), a known repressive chromatin mark, increases upon p53 sumoylation **(B)**. ChIP was quantified relative to input, according to the comparative $^{\Delta\Delta}$Ct-method. Results are displayed as mean of $2^{\Delta\Delta}$Ct values obtained from 3 independent experiments. Error bars represent the standard error of the mean. *p value<0.05, as calculated by an unpaired student t-test.

The presence of reduced H3 acetylation and increased H3K9 methylation associated with the promoters of p21 and PUMA in cells with sumoylated p53 indicates that these regions are less permissive for gene expression. Furthermore, these findings substantiate the results retrieved by qRT-PCR, whereby p53 sumoylation dampens the expression of p53-targets p21 and PUMA.

Chromatin remodelling is an important step to allow the transcription initiation function of p53. Upon binding to the RE within the promoter, p53 is involved in the recruitment of co-activators such as Histone Acetyltransferases (HATs) and Histone Methyltransferases (HMTs), which acetylate and methylate histones in the vicinity of the promoter region. The recruitment of HATs such as CBP/p300, PCAF or TIP60 leads to the alteration of chromatin structure that facilitates the recruitment of the pre-initiation complex (PIC), which in turn permits p53 transactivation of target genes. Conversely, the recruitment of transcriptional co-repressors such as Histone deacetylases (HDACs) causes the deacetylation of histones, leading to chromatin condensation and heterochromatin formation of these regions, and thus promoting gene silencing (Beckerman & Prives 2010).

To further investigate whether the observed chromatin marks in target promoters are a result of the recruitment of co-transcription factors, ChIP assays were carried out for co-repressor HDAC2 and co-activator CBP [**Figure 4.5**]. Indeed, chromatin Immunoprecipitation of HDAC2 revealed a significant enrichment of this co-repressor to the promoter of p21 and PUMA in cells where sumoylated p53 is present [**Figure 4.5a**]. On the contrary, analysis of CBP chromatin Immunoprecipitation showed a higher association of CBP to the promoter region of target genes in cells expressing sumoylation deficient mutant K386R [**Figure 4.5b**]. The enrichment of transcriptional co-repressor HDAC2 and the reduced binding of CBP to these promoters upon p53 sumoylation, correlates with the decrease of Histone H3 acetylation shown in **Figure 4.4a**. Moreover, the differential binding affinities of these co-factors are dependent on p53 sumoylation status, indicating that sumoylation may modulate p53's transcriptional activity both through the recruitment of transcriptional co-repressors, such as HDAC2, as well as by hindering the recruitment of co-activator factors such as CBP.

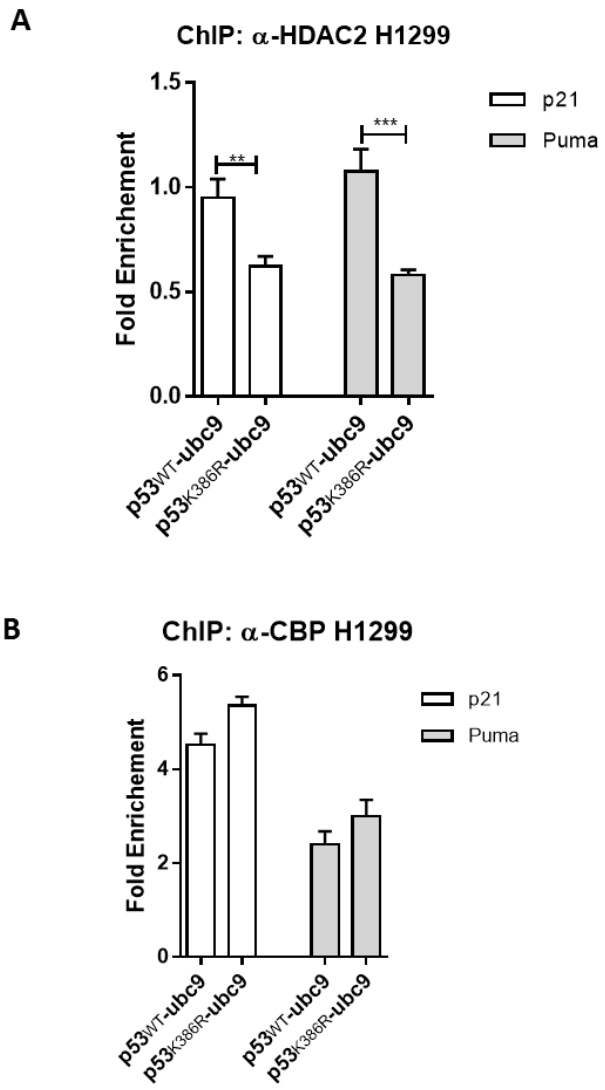

Figure 4.5. Sumoylation of p53 leads to differential enrichment of co-repressor HDAC2 and co-activator CBP on p53-target promoters' p21 and PUMA, in H1299 cells.

H1299 cells were transfected with $p53_{WT}$-ubc9 or mutant $p53_{K386R}$-ubc9 constructs. Cells were then cross-linked and analysed by ChIP.

(A) HDAC2 enrichment to p53-target promoters is reduced in the presence of the sumoylation deficient mutant $p53_{K386R}$-ubc9, when compared to the wild type.

(B) CBP protein binds more efficiently to p53-target promoters in the presence of the sumoylation deficient mutant $p53_{K386R}$-ubc9, when compared to the wild type.

ChIP was quantified relative to input and the housekeeping gene actin, according to the comparative ΔΔCt-method. Results are displayed as mean of $2^{\Delta\Delta}$Ct values obtained from 3 independent experiments. Error bars represent the standard error of the mean. **p-value<0.001, ***p-value<0.0005 as calculated by an unpaired student t-test.

The results shown in this section evidence that p53 sumoylation has small but significant effects in the transactivation activity of p53. SUMO modification of p53 leads to a decrease in its transactivation potential, which is coupled with an increased binding ability of p53 to target-promoters, suggesting that sumoylation promotes p53 binding to target promoters, resulting in transcriptional repression. Accordingly, H3ac chromatin mark and co-activator CBP's enrichment is reduced in the presence of p53 sumoylation in the promoter regions of the target genes tested. Conversely, HDAC2 recruitment to these promoter regions seems to increase in the presence of p53 sumoylation, along with the presence of H3K9me mark. In sum, these results indicate that p53 sumoylation can act as a signal for the recruitment of co-repressor complexes such as HDAC2 to the nearby chromatin, and thus contribute to transcriptional repression of p53-target genes.

4.2.2 Endogenous p53 transactivation is affected by SUMO

In order to determine whether the results obtained in H1299 cells were transferrable to other cell lines, I investigated sumoylation-dependent p53 activity in two other cell lines, U2OS and HCT116 cells. U2OS is a human osteosarcoma cancer cell line, and HCT116 cells derive from human colorectal carcinoma. Both these cells lines have endogenous expression of p53, allowing the study of the effect of sumoylation on endogenous p53.

The level of transcripts for p53-targets p21, PUMA and BAX was monitored by qRT-PCR, from U2OS cells transiently transfected with SUMO-1, SUMO-2 and the E3 ligase PIASx. Western blots confirmed the transfection efficiency of transfection of the different plasmids. SUMO-modified p53 is visible with anti-FLAG antibody at approximately 72kDa, and SUMO-2 poly-conjugates at higher molecular weights (indicated with *)[**Figure 4.6a**]. Doxorubicin, a chemotherapeutic drug that causes DNA double-strand breaks, was utilized to stimulate stabilization and activation of p53, observable by a significant increase in the p53 protein level in cells treated with 0.5µM of doxorubicin [**Figure 4.6a**]. Doxorubicin treatment also led to a significant increase in the activation of p53-dependent transcription, shown by a 3-4 fold increase in target-gene expression quantified by qRT-PCR [**Figure 4.6b**]. Interestingly, over-expression of sumoylation machinery SUMO-1 or SUMO-2, in combination with PIASx led to a significant decrease in gene expression of p53 targets [**Figure 4.6b**]. A very similar effect was seen for both SUMO-1 and SUMO-2 isoforms, indicating that both isoforms lead a decrease in p53's transcriptional activity. These results were consistent for all p53-responsive genes analysed, and the presence of doxorubicin does not seem to change the pattern of response. This indicates that endogenous p53 has impaired ability to activate target genes p21, PUMA and BAX upon over-expression of SUMO proteins.

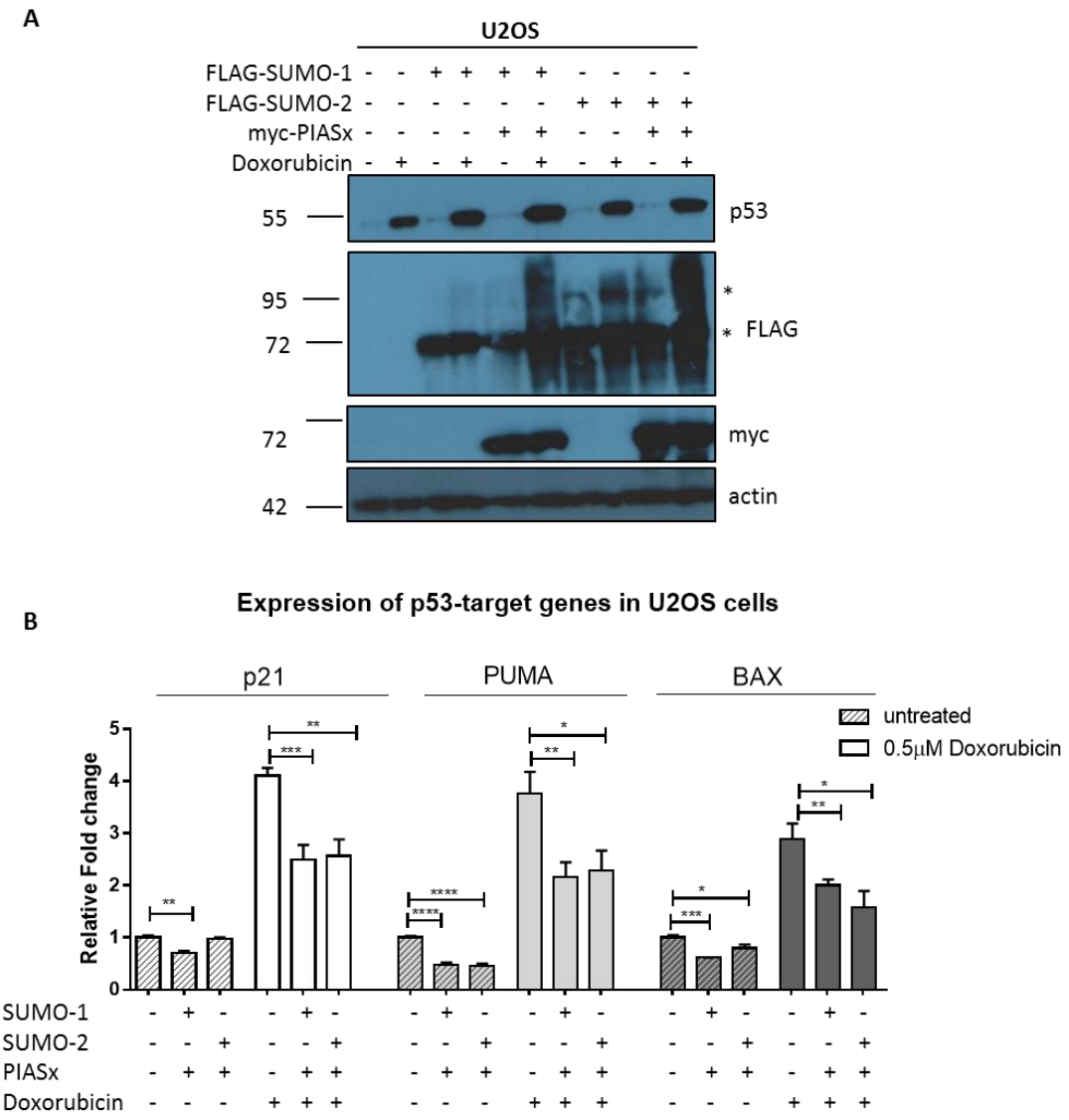

Figure 4.6. p53-target gene expression is affected by p53 Sumoylation in U2OS cells.

U2OS cells were transiently transfected with FLAG-SUMO-1, FLAG-SUMO-2 and Myc-PIASx, and analysed by qRT-PCR.

(A) Representative western blot showing over-expression of FLAG-SUMO-1, FLAG-SUMO-2 and myc-PIASx constructs, and expression of p53 with and without treatment with 0.5μM Doxorubicin. * Shows sumoylated p53 proteins.

(B) Real-time qRT-PCR showing differential gene expression of p53-target genes upon over-expression of sumoylation machinery. Results are displayed as mean of $2^{\Delta\Delta}$Ct values obtained from 3 independent experiments. Error bars represent the standard error of the mean. *pvalue<0.05,**pvalue<0.005, ***p-value<0.001, ****p-value<0.0001 as calculated by an unpaired student t-test.

To investigate whether the changes in transcription of target genes were a result of chromatin remodeling, I next examined the chromatin marks associated with the promoter region of the genes tested. Histone H3 acetylation (H3ac) and Histone H3 Lysine 9 tri-methylation (H3K9me), marks commonly associated with activation and repression, respectively, were assessed via ChIP assay [**Figure 4.7**]. Expectedly, H3 acetylation is enriched at the target-promoters in cells treated with doxorubicin, consistent with the activation of transcription of p21, PUMA and BAX upon treatment. Moreover, over-expression of SUMO proteins in combination with PIASx leads to a clear decrease of H3 acetylation in p21 and BAX promoters with and without treatment, as well as in PUMA promoter in cells treated with doxorubicin [**Figure 4.7a**]. Conversely, untreated cells show a significant increase in H3K9 tri-methylation of target-promoters when the SUMO machinery is over-expressed [**Figure 4.7b**]. The patterns of H3K9methylation were not significantly affected in cells treated with doxorubicin; this is probably the result of the overall gene activation caused by doxorubicin treatment, which leads to the depletion of H3K9me marks from these regions.

The overall decrease in H3ac and increase in H3K9me associated with p53-target promoters upon over-expression of the sumoylation machinery correlates with the decreased expression of p21, PUMA and BAX seen by qRT-PCR [**Figure 4.6**].

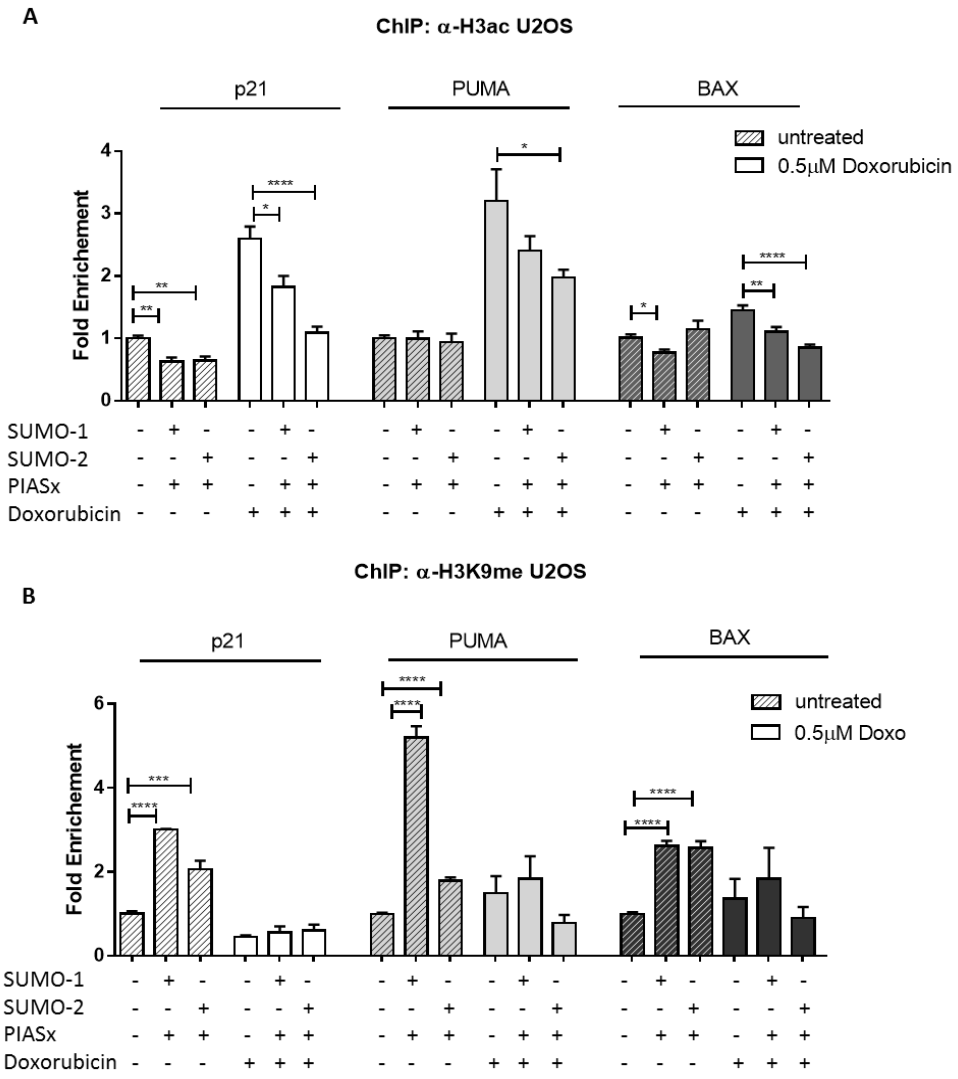

Figure 4.7. Over-expression of SUMO machinery leads to differential enrichment of chromatin marks on Histone H3 on p53-target promoters p21, PUMA and BAX, in U2OS cells.

U2OS cells were transiently transfected with SUMO-1, SUMO-2 and PIASx constructs and treated or not with 0.5μM doxorubicin for a period of 16h. Cells were then cross-linked and analysed by ChIP for the promoter regions of p21, PUMA and BAX.

(A) Histone H3 acetylation is reduced in p53-target promoters upon over-expression of sumoylation machinery in U2OS cells before and after doxorubicin treatment.

(B) ChIP shows an enrichment of Histone H3 Lysine9 tri-methylation to p53-target promoters upon over-expression of sumoylation machinery in U2OS cells.

ChIP was quantified relative to input and the housekeeping gene actin, according to the comparative $^{\Delta\Delta}$Ct-method, and normalized to U2OS non-treated cells. Results are displayed as mean of $2^{\Delta\Delta}$Ct values obtained from 3 independent experiments. Error bars represent the standard error of the mean. *pvalue<0.05,**pvalue<0.005, ***p-value<0.001 as calculated by an unpaired student t-test.

The next step was to evaluate whether the decreased transactivation potential of endogenous p53 resultant from SUMO modifications was caused by a change in the affinity of p53 for its target-promoters. The enrichment of p53 on the promoter regions of p21, PUMA and BAX was assessed via chromatin Immunoprecipitation (ChIP) assay. U2OS cells transiently transfected with SUMO-1 or SUMO-2 proteins, in combination with the E3 ligase PIASx and treated (or not) with 0.5µM of doxorubicin, were cross-linked and immunoprecipitated with anti-p53 antibody. The p53-bound chromatin was treated with protease K and the recovered DNA was amplified via qRT-PCR for the promoter regions of the targets tested. As expected, doxorubicin treatment led to a 2-6 fold increase in the ability of p53 to bind to DNA, when compared to non-treated cells [**Figure 4.8**].

Similarly to the results obtained in H1299 cells, ChIP analysis of p21 and PUMA promoters revealed an enrichment of p53 to these promoters in cells where SUMO proteins were over-expressed. BAX promoter region does not show a preferential binding of p53, irrespective of over-expression of SUMO proteins, indicating that the reduction of BAX transcript expression seen by qRT-PCR [**Figure 4.6**] does not depend on p53's binding ability.

Interestingly, doxorubicin treatment seems to promote the differential binding of p53 depending on its modification with SUMO-1 or SUMO-2. While non-treated cells show a higher enrichment of p53 to p21 and PUMA promoters with SUMO-1 over-expression, SUMO-2 over-expression leads to an increased ability of p53 to bind to these promoters in doxorubicin-treated cells. One possible explanation is the fact that cellular stresses promote the conjugation of SUMO-2 to substrates (Saitoh & Hinchey 2000). A proteome-wide analysis has shown that DNA damage and replication stress induce SUMO-2, but not SUMO-1 modification of substrate proteins. Notably, this study observed increased levels of p53 sumoylation with SUMO-2 upon DNA replication stress (Bursomanno et al. 2015). In another study, doxorubicin-treated cells showed a reduction in p53 sumoylation levels with SUMO-1, attributed to the increased levels of Ser20 phosphorylation (Lin et al. 2004).

The differential modification of p53 with SUMO isoforms before and after doxorubicin treatment was monitored by western blot, which showed p53 sumoylation is stronger after doxorubicin treatment [**Figure 4.6a**]. Contrary to Lin et al. report, SUMO-1 modification of p53 is not reduced upon doxorubicin treatment, but rather increases. Nevertheless, SUMO-2

conjugation to p53 appears stronger upon doxorubicin treatment, consistent with previous reports suggesting that stress induces substrate SUMO-2 modification.

As such, the differential affinity of p53 to its target-promoters could be a result of its differential sumoylation status, where doxorubicin treatment leads to the preferential modification of p53 with SUMO-2, whereas in untreated cells, sumoylation with SUMO-1 is favored. While this hypothesis would have to be further investigated by performing for example immunoprecipitation experiments, it appears that sumoylated p53 has an increased ability to bind to its target promoters p21 and PUMA.

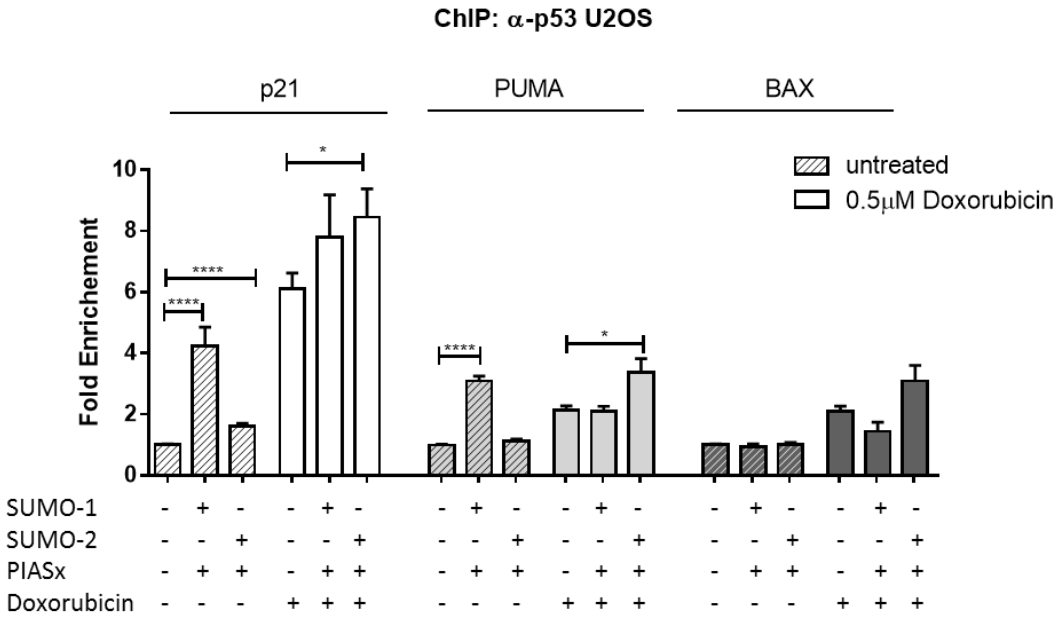

Figure 4.8. p53 shows an increased ability to bind to target promoters upon over-expression of sumoylation machinery in U2OS cells before and after 16h of doxorubicin treatment.

U2OS cells were transiently transfected with SUMO-1, SUMO-2 and PIASx constructs and treated or not with 0.5μM doxorubicin for a period of 16h. Cells were then cross-linked and analysed by ChIP for the promoter regions of p21, PUMA and BAX.

ChIP was quantified relative to input and the housekeeping gene actin, according to the comparative $^{\Delta\Delta}$Ct-method, and normalized to U2OS non-treated cells. Results are displayed as mean of $2^{\Delta\Delta}$Ct values obtained from 3 independent experiments. Error bars represent the standard error of the mean. *pvalue<0.05,**pvalue<0.005, ***p-value<0.001 as calculated by an unpaired student t-test.

As these results were consistent with the ones obtained with over-expression of p53-ubc9 in H1299 cells, I sought to investigate whether preferential ability of SUMO-p53 to target promoters and the resulting effect on target-gene expression was caused by the recruitment of co-repressors to the nearby chromatin. Therefore, I assessed the association of co-repressors HDAC2 and LSD1 to the promoter regions of p21 and PUMA [**Figure 4.9**].

ChIP analysis of HDAC2 association with p53-target promoters revealed that, unexpectedly, HDAC2 binding is not significantly reduced upon treatment with doxorubicin. Moreover, in untreated cells, HDAC2 is enriched when SUMO-1 is over-expressed to the promoter region of both p21 and PUMA, while its affinity to these promoters is reduced when SUMO-2 is over-expressed. In contrast, in doxorubicin treated cells, HDAC2 has increased binding affinity to both promoters when SUMO-2 is over-expressed [**Figure 4.9a**]. These data indicate that HDAC2 is present at the promoter region of p21 and PUMA even upon DNA damage stimulus (doxorubicin). However, its enrichment to these promoters upon stimulation of p53 sumoylation (SUMO-1 with no treatment and SUMO-2 with doxorubicin treatment) indicates that sumoylation contributes to the recruitment of HDAC2 to the promoter vicinity, likely contributing to gene repression.

On the other hand, LSD1 association with p21 and PUMA promoters is reduced by half upon genotoxic insult induced by doxorubicin [**Figure 4.9b**]. Interestingly though, the pattern of binding affinity to these promoters upon over-expression of SUMO proteins closely follows that of HDAC2. In untreated cells, LSD1 association to p21 promoter increases significantly upon over-expression of SUMO-1, whilst SUMO-2 over-expression results in a significant decrease in LSD1 association. Conversely, doxorubicin treated cells show a significant increase in LSD1 affinity to PUMA promoter upon over-expression of SUMO-2 [**Figure 4.9b**]. Therefore, these findings provide circumstantial evidence that sumoylation stimulates co-repressor recruitment to chromatin regions in the vicinity of p53-target promoters.

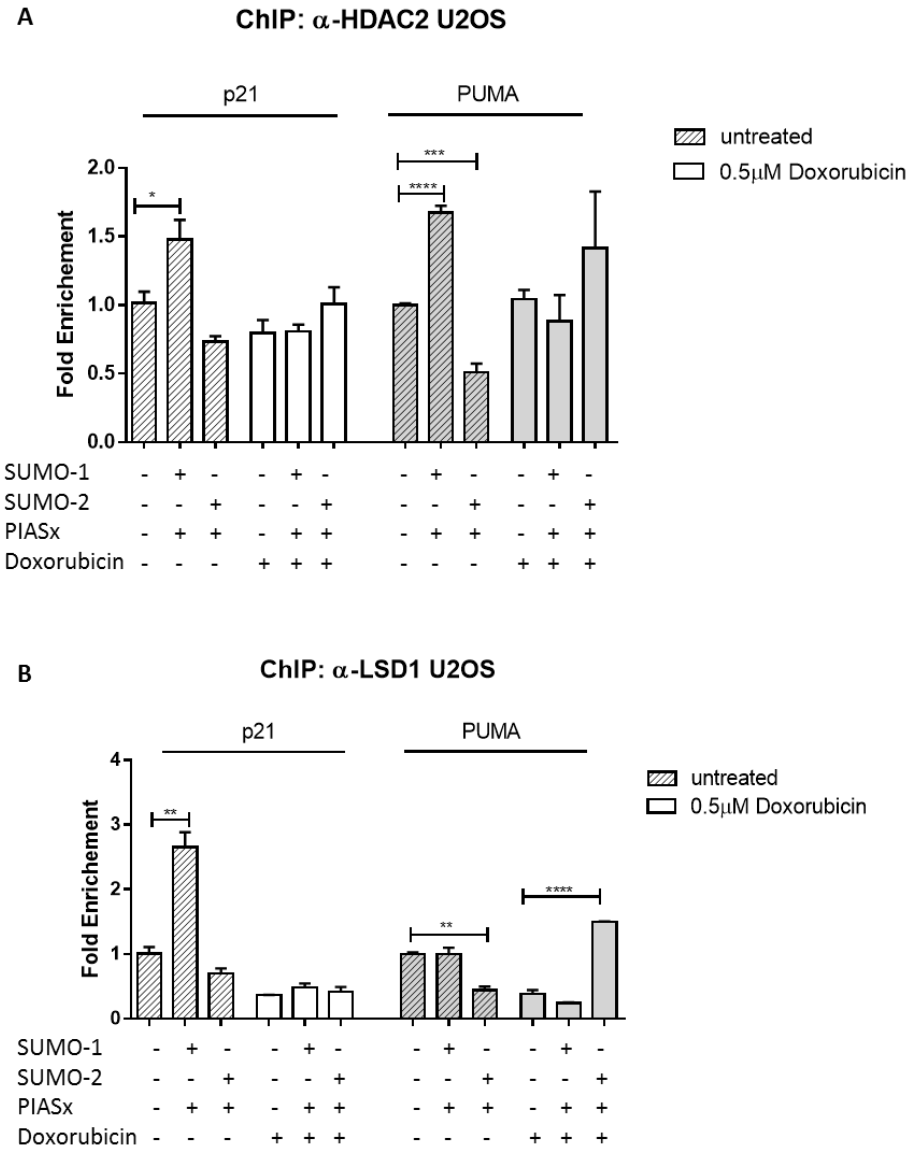

Figure 4.9. ChIP assay shows differential ability of co-repressors HDAC2 and LSD1 to associate to p53-target promoters upon over-expression of sumoylation machinery in U2OS cells.

U2OS cells were transiently transfected with SUMO-1, SUMO-2 and PIASx constructs and treated or not with 0.5μM doxorubicin for a period of 16h. Cells were then cross-linked and analysed by ChIP for the promoter regions of p21 and PUMA.

ChIP was quantified relative to input and the housekeeping gene actin, according to the comparative $^{\Delta\Delta}$Ct-method, and normalized to U2OS non-treated cells. Results are displayed as mean of $2^{\Delta\Delta}$Ct values obtained from 2 independent experiments. Error bars represent the standard error of the mean. *pvalue<0.05,**pvalue<0.005, ***p-value<0.001 as calculated by an unpaired student t-test.

In summary, this section aimed to investigate the effect of sumoylation of endogenous p53 activity. My findings indicate that expression of p53-responsive genes p21, PUMA and BAX is reduced with the over-expression of both SUMO isoforms used, under normal and stress conditions. However, the addition of doxorubicin leads to the differential sumoylation of p53, with doxorubicin promoting modification with SUMO-2, rather than SUMO-1. This affects the binding abilities of p53, and also the recruitment of co-repressors to the vicinity of p53-target promoters, such as HDAC2 and LSD1. These data corroborates the findings of section **4.2.1**, whereby p53 sumoylation increases p53-binding affinity to the promoters of p21 and PUMA, and causes transcriptional repression of these genes by the recruitment of the transcriptional repressor HDAC2.

To verify that the effects observed in p53-target genes by over-expression of SUMO proteins were a result of p53-dependent transcription, U2OS cells containing a shRNA against p53 (U2OS pLKO), in which p53 expression is knocked down, were used for qRT-PCR and ChIP analysis. Successful knock-down of p53 in U2OS plKO cells and transient transfections with SUMO and PIASx proteins were monitored via western blot [**Figure 4.10a**]. As predicted, expression of p53-target genes p21, PUMA and BAX by qRT-PCR was significantly increased in U2OS cells, when compared to p53 knock-down pLKO. Consistently with the results shown previously, over-expression of sumoylation machinery in U2OS cells resulted in a significant decrease in p53-target gene expression. However the same pattern is not observed in U2OS pLKO p53-/- cells, in which the over-expression of SUMO system proteins does not alter significantly the expression of these target-genes [**Figure 4.10b**]. Thus, the results observed upon over-expression of SUMO proteins are the function of p53-dependent transcriptional activity, most likely caused due to p53 sumoylation. To validate the prior ChIP experiments where an enrichment of p53 to target promoters was observed after over-expression of SUMO machinery, I performed ChIP in p53-/- U2OS pLKO cells. ChIP analysis of U2OSplKO cells with anti-p53 antibody showed, as expected, no variation of p53 enrichment for p53-promoters [**Figure 4.11**]. This demonstrated that the increased association of p53 to target promoters seen in U2OS cells over-expressing SUMO system proteins was not an artifact of the antibody used.

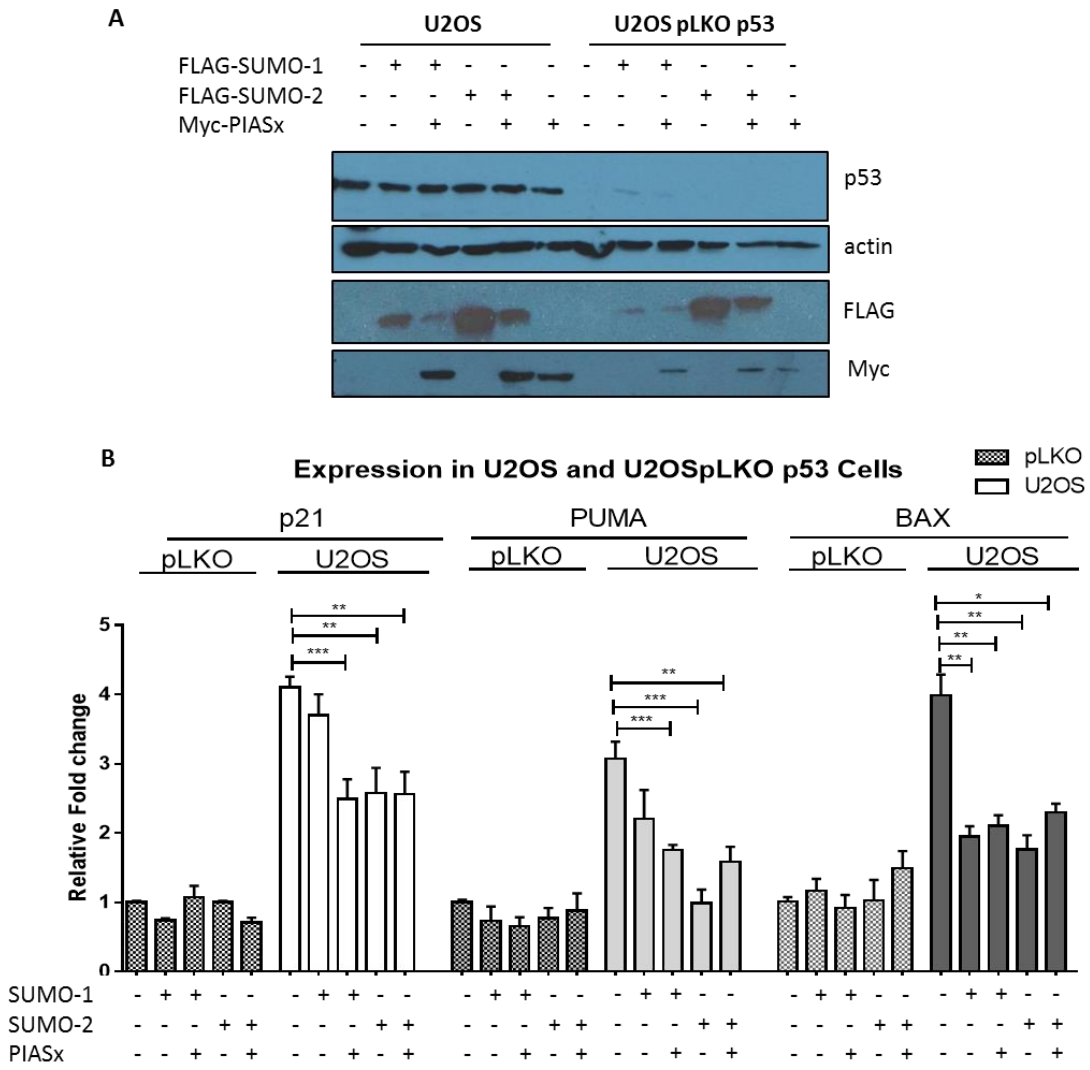

Figure 4.10. Comparison of expression of p53-target genes in U2OS and U2OSpLKO p53-/- cells upon 16h of doxorubicin treatment.

(A) Representative western blot showing the overexpression of FLAG-SUMO-1, FLAG-SUMO-2 and myc-PIASx constructs, and the efficient knock down of p53 on U2OS pLKO cell line.

(B) qRT-PCR analysis of p21, PUMA and BAX expression shows a decrease of transcription of p53-target-genes upon overexpression of sumoylation machinery in U2OS but not in U2OS pLKO p53-/- cells.

Results are displayed as mean of $2^{\Delta\Delta}$Ct values obtained from 2 independent experiments. Error bars represent the standard error of the mean. *p-value<0.05,**p-value<0.005, ***p-value<0.001 as calculated by an unpaired student t-test.

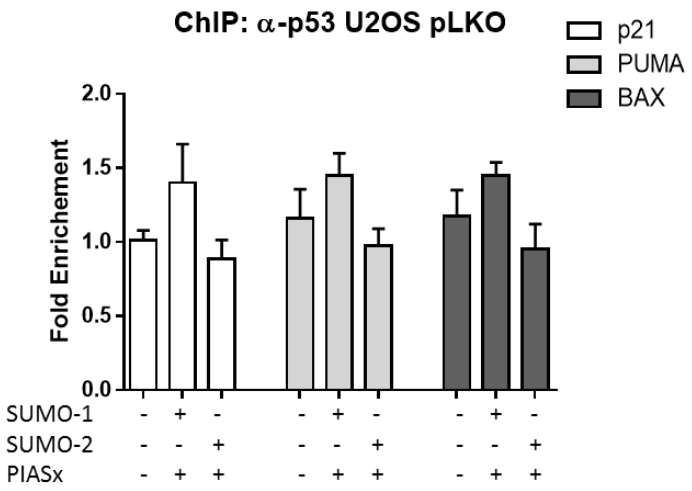

Figure 4.11. p53 deficient cells U2OSpLKO do not show differential enrichment of p53 to p53-target promoters upon 16h of Doxorubicin treatment.

ChIP results are displayed as mean of $2^{\Delta\Delta}$Ct values obtained from 2 independent experiments. Error bars represent the standard error of the mean. Unpaired student t-tests showed non-significant differences, comparing to the un-transfected negative control U2OS pLKO.

To further validate that the effects seen were p53-dependent, experiments were repeated in HCT116 cells. Like U2OS cells, HCT116 express endogenous p53. Homologous recombination performed in Bert Vogelstein lab led to the formation of p53-null HCT116 cells. Thus, HCT116 p53+/+ and HCT116 p53-/- are isogenic human colon cancer cells, only differing in their ability to express p53. These cells were transiently transfected with SUMO and PIASx proteins, and used for the analysis of p53 transactivation and binding abilities. After confirming that cells were successfully transfected via western blot [**Figure 4.12a**], cellular mRNA was extracted, converted to cDNA and analysed by qRT-PCR. Analysis of p53-responsive gene transcription by qRT-PCR in HCT116 p53+/+ shows similar results to those obtained in U2OS cells, where over-expression of SUMO proteins, together with E3 ligase PIASx results in a significant decrease in the expression of p21 and PUMA. Moreover, in p53-null HCT116 cells, over-expression of SUMO machinery does not affect the expression of the same p53-targets [**Figure 4.12b**].

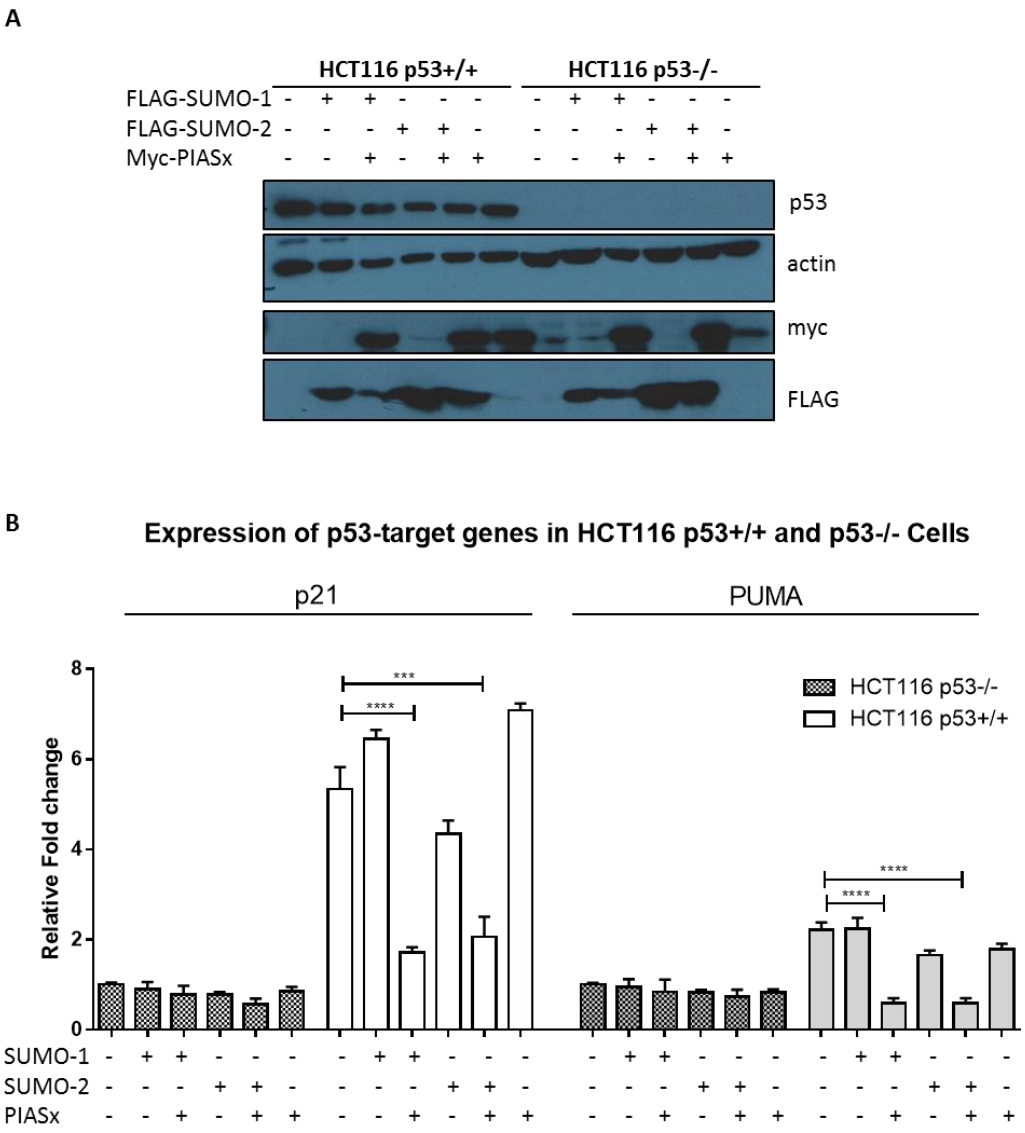

Figure 4.12. Expression of p53-target genes in HCT116 p53+/+ and p53-/- cells upon 16h of doxorubicin treatment.

(A) Representative western blot showing the overexpression of FLAG-SUMO-1, FLAG-SUMO-2 and myc-PIASx constructs, as well as p53 silencing in HCT116 p53-null cells.

(B) qRT-PCR shows p53-dependent transactivation is affected by SUMO system over-expression in HCT116 cells, but not in p53-null HCT116 cells. Results are displayed as mean of $2^{\Delta\Delta}$Ct values obtained from 2 independent experiments. Error bars represent the standard error of the mean. *p-value<0.05,**p-value<0.005, ***p-value<0.001,****p-value<0.0001 as calculated by an unpaired student t-test.

These findings are consistent with the results obtained in both U2OS and H1299, indicating that p53-dependent transcription of p21 and PUMA genes is affected by sumoylation. To investigate if the mechanism by which sumoylation dampens p53 activity in HCT116 cells is similar to the one observed in the other two cell lines, ChIP assay was performed to assess the binding affinity of p53 to these promoters. As shown in **Figure 4.13**, endogenous p53 has increased ability to bind to its target-promoters in HCT116 cells treated with doxorubicin and over-expressing SUMO-2 proteins. Over-expression of SUMO-1 did not have such a dramatic effect in the enrichment of p53 to the promoters. This observation is consistent with the results obtained in U2OS, indicating that doxorubicin treatment might favour SUMO-2 modification of p53 and thus enhance p53-SUMO-2 binding to chromatin. Further investigation on this matter would involve over-expression of SUMO proteins, together with PIASx, in unstressed HCT116 cells, to examine whether p53 binding would be favoured with SUMO-1 overexpression in these conditions.

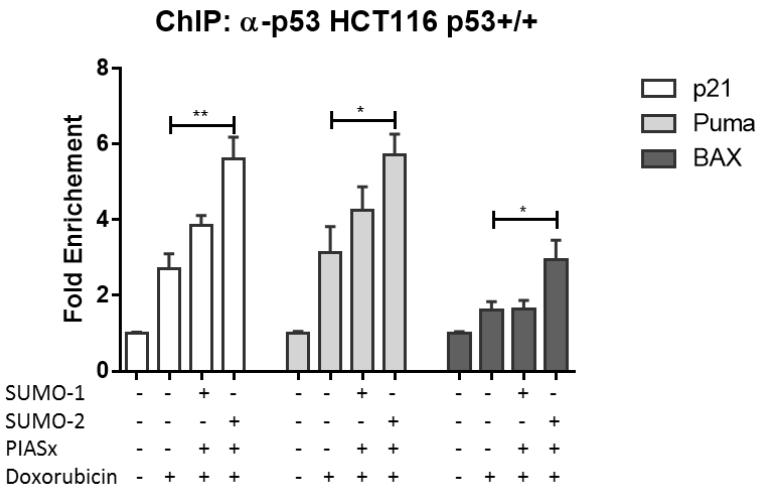

Figure 4.13. p53 shows an increased ability to bind to target promoters upon over-expression of sumoylation machinery in HCT116 p53+/+ cells after 16h of doxorubicin treatment.

ChIP assay results are displayed as mean of $2^{\Delta\Delta}$Ct values obtained from 3 independent experiments. Error bars represent the standard error of the mean. *p-value<0.05,**p-value<0.005, as calculated by an unpaired student t-test.

The aim of this chapter was to elucidate the role of p53 sumoylation in the transactivation functions of p53. Utilizing different transfection approaches in three different established cell lines, I show here that sumoylation has an overall negative effect in p53's transcriptional activity. Moreover, the present results demonstrate that rather than preventing p53 from binding, sumoylation leads to an increase in the binding ability of p53 to its responsive genes. The reduction of Histone H3 acetylation (H3ac) (a chromatin activation mark) in the presence of p53 sumoylation in the promoter regions of the target genes tested correlates with the increase of is HDAC2 recruitment to these promoter regions. These results indicate that sumoylation of p53 can act as a mark for the recruitment of co-repressor complexes such as HDAC2 to the nearby chromatin, and thus contribute to transcriptional repression of p53-target genes.

4.3 Discussion

4.3.1 Down-regulation of p53-targets vs increased p53 binding activity

p53 regulation through ubiquitin-like proteins such as SUMO has been known for many years. Unlike ubiquitin, SUMO modification of p53 does not lead to its proteasomal degradation, but likely alters p53's function. Previous research data has shown that p53 sumoylation modulates p53's transcriptional potential, though the exact mechanism and consequences remained controversial. In this chapter I investigated the effect of SUMO modification of p53 utilizing both endogenous and over-expressed p53 proteins, in three different human cancer cell lines.

Over-expression of p53-fused proteins in H1299 cells showed a clear reduction of p53 transcriptional activity, as p53 protein with disrupted SUMO consensus motif (K386R) induced endogenous p53-target genes p21 and PUMA more strongly when compared to WT p53, which can be potentially sumoylated. This effect was visible at both mRNA and protein levels. Similarly, expression of p53 proteins together with SUMO machinery proteins lead to a significant decrease in the ability of p53 to activate transcription of target-gene p21. These data are in line with previous observations, where K386R mutant expression led to the enhanced activation of p21 in both luciferase-reporter assays and at mRNA level (Wu & Chiang 2009a; Stindt et al. 2011). Moreover, the reduction on p53-dependent transcription by SUMO-modified p53 is substantiated by epigenetic changes in chromatin, namely changes in Histone H3 acetylation and Histone H3K9 tri-methylation. Thus, reduced mRNA levels of p53-targets p21, PUMA and even BAX (although to a lower extent) correlated with reduced levels of Histone H3 acetylation and enrichment of H3K9 methylation on the vicinity of these promoters. Importantly, such changes were consistent in all cell lines tested, with both endogenous and over-expressed p53 proteins, associating p53 sumoylation with a decreased capacity of p53 transactivation.

More surprisingly was the observation that sumoylation led to the augmented affinity of p53 to its targets promoters. In H1299, WT p53 was more prone to bind to its target promoters p21 and PUMA than the sumoylation-deficient mutant K396R, and exogenous expression of sumoylated machinery proteins together with p53 led to an enhanced ability of p53 to bind to these promoters. Similarly, in U2OS and HCT116 cells containing endogenous

p53, over-expression of SUMO proteins in combination with PIASx led to the enrichment of p53 to the promoters tested. Taken together, these results indicate that p53 sumoylation results in enhanced stabilization of p53-chromatin complex at the p21 and PUMA promoters. These observations contrast with a previously published report, where the authors observed a decrease in p53's ability to bind to p21 promoter in SUMO-1 modified p53 (Wu & Chiang 2009a).

Although intriguing, these results indicate a novel mechanism for the transcriptional control of p53 by SUMO, via its stabilization with the chromatin whilst hindering its transactivation potential. The attachment of SUMO to p53 might represent a signal for the recruitment of chromatin remodeling factors, leading to heterochromatin configuration characterized by low levels of Histone acetylation and H3K4 methylation, and high levels of H3K9 and H3K27 methylation (Garcia-Dominguez & Reyes 2009). Indeed, sumoylation of numerous transcription regulators has been shown to mediate the recruitment of chromatin remodeling complexes and histone modifying factors, leading to heterochromatin formation. One such example is the transcription factor Sp3, whose sumoylation promotes the recruitment of several heterochromatin factors, such as HP1 and Histone methyl-transferases SETDB1 and SUV4-20H (Stielow, Sapetschnig, Wink, et al. 2008). Sumoylation of Krüppel-like zinc finger DNA-binding repressor ZEB1 leads to its stabilization in the chromatin and is required for its full repressive functions (Wang et al. 2007).

The differential ability of p53 to bind to its target promoters may explain why previous publications linked p53 sumoylation with an increase in p53's transcriptional potential (Gostissa et al. 1999; Rodriguez et al. 1999; Bischof et al. 2006). Many of these studies used artificial reporter systems, which not always reflect the expression of endogenous targets. In addition, reporter assays do not measure only the potential for transcriptional activation, but also assess the ability of p53 to bind to the REs enclosed within the luciferase constructs, which are, in many cases, not naturally occurring p53-binding sites. As so, it is not possible to discern whether the activation of transcription seen through these luciferase reporters was due to p53's transactivation or due to the increased binding ability of p53 to these REs. The methods used here, such as quantification of mRNA of specific targets by qRT-PCR, and assessment of the binding ability to p53-specific promoters via ChIP represent a more physiological approach to the effects of sumoylation on p53's function.

Given the results obtained for p53-activated genes it would be interesting to determine how sumoylation affects p53-repressive gene transcription. A previous study addressing the role of SUMO-2/3 modification on p53 has shown that mRNA levels of p53-repressive genes CDK1 and CyclinA2 are significantly reduced in the sumoylation-deficient mutants, suggesting that SUMO-2/3 modification of p53 can relieve p53-mediated repression (Stindt et al. 2011). The mechanism of action, remains, however, undetermined, and could simply be an indirect effect of p21 activation. This is, in fact, one of the mechanism of p53-mediated repression, as p21 inactivates CDKs leading to the hypophosphorylation of Rb (Retinoblastoma), which, in turn, results in the repression of E2F-target genes, such as Cyclin A2 and CDK1 (Löhr et al. 2003). Moreover, as most of p53-repressive genes known, neither of the above contain p53-REs within their promoter regions, indicating that in this case, p53-mediated repression is indirect (Rinn & Huarte 2011).

Investigation of p53-repression in target-genes that contain p53-binding sites, such as Cdc25C or Survivin (St Clair & Manfredi 2006; Hoffman et al. 2002), and how SUMO-modification affects p53 repression of these genes would, therefore, provide further insight on our understanding of p53 sumoylation. Whether p53 sumoylation leads to an incremented affinity to p53-repressive promoters, and promotes the recruitment/disassembly of co-factors which dampen its repressive functions, or, on the contrary leads to its disassembly from chromatin remains to be investigated.

4.3.2 Recruitment of co-repressors

Analysis of co-repressor proteins enrichment within the vicinity of p21 and PUMA promoters via chromatin immunoprecipitation suggests that the SUMO moiety present in p53 promotes the recruitment of co-repressor proteins to the promoter region. The increased affinity of co-repressor HDAC2 to p53-target promoters in cells containing sumoylated p53, along with the reduction of co-activator CBP enrichment, correlate with the reduction in Histone H3 acetylation in these regions. Moreover, in U2OS cells expressing endogenous p53, LSD1 recruitment to p53-target promoters seems to be favoured by the presence of exogenous sumoylation machinery.

These observations agree with the current model for SUMO-mediated transcriptional repression, in which SUMO provides a new interaction surface for the attachment of co-repressor complexes (Ouyang & Gill 2009). In fact, a number of studies has connected SUMO with HDAC-transcriptional repression. For example, the transcription factor Elk-1 was specifically associated with HDAC2 when SUMO-modified. Utilizing chromatin immunoprecipitation techniques, the authors demonstrated that sumoylated Elk-1 correlated with the recruitment of HDAC2 to its target-promoter, and reduced acetylation of histones (Yang & Sharrocks 2004). Sumoylation of co-activator p300 has been connected with transcriptional repression via recruitment of HDAC6 (Girdwood et al. 2003). Also co-activator CBP can be modified by SUMO-1 and this modification negatively regulates its transcriptional functions. CBP sumoylation promotes its interaction with the transcriptional co-repressor Daxx, which in turns facilitates the recruitment of HDAC2 (Kuo et al. 2005).

The recruitment of HDACs to chromatin in response to sumoylated factors could occur in different ways. One possibility is that HDACs bind non-covalently to SUMO via inner SUMO Interacting Motifs (SIMs), as is the case for HDAC1 recruitment to sumoylated transcriptional co-repressor Groucho (Ahn et al. 2009). Another possibility is that HDACs do not bind directly to sumoylated substrates, but are recruited indirectly through HDAC-associated co-factors, which bridge the interaction between SUMO and HDACs (Ouyang & Gill 2009). Together with other proteins, HDACs 1 and 2 can form three co-repressor complexes: CoREST (co-repressor for element-1-Silencing Transcription factor), Mi2/NuRD (Nucleosome Remodeling and Deacetylation) and mSin3A (Kelly & Cowley 2013). Interestingly, CoREST1 co-repressor was

shown to associate specifically with SUMO-2/3, potentially bridging the association of HDACs 1 and 2 with SUMO-2 (Ouyang et al. 2009). Also, Mi-2, component of the NuRD complex has been found associated with SUMO-modified Sp3 in a genome-wide RNAi screen in *Drosophila* (Stielow, Sapetschnig, Kru, et al. 2008) and the cellular co-repressor mSin3A was preferably recruited by SUMO-modified p53 (Wu & Chiang 2009a).

Notably, both NuRD and CoREST complexes associate with LSD1 (Wang et al. 2009; Wang et al. 2007), identified in the previous chapter as a specific interactor of SUMO-modified p53. Moreover, enrichment of LSD1 to p53-target promoters correlated with the over-expression of SUMO proteins. Taken together, these findings suggest LSD1 as the primary recruitment protein to sumoylated p53, which by direct association with CoREST and NuRD complexes, could bridge the association between p53-SUMO and HDAC2. Future work would involve ChIP assays for HDAC1 and other proteins of these complexes to further define the mechanism of LSD1-mediated transcriptional repression.

Therefore, I suggest a mechanism by which SUMO-modified p53 recruits LSD1 possibly via SIM, which by association with HDAC co-repressor complexes leads to the transcriptional silencing of p53 responsive-genes [**Figure 4.14**].

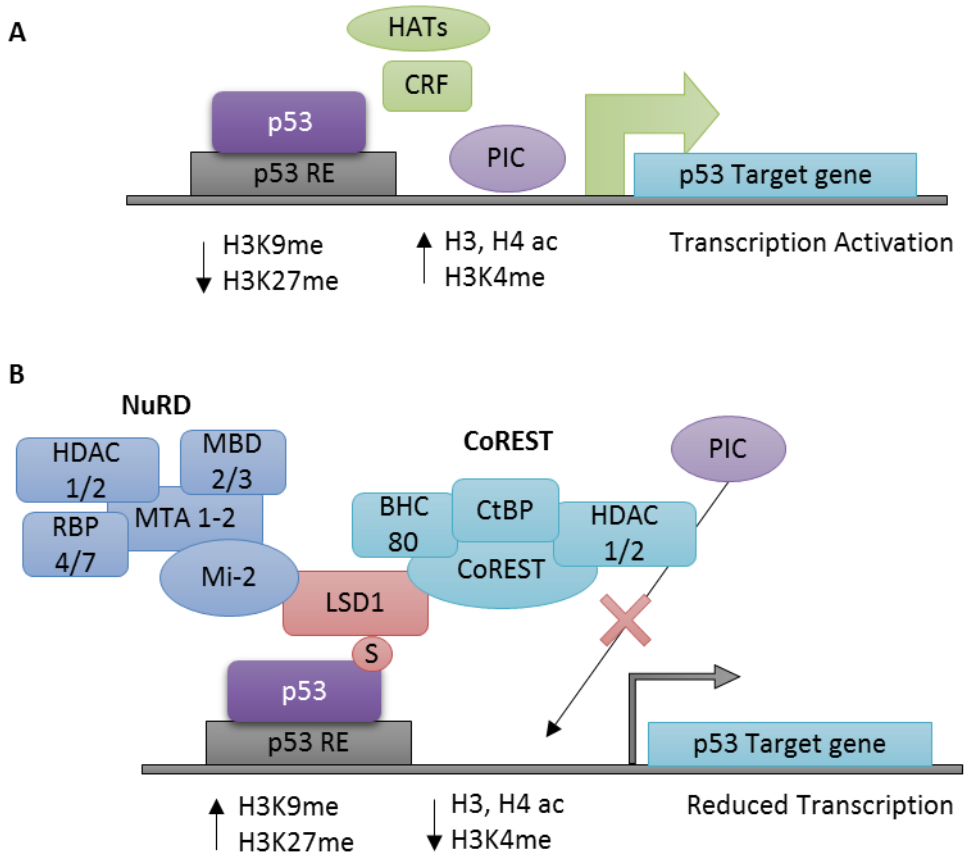

Figure 4.14. Proposed Model for p53-transcriptional silencing following p53 sumoylation.

(A) Upon activation, p53 binds DNA recognizing specific p53 Responsive Elements (p53 RE) and promotes the recruitment of co-activators such as Histone Acetyl-Transferases (HAT) and Chromatin Remodelling Factors (CRF), promoting a state of active chromatin with enriched Histone acetylation and H3K4 methylation, and low levels of H3K9 and H3K27 methylation. This facilitates the recruitment of the Pre-initiation transcription complex (PIC) and promote p53-mediated transcription of target genes.

(B) In the event of p53 sumoylation, LSD1 is recruited, likely via SIM, to SUMO-p53. By association with CoREST and/or NuRD co-repressor complexes, LSD1 promotes their recruitment to the nearby chromatin, favouring heterochromatin formation, characterized by low levels of Histone acetylation and H3K4 methylation, and high levels of H3K9 and H3K27 methylation. The association of co-repressor complexes to the promoter region of p53-target genes prevents the recruitment of the Pre-initiation transcription complex (PIC), leading to the transcriptional silencing of p53 responsive-genes.

CHAPTER 5

Other Effects of p53 Sumoylation

Chapter 5. Other effects of p53 Sumoylation

5.1 Introduction

Apart from modulating p53's transactivation functions, SUMO can affect p53 activity through other mechanisms, including the regulation of other PTMs and the regulation of its subcellular localization.

While single modifications can have a significant impact on p53's function, it is the combination of PTMs occurring in p53 that permits the tight control and regulation of its activities. For example, the initial response to stress is the phosphorylation of Serine 15, which leads to the phosphorylation of S20 and T18 to allow p53's activation (Sakaguchi et al. 2000). Amino-terminal phosphorylation can lead to the subsequent acetylation of lysine residues in the C-terminus of p53 (Sakaguchi et al. 1998), but phosphorylation of C-terminal residues T377 and S378 results in reduced acetylation of K320, K373 and K382 (Ou et al. 2005). Methylation of p53 C-terminal lysines can also promote or hinder adjacent modifications. SET7/9-mediated methylation of K372 promotes acetylation of K373 and K382 residues (Ivanov et al. 2007), and also prevents SMYD2-mediated methylation of K370. Additionally, many residues of p53 can be modified by different PTMs, which can have opposing effects: the acetylation of C-terminal residues prevents the ubiquitylation of the same lysines, and thus act to prevent p53 proteasomal degradation (Li, Luo, et al. 2002). The dynamics of PTMs and their co-operative role to modulate p53's activity has led to the idea of a PTM code for p53, which, much like the histone code hypothesis (Jenuwein & Allis 2001), can be read by effector molecules to mediate differential outcomes (Sims & Reinberg 2008; Gu & Zhu 2012).

Another relatively unexplored role of SUMO-modification is its effect on p53's subcellular distribution. The role of ubiquitin in p53's nuclear-cytoplasmatic traffic is well-defined, as MDM2-mediated mono-ubiquitylation of C-terminal lysines leads to the nuclear export of p53 (Brooks & Gu 2006). Sumoylation has also been implicated in the nuclear export of p53 (Carter et al. 2007)(Santiago et al. 2013). Yet other studies link p53-sumoylation with the accumulation of p53 to specific structures within the nucleus, known as PML nuclear bodies (Muller & Dobner 2008; Pennella et al. 2010; Mauri et al. 2008).

In the first part of this chapter, I aim to investigate the effect of K386 sumoylation on other C-terminal lysine PTMs, namely methylation and acetylation. The second part of this chapter aims to investigate the role of sumoylation in the trafficking of p53 within the cell.

5.2 Results

5.2.1 Crosstalk between Sumoylation and other PTMs in the C-Terminus of p53

The C-terminal region of p53 is a lysine rich region, and is one of the major regions for PTMs to occur. Several enzymes promote different modifications [**Figure 5.1**], which can either stimulate or sometimes counteract further modifications. The interplay among these modifications modulates the stability and activity of p53.

Therefore I aimed to investigate how sumoylation of p53 may interact with other post-translational modifications, and how these interactions affect p53 response. To assess the mutual effect of p53 sumoylation and other PTMs, *in vitro* acetylation and methylation reactions were performed prior, after or simultaneously to p53 sumoylation.

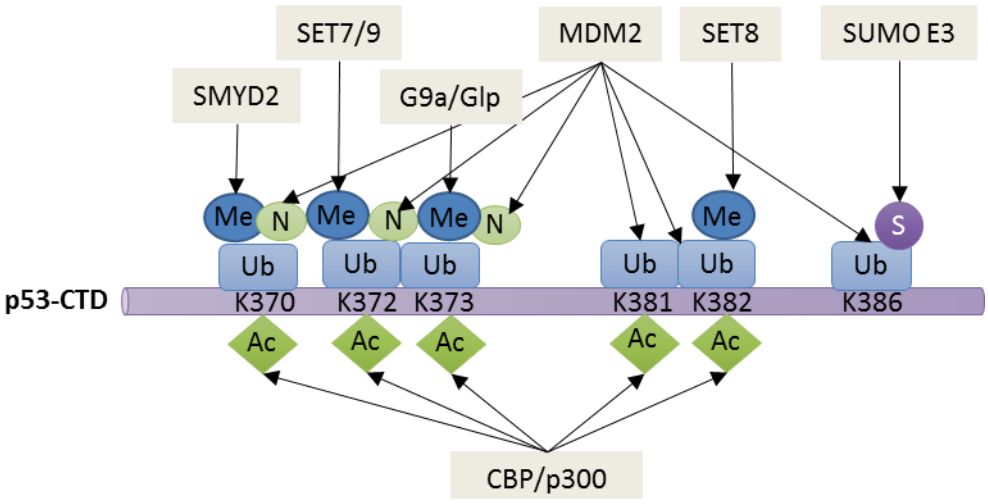

Figure 5.1. Lysine PTMs of the C-terminal domain of p53.

CTD (C-terminal domain) of p53 is a major site for Post-translational modifications. Lysine residues (K) can be modified by acetylation (Ac), ubiquitylation (Ub), methylation (Me), neddylation (N) and sumoylation (S). The enzymes promoting these modifications are indicated.

5.2.1.1 Methylation-Sumoylation Interactions

I started by testing the mutual influence of p53 methylation-sumoylation. p53 methylation occurs in four lysine residues, located in the C-terminal region: K370, K372, K373 and K382. K370 and K382 are mono-methylated by SMYD2 and SET8 methyltransferases, respectively, and both lead to p53's transcriptional repression (Huang et al. 2006; Shi et al. 2007). Lysine 373 is di-methylated by G9a/Glp homologues, and this modification also results in the transcriptional repression of p53 (Huang et al. 2010). Mono-methylation of K372 is catalyzed by SET7/9 methyltransferase, which leads to p53's transcriptional activation by promoting the acetylation of nearby residues (Chuikov et al. 2004; Ivanov et al. 2007).

Since the focus of our lab was directed towards in SET7/9 methyltransferase, I investigated the effect of p53 sumoylation on SET7/9-mediated methylation. For these experiments, I utilized recombinant GST-C-terminal p53 proteins WT and K386R, and proteins of the sumoylation machinery SAE2/1, 6His-Ubc9 and 6His-SUMO-1, purified for *in vitro* studies in **Chapter 3** [**Figure 3.1**;**Figure 3.2**;**Figure 3.3**]. Additionally, for methylation reactions, recombinant GST-SET7/9 was expressed in bacterial cells and subsequently purified with glutathione beads [**Figure 5.2**].

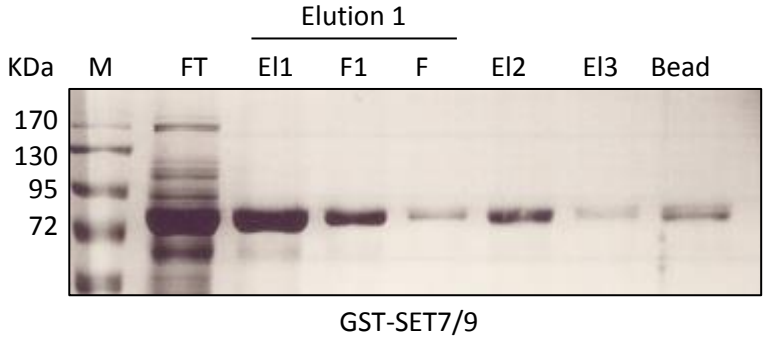

Figure 5.2. Bacterial expression and subsequent purification of GST-tagged recombinant SET7/9 proteins used for *in vitro* methylation studies.

Bacterial expression plasmids for Glutathione-S-Transferase-tagged SET7/9 proteins were induced in *E. coli* (*Rosetta* strain). Bacterial lysate expressing GST-SET7/9 protein was incubated with glutathione beads and the flow through (FT) was run on the gel. Sequential elutions (El1, El2, El3) were made and were then passed through a buffer exchanging column, and different fractions were collected (F1,2).

To assess the mutual influence of sumoylation and SET7/9-mediated methylation on p53, *in vitro* methylation reactions were performed prior, after or simultaneously to its sumoylation [**Figure 5.3**]. Hence, p53 was either firstly methylated, and subsequently sumoylated; or vice-versa, firstly sumoylated and then methylated; or the reactions occurred simultaneously, in the presence of all the enzymes and substrates.

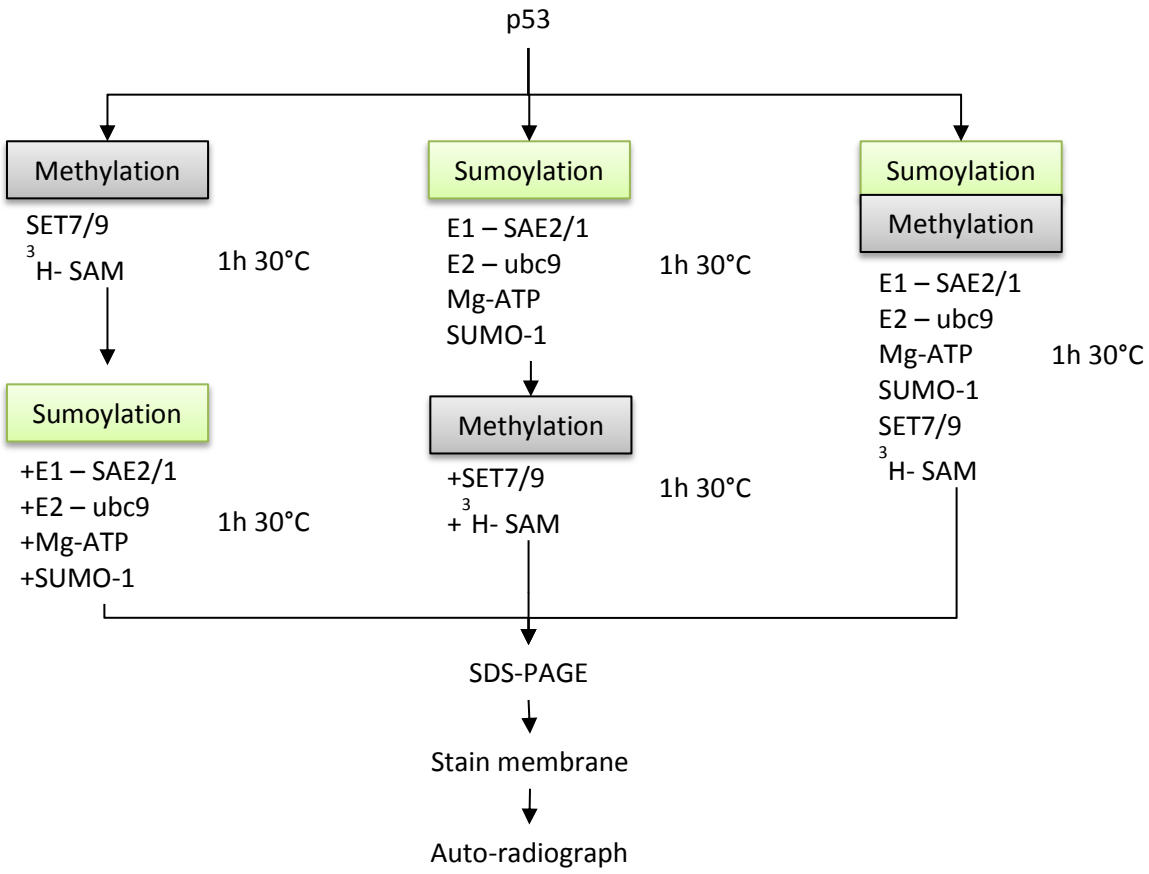

Figure 5.3. Diagram representing *in vitro* crosstalk of methylation and sumoylation of p53.

To assess the mutual influence of sumoylation and SET7/9-mediated methylation on p53, *in vitro* methylation reactions were performed prior, after or simultaneously to its sumoylation. GST-p53$_{300\text{-}93}$ proteins were methylated in the presence of SET7/9 and methyl-group donor SAM. Sumoylation reactions involved the presence of SAE2/1, Ubc9, SUMO-1 and Mg^{2+}-ATP. Subsequent or simultaneously reactions were separated on SDS-PAGE, transferred to a nitrocellulose membrane and stained to assess p53 sumoylation. Methylation efficiency was quantified by autoradiograph, after exposing the membrane to a ^{3}H-enhancer.

Negative control reactions, where either methylation or sumoylation did not occur prior to the converse modification, were used to test their influence on the C-terminus of p53. These are indicated by a minus sign (–) on either Me (methylation) or S1 (SUMO-1 modification) on **Figure 5.4**, representing the absence of GST-SET7/9 or Mg^{2+}-ATP, respectively. To assess whether sumoylation was affected by its prior methylation, the products were run on SDS-PAGE and transferred to a nitrocellulose membrane, which was then stained. The ~17kDa shift on the molecular weight of GST-$p53_{300-393}$, from 38 to 55kDa, shows its efficient sumoylation by SUMO-1 [**Figure 5.4**]. p53 sumoylation does not seem to be affected by its prior methylation, as the levels of sumoylation remain unchanged independently of its methylation. Protein methylation levels were visualized by ^{3}H isotope autoradiography. Analysis of methylated proteins reveals that p53 methylation levels significantly decrease in the sumoylated p53 fraction when sumoylation occurs prior to methylation [**Figure 5.4**, lanes 1 and 3, upper bands and quantified in the lower panel]. Similarly, if the reactions occur simultaneously, methylation levels of sumoylated p53 drop significantly [**Figure 5.4**, lane 5, upper band]. However, sumoylation of K386 has no effect if methylation on K372 precedes sumoylation [**Figure 5.4**, lane 3, upper band]. In contrast, methylation levels of the unsumoyated p53 fraction did not undergo a significant change, whether sumoylation reactions occurred prior or after methylation reactions [**Figure 5.4**, lower bands, quantified on the lower panel]. These findings indicate that while SUMO-1 moiety on p53 K386 might hinder further methylation on K372, sumoylation does not reduce the levels of K372 methylation if SET7/9-mediated methylation had already occurred.

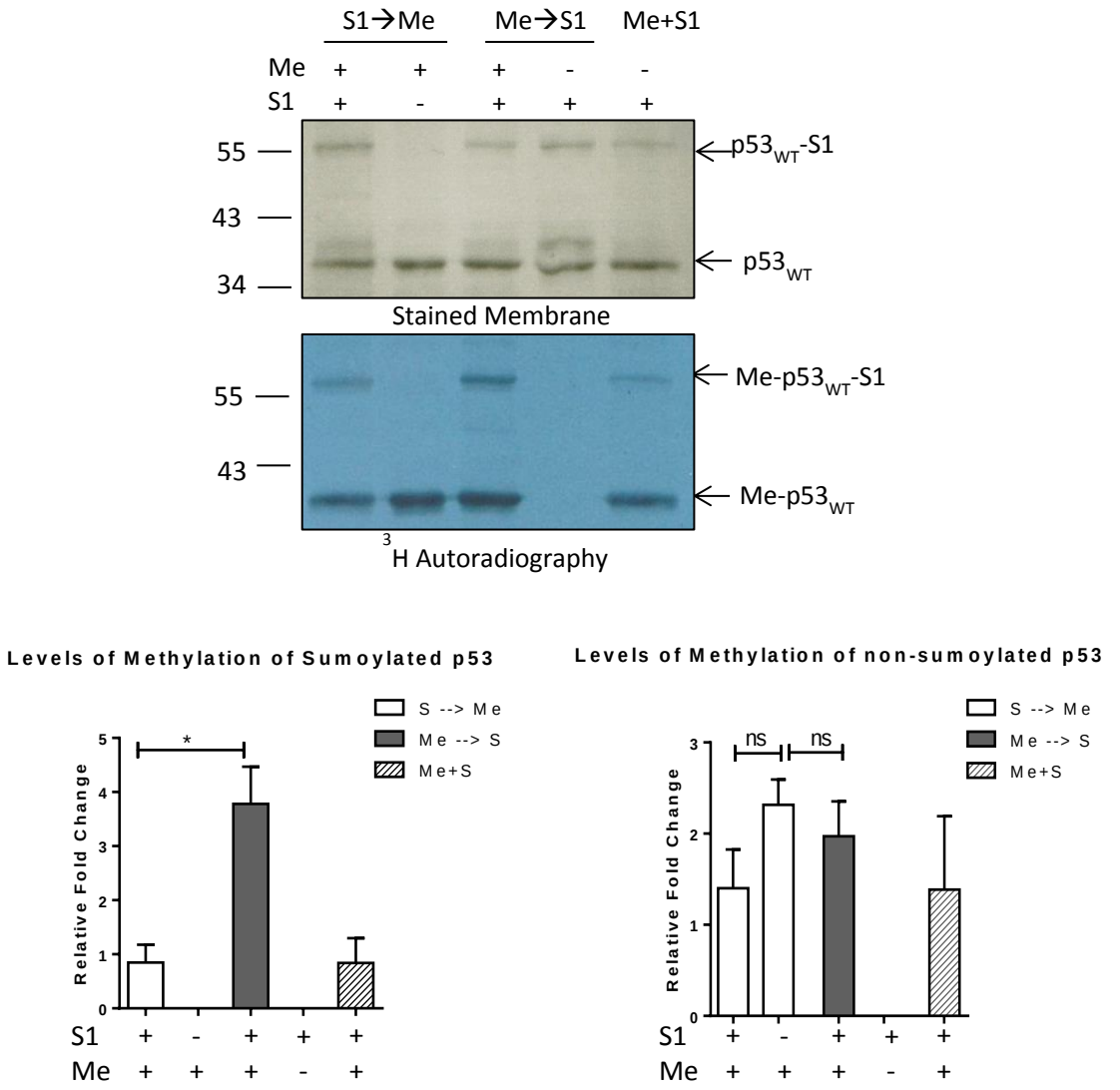

Figure 5.4. In *vitro* p53 sumoylation on K386 reduces its subsequent methylation by SET7/9 on K372.

In vitro sumoylation reactions were performed on GST-p53$_{300-393}$ prior (S1→Me), after (Me→S1) or simultaneously (S1+Me) to methylation reactions with the methyltransferase GST-SET7/9. The reactions were run on SDS-PAGE and transferred to a membrane. The proteins were visualized by DB-71 staining, and methylated proteins were visualized exposing the radio labelled membrane to a ^{3}H enhancer. Molecular weights (kDa) are indicated. Quantification of methylated proteins is shown on the lower panels. Results obtained from 5 independent experiments. Error bars represent the standard error of the mean. *p-value<0.05 as calculated by a paired student t-test.

To further investigate whether sumoylation indeed hampers SET7/9-mediated methylation, I repeated the experiments with K386R sumoylation-deficient mutant. Indeed, methylation levels remain unchanged in the sumoylation-deficient mutant $p53_{K386R}$, irrespective of prior sumoylation [**Figure 5.5**, lanes 1 and 2 and quantified in the lower panel]. However, the simultaneous methylation and SUMO modification resulted in a decreased level of SET7/9 mediated methylation [**Figure 5.5**, lane 5]. It is possible that although K386R mutant lacks the SUMO-target lysine, the E2 conjugating enzyme is still able to recognize and bind the consensus motif, thus preventing SET7/9-mediated methylation on K372. In fact in an early study, Sampson and colleagues showed that although ubc9 binding is mediated by residues surrounding the SUMO-modification site, the modification of the target lysine in RanGAP1 did not affect ubc9 binding (Sampson et al. 2001). Therefore, modifications of residues surrounding the SUMO consensus motif on p53 might be impaired not only by the SUMO moiety covalently conjugated, but also by the transient interaction of ubc9 with the consensus site.

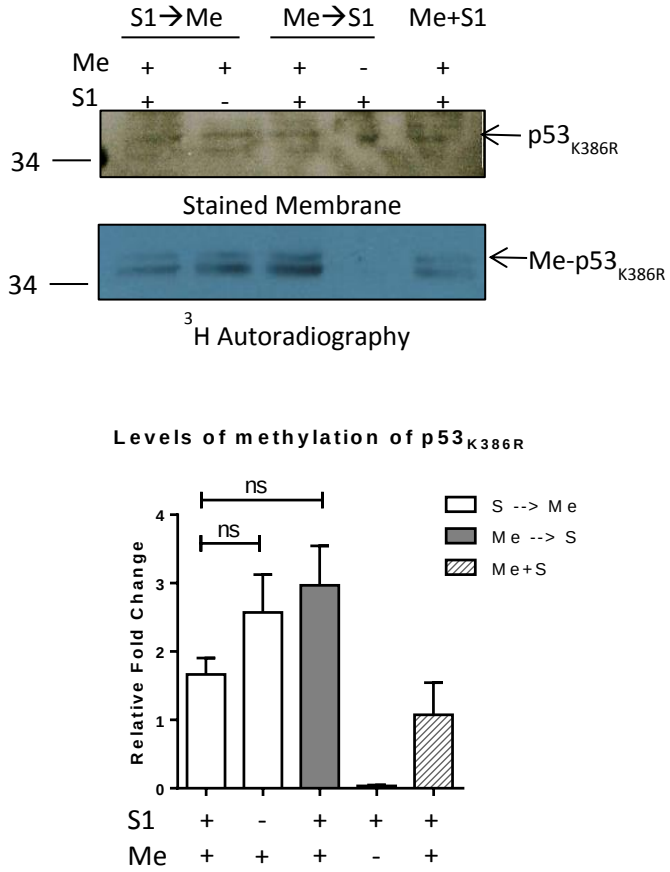

Figure 5.5. Effect of sumoylation of p53 sumoylation-deficient K386R on its subsequent methylation by SET7/9 on K372.

In vitro sumoylation reactions were performed on GST-$p53_{300-393}$ prior (S1→Me), after (Me→S1) or simultaneously (S1+Me) to methylation reactions with the methyltransferase GST-SET7/9. The reactions were run on SDS-PAGE and transferred to a membrane. The proteins were visualized by DB-71 staining, and methylated proteins were visualized exposing the radio labelled membrane to a ^{3}H enhancer. Molecular weights (kDa) are indicated. Quantification of methylated proteins is shown on the lower panel. Results displayed from 2 independent experiments. Error bars represent the standard error of the mean. ns - non-significant (p-value>0.05) as calculated by a paired student t-test.

To understand whether the reduction in methylation was due to the covalent conjugation of SUMO, and not due the transient interaction with ubc9, H1299 cells were transiently transfected with fused p53-ubc9 proteins WT and K386R. Transfected cells were lysed and used for immunoprecipitation with mono-methyl K372p53 antibody (meK372p53). Soluble lysates and IPs were resolved by SDS-PAGE and immuno-blotted with anti-p53 antibody [**Figure 5.6**].

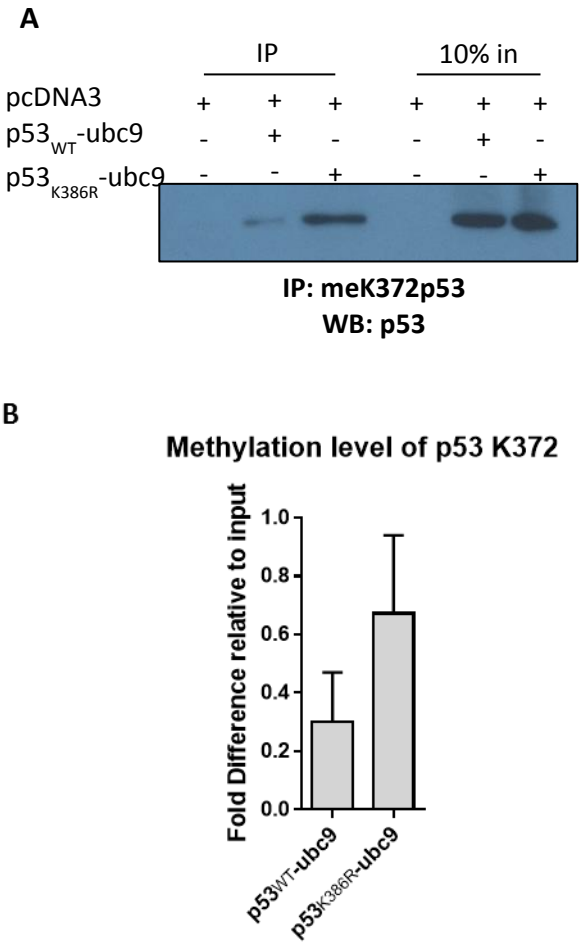

Figure 5.6. Methylation of Lysine 372 is affected by K386 sumoylation.

H1299 cells transiently transfected with either $p53_{WT}$-ubc9 or mutant $p53_{K386R}$-ubc9 plasmids, or with an empty vector (pcDNA3) were lysed and immunoprecipitated with mono-methyl K372 p53 antibody. The immunoprecipitates (IP) were then run on SDS-PAGE, alongside 10% input, and analyzed by western blot with anti-p53 antibody (AB-6).
(A) Representative western blot of the immunoprecipitates analyzed with p53 antibody.
(B) Quantification of methylated K372 p53 in the immunoprecipitates relative to input. Results obtained from 2 independent experiments. Error bars represent the standard error of the mean.

In cells, overexpression of sumoylatable p53 protein (WT) led to the decrease in methylation levels of lysine K372, compared to levels obtained in sumoylation-deficient mutant K386R [**Figure 5.6**]. The impaired methylation of K372 indicates that it is the SUMO moiety, rather than the transitional binding of ubc9 to the consensus SUMO motif that leads to the reduction in p53 methylation.

5.2.1.2 Acetylation-sumoylation interactions

Next, I aimed to investigate the mutual effect of SUMO and acetylation on the C-terminal domain of p53. C-terminal acetylation is catalyzed by co-activator and histone acetyl-transferase p300/CBP, and its target lysines include K370, K372, K373, K381 and K382 (Gu & Roeder 1997). The acetylation of these residues promotes p53 stabilization and transactivation functions, although the mutation of individual lysines does not have a significant effect on p53 activity, pointing to the redundancy of acetylation sites in p53 (Tang et al. 2008).

To investigate the cross-talk between sumoylation and acetylation of C-terminal p53, a similar approach to the one described in the **Figure 5.3** was used. In this case, *in vitro* acetylation reactions, rather than methylation, were performed prior, after or simultaneously to sumoylation. Negative control reactions, where either acetylation or sumoylation did not occur prior to the converse modification, were used to test their influence on the C-terminus of p53. These are indicated by a minus sign (–) on either Ac (acetylation) or S1 (SUMO-1 modification) on **Figure 5.7**, representing the absence of Acetyl-CoA or Mg^{2+}-ATP, respectively.

The reactions were resolved on SDS-PAGE and transferred to nitrocellulose membrane. Proteins were visualized by membrane staining, and a ~17kDa shift on p53 indicates its successful sumoylation [**Figure 5.7**, upper panel]. Acetylation reactions performed prior to p53 sumoylation reveal a slight decrease in the levels of p53-SUMO-1 conjugates [lanes 3 and 4]. However, because this decrease is seen in both reactions independently of Acetyl-CoA addition, this is not an effect of p53 lysine acetylation. In contrast, levels of acetylated p53, are greatly reduced when sumoylation reactions occur prior to acetylation [**Figure 5.7**, upper bands lanes 1 and 3, and quantified in the lower panel]. This is seen in both SUMO-modified and unmodified fractions of p53, indicating that the presence of the SUMO machinery in the reaction is enough to reduce subsequent acetylation of the C-terminus

[**Figure 5.7**, lower bands lanes 1 and 3, and quantified in the lower panel]. Similarly, simultaneous acetylation and sumoylation lead to reduced levels of acetylated p53, independently of its sumoylation status [**Figure 5.7**, lane 5].

To investigate the effect of p53 sumoylation of its subsequent acetylation, I repeated the experiments utilizing sumoylation-deficient GST-$p53_{300\text{-}393}$K386R proteins. Here, the acetylation levels of p53 measured with polyclonal anti-acetyl Lys373 (AcK373p53) antibody did not differ, irrespective of its prior sumoylation [**Figure 5.8**, lanes 1 and 2 and quantified in the lower panel]. However, and similarly to the results obtained in the methylation experiments [**Figure 5.5**], the simultaneous sumoylation and acetylation leads to the reduction of p53 acetylation levels in $p53_{K386R}$ [**Figure 5.8**, lane 5]. This indicates that the presence of SUMO machinery reduces lysine acetylation, possibly due to competition between ubc9 and CBP/p300 for p53 interaction.

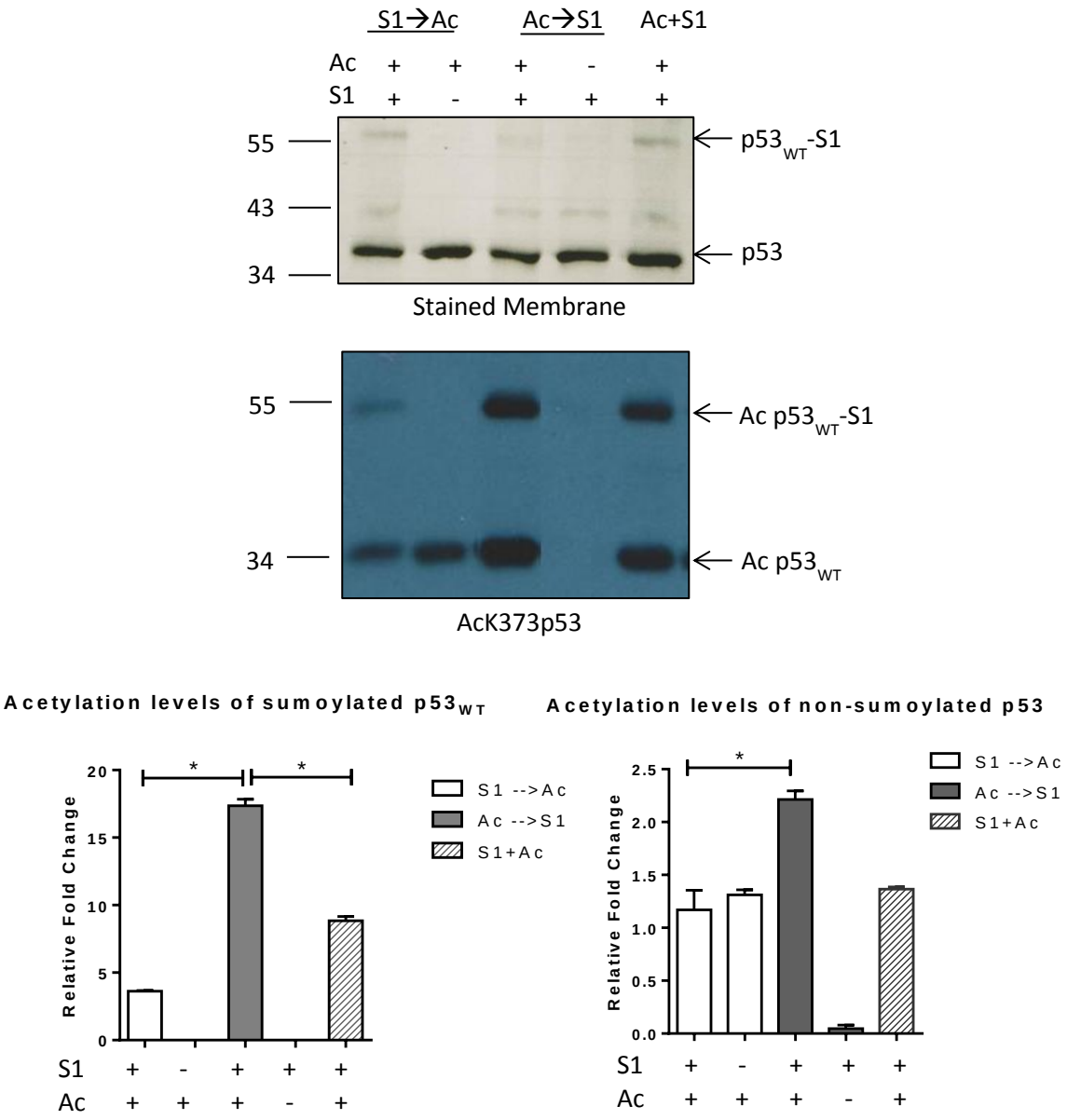

Figure 5.7. *In vitro* p53 sumoylation on K386 reduces its subsequent acetylation by CBP/p300.

In vitro sumoylation reactions were performed on GST-p53$_{300-393}$ prior (S1→Ac), after (Ac→S1) or simultaneously (S1+Ac) to acetylation reactions with the acetyltransferases CBP/p300. The reactions were run on SDS-PAGE and transferred to a membrane. The proteins were visualized by DB-71 staining, and acetylated proteins were visualized by western blot with anti-acetyl K373 (AcK373p53) polyclonal antibody. Molecular weights (kDa) are indicated. Quantification of acetylated proteins is shown on the lower panel. Results obtained from 3 independent experiments. Error bars represent the standard deviation. *p-value<0.05 as calculated by a paired student t-test.

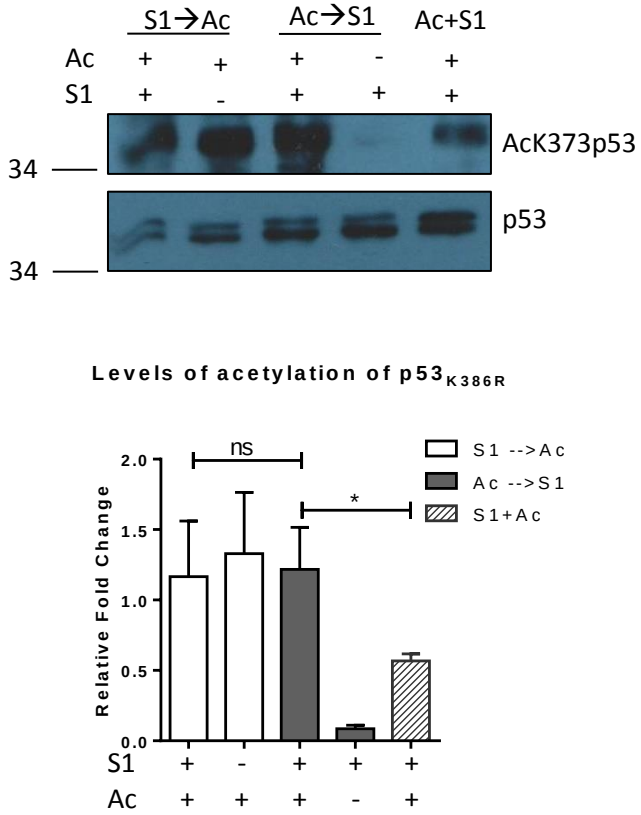

Figure 5.8. Effect of sumoylation of p53 sumoylation-deficient K386R on its subsequent C-terminal acetylation.

In vitro sumoylation reactions were performed on GST-p53$_{300-393}$ prior (S1→Ac), after (Ac→S1) or simultaneously (S1+Ac) to acetylation reactions with the acetyltransferase CBP/p300. The reactions were run on SDS-PAGE and transferred to a membrane. Acetylated proteins were visualized by western blot with anti-acetyl K373 (AcK373p53) polyclonal antibody, stripped and then probed with anti-p53 (Ab-1) monoclonal antibody to calculate the total amount of loaded p53. Molecular weights (kDa) are indicated. Quantification of acetylated proteins is shown on the lower panel. Results displayed from 2 independent experiments. Error bars represent the standard deviation. *p-value<0.05, ns - non-significant (p-value>0.05) as calculated by a paired student t-test.

To investigate whether p53 acetylation was hindered by the presence of SUMO conjugation *in vivo*, H1299 cells were transiently transfected with p53-ubc9 fused proteins and acetylated p53 proteins were immunoprecipitated with anti-acetyl lysine 373 (p53). Soluble lysates and IPs were resolved by SDS-PAGE and immuno-blotted with anti-p53 antibody [**Figure 5.9**].

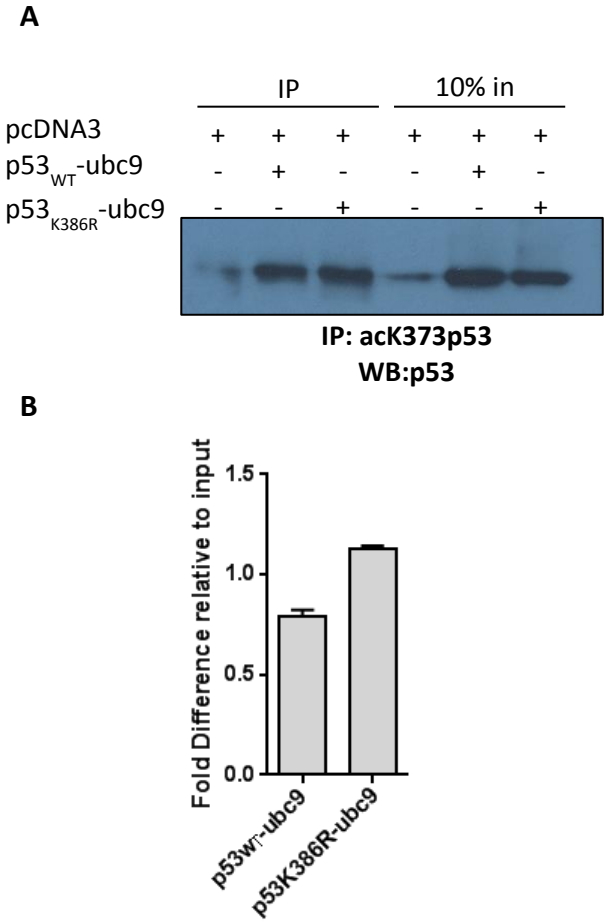

Figure 5.9. C-terminal p53 acetylation is affected by K386 sumoylation.

H1299 cells transiently transfected with either $p53_{WT}$-ubc9 or mutant $p53_{K386R}$-ubc9 plasmids, or with an empty vector (pcDNA3) were lysed and immunoprecipitated with acetyl K373 p53 antibody. The immunoprecipitates (IP) were then run on SDS-PAGE, alongside 10% input, and analyzed by western blot with anti-p53 antibody (AB-6).
(A) Representative western Blot of the immunoprecipitates analyzed with p53 antibody.
(B) Quantification of p53-K373 acetylation in the immunoprecipitates relative to input. Results obtained from 2 independent experiments. Error bars represent the standard error of the mean.

The immunoprecipitates were quantified relative to input, and the results indicate that the sumoylation-deficient mutant K386 shows slightly increased levels of p53 acetylation. Though the difference seen in the immunoprecipitates is not major, these results substantiate the previous findings, indicating that p53 sumoylation leads to decreased levels of C-terminal CBP/p300-mediated acetylation.

5.2.2 Sumoylation causes differential cellular distribution of p53

As p53 functions mostly as a transcription factor, it is found predominantly in the nucleus. The re-localization of p53 to the cytoplasm or other organelles such as the mitochondria, has, therefore a significant impact on p53-transcriptional dependent functions. PTMs such as mono-ubiquitylation by MDM2 have been described as functioning as a signal for p53's nuclear export (Li et al. 2003). Modification of p53 by SUMO has also been associated with p53's subcellular distribution, and the use of fused p53-SUMO proteins showed partial cytoplasmic localization, compared to nuclear un-fused p53 (Carter & Vousden 2008). Although these findings provide circumstantial evidence that p53 sumoylation may promote its nuclear export, the use of fused p53-SUMO proteins could raise questions as to whether they represent a good model for p53 sumoylation.

Therefore, I aimed to investigate whether p53 sumoylation would lead to its cellular redistribution. For that purpose, H1299 cells were transiently transfected with p53 WT and K386R mutants and observed by immunofluorescence microscopy [**Figure 5.10**]. All p53 proteins localized mostly in the nucleus, with no detectable cytoplasmic p53. However, the patterns of localization of localization differ slightly when comparing WT and K386R p53 proteins. Whereas K386R SUMO mutant p53 localizes exclusively within the nucleus, WT p53 proteins showed higher levels of nuclear membrane association. In cells expressing p53-ubc9 fused proteins, p53 WT shows increased nuclear membrane localization, as well as some cytoplasmic distribution. These observations agree with a recent report, which links p53 sumoylation with its interaction with nuclear export receptor CRM1, allowing p53 to be released to the cytoplasm (Santiago et al. 2013).

Fused p53-ubc9 proteins greatly increase sumoylation efficiency *in vivo* (Jakobs et al. 2007), and thus their use enhances the effects of p53 sumoylation. Arguably, the ubc9 attachment of these proteins could promote the re-localization of the fused proteins, as it has been reported that ubc9 localizes to the nuclear pore complex (Zhang et al. 2002). However, according to my observations, only the WTp53, but not sumoylation-mutant K386R localizes to the nuclear membrane and cytoplasm [**Figure 5.10**].

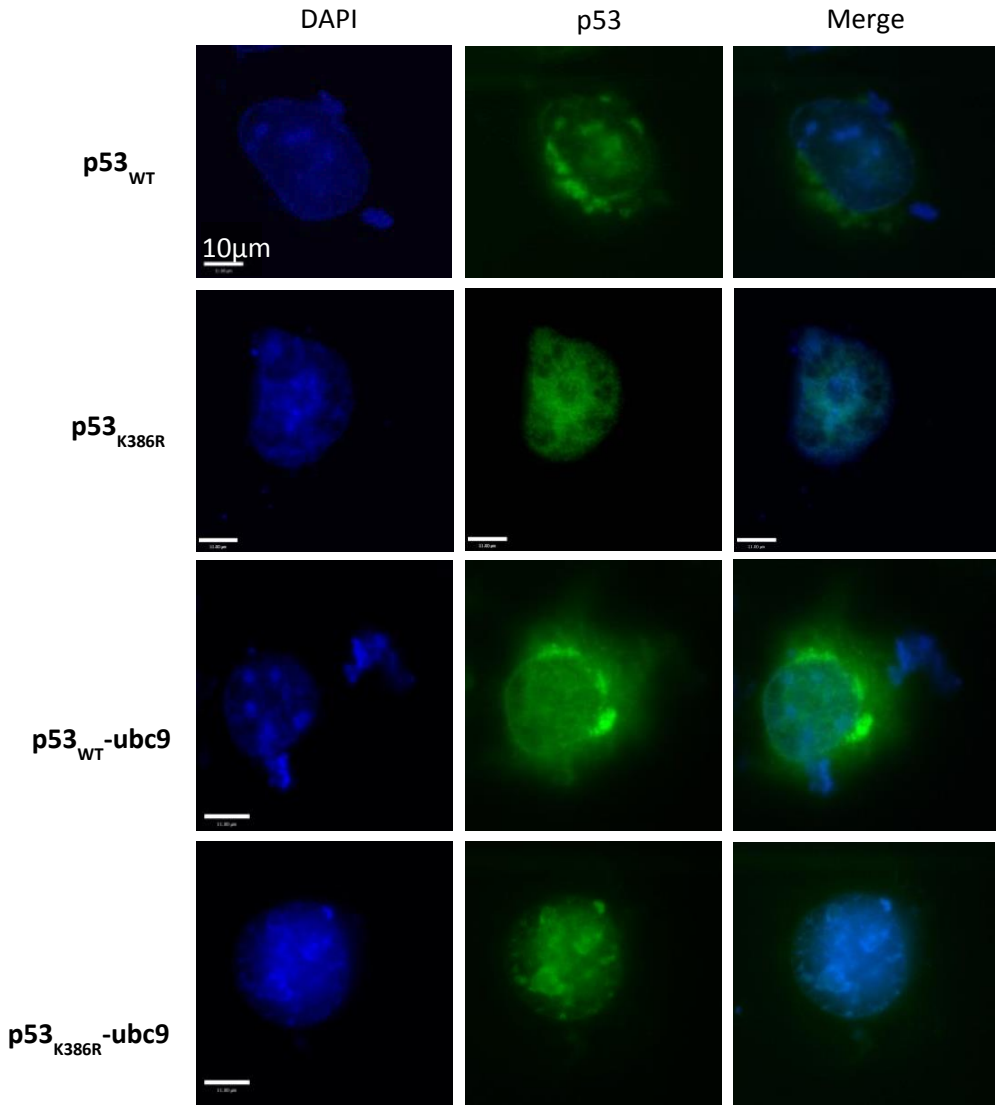

Figure 5.10. Distribution of p53 proteins with and without SUMO site.

H1299 cells were transfected with wild-type or sumoylation-deficient mutant (K386R) p53 alone, or p53-ubc9 fused proteins. p53 was immuno-stained with monoclonal p53 (DO-1) FITC antibody. Nuclei were stained with DAPI. Scale bar 10µm.

To take advantage of the increased sumoylation efficiency provided by the UFDS system whilst preventing accessory effects of the ubc9 fusion, a TEV cleavage site was introduced between p53 and ubc9, resulting in new constructs p53-TEV-ubc9 [**Figure 5.11a**]. Alongside, a TEV protease was cloned into a mammalian expression vector, to be transiently transfected along with the new p53-TEV-ubc9 constructs. To test the efficiency of TEV cleavage in cells, H1299 cells transfected with p53-TEV-ubc9 constructs were subsequently transfected with TEV protease at different time-points, from 0h-24h [**Figure 5.11b**]. Surprisingly shorter time-points (0-4h) gave a more efficient cleavage of the protein, as seen by the presence of a 55kDa band representing p53. TEV protease was then transiently transfected simultaneously or upon 4h of p53-TEV-ubc9 transfections, at increasing concentrations [**Figure 5.11c**]. Efficient cleavage was seen with co-transfection of TEV at 4:1 ratio of p53-TEV-ubc9, with virtually no p53-ubc9 fused for the mutant K386R. Because ubc9 and SUMO-1 have approximately the same molecular weight (15 and 17kDa, respectively), the band of 72kDa seen for p53WT-ubc9 after treatment with TEV could be a mixture of p53-ubc9 and conjugated p53-SUMO-1. However, the efficiency of TEV cleavage in the mutant provided sufficient evidence that TEV cleavage was effective.

The constructs were then transfected in H1299 cells and p53 localization was observed by immunofluorescence microscopy. Efficient cleavage of ubc9 by TEV is shown by western blot [**Figure 5.12a**], in both wild type and mutant K386R proteins. A small portion of WT p53 is modified by SUMO, as shown by the 72kDa band present in the WT p53 after cleavage, but absent in the sumoylation deficient mutant. Analysis of p53 localization by immunofluorescence microscopy shows a pattern similar to the ones seen in **Figure 5.10**. Whereas sumoylation-deficient mutant p53 proteins are restrained to the nucleus, a percentage of sumoylatable p53 (WT) localizes to the nuclear membrane [**Figure 5.12b**]. These results agree with the notion that SUMO promotes the nuclear export of p53, and that this is not dependent on ubc9 attachment.

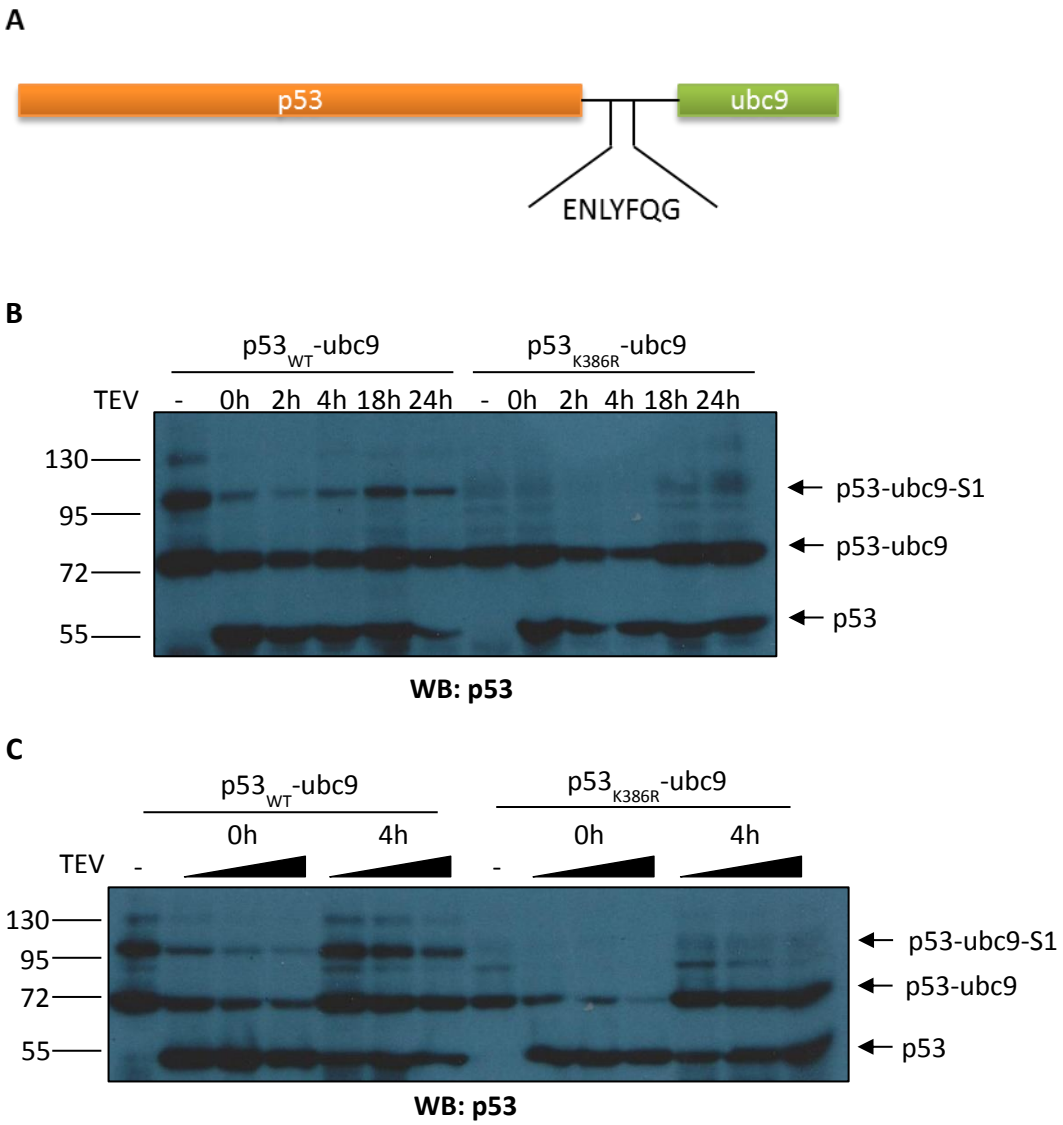

Figure 5.11. p53-TEV-ubc9 constructs and cleavage optimization.

(A) p53-TEV-ubc9 plasmids were constructed by molecular cloning, inserting TEV recognition site (ENLYFQG) between p53 and ubc9. **(B)(C)** Ubc9 Cleavage optimization. TEV protease was transfected at different time-points and increasing TEV concentrations. Proteins were visualized by Western blot with anti-p53 (Ab-6 DO-1) antibody. Molecular Weights (kDa) are indicated.

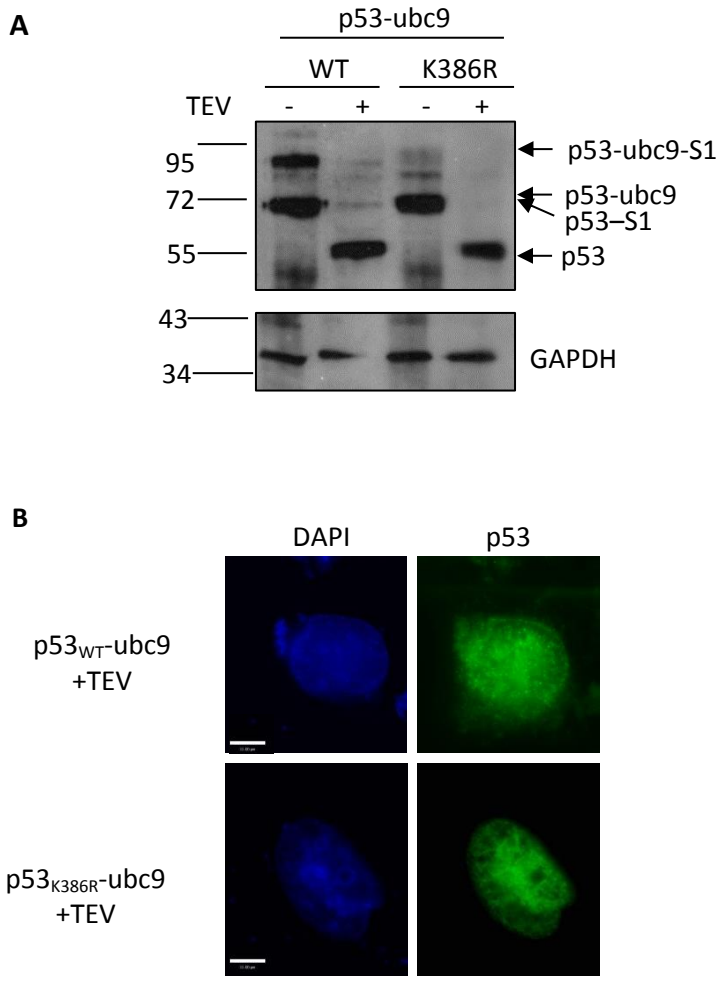

Figure 5.12. Immunofluorescence microscopy with p53-TEV-ubc9 proteins shows partial nuclear envelope localization of WT p53.

(A) Western blot showing the efficient cleavage of p53-ubc9 proteins with TEV protease. GAPDH was used as a loading control. Molecular weights (kDa) are indicated.

(B) Immunofluorescence microscopy. H1299 cells were co-transfected with wild-type or sumoylation-deficient mutant (K386R) p53-TEV-ubc9 fused proteins and TEV protease. p53 was immuno-stained with monoclonal p53 (DO-1) FITC antibody. Nuclei were stained with DAPI. Scale bar 10µm.

5.2.3 Cell survival is affected by p53 Sumoylation

As defined in **Chapter 4**, SUMO conjugation leads to the decrease of p53's transcriptional activity, particularly by reducing the expression of cell cycle arrest gene p21 and pro-apoptotic PUMA. As such, it is likely that sumoylation affects the ability of p53 to act as a tumour suppressor, by reducing its ability to induce cell arrest and apoptosis, and consequently the spread of tumourigenic cells. To investigate whether sumoylation affects cell survival, colony formation assays were performed. These assays evaluate the ability of a single cell to form a colony, and represent a way to determine cell proliferation. H1299 cells were transfected with p53-ubc9 proteins or an empty vector (pcDNA3) and cultured for a period of 2-3 weeks, after which colonies were counted [**Figure 5.13**]. The number of colonies was significantly reduced in cells where p53 proteins were transfected, as expected. Importantly, cells transfected with wild type p53 showed a fewer and smaller colonies when compared to the sumoylation deficient mutant K386R transfected cells.

These results indicate that although p53's transcriptional abilities are hampered by SUMO, these do not reflect a reduction in p53's tumour suppressor functions. On the contrary, the fact that sumoylation-deficient mutant K386R shows a reduced ability to suppress colony formation indicates that sumoylation plays a role in maintaining p53's tumour suppressor function.

A

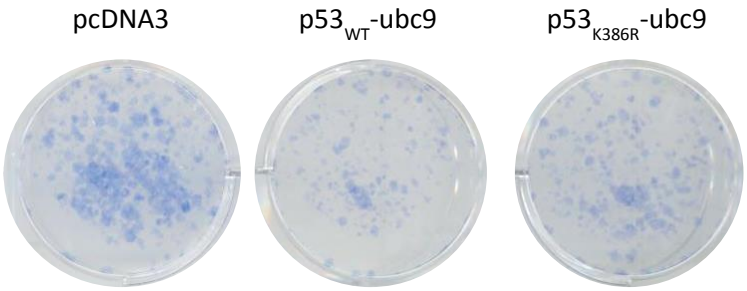

B

pcDNA3	$p53_{WT}$-ubc9	$p53_{K386R}$-ubc9
185.7+/-11.39	87.5+/-12.07	114.17+/-20.69

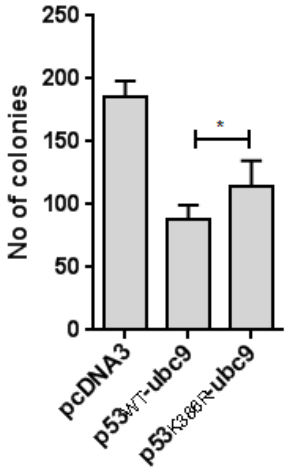

Figure 5.13. p53 sumoylation influences cell survival.

(A) Representative colony formation experiment. 2000 H1299 cells were seeded and transfected with wild-type (WT) or SUMO mutant (K386R) p53-ubc9 proteins, or with an empty control vector (pcDNA3). Cells were cultured for 2-3 weeks, fixed and stained for counting.
(B) Table and graph of number of colonies obtained from 3 independent experiments. Error bars represent the standard deviation. *p-value<0.05 as calculated by an unpaired student t-test.

5.3 Discussion

5.3.1 Sumoylation of K386 leads to reduced SET7/9-mediated methylation and CBP/p300-mediated acetylation of C-terminal residues

Analysis of C-terminal lysine modification patterns and localization of p53 upon its sumoylation revealed a further intricate role for SUMO in the regulation of p53 activity.

Regarding p53, few studies have shown interplay between SUMO and other PTMs. Lin and colleagues showed that the covalent attachment of SUMO to p53 was impaired upon DNA damage due to the phosphorylation of S20, which prevented ubc9 association (Lin et al. 2004). Due to the fact that lysine 386 is shared by both SUMO and ubiquitin, some authors have suggested that sumoylation may impair subsequent ubiquitylation, though this seems unlikely as other residues are available (Stehmeier & Muller 2009). I therefore set to investigate whether sumoylation interplay with other PTMs and thus affect p53 function.

The data presented here shows that sumoylation of lysine 386 partially impairs further C-terminal methylation of lysine 372. The decrease in SET7/9-mediated methylation of K372 upon p53 sumoylation could be caused by the reduced affinity of SET7/9 to p53. SET7/9 recognition site on p53 lies within the surrounding amino acids of K372, recognizing the sequence K370-S371-**K372**-K373 (Chuikov et al. 2004; Morgunkova & Barlev 2006). It has been shown that methylation by SET7/9 is significantly impaired by the modification of residues within the region, particularly phosphorylation of S371 and acetylation of K373 (Couture et al. 2006). While K386 may not be necessary for the interaction between SET7/9 and p53, the conjugation of a bulky SUMO moiety may induce a conformational change, causing reduced affinity of the enzyme to p53. This could be tested by performing immunoprecipitation experiments to evaluate whether SET7/9 binding is reduced in the presence of sumoylation. Also, kinetic analysis would allow the quantification of substrate specificity of SET7/9, depending on the sumoylation status of K386.

Additionally, I present evidence indicating that K386 sumoylation further reduces C-terminal acetylation. These data agreed with an earlier study showing that p53 sumoylation blocks p300-mediated acetylation (Wu & Chiang 2009a). This could be a result of reduced CBP/p300 association with p53. Intriguingly, the same study reports that although there is a reduction in p53 acetylation levels, p53-p300 interaction was not affected by K386

sumoylation. Indeed, CBP/p300 interaction with p53 is known to occur in the transactivation domain (TAD), in the N-terminal region of p53 (Lee et al. 2010). Consequently, given that ubc9 recognizes the consensus SUMO sequence located in the C-terminus of p53, it would be unlikely that ubc9 would interfere with CBP/p300 binding. However, in my *in vitro* system the use of recombinant C-terminal p53 proteins (300-393aa) indicates that CBP/p300 is able to bind within this region and acetylate C-terminal lysines. Therefore, it is possible that ubc9 interferes with CBP/p300 association to C-terminal p53. In fact, a more detailed analysis of p300-p53 association with purified p53 or p53-SUMO-1 proteins by Wu and Chiang showed that although p300 could interact efficiently with both proteins, there is a reduction in p53-p300 association in the sumoylated protein (Wu & Chiang 2009a). Validation of these results by immunoprecipitation should elucidate whether CBP/p300 association is impaired upon SUMO conjugation.

Another possibility for the impairment in acetylation levels seen upon sumoylation could be caused by the presence of SUMO-1 itself. My data shows that C-terminal acetylation is impaired if sumoylation occurs first, but not if the reactions occur simultaneously or after p53 sumoylation. This indicates that lysine acetylation is only hindered if sumoylation had already occurred, and that sumoylation does not alter acetylation levels of pre-acetylated lysines. Moreover, lysine 386 is essential for the reduced levels of acetylation seen upon sumoylation, indicating that it is the covalent attachment of SUMO to K386 that prevents further acetylation. The presence of a bulky SUMO moiety attached to K386 may hinder acetylation of nearby lysines possibly due to steric hindrance.

Importantly, both K372 methylation and C-terminal acetylation on p53 contribute for the enhancement of p53 transcriptional activity (Chuikov et al. 2004; Tang et al. 2008). Moreover, it has been shown that SET7/9-mediated methylation of K372 is important for its subsequent acetylation, thereby promoting p53 stability (Ivanov et al. 2007; Kurash et al. 2008). Therefore, sumoylation could hinder further p53 acetylation indirectly, by preventing SET7/9 association with p53, thus reducing K372 mono-methylation levels.

Independently of the mechanism, the reduction in K372 mono-methylation and C-terminal acetylation observed upon K386 sumoylation correlates with the decrease in p53's transcriptional ability reported in **Chapter 4**, indicating that sumoylation may impair p53 function via different mechanisms.

5.3.2 SUMO modification alters p53 localization

Analysis of the p53 SUMO-modification on p53 localization showed an increased localization of sumoylated p53 to the nuclear membrane, when compared to the sumoylation-deficient mutant. Several publications have linked sumoylation with nuclear-cytoplasmic transport of modified proteins. For example, co-repressor CtBP sumoylation correlates with its nuclear localization (Lin et al. 2003), whereas PIASγ-mediated sumoylation of Smad3 transcription factor stimulates its nuclear export (Imoto et al. 2008). The use of p53-SUMO-1 fusion proteins has suggested that p53 sumoylation functions as a mark for nuclear export (Carter & Vousden 2008; Carter et al. 2007). A later study showed that PIASγ-mediated sumoylation of p53 induced its cytoplasmic localization to promote p53-mediated apoptosis in endothelial cells (Heo et al. 2011). Most recently, a mechanism by which conjugation of SUMO promotes p53's nuclear export was identified, by facilitating p53's release from the nuclear export receptor CRM1 (Santiago et al. 2013). Thus, the data presented here reflects the general notion that sumoylation allows the re-localization of p53 from the nucleus, mainly to the nuclear envelope.

Interestingly, some of the proteins identified by the MS screen as p53-SUMO-1 interactors were involved in nuclear-cytoplasmic transport [**Table 3.1**]. Several importin-alpha isoforms, importin-8 and nuclear pore complex protein Nup155 were found associated with non-sumoylated p53, whereas Exportin-7 was found in the fraction containing p53-SUMO-1. Importin-α/β heterodimers are responsible for targeting NLS-containing proteins to the nuclear pore complex (NPC) and facilitate their translocation to the nucleus (Goldfarb et al. 2004). Conversely, exportins function by binding to NES-containing protein cargo, transporting them to the cytoplasm through the NPC (Fried & Kutay 2003). The association of importins and exportins with non-sumoylated and sumoylated p53, respectively, agrees with the proposed role for SUMO in the modulation of nuclear-cytoplasmic traffic.

5.3.3 Sumoylation enhances tumour suppressor function of p53

Despite the reduction in p53 transcriptional activation functions upon sumoylation [**Chapter 4**], sumoylation did not impair tumour suppressor activity of p53. In fact, the

sumoylation-deficient mutant K386R had higher clonogenic potential, indicating that sumoylation may function to maintain p53's tumour suppressor functions [**Figure 5.13**].

Although conflicting, these results indicate that sumoylation may promote transcription-independent tumour suppressor roles of p53, possibly by primarily inducing its nuclear export. In fact, PIASy-mediated sumoylation of p53 led to its cytoplasmic localization, and promoted transcription-independent apoptosis in endothelial cells (Heo et al. 2011). p53 can mediate apoptosis in a transcription-independent way, as shown by over-expression experiments, in which the use of transactivation p53 mutants was able to efficiently induce apoptosis (Chipuk et al. 2004; Kakudo et al. 2005). Two models have been proposed to explain transcriptional-independent p53-mediated apoptosis. The first one involves the localization of p53 to the mitochondria, where it binds anti-apoptotic factors Bcl-xL/Bcl-2 and Mcl-1, allowing pro-apoptotic BAK release and activation. This is followed by MOMP (mitochondria outer membrane permeabilization) and cytochrome c release, resulting in programmed cell death (Leu et al. 2004). p53 is also able to interact with and activate pro-apoptotic BAX, leading to MOMP, and this correlated with the increased cytoplasmic accumulation of p53 (Chipuk et al. 2004). The second mechanism integrates both transcription-dependent and independent apoptosis. Following genotoxic stress, p53 activates the expression of pro-apoptotic gene PUMA. Cytoplasmic p53 is released from its complex with Bcl-xL by PUMA, and is then able to bind to BAX and promote its activation and oligomerization, allowing cytochrome c release from the mitochondria (Chipuk et al. 2005).

Transcriptional-independent p53-mediated apoptosis is preceded by the accumulation of p53 in the cytoplasm after specific stimuli, including DNA damaging agents, hypoxia, proteasome inhibition and ischemia (Erster et al. 2004; Speidel et al. 2006; Nair et al. 2006; Kojima et al. 2006). The role of certain PTMs specific for non-nuclear p53 have been linked with p53-mediated apoptosis. For example, upon DNA damage, acetylated K120-p53 localizes to the mitochondria outer membrane, and is required to remove Mcl-1 from BAK complex, allowing BAK activation (Sykes et al. 2009). Also, S46 phosphorylation is important to maintain p53 mitochondrial localization and facilitates its interaction with MDM4, which in turn bridges the interaction between p53 and Bcl-2, leading to cytochrome c release (Sorrentino et al. 2013; Mancini et al. 2009). Mono-ubiquitination has also been demonstrated to be important for p53 translocation to the mitochondria (Marchenko et al. 2007). Similarly, SUMO

modification of K386 could enhance p53-mediated apoptosis through a non-transcriptional mechanism, mainly by relocation of p53 to the cytosol/mitochondria. Further investigation is needed to address the role of SUMO on p53 trafficking. Perhaps the use of transactivation p53 mutants would be helpful to evaluate the role of sumoylation on p53-transcriptional-independent apoptosis.

Another possibility is that the same way sumoylation dampens p53-mediated transcription of p53-activated genes (such as p21 and PUMA), it is possible that SUMO attachment alleviates the repressive activities of p53, thus also de-repressing survival genes (such as survivin and cdc25c). Survivin is a member of inhibitor of apoptosis proteins (IAP), which work by targeting and inhibiting active caspases, thereby preventing the apoptotic program (Mita et al. 2008). Cdc15c is part of a family of phosphatases involved in cell cycle regulation. Cdc25c de-phosphorylates Cdk1, leading to the activation of CyclinB/cdk1 complex and progression from G2 into mitosis (Clair & Manfredi 2006). Both Survivin and Cdc25c have been shown to be down-regulated in a p53-dependent manner. Hence, by preventing p53's transcription functions, SUMO could promote p53-mediated transcription-independent activities like apoptosis.

Alternatively, other cytosolic functions of p53 may be induced by p53 sumoylation. Among other functions, cytoplasmic p53 has been shown to prevent autophagy (Tasdemir et al. 2008). Autophagy (or macroautophagy) is the formation of autophagosomes around dysfunctional organelles or proteins that have been targeted for degradation. The autophagosomes are then fused with lysosomes to be catabolized (Berkers et al. 2013). It has been proposed that autophagy is an effective pro-survival response to low metabolic stress (Levine & Kroemer 2009), but it can also lead to enhanced survival of tumour cells in cases of prolonged or extreme stress (Morselli et al. 2009). p53 can control autophagy both in a positive and negative way, depending on its subcellular localization. Whereas nuclear p53 triggers autophagy in response to cellular stresses, via the activation of a number of autophagy-inducing proteins including DRAM-1 (damage-regulated autophagy modulator), cytoplasmic p53, on the contrary, prevents autophagic response (Tasdemir et al. 2008). Thus, by inducing p53 cytosolic localization, sumoylation may prevent survival due to reduced autophagy.

CHAPTER 6

General Discussion

Chapter 6. General Discussion

The Small Ubiquitin Modifier protein SUMO is known to modify a variety of proteins, altering their function, stability and/or localization. Although p53 has been a long-known target of SUMO, the effects of its modification have been a matter of debate. Here, I provide evidence that SUMO modification of p53 leads to the alteration of p53's interactome, both by promoting p53 association with novel partners, and impeding existing protein-protein interactions. Additionally, sumoylation of K386 promotes p53-mediated transcriptional silencing, which is not caused by the reduced affinity of p53 to chromatin, but rather by the recruitment of transcriptional co-repressor factors. Moreover, p53 sumoylation hinders subsequent C-terminal acetylation and K372 methylation, marks associated with increased transcriptional potential. Finally, I show that sumoylation increases p53's nuclear envelope and cytoplasmic localization, pointing to a possible role of SUMO in the modulation of non-transcriptional activities of p53.

6.1 LSD1 as a specific p53-SUMO binding protein

The proteomics screen carried out in this study aimed to investigate whether SUMO-1 modification of p53 led to a change in protein-protein interactions. Indeed, MS analysis predicted a number of proteins to be specific binding partners of sumoylated p53, from which Lysine Specific Demethylase 1 (LSD1) showed to have preferential binding affinity to SUMO-1-modified p53. LSD1 is involved in chromatin remodeling, primarily by de-methylating H3K4me1/2, and thus leading to heterochromatin formation (Shi & Whetstine 2007). Interestingly, LSD1 can also de-methylate H3K9me2/me1, and this substrate selectivity is dictated by associated co-factors (Wysocka et al. 2005). For example, association with nuclear receptors like Androgen Receptor (AR) lead to H3K9 de-methylation (Metzger et al. 2005; Wissmann et al. 2007), whereas interaction with co-factors such as HDACs, CoREST and BHC80 promote H3K4 de-methylation (Shi et al. 2005). LSD1 is also an integral component of co-repressor complexes NurD and CoREST (Wang et al. 2007; Wang et al. 2009). Association of LSD1 with CoREST and HDAC1/2 leads to the formation of the core ternary complex LCH, which bears both de-methylase and de-acetylase activities (Lee et al. 2006). The interaction of LSD1 with CoREST stabilizes LSD1, and has been shown to be important for nucleossomal

targeting and de-methylation by LSD1 (Lee et al. 2005; Shi et al. 2005). More recently, Wang and colleagues proposed that LSD1 is also part of the Mi-2/nucleosome remodeling and deacetylase (NuRD) complex (Wang et al. 2009).

A direct interaction between LSD1 and p53 has been described previously, and correlated with alteration of chromatin structure and repression of alpha-fetoprotein (AFP) during liver development (Tsai et al. 2008). The authors show that LSD1 and p53 co-occupy a p53-RE within AFP gene and that co-related with decrease in H3K4 di-methylation levels. However, LSD1 was not recruited to p53-target gene promoter p21 in MEFs, and the authors concluded that LSD1 might be recruited by p53 in a gene-specific manner. My data, however, suggests that LSD1 is recruited to p53 in a SUMO-dependent manner, possibly bridging the association with HDAC2 repressor-containing complexes such as CoREST or NuRD.

Previously, the association of p53 and LSD1 was shown to promote p53 K370me2 de-methylation *in vivo*, and correlated with a decrease in p53 transcription functions (Huang et al. 2007). The authors demonstrate that de-methylation by LSD1 abolishes the interaction of p53 with co-activator 53BP1, thereby maintaining p53 in an inactive state. The observation that LSD1 has higher affinity to sumoylated p53 may add to this model, whereby SUMO-1 attachment mediates LSD1 recruitment. In retrospective, it would have been interesting to investigate whether sumoylated p53 has diminished affinity to 53BP1, thus supporting this model. Additionally, it would have been worth investigating the levels of K370 methylation *in vivo*, in both WT and K386R mutant p53.

The augmented affinity of LSD1 to SUMO-modified p53 could be caused by non-covalent interactions between LSD1 and the SUMO moiety. These could be conferred by SUMO Interacting Motifs (SIMs) on the surface of LSD1. *In silico* predictions revealed 5 possible SIMs within the LSD1 sequence, although these were not confirmed *in vivo*. Alternatively, LSD1 recruitment to sumoylated p53 can occur via the new interaction domain at the SUMO-p53 interface. Structural studies on p53 PTMs are scarce, and most published results focus on phosphorylation and acetylation (Saha et al. 2015). Such studies could greatly increase the general understanding of the changes in p53 protein-protein interactions upon specific modifications. In particular, bulky modifications such as the addition of SUMO proteins can very well alter the structure of p53, providing new surfaces for protein

interactions, or, on the contrary, abolish existing interacting sites. Therefore, structural work could contribute to define how PTMs alter p53 function.

The possibility that SUMO could alter the network of protein interactions of its substrates was explored here, and in addition to the identification of specific p53-SUMO-1 binding partner LSD1, a number of proteins were found associated only with non-modified p53. These were mostly involved in transcriptional regulation, either by promoting histone modifications and chromatin remodeling (such as WD repeat-containing proteins and SMARCA1), modulation transcription (UPF0568 protein C14orf166), or involved in mRNA processing to facilitate gene expression (as is the case for RNA helicases of the DEAD-box helicase (DDX) family and RNA-binding protein4). Although not confirmed *in vivo*, the loss of these interactions with sumoylated p53 suggests that SUMO modification can also function to prevent protein interactions with existing partners. Interestingly, most of the interactions lost upon p53 sumoylation identified in the MS screen were proteins involved in the promotion of gene expression, supporting the transcriptional repression role addressed to SUMO.

The findings discussed here focused on the changes of protein-p53 interactions that happen upon SUMO-1 modification of K386. Future studies could include the investigation of SUMO-2/3-p53 specific binding partners, and ascertain whether these would differ from p53-SUMO-1 interactors. Given the ability of SUMO-2/3 isoforms to form mixed chains, and the recent bridge between ubiquitin-SUMO systems provided by the discovery of STUbLs, it is tempting to postulate that protein interactions would be different. In any case, these findings present an exciting new approach to the study of p53 sumoylation and its downstream effects.

6.2 p53 sumoylation as a mark for transcriptional silencing

Data presented in this thesis supports a negative effect of SUMO-modification on p53 transcriptional abilities. Over-expression of p53 WT in p53 null H1299 cells leads to the reduction of expression of p53-responsive genes, when compared to the sumoylation-deficient K386R mutant proteins. Similarly, over-expression of components of the sumoylation

machinery lead to the reduction of p53-dependent transcription. This was accompanied by the reduction of Histone H3 acetylation and an increase in H3K9me3 marks on the promoter region of these genes. Intriguingly, and in contrast with a previous publication (Wu & Chiang 2009a), decreased gene expression correlated with an increase in p53 affinity to target promoters, measured by chromatin immunoprecipitation experiments. This observation, consistent in all cell lines tested, was followed by other ChIP experiments to assess the binding of co-factors to these regions. I found that while HDAC2 was enriched in the promoters where sumoylated p53 was present, co-activator CBP recruitment was diminished in these regions, in conformity with the decrease in histone H3 acetylation. This suggests that sumoylation of K386 could enhance stabilization of p53 to chromatin while promoting HDAC2-containing complexes, which via de-acetylation of nearby histones cause heterochromatin formation, leading to transcriptional silencing. These data, together with the preferential recruitment of LSD1 to SUMO-modified p53 led me to propose the model represented in **Figure 4.14**, whereby the covalent attachment of SUMO to p53 leads to the recruitment of HDAC complexes, initiated by the recruitment of LSD1 to sumoylated p53. The recruitment of these co-repressor complexes would then promote chromatin remodeling, resulting in silencing of p53-responsive genes.

Association of p53 with co-repressor complexes in the vicinity of p53-RE has been previously reported. For instance, recruitment of HDAC complexes to p53-target promoters upon p53 binding was shown to be mediated by co-factors, such as Sin3A (Murphy et al. 1999). Sin3A/HDAC recruitment is essential for p53-mediated repression of target genes such as MAP4 (Microtubule Associated Protein 4), c-myc and MAD1 (Mitosis Arrest Deficiency 1), and is associated with a decrease in histone acetylation (Murphy et al. 1996; Ho et al. 2005; Chun & Jin 2003). Another gene repressed by p53 is AFP, which requires the recruitment of Sin3A complex as well as HP1 (Heterochromatin Protein 1), and is associated with H3K9 di-methylation (Nguyen et al. 2005). More recently, Sin3B has also been shown to be recruited by p53, to the promoters of HSPA8, MAD1 and CRYZ (Bansal et al. 2011). Interestingly, p53 appears to be able to function both as an activator and as a repressor for the same gene. An example is the target gene encoding heat-shock protein HSP90β, which can be up- or down-regulated by p53 depending on the recruitment of co-activator p300 or co-repressor Sin3A/HDAC1, in response to UV irradiation (Zhang et al. 2004). Importantly, other proteins

seem to influence p53's transcriptional abilities at target-promoters. Its key regulator, MDM2, was shown to inhibit p53 transcriptional function by displacing co-activators and HATs such as p300 (Teufel et al. 2007), and recruiting co-repressors such as KAP1 and HDACs (C. Wang et al. 2005). Moreover, MDM2 was shown to co-precipitate with histone methyltransferases SUV39H1 and Glp, and the formation of this complex correlated with increased H3K9 methylation on p53-target promoters (Chen et al. 2010). Thus, it would be interesting to explore whether sumoylation of p53 augments the recruitment of MDM2 to specific promoters.

On the related note, Sin3A association with chromatin-bound p53 was dramatically increased when p53 was modified by SUMO-1 (Wu & Chiang 2009a). Although a preferential HDAC recruitment to p53 protein was not observed in the presence of SUMO (Wu & Chiang 2009a and this study), here I showed that HDAC2 was enriched in p53-target promoters in the presence of SUMO-modified p53 [**Figure 4.5**, **Figure 4.9**]. This observation indicates that HDAC2 recruitment is not direct, but rather mediated thought other co-factors, namely Sin3A, LSD1 or CoREST. The preferential recruitment of LSD1 to sumoylated p53 described here makes it an ideal candidate to mediate the recruitment of HDAC2 to chromatin. Since LSD1 and HDAC2 can co-exist in two protein complexes, it would be interesting to investigate whether these proteins are recruited in a complex to p53-target promoters in a SUMO-p53 dependent manner. Also, knock-down experiments of LSD1 would answer the question as to whether LSD1 recruitment is necessary for the assembly of HDAC2 to p53-target promoters. It is also not clear how LSD1 executes its function on sumoylated p53. On one hand, LSD1 could act as a histone demethylase. Since H3K9 methylation levels raised upon p53 sumoylation, it is likely that the specificity of LSD1 stands is aimed towards H3K4. Further studies of histone epigenetic marks related to LSD1 activity, particularly the state of H3K4 di-methylation, upon p53 sumoylation would clarify its specific association. It is also possible that LSD1 function in this context is the one of a bridging protein to other chromatin remodeling complexes, including HDACs. HDAC recruitment to the promoter regions tested was clearly associated with a reduction in Histone acetylation, indicating a clear histone deacetylase activity. Finally, a third mode of regulation by LSD1 in this context could be its specificity towards K370 on p53 itself. As mentioned above, di-methylation of K370 by a yet unidentified methyltransferase results in p53's transcriptional activation; LSD1-dependent demethylation of K370me2

represses p53 functions, by reducing its interaction with 53BP1 (Huang et al. 2007). Thus, SUMO-p53-dependent recruitment of LSD1 could have three different functions: a) as a histone demethylase; b) as a co-factor for the recruitment of repressor/chromatin remodeling complexes; or c) as a p53-specific demethylase.

6.3 The involvement and interaction of SUMO-1 with other PTMs on p53

The interplay between SUMO modification and other PTMs was also explored. The results shown here suggest that SUMO-1 modification on p53K386 leads to the reduction of K372 SET7/9-mediated methylation, and also interferes with C-terminal CBP/p300-mediated acetylation. Notably, both modifications affected by sumoylation are known to enhance p53 transcriptional abilities (Chuikov et al. 2004; Tang et al. 2008). SET7/9-mediated methylation of K372 correlated with increased transcription of p21, BAX and MDM2 genes, and demonstrated to be an important step for C-terminal lysine acetylation (Chuikov et al. 2004; Ivanov et al. 2007). While p53's acetylation results in its activation, the mechanism behind this phenomenon remains unclear. On one hand, p53 acetylation is thought to enhance p53-DNA binding, which in turn promotes transcription (Gu & Roeder 1997). On the other hand, it was proposed that the increased transcriptional potential resulting from p53 acetylation is triggered by the recruitment of co-activators to chromatin (Barlev et al. 2001; Espinosa & Emerson 2001). In line with the latter, is the observation that p53 acetylation by co-activator HAT p300/CBP is more efficient when p53 is bound to chromatin (Cesková et al. 2006).

It remains unclear whether the negative effect of sumoylation on the subsequent acetylation of p53 is caused by the reduced affinity of HAT CBP/p300 (to either chromatin or p53 itself) or due to the steric interference of the SUMO molecule. According to a previous publication, p53 sumoylation did not interfere with the p53-p300 interaction, and therefore the authors propose a model in which sumoylation hinders C-terminal acetylation due to steric hindrance (Wu & Chiang 2009a). However, chromatin immunoprecipitation experiments showed that along with the increased recruitment of HDAC2 to p53-promoters, there was a slight decrease in the levels of CBP bound to chromatin when p53 was sumoylated [**Figure 4.5**]. In an *in cellulo* context, this could explain the reduced acetylation of p53 following its

sumoylation, where p53 acetylation results from HAT recruitment to chromatin, rather than to p53 itself. On the other hand, *in vitro* experiments revealed p53 acetylation levels despite the lack of chromatin-associated p53 [**Figure 5.7**], indicating that CBP/p300 is able to bind C-terminal p53 in a chromatin-free context. Together, these data suggest that while CBP/p300 recruitment to chromatin may be important for further p53 acetylation, the physical presence of the SUMO moiety on K386 is sufficient to reduce subsequent acetylation of C-terminal lysines. Alternatively, the reduction of acetylation levels could instead be an indirect consequence of sumoylation on K372 SET7/9-mediated mono-methylation. The use of a K372 methylation deficient mutant in the acetylation studies would be important to address this question.

In the context of DNA-bound p53, the presence of HATs and HDACs in the surrounding chromatin likely influences p53 acetylation and function. Deacetylation of p53 is catalysed by HDACs, and strongly correlates with repression of p53 activity (Luo et al. 2000). Thus, the favourable recruitment of HDAC2 to p53-target promoters by SUMO-modified p53 could lead not only to histone deacetylation, but also deacetylation of p53 itself. It would be interesting to investigate the enrichment of acetylated p53 towards target-promoters, depending on its sumoylation status. This could be assessed by chromatin immunoprecipitation techniques as used here, with a specific anti-acetyl p53 antibody. Deacetylation of both histone and non-histone proteins by HDACs is an important regulator of gene expression, and studies in knock-out mice show that loss of HDAC1/2 results in a reduction of cell proliferation (Wilting et al. 2010; Yamaguchi et al. 2010). As such, due to their biological significance, HDAC inhibitors have long been exploited for their potential as anti-cancer agents (Marks & Xu 2009).

Importantly, p53 deacetylation is strongly linked with its ubiquitylation, and MDM2 has been shown to promote HDAC1-mediated deacetylation, resulting in p53 degradation (Ito et al. 2001; Jin et al. 2002; Ito et al. 2002). The competition between ubiquitin and acetyl groups for the same C-terminal lysines on p53 presents an effective method of p53 regulation. Given the unidirectional effect of sumoylation on C-terminal p53 acetylation, it is worth investigating whether sumoylation would have an effect on ubiquitylation. *In vitro* MDM2-mediated ubiquitylation of C-terminal p53 did not show any variation irrespective of its prior sumoylation [data not shown], though a previous study suggested that p53 mono-ubiquitylation stimulates PIASy-mediated sumoylation (Carter et al. 2007). Additional studies

on the mutual effect of SUMO and other PTMs would certainly improve the understanding of sumoylation in the regulation of p53. In particular, studies on K370 di-methylation levels would be important to decipher the role of LSD1 recruitment to SUMO-modified p53. Since *in vitro* studies are restricted because the enzyme that catalyses K370 di-methylation is yet to be identified, these studies would have to be done in a cellular context.

6.4 SUMO as a modulator of tumor suppressor functions of p53

Finally, although SUMO plays a clear repressive role on the transcription activity of p53, data presented here suggested that it may also promote tumour suppressor abilities of p53. This was evidenced by the fact that a sumoylation-deficient mutant had higher clonogenic potential that the WT protein [**Figure 5.13**]. A possible explanation for this phenomenon is that SUMO promotes non-nuclear functions of p53. Indeed, although p53 exerts its function mainly as a sequence-specific transcription factor, over the years a number of transcription-independent functions have been addressed to p53. In line with this idea, is the observation that sumoylation increases p53 localization to the nuclear membrane and cytoplasm [**Figure 5.10**, **Figure 5.12**] (Carter et al. 2007; Pennella et al. 2010; Santiago et al. 2013). Thus, by promoting nuclear export, SUMO may be contributing for cytoplasmic functions of p53.

One of the first p53 non-nuclear functions described was transcription-independent apoptosis (Caelles et al. 1994; Haupt et al. 1995). The translocation of p53 to the mitochondria is part of a rapid response to γ-irradiation in radiosensitive organs, triggering early apoptosis before induction of p53 target genes (Erster et al. 2004). Studies with irradiated mouse fibroblasts showed that the primary cause of p53-mediated apoptosis depends on p53 non-transcriptional activities (Speidel et al. 2006). Accordingly, treatment with a small-molecule inhibitor of p53 Pifithrin-μ (PFTμ), which inhibits p53 mitochondrial translocation but does not affect its transactivation potential, prevented cell death in thymocytes (Strom et al. 2006). Modification of p53 with SUMO-1 has been shown to increase apoptosis in Saos-2 cells and *Drosophila*, although these studies did not address whether this induction was via transcription-dependent or independent mechanisms (Müller et al. 2000; Mauri et al. 2008).

Similarly, in mice ovarian cells, a shorter isoform of p53 resultant from alternative splicing (p53b) has been shown to be modified by SUMO-1 at K375, and correlated with increased protein stability and p53-mediated apoptosis (Liu et al. 2013). Whilst these studies demonstrate a clear role for SUMO in stimulating p53-mediated apoptosis, it is unclear whether this effect relies on p53 transcription-independent functions. On the other hand, a recent study has linked p53 sumoylation with the increased transcription of pro-apoptotic genes PUMA, NOXA and BAX, and the consequent increase in apoptosis in podocytes (Wang et al. 2014). Although these results discord with the data presented in this thesis, it is possible that the function of p53 sumoylation is stimuli and cell-specific.

In addition to apoptosis, cytoplasmic p53 is able to mediate other non-transcriptional functions, such as autophagy and inhibition of glucose metabolism (Comel et al. 2014). The latter may be important to prevent the Warburg effect typical of cancer cells, in which the use of glycolysis for ATP production is preferred, even in the presence of sufficient oxygen levels. Interestingly, PIASγ-mediated sumoylation of p53K386, together with Tip60-mediated acetylation on K120, were shown to act as a powerful binary signal for p53 cytoplasmic accumulation and induce autophagy (Naidu et al. 2012). Clearly, the effect of PTMs and their combinatorial effect on p53 is important for both transcriptional and non-transcriptional functions of p53.

Most research relating to p53 sumoylation focused on the effects of SUMO on p53 transcriptional activities. Although undoubtedly important, perhaps the mystery of p53-SUMO relationship lies beyond p53-mediated transcription. The results presented here suggest that sumoylation affects p53 activity via three different mechanisms. First, sumoylation stabilizes p53-chromatin association whilst repressing p53 transcriptional activity via recruitment of corepressors. Second, sumoylation prevents the C-terminal acetylation and K372 mono-methylation, thus contributing for p53 inactivation. And finally, sumoylation leads to p53 nuclear export, likely enhancing cytoplasmic functions of p53 [**Figure 6.1**].

The implications of p53 sumoylation *in vivo* remain to be elucidated. Whilst the generation of human p53 knock-in mice models with SUMO consensus motif mutations would provide useful information for the role of SUMO-p53 in tumourigenesis, it is important to take into consideration that this may not reproduce the effects in human. Several mouse models

for C-terminal lysine modifications (including acetylation and ubiquitylation) showed phenotypes that resembled wild type ones (Toledo & Wahl 2006), posing questions about the functional effect of these modifications *in vivo*. Additionally, the most common isoform of p53 in mouse does not contain a SUMO consensus motif, and accordingly, cannot be sumoylated (Stindt et al. 2011). Strikingly, studies in rat neurons have shown that rat p53 can be SUMO-1 modified, even though rat p53 lacks a SUMO consensus motif and the targeted lysine is yet to be identified (Gowran et al. 2009). Also, conclusions from experiments with *Drosophila* as an animal model for p53 sumoylation have to be done with caution, as unlike human p53, flies have two SUMO sites, and none of these correlates with the C-terminal SUMO site conserved in human p53 (Mauri et al. 2008; Pardi et al. 2011). A promising alternative model to study p53 sumoylation *in vivo* is zebrafish. In one study, depletion of all three SUMO paralogues triggered p53-dependent apoptosis, which could be rescued by p53 inactivation (Yuan et al. 2010). Zebrafish p53 contains a SUMO motif in the C-terminus of the protein, homologous to the human p53. Thus, mutation of this site in zebrafish could provide valuable information about the role of p53 sumoylation *in vivo*.

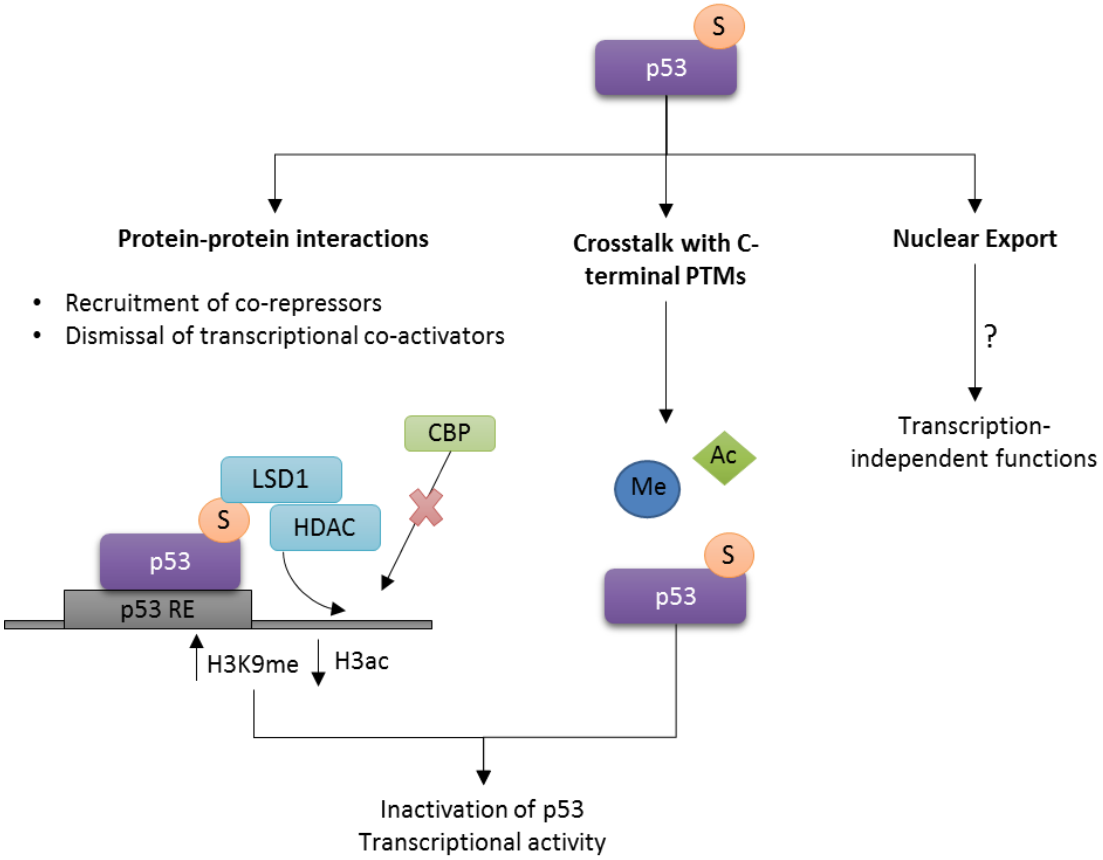

Figure 6.1. Effects of SUMO proteins on p53 function.

SUMO modification of tumour suppressor p53 can contribute to p53 function via different mechanisms. 1) p53 sumoylation leads to p53-transcription inactivation due to recruitment of co-repressors to the p53-target promoters, which contribute for histone modification and heterochromatin formation. 2) Sumoylation of K386 impedes further C-terminal modifications, including lysine acetylation and K372 mono-methylation. 3) Sumoylation induces the nuclear export of p53, possibly contributing to p53 cytoplasmic functions.

Chapter 7. Bibliography

Ahn, J.-W. et al., 2009. Covalent conjugation of Groucho with SUMO-1 modulates its corepressor activity. *Biochemical and biophysical research communications*, 379(1), pp.160–5.

Alkuraya, F.S. et al., 2006. SUMO1 haploinsufficiency leads to cleft lip and palate. *Science (New York, N.Y.)*, 313(5794), p.1751.

Anckar, J. & Sistonen, L., 2007. SUMO: getting it on. *Biochemical Society transactions*, 35(Pt 6), pp.1409–13.

Andrews, E.A. et al., 2005. Nse2, a component of the Smc5-6 complex, is a SUMO ligase required for the response to DNA damage. *Molecular and cellular biology*, 25(1), pp.185–96.

Appella, E. & Anderson, C.W., 2001. Post-translational modifications and activation of p53 by genotoxic stresses. *European Journal of Biochemistry*, 268, pp.2764–2772.

Artandi, S.E. & DePinho, R.A., 2010. Telomeres and telomerase in cancer. *Carcinogenesis*, 31(1), pp.9–18.

Ayaydin, F. & Dasso, M., 2004. Distinct in vivo dynamics of vertebrate SUMO paralogues. *Molecular biology of the cell*, 15(12), pp.5208–18.

Baba, D. et al., 2005. Crystal structure of thymine DNA glycosylase conjugated to SUMO-1. *Nature*, 435(7044), pp.979–82.

Ban, R., Nishida, T. & Urano, T., 2011. Mitotic kinase Aurora-B is regulated by SUMO-2/3 conjugation/deconjugation during mitosis. *Genes to cells : devoted to molecular & cellular mechanisms*, 16(6), pp.652–69.

Bansal, N. et al., 2011. Tumor suppressor protein p53 recruits human Sin3B/HDAC1 complex for down-regulation of its target promoters in response to genotoxic stress. *PloS one*, 6(10), p.e26156.

Barlev, N. a et al., 2001. Acetylation of p53 activates transcription through recruitment of coactivators/histone acetyltransferases. *Molecular cell*, 8(6), pp.1243–54.

Bartek, J. & Hodny, Z., 2010. SUMO Boosts the DNA Damage Response Barrier against Cancer. *Cancer Cell*, 17(1), pp.9–11.

Bawa-Khalfe, T. & Yeh, E.T.H., 2010. SUMO Losing Balance: SUMO Proteases Disrupt SUMO Homeostasis to Facilitate Cancer Development and Progression. *Genes & cancer*, 1(7), pp.748–752.

Beckerman, R. & Prives, C., 2010. Transcriptional regulation by p53. *Cold Spring Harbor perspectives in biology*, 2(8), p.a000935.

Bell, S. et al., 2002. p53 contains large unstructured regions in its native state. *Journal of molecular biology*, 322(5), pp.917–27.

Bennett, R.L. et al., 2012. The RAX/PACT-PKR stress response pathway promotes p53 sumoylation and activation, leading to G_1 arrest. *Cell Cycle*, 11(2), pp.407–17.

Bensaad, K. & Vousden, K.H., 2007. P53: New Roles in Metabolism. *Trends in cell biology*, 17(6), pp.286–91.

Berkers, C.R. et al., 2013. Metabolic regulation by p53 family members. *Cell metabolism*, 18(5), pp.617–33.

Bertolotto, C. et al., 2011. A SUMOylation-defective MITF germline mutation predisposes to melanoma and renal carcinoma. *Nature*, 480(7375), pp.94–98.

Bhat, K.P. et al., 2004. Essential role of ribosomal protein L11 in mediating growth inhibition-induced p53 activation. *The EMBO journal*, 23(12), pp.2402–12.

Bieging, K.T. & Attardi, L.D., 2012. Deconstructing p53 transcriptional networks in tumor suppression. *Trends in cell biology*, 22(2), pp.97–106.

Bischof, O. et al., 2006. The E3 SUMO Ligase PIASy Is a Regulator of Cellular Senescence and Apoptosis. *Molecular Cell*, 22, pp.783–794.

Bischof, O. & Dejean, A., 2007. SUMO is Growing Senescent. *Cell Cycle*, 6(6), pp.677–681.

Boddy, M.N. et al., 1996. PIC 1, a novel ubiquitin-like protein which interacts with the PML component of a multiprotein complex that is disrupted in acute promyelocytic leukaemia. *Oncogene*, 13(5), pp.971–82.

Böhlig, L. & Rother, K., 2011. One function--multiple mechanisms: the manifold activities of p53 as a transcriptional repressor. *Journal of biomedicine & biotechnology*, 2011, p.464916.

Bohren, K.M. et al., 2004. A M55V polymorphism in a novel SUMO gene (SUMO-4) differentially activates heat shock transcription factors and is associated with susceptibility to type I diabetes mellitus. *The Journal of biological chemistry*, 279(26), pp.27233–8.

Bossis, G. et al., 2005. Down-regulation of c-Fos/c-Jun AP-1 dimer activity by sumoylation. *Molecular and cellular biology*, 25(16), pp.6964–79.

Bossis, G. & Melchior, F., 2006a. Regulation of SUMOylation by reversible oxidation of SUMO conjugating enzymes. *Molecular cell*, 21(3), pp.349–57.

Bossis, G. & Melchior, F., 2006b. SUMO: regulating the regulator. *Cell division*, 1(Figure 1), p.13.

Bouvard, V. et al., 2000. Tissue and cell-specific expression of the p53-target genes: bax, fas, mdm2 and waf1/p21, before and following ionising irradiation in mice. *Oncogene*, 19(5), pp.649–60.

Brooks, C.L. & Gu, W., 2006. p53 ubiquitination: Mdm2 and beyond. *Molecular cell*, 21(3), pp.307–15.

Bursomanno, S. et al., 2015. Proteome-wide analysis of SUMO2 targets in response to pathological DNA replication stress in human cells. *DNA repair*, 25, pp.84–96.

Caelles, C., Helmberg, A. & Karin, M., 1994. p53-dependent apoptosis in the absence of transcriptional activation of p53-target genes. *Nature*, 370(6486), pp.220–3.

Carter, S. et al., 2007. C-terminal modifications regulate MDM2 dissociation and nuclear export of p53. *Group*, 9(4).

Carter, S. & Vousden, K.H., 2008. p53-Ubl fusions as models of ubiquitination, sumoylation and neddylation of p53. *Cell Cycle*, 7(15), pp.2519–2528.

Carvajal, L. a & Manfredi, J.J., 2013. Another fork in the road-life or death decisions by the tumour suppressor p53. *EMBO reports*, 14(5), pp.414–21.

Cesková, P. et al., 2006. On the mechanism of sequence-specific DNA-dependent acetylation of p53: the acetylation motif is exposed upon DNA binding. *Journal of molecular biology*, 357(2), pp.442–56.

Cheema, A. et al., 2010. Functional mimicry of the acetylated C-terminal tail of p53 by a SUMO-1 acetylated domain, SAD. *Journal of cellular physiology*, 225(2), pp.371–84.

Chen, L. et al., 2010. MDM2 recruitment of lysine methyltransferases regulates p53 transcriptional output. *The EMBO journal*, 29(15), pp.2538–52.

Chen, L. & Chen, J., 2003. MDM2-ARF complex regulates p53 sumoylation. *Oncogene*, 22(34), pp.5348–57.

Chen, X. et al., 1996. p53 levels, functional domains, and DNA damage determine the extent of the apoptotic response of tumor cells. *Genes & Development*, 10(19), pp.2438–2451.

Cheng, J. et al., 2007. SUMO-specific protease 1 is essential for stabilization of HIF1alpha during hypoxia. *Cell*, 131(3), pp.584–95.

Cheng, Z. et al., 2008. Functional characterization of TIP60 sumoylation in UV-irradiated DNA damage response. *Oncogene*, 27(7), pp.931–41.

Chipuk, J.E. et al., 2004. Direct activation of Bax by p53 mediates mitochondrial membrane permeabilization and apoptosis. *Science (New York, N.Y.)*, 303(5660), pp.1010–4.

Chipuk, J.E. et al., 2005. PUMA couples the nuclear and cytoplasmic proapoptotic function of p53. *Science (New York, N.Y.)*, 309(5741), pp.1732–5.

Chiu, S.-Y. et al., 2008. SUMO-specific protease 2 is essential for modulating p53-Mdm2 in development of trophoblast stem cell niches and lineages. *PLoS biology*, 6(12), p.e310.

Chow, K.-H. et al., 2014. The SUMO proteases SENP1 and SENP2 play a critical role in nucleoporin homeostasis and nuclear pore complex function. *Molecular biology of the cell*, 25(1), pp.160–8.

Chu, Y. & Yang, X., 2011. SUMO E3 ligase activity of TRIM proteins. *Oncogene*, 30, pp.1108–1116.

Chuikov, S. et al., 2004. Regulation of p53 activity through lysine methylation. *Nature*, 432(18), pp.353–360.

Chun, A.C.S. & Jin, D.-Y., 2003. Transcriptional regulation of mitotic checkpoint gene MAD1 by p53. *The Journal of biological chemistry*, 278(39), pp.37439–50.

Cimarosti, H. et al., 2008. Increased protein SUMOylation following focal cerebral ischemia. *Neuropharmacology*, 54(2), pp.280–9.

Clair, S. St. & Manfredi, J.J., 2006. The Dual Specificity Phosphatase Cdc25C is a Direct Target for Transcriptional Repression by the Tumor Suppressor p53. *Cell Cycle*.

Comel, A. et al., 2014. The cytoplasmic side of p53's oncosuppressive activities. *FEBS letters*, 588(16), pp.2600–9.

Comerford, K.M. et al., 2003. Small ubiquitin-related modifier-1 modification mediates resolution of CREB-dependent responses to hypoxia. *Proceedings of the National Academy of Sciences of the United States of America*, 100(3), pp.986–91.

Couture, J.-F. et al., 2006. Structural basis for the methylation site specificity of SET7/9. *Nature structural & molecular biology*, 13(2), pp.140–6.

Cummins, J.M. et al., 2004. Tumour suppression: disruption of HAUSP gene stabilizes p53. *Nature*, 428(6982), p.1 p following 486.

Dai, C. & Gu, W., 2010. P53 Post-Translational Modification: Deregulated in Tumorigenesis. *Trends in Molecular Medicine*, 16(11), pp.528–36.

Das, S. et al., 2007. Hzf Determines cell survival upon genotoxic stress by modulating p53 transactivation. *Cell*, 130(4), pp.624–37.

DeHart, C.J. et al., 2014. Extensive post-translational modification of active and inactivated forms of endogenous p53. *Molecular & cellular proteomics : MCP*, 13(1), pp.1–17.

DeLeo, A.B. et al., 1979. Detection of a transformation-related antigen in chemically induced sarcomas and other transformed cells of the mouse. *Proceedings of the National Academy of Sciences of the United States of America*, 76(5), pp.2420–4.

Desterro, J.M., Rodriguez, M.S. & Hay, R.T., 1998. SUMO-1 modification of IkappaBalpha inhibits NF-kappaB activation. *Molecular cell*, 2(2), pp.233–9.

Dünnebier, T. et al., 2009. Common variants in the UBC9 gene encoding the SUMO-conjugating enzyme are associated with breast tumor grade. *International journal of cancer. Journal international du cancer*, 125(3), pp.596–602.

Efeyan, A. & Serrano, M., 2007. p53: Guardian of the Genome and Policeman of the Oncogenes. *Cell Cycle*, 6(9), pp.1006–1010.

Eischen, C.M. & Lozano, G., 2014. The mdm network and its regulation of p53 activities: A rheostat of cancer risk. *Human Mutation*, 35, pp.728–737.

el-Deiry, W.S. et al., 1992. Definition of a consensus binding site for p53. *Nature genetics*, 1(1), pp.45–9.

El-Deiry, W.S., 1998. Regulation ofp53downstream genes. *Seminars in Cancer Biology*, 8, pp.345–357.

Erker, Y. et al., 2013. Arkadia, a novel SUMO-targeted ubiquitin ligase involved in PML degradation. *Molecular and cellular biology*, 33, pp.2163–77.

Erster, S. et al., 2004. In vivo mitochondrial p53 translocation triggers a rapid first wave of cell death in response to DNA damage that can precede p53 target gene activation. *Molecular and cellular biology*, 24(15), pp.6728–41.

Espinosa, J.M. & Emerson, B.M., 2001. Transcriptional regulation by p53 through intrinsic DNA/chromatin binding and site-directed cofactor recruitment. *Molecular cell*, 8(1), pp.57–69.

Evdokimov, E. et al., 2008. Loss of SUMO1 in mice affects RanGAP1 localization and formation of PML nuclear bodies, but is not lethal as it can be compensated by SUMO2 or SUMO3. *Journal of cell science*, 121(Pt 24), pp.4106–13.

Faus, H. & Haendler, B., 2006. Post-translational modifications of steroid receptors. *Biomedicine & pharmacotherapy = Biomédecine & pharmacothérapie*, 60(9), pp.520–8.

Feng, L. et al., 2005. Functional analysis of the roles of posttranslational modifications at the p53 C terminus in regulating p53 stability and activity. *Molecular and cellular biology*, 25(13), pp.5389–95.

Flotho, A. & Melchior, F., 2013. Sumoylation: a regulatory protein modification in health and disease. *Annual review of biochemistry*, 82, pp.357–85.

Fried, H. & Kutay, U., 2003. Nucleocytoplasmic transport: taking an inventory. *Cellular and Molecular Life Sciences (CMLS)*, 60(8), pp.1659–1688.

Gao, C. et al., 2008. Histone deacetylase 7 promotes PML sumoylation and is essential for PML nuclear body formation. *Molecular and cellular biology*, 28(18), pp.5658–67.

Garcia-Dominguez, M. & Reyes, J.C., 2009. SUMO association with repressor complexes, emerging routes for transcriptional control. *Biochimica et biophysica acta*, 1789(6-8), pp.451–9.

Gärtner, A. & Muller, S., 2014. PML, SUMO, and RNF4: Guardians of Nuclear Protein Quality. *Molecular cell*, 55(1), pp.1–3.

Geiss-Friedlander, R. & Melchior, F., 2007. Concepts in sumoylation: a decade on. *Nature reviews. Molecular cell biology*, 8(december), pp.947–956.

Ghisletti, S. et al., 2007. Parallel SUMOylation-dependent pathways mediate gene- and signal-specific transrepression by LXRs and PPARgamma. *Molecular cell*, 25(1), pp.57–70.

Gill, G., 2003. Post-translational modification by the small ubiquitin-related modifier SUMO has big effects on transcription factor activity. *Current Opinion in Genetics & Development*, 13(2), pp.108–113.

Gill, G., 2005. Something about SUMO inhibits transcription. *Current opinion in genetics & development*, 15(5), pp.536–41.

Girdwood, D. et al., 2003. p300 Transcriptional Repression Is Mediated by SUMO Modification. *Molecular Cell*, 11(4), pp.1043–1054.

Goeres, J. et al., 2011. The SUMO-specific isopeptidase SENP2 associates dynamically with nuclear pore complexes through interactions with karyopherins and the Nup107-160 nucleoporin subcomplex. *Molecular biology of the cell*, 22(24), pp.4868–82.

Gogna, R. et al., 2012. Re-oxygenation causes hypoxic tumor regression through restoration of p53 wild-type conformation and post-translational modifications. *Cell death & disease*, 3, p.e286.

Goldfarb, D.S. et al., 2004. Importin α: a multipurpose nuclear-transport receptor. *Trends in Cell Biology*, 14(9), pp.505–514.

Golebiowski, F. et al., 2009. System-wide changes to SUMO modifications in response to heat shock. *Science signaling*, 2(72), p.ra24.

Gostissa, M. et al., 1999. Activation of p53 by conjugation to the ubiquitin-like protein SUMO-1. *The EMBO journal*, 18(22), pp.6462–6471.

Gowran, A., Murphy, C.E. & Campbell, V.A., 2009. Delta(9)-tetrahydrocannabinol regulates the p53 post-translational modifiers Murine double minute 2 and the Small Ubiquitin MOdifier protein in the rat brain. *FEBS letters*, 583(21), pp.3412–8.

Green, D.R. & Kroemer, G., 2009. Cytoplasmic functions of the tumour suppressor p53. *Nature*, 458(7242), pp.1127–30.

Grégoire, S., Yang, X. & Gre, S., 2005. Association with Class IIa Histone Deacetylases Upregulates the Sumoylation of MEF2 Transcription Factors. *Molecular and cellular biology*, 25(6), pp.2273–2287.

Grönroos, E. et al., 2004. YY1 inhibits the activation of the p53 tumor suppressor in response to genotoxic stress. *Proceedings of the National Academy of Sciences of the United States of America*, 101(33), pp.12165–70.

Gu, B. & Zhu, W.-G., 2012. Surf the post-translational modification network of p53 regulation. *International journal of biological sciences*, 8(5), pp.672–84.

Gu, W. & Roeder, R.G., 1997. Activation of p53 sequence-specific DNA binding by acetylation of the p53 C-terminal domain. *Cell*, 90(4), pp.595–606.

Gu, W., Shi, X.L. & Roeder, R.G., 1997. Synergistic activation of transcription by CBP and p53. *Nature*, 387(6635), pp.819–23.

Guo, B. & Sharrocks, A.D., 2009. Extracellular signal-regulated kinase mitogen-activated protein kinase signaling initiates a dynamic interplay between sumoylation and ubiquitination to regulate the activity of the transcriptional activator PEA3. *Molecular and cellular biology*, 29(11), pp.3204–18.

Guo, C. & Henley, J.M., 2014. Wrestling with stress: Roles of protein SUMOylation and deSUMOylation in cell stress response. *IUBMB Life*, 66, pp.71–77.

Guo, D. et al., 2004. A functional variant of SUMO4, a new I kappa B alpha modifier, is associated with type 1 diabetes. *Nature genetics*, 36(8), pp.837–41.

Guo, L. et al., 2014. A Cellular System that Degrades Misfolded Proteins and Protects against Neurodegeneration. *Molecular cell*, 55(1), pp.15–30.

Van Hagen, M. et al., 2010. RNF4 and VHL regulate the proteasomal degradation of SUMO-conjugated Hypoxia-Inducible Factor-2alpha. *Nucleic acids research*, 38(6), pp.1922–31.

Hammer, E., Heilbronn, R. & Weger, S., 2007. The E3 ligase Topors induces the accumulation of polysumoylated forms of DNA topoisomerase I in vitro and in vivo. *FEBS letters*, 581(28), pp.5418–24.

Hardeland, U. et al., 2002. Modification of the human thymine-DNA glycosylase by ubiquitin-like proteins facilitates enzymatic turnover. *The EMBO journal*, 21(6), pp.1456–64.

Haupt, Y. et al., 1995. Induction of apoptosis in HeLa cells by trans-activation-deficient p53. *Genes & development*, 9(17), pp.2170–83.

Hay, R.T., 2013. Decoding the SUMO signal. *Biochemical Society transactions*, 41(2), pp.463–73.

Hay, R.T., 2005. SUMO: a history of modification. *Molecular cell*, 18(1), pp.1–12.

Hay, R.T., 2007. SUMO-specific proteases: a twist in the tail. *Trends in Cell Biology*, 17(8), pp.370–376.

He, X. et al., 2015. Characterization of the loss of SUMO pathway function on cancer cells and tumor proliferation. *PloS one*, 10(4), p.e0123882.

Hendriks, I. a et al., 2014. Uncovering global SUMOylation signaling networks in a site-specific manner. *Nature structural & molecular biology*, 21(10), pp.927–936.

Heo, K.-S. et al., 2011. PKCζ mediates disturbed flow-induced endothelial apoptosis via p53 SUMOylation. *The Journal of cell biology*, 193(5), pp.867–84.

Hermeking, H. & Benzinger, A., 2006. 14-3-3 proteins in cell cycle regulation. *Seminars in cancer biology*, 16(3), pp.183–92.

Hickey, C.M., Wilson, N.R. & Hochstrasser, M., 2012. Function and regulation of SUMO proteases. *Nature reviews. Molecular cell biology*, 13(12), pp.755–66.

Hietakangas, V. et al., 2006. PDSM, a motif for phosphorylation-dependent SUMO modification. *Proceedings of the National Academy of Sciences of the United States of America*, 103(1), pp.45–50.

Ho, J.S.L. et al., 2005. p53-Dependent transcriptional repression of c-myc is required for G1 cell cycle arrest. *Molecular and cellular biology*, 25(17), pp.7423–31.

Hoffman, W.H. et al., 2002. Transcriptional repression of the anti-apoptotic survivin gene by wild type p53. *The Journal of biological chemistry*, 277(5), pp.3247–57.

Hohmann, A.F. & Vakoc, C.R., 2014. A rationale to target the SWI/SNF complex for cancer therapy. *Trends in genetics : TIG*, 30(8), pp.356–63.

Hollstein, M. & Hainaut, P., 2010. Massively regulated genes : the example of TP53. *Journal of Pathology, The*, 220, pp.164–173.

Huang, J. et al., 2010. G9a and Glp Methylate Lysine 373 in the Tumor Supressor p53. *The Journal of biological chemistry*, 285(13), pp.9636–9641.

Huang, J. et al., 2007. p53 is regulated by the lysine demethylase LSD1. *Nature*, 449(7158), pp.105–8.

Huang, J. et al., 2006. Repression of p53 activity by Smyd2-mediated methylation. *Nature*, 444(30), pp.629–632.

Huang, L. et al., 2011. The p53 inhibitors MDM2/MDMX complex is required for control of p53 activity in vivo. *Proceedings of the National Academy of Sciences of the United States of America*, 108(29), pp.12001–6.

Huang, T.T. et al., 2003. Sequential modification of NEMO/IKKgamma by SUMO-1 and ubiquitin mediates NF-kappaB activation by genotoxic stress. *Cell*, 115(5), pp.565–76.

Hussain, S.P., Hofseth, L.J. & Harris, C.C., 2003. Radical causes of cancer. *Nature reviews. Cancer*, 3(4), pp.276–85.

Imoto, S. et al., 2008. Sumoylation of Smad3 stimulates its nuclear export during PIASy-mediated suppression of TGF-beta signaling. *Biochemical and biophysical research communications*, 370(2), pp.359–65.

Inga, A. et al., 2002. Differential Transactivation by the p53 Transcription Factor Is Highly Dependent on p53 Level and Promoter Target Sequence. *Molecular and cellular biology*, 22(24), pp.8612–8625.

Itahana, K. et al., 2007. Targeted Inactivation of Mdm2 RING Finger E3 Ubiquitin Ligase Activity in the Mouse Reveals Mechanistic Insights into p53 Regulation. *Cancer Cell*, 12(October), pp.355–366.

Ito, A. et al., 2002. MDM2-HDAC1-mediated deacetylation of p53 is required for its degradation. *The EMBO journal*, 21(22), pp.6236–45.

Ito, A. et al., 2001. p300/CBP-mediated p53 acetylation is commonly induced by p53-activating agents and inhibited by MDM2. *The EMBO journal*, 20(6), pp.1331–40.

Ivanov, G.S. et al., 2007. Methylation-acetylation interplay activates p53 in response to DNA damage. *Molecular and cellular biology*, 27(19), pp.6756–69.

Jackson, J.G., Post, S.M. & Lozano, G., 2011. Regulation of tissue- and stimulus-specific cell fate decisions by p53 in vivo. *The Journal of pathology*, 223(2), pp.127–36.

Jakobs, A. et al., 2007. Ubc9 fusion – directed SUMOylation (UFDS): a method to analyze function of protein SUMOylation. *Nature Methods*, 4(3), pp.245–250.

Jenkins, J.R., Rudge, K. & Currie, G.A., 1984. Cellular immortalization by a cDNA clone encoding the transformation-associated phosphoprotein p53. *Nature*, 312(5995), pp.651–4.

Jentsch, S. & Psakhye, I., 2013. Control of nuclear activities by substrate-selective and protein-group SUMOylation. *Annual review of genetics*, 47, pp.167–86.

Jenuwein, T. & Allis, C.D., 2001. Translating the histone code. *Science*, 293, pp.1074–80.

Jin, Y. et al., 2002. MDM2 inhibits PCAF (p300/CREB-binding protein-associated factor)-mediated p53 acetylation. *The Journal of biological chemistry*, 277(34), pp.30838–43.

Joerger, A.C. & Fersht, A.R., 2010. The tumor suppressor p53: from structures to drug discovery. *Cold Spring Harbor perspectives in biology*, 2(6), p.a000919.

Jones, S.N. et al., 1995. Rescue of embryonic lethality in Mdm2-deficient mice by absence of p53. *Nature*, 378(6553), pp.206–8.

Junttila, M.R. & Evan, G.I., 2009. p53--a Jack of all trades but master of none. *Nature reviews. Cancer*, 9(11), pp.821–9.

Kagey, M.H., Melhuish, T. a & Wotton, D., 2003. The polycomb protein Pc2 is a SUMO E3. *Cell*, 113(1), pp.127–37.

Kagey, M.H., Melhuish, T.A. & Wotton, D., 2003. The polycomb protein Pc2 is a SUMO E3. *Cell*, 113(1), pp.127–37.

Kahyo, T., Nishida, T. & Yasuda, H., 2001. Involvement of PIAS1 in the sumoylation of tumor suppressor p53. *Molecular cell*, 8(3), pp.713–8.

Kakudo, Y. et al., 2005. Lack of correlation between p53-dependent transcriptional activity and the ability to induce apoptosis among 179 mutant p53s. *Cancer research*, 65(6), pp.2108–14.

Kang, J.S. et al., 2008. The type I TGF-beta receptor is covalently modified and regulated by sumoylation. *Nature cell biology*, 10(6), pp.654–64.

Kang, X. et al., 2010. SUMO-specific protease 2 is essential for suppression of polycomb group protein-mediated gene silencing during embryonic development. *Molecular cell*, 38(2), pp.191–201.

Kelly, R.D.W. & Cowley, S.M., 2013. The physiological roles of histone deacetylase (HDAC) 1 and 2: complex co-stars with multiple leading parts. *Biochemical Society transactions*, 41(3), pp.741–9.

Kessler, J.D. et al., 2012. A SUMOylation-dependent transcriptional subprogram is required for Myc-driven tumorigenesis. *Science (New York, N.Y.)*, 335(6066), pp.348–53.

Kim, J.H. et al., 2006. Roles of sumoylation of a reptin chromatin-remodelling complex in cancer metastasis. *Nature cell biology*, 8(6), pp.631–9.

Kim, K. Il & Baek, S.H., 2009. Small ubiquitin-like modifiers in cellular malignancy and metastasis. *International review of cell and molecular biology*, 273, pp.265–311.

Kim, K. Il & Baek, S.H., 2006. SUMOylation Code in Cancer Development and Metastasis. , 22(3), pp.247–253.

Kitayner, M. et al., 2006. Structural basis of DNA recognition by p53 tetramers. *Molecular cell*, 22(6), pp.741–53.

Klein, U.R. et al., 2009. RanBP2 and SENP3 function in a mitotic SUMO2/3 conjugation-deconjugation cycle on Borealin. *Molecular biology of the cell*, 20(1), pp.410–8.

Kojima, K. et al., 2006. Mdm2 inhibitor Nutlin-3a induces p53-mediated apoptosis by transcription-dependent and transcription-independent mechanisms and may overcome Atm-mediated resistance to fludarabine in chronic lymphocytic leukemia. *Blood*, 108(3), pp.993–1000.

Kolli, N. et al., 2010. Distribution and paralogue specificity of mammalian deSUMOylating enzymes. *The Biochemical journal*, 430(2), pp.335–44.

Kortlever, R.M., Higgins, P.J. & Bernards, R., 2006. Plasminogen activator inhibitor-1 is a critical downstream target of p53 in the induction of replicative senescence. *Nature cell biology*, 8(8), pp.877–84.

Krummel, K.A. et al., 2005. The C-terminal lysines fine-tune P53 stress responses in a mouse model but are not required for stability control or transactivation. *Proceedings of the National Academy of Sciences of the United States of America*, 102(29), pp.10188–93.

Kuo, H.-Y. et al., 2005. SUMO modification negatively modulates the transcriptional activity of CREB-binding protein via the recruitment of Daxx. *Proceedings of the National Academy of Sciences of the United States of America*, 102(47), pp.16973–8.

Kurash, J.K. et al., 2008. Methylation of p53 by Set7/9Mediates p53 Acetylation and Activity In Vivo. *Molecular cell*, (29), pp.392–400.

Kussie, P.H. et al., 1996. Structure of the MDM2 oncoprotein bound to the p53 tumor suppressor transactivation domain. *Science (New York, N.Y.)*, 274(5289), pp.948–53.

Kwek, S.S.S. et al., 2001. Functional analysis and intracellular localization of p53 modified by SUMO-1. *Oncogene*, 20, pp.2587–99.

Lallemand-Breitenbach, V. et al., 2008. Arsenic degrades PML or PML-RARalpha through a SUMO-triggered RNF4/ubiquitin-mediated pathway. *Nature cell biology*, 10(5), pp.547–555.

Lallemand-Breitenbach, V. & de Thé, H., 2010. PML nuclear bodies. *Cold Spring Harbor perspectives in biology*, 2(5), p.a000661.

Lane, D.P. & Crawford, L. V, 1979. T antigen is bound to a host protein in SV40-transformed cells. *Nature*, 278(5701), pp.261–3.

Laptenko, O. & Prives, C., 2006. Transcriptional regulation by p53: one protein, many possibilities. *Cell death and differentiation*, 13(6), pp.951–61.

Lee, C.W. et al., 2010. Structure of the p53 transactivation domain in complex with the nuclear receptor coactivator binding domain of CREB binding protein. *Biochemistry*, 49(46), pp.9964–71.

Lee, D. et al., 2002. SWI/SNF complex interacts with tumor suppressor p53 and is necessary for the activation of p53-mediated transcription. *Journal of Biological Chemistry*, 277(25), pp.22330–22337.

Lee, F.Y. et al., 2011. Eliminating SF-1 (NR5A1) sumoylation in vivo results in ectopic hedgehog signaling and disruption of endocrine development. *Developmental cell*, 21(2), pp.315–27.

Lee, J.-S. & Thorgeirsson, S.S., 2004. Genome-scale profiling of gene expression in hepatocellular carcinoma: classification, survival prediction, and identification of therapeutic targets. *Gastroenterology*, 127(5 Suppl 1), pp.S51–5.

Lee, M.G. et al., 2005. An essential role for CoREST in nucleosomal histone 3 lysine 4 demethylation. *Nature*, 437(7057), pp.432–5.

Lee, M.G. et al., 2006. Functional interplay between histone demethylase and deacetylase enzymes. *Molecular and cellular biology*, 26(17), pp.6395–402.

Lee, Y., Chong, M.J. & McKinnon, P.J., 2001. Ataxia telangiectasia mutated-dependent apoptosis after genotoxic stress in the developing nervous system is determined by cellular differentiation status. *The Journal of neuroscience : the official journal of the Society for Neuroscience*, 21(17), pp.6687–93.

Leu, J.I.-J. et al., 2004. Mitochondrial p53 activates Bak and causes disruption of a Bak-Mcl1 complex. *Nature cell biology*, 6(5), pp.443–50.

Levine, B. & Kroemer, G., 2009. Autophagy in aging, disease and death: the true identity of a cell death impostor. *Cell death and differentiation*, 16(1), pp.1–2.

Li, B. et al., 2007. Polycomb protein Cbx4 promotes SUMO modification of de novo DNA methyltransferase Dnmt3a. *The Biochemical journal*, 405(2), pp.369–78.

Li, M. et al., 2004. A dynamic role of HAUSP in the p53-Mdm2 pathway. *Molecular cell*, 13(6), pp.879–86.

Li, M., Luo, J., et al., 2002. Acetylation of p53 inhibits its ubiquitination by Mdm2. *The Journal of biological chemistry*, 277(52), pp.50607–11.

Li, M., Chen, D., et al., 2002. Deubiquitination of p53 by HAUSP is an important pathway for p53 stabilization. *Nature*, 416(April), pp.648–653.

Li, M. et al., 2003. Mono- versus polyubiquitination: differential control of p53 fate by Mdm2. *Science (New York, N.Y.)*, 302(5652), pp.1972–5.

Li, T. et al., 2006. Expression of SUMO-2/3 induced senescence through p53- and pRB-mediated pathways. *The Journal of biological chemistry*, 281(47), pp.36221–7.

Li, X. et al., 2007. Role for KAP1 serine 824 phosphorylation and sumoylation/desumoylation switch in regulating KAP1-mediated transcriptional repression. *The Journal of biological chemistry*, 282(50), pp.36177–89.

Li, Y. et al., 2014. Structural insights into the TRIM family of ubiquitin E3 ligases. *Cell research*, 24, pp.762–5.

Liang, Q. et al., 2011. Tripartite motif-containing protein 28 is a small ubiquitin-related modifier E3 ligase and negative regulator of IFN regulatory factor 7. *Journal of immunology (Baltimore, Md. : 1950)*, 187(9), pp.4754–63.

Lin, J.-Y., Ohshima, T. & Shimotohno, K., 2004. Association of Ubc9, an E2 ligase for SUMO conjugation, with p53 is regulated by phosphorylation of p53. *FEBS letters*, 573(1-3), pp.15–8.

Lin, L. et al., 2005. topors, a p53 and topoisomerase I-binding RING finger protein, is a coactivator of p53 in growth suppression induced by DNA damage. *Oncogene*, 24(21), pp.3385–96.

Lin, X. et al., 2003. Opposed regulation of corepressor CtBP by SUMOylation and PDZ binding. *Molecular cell*, 11(5), pp.1389–96.

Linares, L.K. et al., 2003. HdmX stimulates Hdm2-mediated ubiquitination and degradation of p53. *Proceedings of the National Academy of Sciences of the United States of America*, 100(21), pp.12009–14.

Linke, S.P. et al., 1996. A reversible, p53-dependent G0/G1 cell cycle arrest induced by ribonucleotide depletion in the absence of detectable DNA damage. *Genes & development*, 10(8), pp.934–47.

Linzer, D.I. & Levine, A.J., 1979. Characterization of a 54K dalton cellular SV40 tumor antigen present in SV40-transformed cells and uninfected embryonal carcinoma cells. *Cell*, 17(1), pp.43–52.

Liu, G. et al., 2004. Chromosome stability, in the absence of apoptosis, is critical for suppression of tumorigenesis in Trp53 mutant mice. *Nature genetics*, 36(1), pp.63–8.

Liu, X.-M. et al., 2013. SUMOylation of mouse p53b by SUMO-1 promotes its pro-apoptotic function in ovarian granulosa cells. *PloS one*, 8(5), p.e63680.

Löhr, K. et al., 2003. p21/CDKN1A mediates negative regulation of transcription by p53. *The Journal of biological chemistry*, 278(35), pp.32507–16.

Long, J., Zuo, D. & Park, M., 2005. Pc2-mediated sumoylation of Smad-interacting protein 1 attenuates transcriptional repression of E-cadherin. *The Journal of biological chemistry*, 280(42), pp.35477–89.

Lowe, S.W., 1999. Activation of p53 by oncogenes. *Endocrine-related cancer*, 6(1), pp.45–8.

Luo, J. et al., 2000. Deacetylation of p53 modulates its effect on cell growth and apoptosis. *Nature*, 408(6810), pp.377–81.

Luo, J. et al., 2001. Negative control of p53 by Sir2alpha promotes cell survival under stress. *Cell*, 107(2), pp.137–48.

Mabb, A.M. & Miyamoto, S., 2007. SUMO and NF-kappaB ties. *Cellular and molecular life sciences : CMLS*, 64(15), pp.1979–96.

MacCallum, D.E. et al., 1996. The p53 response to ionising radiation in adult and developing murine tissues. *Oncogene*, 13(12), pp.2575–87.

Maddocks, O.D.K. et al., 2013. Serine starvation induces stress and p53-dependent metabolic remodelling in cancer cells. *Nature*, 493(7433), pp.542–6.

Maddocks, O.D.K. & Vousden, K.H., 2011. Metabolic regulation by p53. *Journal of molecular medicine (Berlin, Germany)*, 89(3), pp.237–45.

Mahajan, R. et al., 1997. A small ubiquitin-related polypeptide involved in targeting RanGAP1 to nuclear pore complex protein RanBP2. *Cell*, 88(1), pp.97–107.

Malkin, D. et al., 1990. Germ line p53 mutations in a familial syndrome of breast cancer, sarcomas, and other neoplasms. *Science (New York, N.Y.)*, 250(4985), pp.1233–8.

Mancini, F. et al., 2009. MDM4 (MDMX) localizes at the mitochondria and facilitates the p53-mediated intrinsic-apoptotic pathway. *The EMBO journal*, 28(13), pp.1926–39.

Marchenko, N.D. et al., 2007. Monoubiquitylation promotes mitochondrial p53 translocation. *The EMBO Journal*, 26(4), pp.923–934.

Marcos-Villar, L. et al., 2013. SUMOylation of p53 mediates interferon activities. *Cell Cycle*, 12, pp.2809–2816.

Marks, P.A. & Xu, W.-S., 2009. Histone deacetylase inhibitors: Potential in cancer therapy. *Journal of cellular biochemistry*, 107(4), pp.600–8.

Marouco, D. et al., 2013. Lysine-specific modifications of p53: a matter of life and death? *Oncotarget*, 4(10), pp.1556–71.

Martin, N. et al., 2009. PARP-1 transcriptional activity is regulated by sumoylation upon heat shock. *The EMBO journal*, 28(22), pp.3534–48.

Martin, S., Wilkinson, K. a, et al., 2007. Emerging extranuclear roles of protein SUMOylation in neuronal function and dysfunction. *Nature reviews. Neuroscience*, 8(12), pp.948–959.

Martin, S., Wilkinson, K.A., et al., 2007. Emerging extranuclear roles of protein SUMOylation in neuronal function and dysfunction. *Nature reviews. Neuroscience*, 8(12), pp.948–59.

Matunis, M.J., Coutavas, E. & Blobel, G., 1996. A novel ubiquitin-like modification modulates the partitioning of the Ran-GTPase-activating protein RanGAP1 between the cytosol and the nuclear pore complex. *The Journal of cell biology*, 135(6 Pt 1), pp.1457–70.

Mauri, F. et al., 2008. Modification of Drosophila p53 by SUMO Modulates Its Transactivation and Pro-apoptotic Functions * □. *Journal of Biological Chemistry*, 283(30), pp.20848 – 20856.

McDoniels-Silvers, A.L. et al., 2002. Differential gene expression in human lung adenocarcinomas and squamous cell carcinomas. *Clinical cancer research : an official journal of the American Association for Cancer Research*, 8(4), pp.1127–38.

Meek, D.W. & Anderson, C.W., 2009. Posttranslational modification of p53: cooperative integrators of function. *Cold Spring Harbor perspectives in biology*, 1(6), p.a000950.

Megidish, T., Xu, J.H. & Wilson Xu, C., 2002. Activation of p53 by protein inhibitor of activated Stat1 (PIAS1). *Journal of Biological Chemistry*, 277(10), pp.8255–8259.

Melchior, F., 2003. SUMO: ligases, isopeptidases and nuclear pores. *Trends in Biochemical Sciences*, 28(11), pp.612–618.

Melchior, F. & Hengst, L., 2002. SUMO-1 and p53. *Cell Cycle*, (August), pp.245–249.

Menendez, D. et al., 2007. Changing the p53 master regulatory network: ELEMENTary, my dear Mr Watson. *Oncogene*, 26(15), pp.2191–201.

Meroni, G. & Diez-Roux, G., 2005. TRIM/RBCC, a novel class of “single protein RING finger” E3 ubiquitin ligases. *BioEssays*, 27, pp.1147–1157.

Metzger, E. et al., 2005. LSD1 demethylates repressive histone marks to promote androgen-receptor-dependent transcription. *Nature*, 437(7057), pp.436–9.

Michalak, E.M. et al., 2008. In several cell types tumour suppressor p53 induces apoptosis largely via Puma but Noxa can contribute. *Cell death and differentiation*, 15(6), pp.1019–29.

Midgley, C.A. et al., 1995. Coupling between gamma irradiation, p53 induction and the apoptotic response depends upon cell type in vivo. *Journal of cell science*, 108 (Pt 5, pp.1843–8.

Mikkonen, L., Hirvonen, J. & Jänne, O. a., 2013. SUMO-1 regulates body weight and adipogenesis via PPARγ in male and female mice. *Endocrinology*, 154(February 2013), pp.698–708.

Mita, A.C. et al., 2008. Survivin: key regulator of mitosis and apoptosis and novel target for cancer therapeutics. *Clinical cancer research : an official journal of the American Association for Cancer Research*, 14(16), pp.5000–5.

Mo, Y.-Y. et al., 2005. A role for Ubc9 in tumorigenesis. *Oncogene*, 24(16), pp.2677–83.

Montes de Oca Luna, R., Wagner, D.S. & Lozano, G., 1995. Rescue of early embryonic lethality in mdm2-deficient mice by deletion of p53. *Nature*, 378(6553), pp.203–6.

Morgunkova, A. & Barlev, N.A., 2006. Lysine Methylation goes global. *Cell Cycle*, 12(5), pp.1308–1312.

Morselli, E. et al., 2009. Anti- and pro-tumor functions of autophagy. *Biochimica et biophysica acta*, 1793(9), pp.1524–32.

Mukhopadhyay, D., Arnaoutov, A. & Dasso, M., 2010. The SUMO protease SENP6 is essential for inner kinetochore assembly. *The Journal of cell biology*, 188(5), pp.681–92.

Mukhopadhyay, D. & Dasso, M., 2007. Modification in reverse: the SUMO proteases. *Trends in biochemical sciences*, 32(6), pp.286–95.

Müller, S. et al., 2000. c-Jun and p53 activity is modulated by SUMO-1 modification. *Journal of Biological Chemistry*, 275(18), pp.13321–13329.

Muller, S. & Dobner, T., 2008. The adenovirus E1B-55K oncoprotein induces SUMO modification of p53. *Cell cycle (Georgetown, Tex.)*, 7(6), pp.754–8.

Müller, S., Matunis, M.J. & Dejean, A., 1998. Conjugation with the ubiquitin-related modifier SUMO-1 regulates the partitioning of PML within the nucleus. *The EMBO journal*, 17(1), pp.61–70.

Murphy, M. et al., 1999. Transcriptional repression by wild-type p53 utilizes histone deacetylases, mediated by interaction with mSin3a. *Genes & development*, 13(19), pp.2490–501.

Murphy, M., Hinman, A. & Levine, A.J., 1996. Wild-type p53 negatively regulates the expression of a microtubule-associated protein. *Genes & development*, 10(23), pp.2971–80.

Murray-Zmijewski, F., Slee, E. a & Lu, X., 2008. A complex barcode underlies the heterogeneous response of p53 to stress. *Nature reviews. Molecular cell biology*, 9(9), pp.702–12.

Nacerddine, K. et al., 2005. The SUMO pathway is essential for nuclear integrity and chromosome segregation in mice. *Developmental cell*, 9(6), pp.769–79.

Naidu, S.R. et al., 2009. The SWI/SNF chromatin remodeling subunit BRG1 is a critical regulator of p53 necessary for proliferation of malignant cells. *Oncogene*, 28(27), pp.2492–501.

Naidu, S.R., Lakhter, A.J. & Androphy, E.J., 2012. PIASy-mediated Tip60 sumoylation regulates p53-induced autophagy. *Cell cycle (Georgetown, Tex.)*, 11(14), pp.2717–28.

Nair, V.D. et al., 2006. p53 mediates nontranscriptional cell death in dopaminergic cells in response to proteasome inhibition. *The Journal of biological chemistry*, 281(51), pp.39550–60.

Nelson, V., Davis, G.E. & Maxwell, S.A., 2001. A putative protein inhibitor of activated STAT (PIASy) interacts with p53 and inhibits p53-mediated transactivation but not apoptosis. *Apoptosis : an international journal on programmed cell death*, 6(3), pp.221–34.

Nguyen, T.T. et al., 2005. Transcription factor interactions and chromatin modifications associated with p53-mediated, developmental repression of the alpha-fetoprotein gene. *Molecular and cellular biology*, 25(6), pp.2147–57.

Nishida, T. & Yasuda, H., 2002. PIAS1 and PIASxalpha function as SUMO-E3 ligases toward androgen receptor and repress androgen receptor-dependent transcription. *The Journal of biological chemistry*, 277(44), pp.41311–7.

Oda, K. et al., 2000. p53AIP1, a potential mediator of p53-dependent apoptosis, and its regulation by Ser-46-phosphorylated p53. *Cell*, 102(6), pp.849–62.

Oh, J. et al., 2008. BAF60a interacts with p53 to recruit the SWI/SNF complex. *Journal of Biological Chemistry*, 283(18), pp.11924–11934.

Oh, S.-M. et al., 2010. Ebp1 sumoylation, regulated by TLS/FUS E3 ligase, is required for its anti-proliferative activity. *Oncogene*, 29(7), pp.1017–30.

Oh, Y. & Chung, K.C., 2013. UHRF2, a ubiquitin E3 ligase, acts as a small ubiquitin-like modifier E3 ligase for zinc finger protein 131. *The Journal of biological chemistry*, 288(13), pp.9102–11.

Okorokov, A.L. et al., 2006. The structure of p53 tumour suppressor protein reveals the basis for its functional plasticity. *The EMBO journal*, 25(April), pp.5191–5200.

Olsson, a et al., 2007. How important are post-translational modifications in p53 for selectivity in target-gene transcription and tumour suppression? *Cell death and differentiation*, 14(9), pp.1561–75.

Ou, Y.-H. et al., 2005. p53 C-terminal phosphorylation by CHK1 and CHK2 participates in the regulation of DNA-damage-induced C-terminal acetylation. *Molecular biology of the cell*, 16(4), pp.1684–95.

Ouyang, J. et al., 2009. Direct binding of CoREST1 to SUMO-2/3 contributes to gene-specific repression by the LSD1/CoREST1/HDAC complex. *Molecular cell*, 34(2), pp.145–54.

Ouyang, J. & Gill, G., 2009. SUMO engages multiple corepressors to regulate chromatin structure and transcription. *Epigenetics*, 4(7), pp.440–444.

Owerbach, D. et al., 2005. A proline-90 residue unique to SUMO-4 prevents maturation and sumoylation. *Biochemical and biophysical research communications*, 337(2), pp.517–20.

Pant, V. et al., 2011. Heterodimerization of Mdm2 and Mdm4 is critical for regulating p53 activity during embryogenesis but dispensable for p53 and Mdm2 stability. *Proceedings of the National Academy of Sciences of the United States of America*, 108(29), pp.11995–2000.

Parant, J. et al., 2001. Rescue of embryonic lethality in Mdm4-null mice by loss of Trp53 suggests a nonoverlapping pathway with MDM2 to regulate p53. *Nature genetics*, 29(1), pp.92–5.

Pardi, N. et al., 2011. In vivo effects of abolishing the single canonical sumoylation site in the C-terminal region of Drosophila p53. *Acta biologica Hungarica*, 62(4), pp.397–412.

Park, J. et al., 2005. Sumoylation of the novel protein hRIP{beta} is involved in replication protein A deposition in PML nuclear bodies. *Molecular and cellular biology*, 25(18), pp.8202–14.

Pennella, M. a et al., 2010. Adenovirus E1B 55-kilodalton protein is a p53-SUMO1 E3 ligase that represses p53 and stimulates its nuclear export through interactions with promyelocytic leukemia nuclear bodies. *Journal of virology*, 84(23), pp.12210–25.

Perry, J.J.P., Tainer, J. a & Boddy, M.N., 2008. A SIM-ultaneous role for SUMO and ubiquitin. *Trends in biochemical sciences*, 33(5), pp.201–8.

Pflaum, J., Schlosser, S. & Müller, M., 2014. p53 Family and Cellular Stress Responses in Cancer. *Frontiers in oncology*, 4, p.285.

Pichler, A. et al., 2005. SUMO modification of the ubiquitin-conjugating enzyme E2-25K. *Nature structural & molecular biology*, 12(3), pp.264–9.

Pichler, A. et al., 2002. The nucleoporin RanBP2 has SUMO1 E3 ligase activity. *Cell*, 108(1), pp.109–20.

Potts, P.R. & Yu, H., 2005. Human MMS21/NSE2 is a SUMO ligase required for DNA repair. *Molecular and cellular biology*, 25(16), pp.7021–32.

Poulsen, S.L. et al., 2013. RNF111/Arkadia is a SUMO-targeted ubiquitin ligase that facilitates the DNA damage response. *The Journal of cell biology*, 201(6), pp.797–807.

Prudden, J. et al., 2007. SUMO-targeted ubiquitin ligases in genome stability. *The EMBO journal*, 26, pp.4089–4101.

Pungaliya, P. et al., 2007. TOPORS functions as a SUMO-1 E3 ligase for chromatin-modifying proteins. *Journal of proteome research*, 6(10), pp.3918–23.

Qu, J. et al., 2007. Nitric oxide destabilizes Pias3 and regulates sumoylation. *PloS one*, 2(10), p.e1085.

Reisman, D., Glaros, S. & Thompson, E.A., 2009. The SWI/SNF complex and cancer. *Oncogene*, 28(14), pp.1653–68.

Reverter, D. & Lima, C.D., 2005. Insights into E3 ligase activity revealed by a SUMO-RanGAP1-Ubc9-Nup358 complex. *Nature*, 435(7042), pp.687–92.

Rinn, J.L. & Huarte, M., 2011. To repress or not to repress: this is the guardian's question. *Trends in cell biology*, 21(6), pp.344–53.

Rodriguez, M.S. et al., 1999. SUMO-1 modification activates the transcriptional response of p53. *The EMBO journal*, 18(22), pp.6455–61.

Roscic, A. et al., 2006. Phosphorylation-dependent control of Pc2 SUMO E3 ligase activity by its substrate protein HIPK2. *Molecular cell*, 24(1), pp.77–89.

Saha, T., Kar, R.K. & Sa, G., 2015. Structural and sequential context of p53: A review of experimental and theoretical evidence. *Progress in biophysics and molecular biology*, 117(2-3), pp.250–63.

Saitoh, H. & Hinchey, J., 2000. Functional heterogeneity of small ubiquitin-related protein modifiers SUMO-1 versus SUMO-2/3. *Journal of Biological Chemistry*, 275(9), pp.6252–6258.

Sakaguchi, K. et al., 2000. Damage-mediated phosphorylation of human p53 threonine 18 through a cascade mediated by a casein 1-like kinase. Effect on Mdm2 binding. *The Journal of biological chemistry*, 275(13), pp.9278–83.

Sakaguchi, K. et al., 1998. DNA damage activates p53 through a phosphorylation-acetylation cascade. *Genes & Development*, 12(18), pp.2831–2841.

Sampson, D.A., Wang, M. & Matunis, M.J., 2001. The small ubiquitin-like modifier-1 (SUMO-1) consensus sequence mediates Ubc9 binding and is essential for SUMO-1 modification. *The Journal of biological chemistry*, 276(24), pp.21664–9.

Samuels-Lev, Y. et al., 2001. ASPP proteins specifically stimulate the apoptotic function of p53. *Molecular cell*, 8(4), pp.781–94.

Santiago, A. et al., 2013. p53 SUMOylation promotes its nuclear export by facilitating its release from the nuclear export receptor CRM1. *Molecular biology of the cell*, 24(17), pp.2739–52.

Sarge, K.D. & Park-Sarge, O.-K., 2011. *SUMO and its role in human diseases.* 1st ed., Elsevier Inc.

Schmidt, D. & Müller, S., 2002. Members of the PIAS family act as SUMO ligases for c-Jun and p53 and repress p53 activity. *Proceedings of the National Academy of Sciences of the United States of America*, 99(5), pp.2872–7.

Schulz, S. et al., 2012. Ubiquitin-specific protease-like 1 (USPL1) is a SUMO isopeptidase with essential, non-catalytic functions. *EMBO reports*, 13(10), pp.930–8.

Sehat, B. et al., 2010. SUMOylation mediates the nuclear translocation and signaling of the IGF-1 receptor. *Science signaling*, 3(108), p.ra10.

Sermeus, A. & Michiels, C., 2011. Reciprocal influence of the p53 and the hypoxic pathways. *Cell death & disease*, 2, p.e164.

Shao, R. et al., 2004. Increase of SUMO-1 expression in response to hypoxia: direct interaction with HIF-1alpha in adult mouse brain and heart in vivo. *FEBS letters*, 569(1-3), pp.293–300.

Shen, Z. et al., 1996. UBL1, a human ubiquitin-like protein associating with human RAD51/RAD52 proteins. *Genomics*, 36(2), pp.271–9.

Shi, X. et al., 2007. Modulation of p53 function by SET8-mediated methylation at lysine 382. *Molecular cell*, 27(4), pp.636–46.

Shi, Y. et al., 2003. Coordinated histone modifications mediated by a CtBP co-repressor complex. *Nature*, 422(6933), pp.735–8.

Shi, Y. et al., 2004. Histone Demethylation Mediated by the Nuclear Amine Oxidase Homolog LSD1. *Cell*, 119, pp.941–953.

Shi, Y. & Whetstine, J.R., 2007. Dynamic regulation of histone lysine methylation by demethylases. *Molecular cell*, 25(1), pp.1–14.

Shi, Y.-J. et al., 2005. Regulation of LSD1 Histone Demethylase Activity by Its Associated Factors. *Molecular Cell*, 19(6), pp.857–864.

Shin, E.J. et al., 2012. DeSUMOylating isopeptidase: a second class of SUMO protease. *EMBO reports*, 13(4), pp.339–46.

Shinbo, Y. et al., 2006. Proper SUMO-1 conjugation is essential to DJ-1 to exert its full activities. *Cell death and differentiation*, 13(1), pp.96–108.

Sif, S. et al., 2001. Purification and characterization of mSin3A-containing Brg1 and hBrm chromatin remodeling complexes. , pp.603–618.

Silver, H.R. et al., 2011. A role for SUMO in nucleotide excision repair. *DNA repair*, 10(12), pp.1243–51.

Sims, R.J. & Reinberg, D., 2008. Is there a code embedded in proteins that is based on post-translational modifications? *Nature reviews. Molecular cell biology*, 9, pp.1–6.

Song, J. et al., 2004. Identification of a SUMO-binding motif that recognizes SUMO-modified proteins. *Proceedings of the National Academy of Sciences of the United States of America*, 101, pp.14373–14378.

Sorrentino, G. et al., 2013. The prolyl-isomerase Pin1 activates the mitochondrial death program of p53. *Cell death and differentiation*, 20(2), pp.198–208.

Speidel, D., Helmbold, H. & Deppert, W., 2006. Dissection of transcriptional and non-transcriptional p53 activities in the response to genotoxic stress. *Oncogene*, 25(6), pp.940–53.

Sriramachandran, A.M. & Dohmen, R.J., 2014. SUMO-targeted ubiquitin ligases. *Biochimica et Biophysica Acta - Molecular Cell Research*, 1843(1), pp.75–85.

Srivastava, S. et al., 1990. Germ-line transmission of a mutated p53 gene in a cancer-prone family with Li-Fraumeni syndrome. *Nature*, 348(6303), pp.747–9.

St Clair, S. & Manfredi, J.J., 2006. The dual specificity phosphatase Cdc25C is a direct target for transcriptional repression by the tumor suppressor p53. *Cell cycle (Georgetown, Tex.)*, 5(7), pp.709–13.

Stankovic-Valentin, N. et al., 2007. An acetylation/deacetylation-SUMOylation switch through a phylogenetically conserved psiKXEP motif in the tumor suppressor HIC1 regulates transcriptional repression activity. *Molecular and cellular biology*, 27(7), pp.2661–75.

Stehmeier, P. & Muller, S., 2009. Regulation of p53 family members by the ubiquitin-like SUMO system. *DNA repair*, 8(4), pp.491–8.

Stielow, B., Sapetschnig, A., Kru, I., et al., 2008. Identification of SUMO-Dependent Chromatin-Associated Transcriptional Repression Components by a Genome-wide RNAi Screen. *Molecular Cell*, (29), pp.742–754.

Stielow, B., Sapetschnig, A., Wink, C., et al., 2008. SUMO-modified Sp3 represses transcription by provoking local heterochromatic gene silencing. *EMBO reports*, 9(9), pp.899–906.

Stindt, M.H. et al., 2011. MDM2 promotes SUMO-2/3 modification of p53 to modulate transcriptional activity. *Cell Cycle*, 10(18), pp.3176–3188.

Strom, E. et al., 2006. Small-molecule inhibitor of p53 binding to mitochondria protects mice from gamma radiation. *Nature chemical biology*, 2(9), pp.474–9.

Sui, G. et al., 2004. Yin Yang 1 Is a Negative Regulator of p53. *Cell*, 117(7), pp.859–872.

Sun, H., Leverson, J.D. & Hunter, T., 2007. Conserved function of RNF4 family proteins in eukaryotes: targeting a ubiquitin ligase to SUMOylated proteins. *The EMBO journal*, 26(18), pp.4102–12.

Sykes, S.M. et al., 2009. Acetylation of the DNA Binding Domain Regulates Transcription-independent Apoptosis by p53. *Journal of Biological Chemistry*, 284(30), pp.20197–20205.

Sykes, S.M. et al., 2006. Acetylation of the p53 DNA-binding domain regulates apoptosis induction. *Molecular cell*, 24(6), pp.841–51.

Takabe, W., Alberts-Grill, N. & Jo, H., 2011. Disturbed flow: p53 SUMOylation in the turnover of endothelial cells. *The Journal of cell biology*, 193(5), pp.805–07.

Tang, Y. et al., 2008. Acetylation is indispensable for p53 activation. *Cell*, 133(4), pp.612–26.

Tang, Y. et al., 2006. Tip60-dependent acetylation of p53 modulates the decision between cell-cycle arrest and apoptosis. *Molecular cell*, 24(6), pp.827–39.

Tasdemir, E. et al., 2008. Regulation of autophagy by cytoplasmic p53. *Nature cell biology*, 10(6), pp.676–87.

Tatham, M.H. et al., 2001. Polymeric Chains of SUMO-2 and SUMO-3 are Conjugated to Protein Substrates by SAE1/SAE2 and Ubc9. *Journal of Biological Chemistry*, 276(38), pp.35368–35374.

Tatham, M.H. et al., 2001. Polymeric chains of SUMO-2 and SUMO-3 are conjugated to protein substrates by SAE1/SAE2 and Ubc9. *The Journal of biological chemistry*, 276(38), pp.35368–74.

Tatham, M.H. et al., 2008. RNF4 is a poly-SUMO-specific E3 ubiquitin ligase required for arsenic-induced PML degradation. *Nature cell biology*, 10(5), pp.538–546.

Taylor, K.M. & Labonne, C., 2005. SoxE factors function equivalently during neural crest and inner ear development and their activity is regulated by SUMOylation. *Developmental cell*, 9(5), pp.593–603.

Tempé, D., Piechaczyk, M. & Bossis, G., 2008. SUMO under stress. *Biochemical Society transactions*, 36, pp.874–878.

Teufel, D.P. et al., 2007. Four domains of p300 each bind tightly to a sequence spanning both transactivation subdomains of p53. *Proceedings of the National Academy of Sciences of the United States of America*, 104(17), pp.7009–14.

Toledo, F. et al., 2006. A mouse p53 mutant lacking the proline-rich domain rescues Mdm4 deficiency and provides insight into the Mdm2-Mdm4-p53 regulatory network. *Cancer cell*, 9(4), pp.273–85.

Toledo, F. & Wahl, G.M., 2006. Regulating the p53 pathway: in vitro hypotheses, in vivo veritas. *Nature reviews. Cancer*, 6(12), pp.909–23.

Tsai, W.-W. et al., 2008. p53-targeted LSD1 functions in repression of chromatin structure and transcription in vivo. *Molecular and cellular biology*, 28(17), pp.5139–46.

Ulrich, H.D., 2009. The SUMO System: An Overview. *Methods in molecular biology (Clifton, N.J.)*, 497, pp.v–vi.

Van der Veen, A.G. & Ploegh, H.L., 2012. Ubiquitin-like proteins. *Annual review of biochemistry*, 81, pp.323–57.

Vertegaal, A.C.O. et al., 2006. Distinct and overlapping sets of SUMO-1 and SUMO-2 target proteins revealed by quantitative proteomics. *Molecular & cellular proteomics : MCP*, 5, pp.2298–2310.

Vousden, K.H. & Lane, D.P., 2007. P53 in Health and Disease. *Nature reviews. Molecular cell biology*, 8(4), pp.275–83.

Vousden, K.H. & Prives, C., 2009. Blinded by the Light: The Growing Complexity of p53. *Cell*, 137(3), pp.413–31.

Wade, M., Wang, Y. V & Wahl, G.M., 2010. The p53 orchestra: Mdm2 and Mdmx set the tone. *Trends in cell biology*, 20(5), pp.299–309.

Wagner, T. et al., 2014. Histone deacetylase 2 controls p53 and is a critical factor in tumorigenesis. *Biochimica et biophysica acta*, 1846(2), pp.524–38.

Wang, C. et al., 2005. MDM2 interaction with nuclear corepressor KAP1 contributes to p53 inactivation. *The EMBO journal*, 24(18), pp.3279–90.

Wang, C.-Y., Podolsky, R. & She, J.-X., 2006. Genetic and functional evidence supporting SUMO4 as a type 1 diabetes susceptibility gene. *Annals of the New York Academy of Sciences*, 1079, pp.257–67.

Wang, C.-Y. & She, J.-X., 2008. SUMO4 and its role in type 1 diabetes pathogenesis. *Diabetes/metabolism research and reviews*, 24(2), pp.93–102.

Wang, J. et al., 2011. Defective sumoylation pathway directs congenital heart disease. *Birth Defects Research Part A - Clinical and Molecular Teratology*, 91(2), pp.468–476.

Wang, J. et al., 2007. Opposing LSD1 complexes function in developmental gene activation and repression programmes. *Nature*, 446(7138), pp.882–7.

Wang, L. et al., 2014. Inhibition of p53 deSUMOylation exacerbates puromycin aminonucleoside-induced apoptosis in podocytes. *International journal of molecular sciences*, 15(11), pp.21314–30.

Wang, L. & Banerjee, S., 2004. Differential PIAS3 expression in human malignancy. *Oncology reports*, 11(6), pp.1319–24.

Wang, Q.-E. et al., 2005. DNA repair factor XPC is modified by SUMO-1 and ubiquitin following UV irradiation. *Nucleic acids research*, 33(13), pp.4023–34.

Wang, Y. et al., 2009. LSD1 is a subunit of the NuRD complex and targets the metastasis programs in breast cancer. *Cell*, 138(4), pp.660–72.

Weger, S., Hammer, E. & Heilbronn, R., 2005. Topors acts as a SUMO-1 E3 ligase for p53 in vitro and in vivo. *FEBS letters*, 579(22), pp.5007–12.

Wei, W. et al., 2008. A stress-dependent SUMO4 sumoylation of its substrate proteins. *Biochemical and Biophysical Research Communications*, 375, pp.454–459.

Weinberg, R.L. et al., 2005. Comparative binding of p53 to its promoter and DNA recognition elements. *Journal of molecular biology*, 348(3), pp.589–96.

Weinberg, R.L., Veprintsev, D.B. & Fersht, A.R., 2004. Cooperative binding of tetrameric p53 to DNA. *Journal of molecular biology*, 341(5), pp.1145–59.

Weisshaar, S.R. et al., 2008. Arsenic trioxide stimulates SUMO-2/3 modification leading to RNF4-dependent proteolytic targeting of PML. *FEBS Letters*, 582, pp.3174–3178.

Wilkinson, K. a & Henley, J.M., 2010. Mechanisms, regulation and consequences of protein SUMOylation. *The Biochemical journal*, 428(2), pp.133–45.

Wilting, R.H. et al., 2010. Overlapping functions of Hdac1 and Hdac2 in cell cycle regulation and haematopoiesis. *The EMBO journal*, 29(15), pp.2586–97.

Wissmann, M. et al., 2007. Cooperative demethylation by JMJD2C and LSD1 promotes androgen receptor-dependent gene expression. *Nature cell biology*, 9(3), pp.347–53.

Wotton, D. & Merrill, J.C., 2007. Pc2 and SUMOylation. *Biochemical Society transactions*, 35, pp.1401–1404.

Wu, S.-Y. & Chiang, C.-M., 2009a. Crosstalk between sumoylation and acetylation regulates p53-dependent chromatin transcription and DNA binding. *The EmBO Journal*, 28(9), pp.1246–59.

Wu, S.-Y. & Chiang, C.-M., 2009b. P53 Sumoylation: Mechanistic Insights From Reconstitution Studies. *Epigenetics : official journal of the DNA Methylation Society*, 4(7), pp.445–51.

Wysocka, J., Milne, T.A. & Allis, C.D., 2005. Taking LSD 1 to a new high. *Cell*, 122(5), pp.654–8.

Xirodimas, D.P. et al., 2004. Mdm2-Mediated NEDD8 Conjugation of p53 Inhibits Its Transcriptional Activity. , 118, pp.83–97.

Xu, J. et al., 2008. A novel method for high accuracy sumoylation site prediction from protein sequences. *BMC bioinformatics*, 9, p.8.

Xu, Y., Yan, W. & Chen, X., 2010. SNF5, a core component of the SWI/SNF complex, is necessary for p53 expression and cell survival, in part through eIF4E. *Oncogene*, 29(28), pp.4090–100.

Xue, W. et al., 2007. Senescence and tumour clearance is triggered by p53 restoration in murine liver carcinomas. *Nature*, 445(February), pp.656–660.

Yamaguchi, T. et al., 2010. Histone deacetylases 1 and 2 act in concert to promote the G1-to-S progression. *Genes & development*, 24(5), pp.455–69.

Yamaguchi, T. et al., 2005. Mutation of SENP1/SuPr-2 reveals an essential role for desumoylation in mouse development. *Molecular and cellular biology*, 25(12), pp.5171–82.

Yan, C. & Boyd, D.D., 2006. Histone H3 acetylation and H3 K4 methylation define distinct chromatin regions permissive for transgene expression. *Molecular and cellular biology*, 26(17), pp.6357–71.

Yan, S. et al., 2010. Redox regulation of the stability of the SUMO protease SENP3 via interactions with CHIP and Hsp90. *The EMBO journal*, 29(22), pp.3773–86.

Yang, S.-H. & Sharrocks, A.D., 2004. SUMO Promotes HDAC-Mediated Transcriptional Repression. *Molecular Cell*, 13(4), pp.611–617.

Yang, W. & Paschen, W., 2009. Gene expression and cell growth are modified by silencing SUMO2 and SUMO3 expression. *Biochemical and biophysical research communications*, 382(1), pp.215–8.

Yang, X. et al., 2009. Plk1-mediated phosphorylation of Topors regulates p53 stability. *The Journal of biological chemistry*, 284(28), pp.18588–92.

Yates, K.E. et al., 2008. Repression of the SUMO-specific protease Senp1 induces p53-dependent premature senescence in normal human fibroblasts. *Aging cell*, 7(5), pp.609–21.

Yokoyama, S. et al., 2011. A novel recurrent mutation in MITF predisposes to familial and sporadic melanoma. *Nature*, 480(7375), pp.99–103.

Yuan, H. et al., 2010. Small ubiquitin-related modifier paralogs are indispensable but functionally redundant during early development of zebrafish. *Cell research*, 20(2), pp.185–96.

Zhang, F.-P. et al., 2008. Sumo-1 function is dispensable in normal mouse development. *Molecular and cellular biology*, 28(17), pp.5381–90.

Zhang, H., Saitoh, H. & Matunis, M.J., 2002. Enzymes of the SUMO modification pathway localize to filaments of the nuclear pore complex. *Molecular and cellular biology*, 22(18), pp.6498–508.

Zhang, X.-D. et al., 2008. SUMO-2/3 modification and binding regulate the association of CENP-E with kinetochores and progression through mitosis. *Molecular cell*, 29(6), pp.729–41.

Zhang, Y. et al., 2004. Repression of hsp90beta gene by p53 in UV irradiation-induced apoptosis of Jurkat cells. *The Journal of biological chemistry*, 279(41), pp.42545–51.

Zhao, Q. et al., 2014. GPS-SUMO: a tool for the prediction of sumoylation sites and SUMO-interaction motifs. *Nucleic acids research*, 42(Web Server issue), pp.W325–30.

Zheng, G. & Yang, Y.-C., 2004. ZNF76, a novel transcriptional repressor targeting TATA-binding protein, is modulated by sumoylation. *The Journal of biological chemistry*, 279(41), pp.42410–21.

Zilfou, J.T. & Lowe, S.W., 2009. Tumor suppressive functions of p53. *Cold Spring Harbor perspectives in biology*, 1(5), p.a001883.

Appendix

Appendix A Vector maps for pLEISC plasmids used for molecular cloning

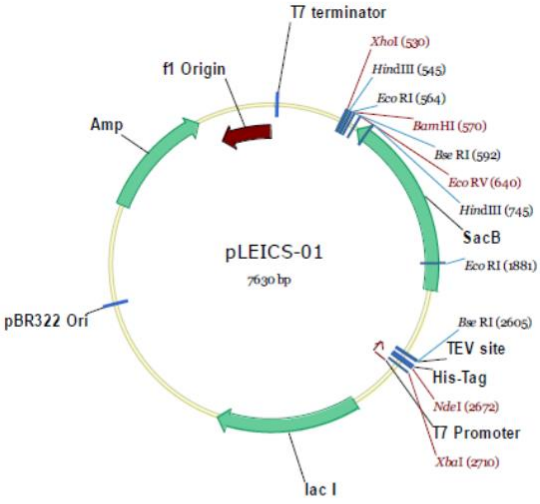

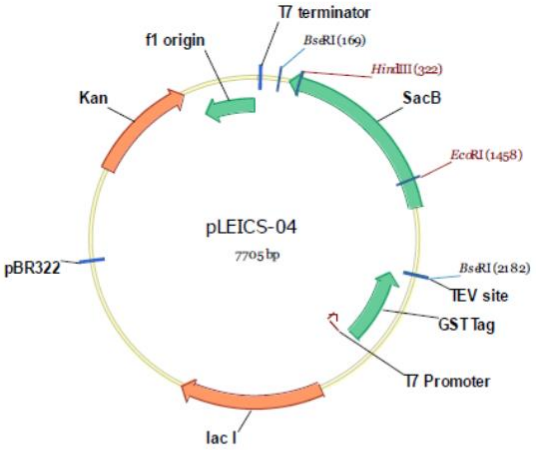

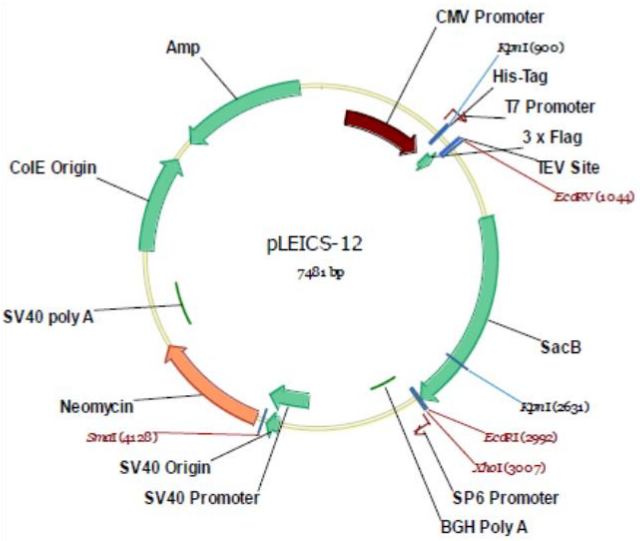

Appendix B Complete list of Plasmids utilized for bacterial and mammalian Expression

Vector name	Expression	Backbone	Tag	Source
GST-$p53_{WT}$	Bacterial	pGEX-5x-3	GST	Dr Barlev's lab
GST-$p53_{K386R}$	Bacterial	pGEX-5x-3	GST	Dr Barlev's lab
GST-$p53_{WT}$300-393	Bacterial	pGEX-5x-3	GST	Dr Barlev's lab
GST-$p53_{K386R}$300-393	Bacterial	pGEX-5x-3	GST	Dr Barlev's lab
GST-$p53_{WT}$-ubc9	Bacterial	pLEIS02	GST	Dr Barlev's lab /PROTEX
GST-$p53_{K386R}$-ubc9	Bacterial	pLEIS02	GST	Dr Barlev's lab /PROTEX
GST-p53Δ 324-355	Bacterial	pGEX-5x-3	GST	Dr Barlev's lab
GST-$p53_{K386R}$Δ 324-355	Bacterial	pGEX-5x-3	GST	Dr Barlev's lab
pLEISC01-Ubc9	Bacterial	pLEISC01	6-HIS	Dr Barlev's lab /PROTEX
GST-SAE2/1	Bacterial	pGEX	GST	Dr Ronald T. Hay
pLEISC01-SUMO-1	Bacterial	pLEISC01	6-HIS	Dr Barlev's lab /PROTEX
pLEISC01-SUMO-2	Bacterial	pLEISC01	6-HIS	Dr Barlev's lab /PROTEX
pcDNA3-$p53_{WT}$-ubc9	Mammalian	pcDNA3	Na	Dr Rainer Niedenthal
pcDNA3-$p53_{K386R}$-ubc9	Mammalian	pcDNA3	Na	Dr Rainer Niedenthal
pcDNA3-$p53_{WT}$	Mammalian	pcDNA3	Na	Dr Barlev's lab
pcDNA3-$p53_{K386R}$	Mammalian	pcDNA3	Na	Dr Barlev's lab
pLEICS12-Sumo-1	Mammalian	pLEISC12	FLAG	Dr Barlev's lab /PROTEX
pLEICS12-Sumo-2	Mammalian	pLEISC12	FLAG	Dr Barlev's lab /PROTEX
Myc-PIASx	Mammalian	pCMV	myc	Dr Barlev's lab
pcDNA3-$p53_{WT}$-TEV-ubc9	Mammalian	pcDNA3	Na	Dr Barlev's lab
pcDNA3-$p53_{K386R}$-TEV-ubc9	Mammalian	pcDNA3	Na	Dr Barlev's lab
pFLAG-TEVpro	Mammalian	pCMV2	FLAG	Dr. Xiaowen Yang

Na: not applicable

Appendix C Complete list of proteins identified by MS 1

UL00932-*-DM

Analysis Type: In-gel trypsin digestion; LC-MS/MS

Mass Spectrometer: LTQ-Orbitrap-Velos-ETD - SN03106B

Database Search Algorithm: Mascot v2.2.04; MS/MS Ion Search

Database Searched: UniProtKB/Swiss-Prot Release 2010_10 of 05-OCT-2010

Idendified Proteins	**$p53_{WT}$ +S1**			**$p53_{K386R}$ +S1**			**$p53_{WT}$**		
	a)	b)	c)	a)	b)	c)	a)	b)	c)
116 kDa U5 small nuclear ribonucleoprotein component OS=Homo sapiens GN=EFTUD2 PE=1 SV=1							+		
14-3-3 protein theta OS=Homo sapiens GN=YWHAQ PE=1 SV=1						+			+
14-3-3 protein zeta/delta OS=Homo sapiens GN=YWHAZ PE=1 SV=1									+
26S protease regulatory subunit 4 OS=Homo sapiens GN=PSMC1 PE=1 SV=1								+	
26S proteasome non-ATPase regulatory subunit 2 OS=Homo sapiens GN=PSMD2 PE=1 SV=3							+		
40S ribosomal protein S10 OS=Homo sapiens GN=RPS10 PE=1 SV=1									+
40S ribosomal protein S12 OS=Homo sapiens GN=RPS12 PE=1 SV=3									+
40S ribosomal protein S13 OS=Homo sapiens GN=RPS13 PE=1 SV=2						+			+
40S ribosomal protein S14 OS=Homo sapiens GN=RPS14 PE=1 SV=3			+			+			+
40S ribosomal protein S15a OS=Homo sapiens GN=RPS15A PE=1 SV=2			+			+			+
40S ribosomal protein S16 OS=Homo sapiens GN=RPS16 PE=1 SV=2									+
40S ribosomal protein S17 OS=Homo sapiens GN=RPS17 PE=1 SV=2									+
40S ribosomal protein S18 OS=Homo sapiens GN=RPS18 PE=1 SV=3						+			+
40S ribosomal protein S19 OS=Homo sapiens GN=RPS19 PE=1 SV=2						+			+

40S ribosomal protein S2 OS=Homo sapiens GN=RPS2 PE=1 SV=2						+			+
40S ribosomal protein S20 OS=Homo sapiens GN=RPS20 PE=1 SV=1						+			+
40S ribosomal protein S21 OS=Homo sapiens GN=RPS21 PE=1 SV=1									+
40S ribosomal protein S23 OS=Homo sapiens GN=RPS23 PE=1 SV=3									+
40S ribosomal protein S24 OS=Homo sapiens GN=RPS24 PE=1 SV=1									+
40S ribosomal protein S25 OS=Homo sapiens GN=RPS25 PE=1 SV=1									+
40S ribosomal protein S3 OS=Homo sapiens GN=RPS3 PE=1 SV=2			+			+			+
40S ribosomal protein S3a OS=Homo sapiens GN=RPS3A PE=1 SV=2									+
40S ribosomal protein S4, X isoform OS=Homo sapiens GN=RPS4X PE=1 SV=2						+			+
40S ribosomal protein S5 OS=Homo sapiens GN=RPS5 PE=1 SV=4									+
40S ribosomal protein S6 OS=Homo sapiens GN=RPS6 PE=1 SV=1									+
40S ribosomal protein S7 OS=Homo sapiens GN=RPS7 PE=1 SV=1						+			+
40S ribosomal protein S8 OS=Homo sapiens GN=RPS8 PE=1 SV=2									+
40S ribosomal protein S9 OS=Homo sapiens GN=RPS9 PE=1 SV=3									+
40S ribosomal protein SA OS=Homo sapiens GN=RPSA PE=1 SV=4			+			+			+
60S acidic ribosomal protein P0 OS=Homo sapiens GN=RPLP0 PE=1 SV=1									+
60S acidic ribosomal protein P0-like OS=Homo sapiens PE=1 SV=1						+			
60S acidic ribosomal protein P1 OS=Homo sapiens GN=RPLP1 PE=1 SV=1									+
60S acidic ribosomal protein P2 OS=Homo sapiens GN=RPLP2 PE=1 SV=1									+
60S ribosomal protein L10a OS=Homo sapiens GN=RPL10A PE=1 SV=2									+
60S ribosomal protein L11 OS=Homo sapiens GN=RPL11 PE=1 SV=2						+			+
60S ribosomal protein L12 OS=Homo sapiens GN=RPL12 PE=1 SV=1						+			+

60S ribosomal protein L13 OS=Homo sapiens GN=RPL13 PE=1 SV=4						+			+
60S ribosomal protein L14 OS=Homo sapiens GN=RPL14 PE=1 SV=4						+			+
60S ribosomal protein L15 OS=Homo sapiens GN=RPL15 PE=1 SV=2									+
60S ribosomal protein L18 OS=Homo sapiens GN=RPL18 PE=1 SV=2									+
60S ribosomal protein L18a OS=Homo sapiens GN=RPL18A PE=1 SV=2									+
60S ribosomal protein L19 OS=Homo sapiens GN=RPL19 PE=1 SV=1						+			+
60S ribosomal protein L22 OS=Homo sapiens GN=RPL22 PE=1 SV=2		+	+			+			+
60S ribosomal protein L23 OS=Homo sapiens GN=RPL23 PE=1 SV=1			+			+			+
60S ribosomal protein L23a OS=Homo sapiens GN=RPL23A PE=1 SV=1									+
60S ribosomal protein L24 OS=Homo sapiens GN=RPL24 PE=1 SV=1						+			+
60S ribosomal protein L26-like 1 OS=Homo sapiens GN=RPL26L1 PE=1 SV=1									+
60S ribosomal protein L27 OS=Homo sapiens GN=RPL27 PE=1 SV=2									+
60S ribosomal protein L27a OS=Homo sapiens GN=RPL27A PE=1 SV=2						+			+
60S ribosomal protein L28 OS=Homo sapiens GN=RPL28 PE=1 SV=3									+
60S ribosomal protein L3 OS=Homo sapiens GN=RPL3 PE=1 SV=2								+	
60S ribosomal protein L30 OS=Homo sapiens GN=RPL30 PE=1 SV=2									+
60S ribosomal protein L31 OS=Homo sapiens GN=RPL31 PE=1 SV=1						+			+
60S ribosomal protein L34 OS=Homo sapiens GN=RPL34 PE=1 SV=3						+			+
60S ribosomal protein L35 OS=Homo sapiens GN=RPL35 PE=1 SV=2			+			+			+
60S ribosomal protein L36 OS=Homo sapiens GN=RPL36 PE=1 SV=3									+
60S ribosomal protein L38 OS=Homo sapiens GN=RPL38 PE=1 SV=2									+
60S ribosomal protein L4 OS=Homo sapiens GN=RPL4 PE=1 SV=5		+			+			+	

60S ribosomal protein L5 OS=Homo sapiens GN=RPL5 PE=1 SV=3									+
60S ribosomal protein L6 OS=Homo sapiens GN=RPL6 PE=1 SV=3									+
60S ribosomal protein L7 OS=Homo sapiens GN=RPL7 PE=1 SV=1			+			+			+
60S ribosomal protein L7a OS=Homo sapiens GN=RPL7A PE=1 SV=2									+
60S ribosomal protein L8 OS=Homo sapiens GN=RPL8 PE=1 SV=2			+			+			+
Acidic leucine-rich nuclear phosphoprotein 32 family member E OS=Homo sapiens GN=ANP32E PE=1 SV=1									+
Actin, cytoplasmic 1 OS=Homo sapiens GN=ACTB PE=1 SV=1		+			+			+	
Alpha-actinin-1 OS=Homo sapiens GN=ACTN1 PE=1 SV=2							+		
Alpha-actinin-2 OS=Homo sapiens GN=ACTN2 PE=1 SV=1							+		
Alpha-actinin-3 OS=Homo sapiens GN=ACTN3 PE=1 SV=2							+		
Alpha-actinin-4 OS=Homo sapiens GN=ACTN4 PE=1 SV=2							+		
Alpha-enolase OS=Homo sapiens GN=ENO1 PE=1 SV=2								+	
Aminoacyl tRNA synthase complex-interacting multifunctional protein 2 OS=Homo sapiens GN=AIMP2 PE=1 SV=2									+
Ankyrin repeat and KH domain-containing protein 1 OS=Homo sapiens GN=ANKHD1 PE=1 SV=1					+	+			
AP-1 complex subunit beta-1 OS=Homo sapiens GN=AP1B1 PE=1 SV=2							+		
Apoptosis inhibitor 5 OS=Homo sapiens GN=API5 PE=1 SV=2					+				
Arginyl-tRNA synthetase, cytoplasmic OS=Homo sapiens GN=RARS PE=1 SV=2								+	
Aspartyl-tRNA synthetase, cytoplasmic OS=Homo sapiens GN=DARS PE=1 SV=2								+	
ATP-binding cassette sub-family F member 1 OS=Homo sapiens GN=ABCF1 PE=1 SV=2							+		
ATP-binding cassette sub-family F member 2 OS=Homo sapiens GN=ABCF2 PE=1 SV=2								+	
ATP-citrate synthase OS=Homo sapiens GN=ACLY PE=1 SV=3							+		
ATP-dependent DNA helicase Q1 OS=Homo sapiens GN=RECQL PE=1 SV=3				+				+	

ATP-dependent RNA helicase A OS=Homo sapiens GN=DHX9 PE=1 SV=4	+			+			+		
ATP-dependent RNA helicase DDX1 OS=Homo sapiens GN=DDX1 PE=1 SV=2								+	
ATP-dependent RNA helicase DDX39 OS=Homo sapiens GN=DDX39 PE=1 SV=2								+	
ATP-dependent RNA helicase DDX3X OS=Homo sapiens GN=DDX3X PE=1 SV=3		+			+			+	
ATP-dependent RNA helicase DDX55 OS=Homo sapiens GN=DDX55 PE=1 SV=3					+				
Bcl-2-associated transcription factor 1 OS=Homo sapiens GN=BCLAF1 PE=1 SV=2							+		
Beta-actin-like protein 2 OS=Homo sapiens GN=ACTBL2 PE=1 SV=2								+	
Bifunctional aminoacyl-tRNA synthetase OS=Homo sapiens GN=EPRS PE=1 SV=5							+		
Bloom syndrome protein OS=Homo sapiens GN=BLM PE=1 SV=1					+				
C-1-tetrahydrofolate synthase, cytoplasmic OS=Homo sapiens GN=MTHFD1 PE=1 SV=3							+		
Caprin-1 OS=Homo sapiens GN=CAPRIN1 PE=1 SV=2				+			+		
Carbonyl reductase [NADPH] 1 OS=Homo sapiens GN=CBR1 PE=1 SV=3									+
Cell division cycle 5-like protein OS=Homo sapiens GN=CDC5L PE=1 SV=2							+		
Cell growth-regulating nucleolar protein OS=Homo sapiens GN=LYAR PE=1 SV=2								+	
Cellular tumor antigen p53 OS=Homo sapiens GN=TP53 PE=1 SV=4	+	+	+	+	+	+	+	+	+
Chloride intracellular channel protein 1 OS=Homo sapiens GN=CLIC1 PE=1 SV=4									+
Clathrin heavy chain 1 OS=Homo sapiens GN=CLTC PE=1 SV=5	+			+					
Clathrin heavy chain 1 OS=Homo sapiens GN=CLTC PE=1 SV=5							+		
Cleavage and polyadenylation specificity factor subunit 5 OS=Homo sapiens GN=NUDT21 PE=1 SV=1									+
Coatomer subunit alpha OS=Homo sapiens GN=COPA PE=1 SV=2							+		
Coatomer subunit delta OS=Homo sapiens GN=ARCN1 PE=1 SV=1								+	
Coatomer subunit gamma OS=Homo sapiens GN=COPG PE=1 SV=1	+			+					

Coatomer subunit gamma OS=Homo sapiens GN=COPG PE=1 SV=1							+		
Coiled-coil domain-containing protein 112 OS=Homo sapiens GN=CCDC112 PE=2 SV=2									+
Coiled-coil domain-containing protein 124 OS=Homo sapiens GN=CCDC124 PE=1 SV=1									+
Coronin-1C OS=Homo sapiens GN=CORO1C PE=1 SV=1					+			+	
Cullin-associated NEDD8-dissociated protein 1 OS=Homo sapiens GN=CAND1 PE=1 SV=2				+					
Cytoskeleton-associated protein 5 OS=Homo sapiens GN=CKAP5 PE=1 SV=3							+		
Dermcidin OS=Homo sapiens GN=DCD PE=1 SV=2	+						+		
Desmin OS=Homo sapiens GN=DES PE=1 SV=3								+	
DNA (cytosine-5)-methyltransferase 1 OS=Homo sapiens GN=DNMT1 PE=1 SV=2							+		
DNA repair protein RAD50 OS=Homo sapiens GN=RAD50 PE=1 SV=1							+		
DNA replication licensing factor MCM3 OS=Homo sapiens GN=MCM3 PE=1 SV=3							+		
DNA replication licensing factor MCM4 OS=Homo sapiens GN=MCM4 PE=1 SV=5							+		
DNA replication licensing factor MCM5 OS=Homo sapiens GN=MCM5 PE=1 SV=5								+	
DNA replication licensing factor MCM7 OS=Homo sapiens GN=MCM7 PE=1 SV=4		+			+			+	
DNA topoisomerase 1 OS=Homo sapiens GN=TOP1 PE=1 SV=2							+		
DNA-binding protein A OS=Homo sapiens GN=CSDA PE=1 SV=4					+				
DNA-dependent protein kinase catalytic subunit OS=Homo sapiens GN=PRKDC PE=1 SV=3	+			+			+		
DNA-directed RNA polymerase I subunit RPA34 OS=Homo sapiens GN=CD3EAP PE=1 SV=1								+	
Dolichyl-diphosphooligosaccharide--protein glycosyltransferase subunit 2 OS=Homo sapiens GN=RPN2 PE=1 SV=3								+	
E3 ubiquitin/ISG15 ligase TRIM25 OS=Homo sapiens GN=TRIM25 PE=1 SV=1								+	
E3 ubiquitin-protein ligase HUWE1 OS=Homo sapiens GN=HUWE1 PE=1 SV=3					+				
ELAV-like protein 1 OS=Homo sapiens GN=ELAVL1 PE=1 SV=2									+

Elongation factor 1-alpha 1 OS=Homo sapiens GN=EEF1A1 PE=1 SV=1		+			+		+	+	
Elongation factor 1-alpha 2 OS=Homo sapiens GN=EEF1A2 PE=1 SV=1								+	
Elongation factor 1-delta OS=Homo sapiens GN=EEF1D PE=1 SV=5									+
Elongation factor 1-gamma OS=Homo sapiens GN=EEF1G PE=1 SV=3					+			+	
Elongation factor 2 OS=Homo sapiens GN=EEF2 PE=1 SV=4							+		
Eukaryotic initiation factor 4A-I OS=Homo sapiens GN=EIF4A1 PE=1 SV=1		+			+			+	
Eukaryotic initiation factor 4A-II OS=Homo sapiens GN=EIF4A2 PE=1 SV=2					+			+	
Eukaryotic translation initiation factor 2 subunit 1 OS=Homo sapiens GN=EIF2S1 PE=1 SV=3						+			+
Eukaryotic translation initiation factor 2 subunit 2 OS=Homo sapiens GN=EIF2S2 PE=1 SV=2								+	
Eukaryotic translation initiation factor 2 subunit 3 OS=Homo sapiens GN=EIF2S3 PE=1 SV=3								+	
Eukaryotic translation initiation factor 2A OS=Homo sapiens GN=EIF2A PE=1 SV=3								+	
Eukaryotic translation initiation factor 3 subunit A OS=Homo sapiens GN=EIF3A PE=1 SV=1							+		
Eukaryotic translation initiation factor 3 subunit B OS=Homo sapiens GN=EIF3B PE=1 SV=3							+		
Eukaryotic translation initiation factor 3 subunit C OS=Homo sapiens GN=EIF3C PE=1 SV=1							+		
Eukaryotic translation initiation factor 3 subunit E OS=Homo sapiens GN=EIF3E PE=1 SV=1								+	
Eukaryotic translation initiation factor 3 subunit F OS=Homo sapiens GN=EIF3F PE=1 SV=1								+	
Eukaryotic translation initiation factor 3 subunit G OS=Homo sapiens GN=EIF3G PE=1 SV=2								+	
Eukaryotic translation initiation factor 3 subunit I OS=Homo sapiens GN=EIF3I PE=1 SV=1									+
Eukaryotic translation initiation factor 3 subunit J OS=Homo sapiens GN=EIF3J PE=1 SV=2									+
Eukaryotic translation initiation factor 3 subunit L OS=Homo sapiens GN=EIF3L PE=1 SV=1								+	
Eukaryotic translation initiation factor 4 gamma 1 OS=Homo sapiens GN=EIF4G1 PE=1 SV=4							+		
Eukaryotic translation initiation factor 4 gamma 2 OS=Homo sapiens GN=EIF4G2 PE=1 SV=1							+		

Eukaryotic translation initiation factor 4 gamma 3 OS=Homo sapiens GN=EIF4G3 PE=1 SV=2							+		
Eukaryotic translation initiation factor 4B OS=Homo sapiens GN=EIF4B PE=1 SV=2								+	
Eukaryotic translation initiation factor 5B OS=Homo sapiens GN=EIF5B PE=1 SV=4							+		
Exosome component 10 OS=Homo sapiens GN=EXOSC10 PE=1 SV=2							+		
Exportin-2 OS=Homo sapiens GN=CSE1L PE=1 SV=3	+			+					
FACT complex subunit SPT16 OS=Homo sapiens GN=SUPT16H PE=1 SV=1							+		
Fanconi anemia group M protein OS=Homo sapiens GN=FANCM PE=1 SV=2				+					
FAST kinase domain-containing protein 2 OS=Homo sapiens GN=FASTKD2 PE=1 SV=1									
Fatty acid synthase OS=Homo sapiens GN=FASN PE=1 SV=3	+						+		
Filamin-A OS=Homo sapiens GN=FLNA PE=1 SV=4	+						+		
Flap endonuclease 1 OS=Homo sapiens GN=FEN1 PE=1 SV=1								+	
Fragile X mental retardation 1 protein OS=Homo sapiens GN=FMR1 PE=1 SV=1								+	
Fragile X mental retardation syndrome-related protein 1 OS=Homo sapiens GN=FXR1 PE=1 SV=3								+	
General transcription factor II-I OS=Homo sapiens GN=GTF2I PE=1 SV=2							+		
General transcription factor II-I repeat domain-containing protein 2A OS=Homo sapiens GN=GTF2IRD2 PE=2 SV=2							+		
Glyceraldehyde-3-phosphate dehydrogenase OS=Homo sapiens GN=GAPDH PE=1 SV=3			+			+			+
GTP-binding protein Di-Ras2 OS=Homo sapiens GN=DIRAS2 PE=1 SV=1					+				
Guanine nucleotide-binding protein subunit beta-2-like 1 OS=Homo sapiens GN=GNB2L1 PE=1 SV=3						+			+
H/ACA ribonucleoprotein complex subunit 4 OS=Homo sapiens GN=DKC1 PE=1 SV=3								+	
Heat shock 70 kDa protein 1A/1B OS=Homo sapiens GN=HSPA1A PE=1 SV=5								+	
Heat shock 70 kDa protein 1-like OS=Homo sapiens GN=HSPA1L PE=1 SV=2								+	
Heat shock 70 kDa protein 6 OS=Homo sapiens GN=HSPA6 PE=1 SV=2								+	

Heat shock cognate 71 kDa protein OS=Homo sapiens GN=HSPA8 PE=1 SV=1					+			+	
Heat shock protein HSP 90-alpha OS=Homo sapiens GN=HSP90AA1 PE=1 SV=5	+			+			+	+	
Heat shock protein HSP 90-beta OS=Homo sapiens GN=HSP90AB1 PE=1 SV=4		+		+	+		+	+	
Heterochromatin protein 1-binding protein 3 OS=Homo sapiens GN=HP1BP3 PE=1 SV=1								+	
Heterogeneous nuclear ribonucleoprotein A/B OS=Homo sapiens GN=HNRNPAB PE=1 SV=2								+	
Heterogeneous nuclear ribonucleoprotein A1-like 2 OS=Homo sapiens GN=HNRNPA1L2 PE=2 SV=2			+			+			
Heterogeneous nuclear ribonucleoprotein A3 OS=Homo sapiens GN=HNRNPA3 PE=1 SV=2					+			+	
Heterogeneous nuclear ribonucleoprotein D0 OS=Homo sapiens GN=HNRNPD PE=1 SV=1		+			+			+	+
Heterogeneous nuclear ribonucleoprotein D-like OS=Homo sapiens GN=HNRPDL PE=1 SV=3		+						+	+
Heterogeneous nuclear ribonucleoprotein F OS=Homo sapiens GN=HNRNPF PE=1 SV=3					+				
Heterogeneous nuclear ribonucleoprotein G OS=Homo sapiens GN=RBMX PE=1 SV=3		+							
Heterogeneous nuclear ribonucleoprotein H OS=Homo sapiens GN=HNRNPH1 PE=1 SV=4					+			+	
Heterogeneous nuclear ribonucleoprotein H3 OS=Homo sapiens GN=HNRNPH3 PE=1 SV=2									+
Heterogeneous nuclear ribonucleoprotein K OS=Homo sapiens GN=HNRNPK PE=1 SV=1		+			+			+	
Heterogeneous nuclear ribonucleoprotein L OS=Homo sapiens GN=HNRNPL PE=1 SV=2		+			+			+	
Heterogeneous nuclear ribonucleoprotein L-like OS=Homo sapiens GN=HNRPLL PE=1 SV=1					+				
Heterogeneous nuclear ribonucleoprotein M OS=Homo sapiens GN=HNRNPM PE=1 SV=3								+	
Heterogeneous nuclear ribonucleoprotein Q OS=Homo sapiens GN=SYNCRIP PE=1 SV=2		+			+			+	
Heterogeneous nuclear ribonucleoprotein R OS=Homo sapiens GN=HNRNPR PE=1 SV=1		+			+				
Heterogeneous nuclear ribonucleoprotein U OS=Homo sapiens GN=HNRNPU PE=1 SV=6	+	+					+		
Heterogeneous nuclear ribonucleoproteins A2/B1 OS=Homo sapiens GN=HNRNPA2B1 PE=1 SV=2						+			+
Heterogeneous nuclear ribonucleoproteins C1/C2 OS=Homo sapiens GN=HNRNPC PE=1 SV=4						+			+

Hexokinase-1 OS=Homo sapiens GN=HK1 PE=1 SV=3		+							
Histone H1.1 OS=Homo sapiens GN=HIST1H1A PE=1 SV=3									+
Histone H1.3 OS=Homo sapiens GN=HIST1H1D PE=1 SV=2									+
Histone H1.4 OS=Homo sapiens GN=HIST1H1E PE=1 SV=2									+
Histone H1.5 OS=Homo sapiens GN=HIST1H1B PE=1 SV=3									+
Histone H2A type 1-A OS=Homo sapiens GN=HIST1H2AA PE=1 SV=3						+			
Histone H2A type 1-J OS=Homo sapiens GN=HIST1H2AJ PE=1 SV=3						+			+
Histone H2B type 1-M OS=Homo sapiens GN=HIST1H2BM PE=1 SV=3									+
Histone H4 OS=Homo sapiens GN=HIST1H4A PE=1 SV=2						+			+
Hsp90 co-chaperone Cdc37 OS=Homo sapiens GN=CDC37 PE=1 SV=1								+	
Hyaluronan synthase 1 OS=Homo sapiens GN=HAS1 PE=1 SV=2								+	
Importin subunit alpha-2 OS=Homo sapiens GN=KPNA2 PE=1 SV=1								+	
Importin subunit beta-1 OS=Homo sapiens GN=KPNB1 PE=1 SV=2				+			+		
Importin-5 OS=Homo sapiens GN=IPO5 PE=1 SV=4							+		
Inosine-5'-monophosphate dehydrogenase 2 OS=Homo sapiens GN=IMPDH2 PE=1 SV=2								+	
Insulin-like growth factor 2 mRNA-binding protein 1 OS=Homo sapiens GN=IGF2BP1 PE=1 SV=2					+			+	
Insulin-like growth factor 2 mRNA-binding protein 2 OS=Homo sapiens GN=IGF2BP2 PE=1 SV=2								+	
Insulin-like growth factor 2 mRNA-binding protein 3 OS=Homo sapiens GN=IGF2BP3 PE=1 SV=2								+	
Interferon-induced, double-stranded RNA-activated protein kinase OS=Homo sapiens GN=EIF2AK2 PE=1 SV=2								+	
Interleukin enhancer-binding factor 2 OS=Homo sapiens GN=ILF2 PE=1 SV=2		+			+			+	
Interleukin enhancer-binding factor 3 OS=Homo sapiens GN=ILF3 PE=1 SV=3							+	+	
Isoleucyl-tRNA synthetase, cytoplasmic OS=Homo sapiens GN=IARS PE=1 SV=2							+		

KH domain-containing, RNA-binding, signal transduction-associated protein 1 OS=Homo sapiens GN=KHDRBS1 PE=1 SV=1		+						+	
La-related protein 1 OS=Homo sapiens GN=LARP1 PE=1 SV=2							+		
Leucyl-tRNA synthetase, cytoplasmic OS=Homo sapiens GN=LARS PE=1 SV=2				+			+		
L-lactate dehydrogenase A chain OS=Homo sapiens GN=LDHA PE=1 SV=2			+			+			+
L-lactate dehydrogenase B chain OS=Homo sapiens GN=LDHB PE=1 SV=2									+
Lysyl-tRNA synthetase OS=Homo sapiens GN=KARS PE=1 SV=3								+	
Matrin-3 OS=Homo sapiens GN=MATR3 PE=1 SV=2							+		
Mediator of DNA damage checkpoint protein 1 OS=Homo sapiens GN=MDC1 PE=1 SV=3							+		
Methionyl-tRNA synthetase, cytoplasmic OS=Homo sapiens GN=MARS PE=1 SV=2							+		
Microtubule-actin cross-linking factor 1, isoforms 1/2/3/5 OS=Homo sapiens GN=MACF1 PE=1 SV=3						+			
Microtubule-associated protein 4 OS=Homo sapiens GN=MAP4 PE=1 SV=3							+		
Myb-binding protein 1A OS=Homo sapiens GN=MYBBP1A PE=1 SV=2							+		
Myosin-11 OS=Homo sapiens GN=MYH11 PE=1 SV=3							+		
Myosin-14 OS=Homo sapiens GN=MYH14 PE=1 SV=1							+		
Myosin-9 OS=Homo sapiens GN=MYH9 PE=1 SV=4							+		
Nascent polypeptide-associated complex subunit alpha OS=Homo sapiens GN=NACA PE=1 SV=1									+
Nesprin-1 OS=Homo sapiens GN=SYNE1 PE=1 SV=3								+	
Neurofilament heavy polypeptide OS=Homo sapiens GN=NEFH PE=1 SV=4								+	
Neurofilament medium polypeptide OS=Homo sapiens GN=NEFM PE=1 SV=3								+	
Nicotinate phosphoribosyltransferase OS=Homo sapiens GN=NAPRT1 PE=1 SV=2		+							
Non-POU domain-containing octamer-binding protein OS=Homo sapiens GN=NONO PE=1 SV=4					+			+	
Nuclease-sensitive element-binding protein 1 OS=Homo sapiens GN=YBX1 PE=1 SV=3								+	

Nucleolar and coiled-body phosphoprotein 1 OS=Homo sapiens GN=NOLC1 PE=1 SV=2							+		
Nucleolar RNA helicase 2 OS=Homo sapiens GN=DDX21 PE=1 SV=5							+		
Nucleolar transcription factor 1 OS=Homo sapiens GN=UBTF PE=1 SV=1							+		
Nucleolin OS=Homo sapiens GN=NCL PE=1 SV=3	+			+			+	+	
Nucleophosmin OS=Homo sapiens GN=NPM1 PE=1 SV=2			+			+			+
Parafibromin OS=Homo sapiens GN=CDC73 PE=1 SV=1								+	
Paraspeckle component 1 OS=Homo sapiens GN=PSPC1 PE=1 SV=1								+	
PC4 and SFRS1-interacting protein OS=Homo sapiens GN=PSIP1 PE=1 SV=1				+				+	
Peptidyl-prolyl cis-trans isomerase A OS=Homo sapiens GN=PPIA PE=1 SV=2									+
Peroxiredoxin-1 OS=Homo sapiens GN=PRDX1 PE=1 SV=1						+			+
Peroxiredoxin-2 OS=Homo sapiens GN=PRDX2 PE=1 SV=5									+
PHD and RING finger domain-containing protein 1 OS=Homo sapiens GN=PHRF1 PE=1 SV=3						+			
Phosphoglycerate kinase 1 OS=Homo sapiens GN=PGK1 PE=1 SV=3		+			+			+	
Plasminogen activator inhibitor 1 RNA-binding protein OS=Homo sapiens GN=SERBP1 PE=1 SV=2								+	
Poly [ADP-ribose] polymerase 1 OS=Homo sapiens GN=PARP1 PE=1 SV=4							+		
Poly(rC)-binding protein 2 OS=Homo sapiens GN=PCBP2 PE=1 SV=1									+
Poly(rC)-binding protein 3 OS=Homo sapiens GN=PCBP3 PE=1 SV=2									+
Poly(U)-binding-splicing factor PUF60 OS=Homo sapiens GN=PUF60 PE=1 SV=1								+	
Polyadenylate-binding protein 1 OS=Homo sapiens GN=PABPC1 PE=1 SV=2								+	
Polyadenylate-binding protein 3 OS=Homo sapiens GN=PABPC3 PE=1 SV=2								+	
Polyadenylate-binding protein 4 OS=Homo sapiens GN=PABPC4 PE=1 SV=1								+	
Polypyrimidine tract-binding protein 1 OS=Homo sapiens GN=PTBP1 PE=1 SV=1					+			+	

Polypyrimidine tract-binding protein 2 OS=Homo sapiens GN=PTBP2 PE=1 SV=1					+			+	
POTE ankyrin domain family member E OS=Homo sapiens GN=POTEE PE=1 SV=3								+	
POTE ankyrin domain family member I OS=Homo sapiens GN=POTEI PE=3 SV=1					+				
Prelamin-A/C OS=Homo sapiens GN=LMNA PE=1 SV=1								+	
Pre-mRNA-processing factor 19 OS=Homo sapiens GN=PRPF19 PE=1 SV=1								+	
Pre-mRNA-processing factor 6 OS=Homo sapiens GN=PRPF6 PE=1 SV=1							+		
Pre-mRNA-processing-splicing factor 8 OS=Homo sapiens GN=PRPF8 PE=1 SV=2							+		
Probable ATP-dependent RNA helicase DDX17 OS=Homo sapiens GN=DDX17 PE=1 SV=1					+			+	
Probable ATP-dependent RNA helicase DDX23 OS=Homo sapiens GN=DDX23 PE=1 SV=3							+		
Probable ATP-dependent RNA helicase DDX46 OS=Homo sapiens GN=DDX46 PE=1 SV=2							+		
Probable ATP-dependent RNA helicase DDX47 OS=Homo sapiens GN=DDX47 PE=1 SV=1								+	
Probable ATP-dependent RNA helicase DDX5 OS=Homo sapiens GN=DDX5 PE=1 SV=1		+			+			+	
Probable ATP-dependent RNA helicase DDX6 OS=Homo sapiens GN=DDX6 PE=1 SV=2								+	
Probable Xaa-Pro aminopeptidase 3 OS=Homo sapiens GN=XPNPEP3 PE=1 SV=1							+		
Profilin-1 OS=Homo sapiens GN=PFN1 PE=1 SV=2		+			+				+
Proliferating cell nuclear antigen OS=Homo sapiens GN=PCNA PE=1 SV=1						+			+
Proliferation-associated protein 2G4 OS=Homo sapiens GN=PA2G4 PE=1 SV=3					+			+	
Prostaglandin E synthase 3 OS=Homo sapiens GN=PTGES3 PE=1 SV=1						+			
Protein DEK OS=Homo sapiens GN=DEK PE=1 SV=1								+	
Protein Shroom3 OS=Homo sapiens GN=SHROOM3 PE=1 SV=2	+	+	+	+	+	+	+	+	+
Putative 40S ribosomal protein S26-like 1 OS=Homo sapiens GN=RPS26P11 PE=5 SV=1			+			+			+
Putative 60S ribosomal protein L13a-like MGC87657 OS=Homo sapiens PE=5 SV=1									+

Putative heat shock 70 kDa protein 7 OS=Homo sapiens GN=HSPA7 PE=5 SV=2								+	
Putative heat shock protein HSP 90-alpha A4 OS=Homo sapiens GN=HSP90AA4P PE=5 SV=1	+	+							
Putative heat shock protein HSP 90-beta-3 OS=Homo sapiens GN=HSP90AB3P PE=5 SV=1		+			+			+	
Putative heterogeneous nuclear ribonucleoprotein A1-like 3 OS=Homo sapiens GN=HNRPA1L3 PE=5 SV=1									+
Putative pre-mRNA-splicing factor ATP-dependent RNA helicase DHX15 OS=Homo sapiens GN=DHX15 PE=1 SV=2	+			+			+	+	
Putative pre-mRNA-splicing factor ATP-dependent RNA helicase DHX16 OS=Homo sapiens GN=DHX16 PE=1 SV=2							+		
Putative ribosomal RNA methyltransferase NOP2 OS=Homo sapiens GN=NOP2 PE=1 SV=2							+		
Putative RNA-binding protein Luc7-like 2 OS=Homo sapiens GN=LUC7L2 PE=1 SV=2								+	
Putative tubulin-like protein alpha-4B OS=Homo sapiens GN=TUBA4B PE=5 SV=2		+			+			+	
Pyruvate kinase isozymes M1/M2 OS=Homo sapiens GN=PKM2 PE=1 SV=4		+			+			+	
Ran GTPase-activating protein 1 OS=Homo sapiens GN=RANGAP1 PE=1 SV=1		+						+	
Ras GTPase-activating protein-binding protein 1 OS=Homo sapiens GN=G3BP1 PE=1 SV=1								+	
Ras GTPase-activating protein-binding protein 2 OS=Homo sapiens GN=G3BP2 PE=1 SV=2								+	
Ras GTPase-activating-like protein IQGAP1 OS=Homo sapiens GN=IQGAP1 PE=1 SV=1							+		
Regulator of chromosome condensation OS=Homo sapiens GN=RCC1 PE=1 SV=1					+			+	
Replication protein A 70 kDa DNA-binding subunit OS=Homo sapiens GN=RPA1 PE=1 SV=2								+	
RNA-binding protein 39 OS=Homo sapiens GN=RBM39 PE=1 SV=2	+	+						+	
RNA-binding protein FUS OS=Homo sapiens GN=FUS PE=1 SV=1								+	
rRNA 2'-O-methyltransferase fibrillarin OS=Homo sapiens GN=FBL PE=1 SV=2									+
RUN and FYVE domain-containing protein 2 OS=Homo sapiens GN=RUFY2 PE=1 SV=2		+			+				
RuvB-like 1 OS=Homo sapiens GN=RUVBL1 PE=1 SV=1								+	
RuvB-like 2 OS=Homo sapiens GN=RUVBL2 PE=1 SV=3								+	

Septin-2 OS=Homo sapiens GN=SEPT2 PE=1 SV=1								+	
Serine/arginine-rich splicing factor 1 OS=Homo sapiens GN=SRSF1 PE=1 SV=2									+
Serine/arginine-rich splicing factor 3 OS=Homo sapiens GN=SRSF3 PE=1 SV=1									+
Serine/arginine-rich splicing factor 4 OS=Homo sapiens GN=SRSF4 PE=1 SV=2		+						+	+
Serine/arginine-rich splicing factor 5 OS=Homo sapiens GN=SRSF5 PE=1 SV=1								+	
Serine/arginine-rich splicing factor 6 OS=Homo sapiens GN=SRSF6 PE=1 SV=2								+	+
Serum albumin OS=Homo sapiens GN=ALB PE=1 SV=2	+	+			+	+	+	+	+
Signal recognition particle 14 kDa protein OS=Homo sapiens GN=SRP14 PE=1 SV=2									+
Sister chromatid cohesion protein PDS5 homolog A OS=Homo sapiens GN=PDS5A PE=1 SV=1							+		
Small nuclear ribonucleoprotein Sm D2 OS=Homo sapiens GN=SNRPD2 PE=1 SV=1									+
Small nuclear ribonucleoprotein Sm D3 OS=Homo sapiens GN=SNRPD3 PE=1 SV=1									+
Small nuclear ribonucleoprotein-associated proteins B and B' OS=Homo sapiens GN=SNRPB PE=1 SV=2									+
Small ubiquitin-related modifier 1 OS=Homo sapiens GN=SUMO1 PE=1 SV=1	+	+	+	+		+			
Spermatid perinuclear RNA-binding protein OS=Homo sapiens GN=STRBP PE=1 SV=1							+	+	
Spliceosome RNA helicase BAT1 OS=Homo sapiens GN=BAT1 PE=1 SV=1								+	
Splicing factor 3A subunit 1 OS=Homo sapiens GN=SF3A1 PE=1 SV=1							+		
Splicing factor 3B subunit 2 OS=Homo sapiens GN=SF3B2 PE=1 SV=2							+		
Splicing factor U2AF 65 kDa subunit OS=Homo sapiens GN=U2AF2 PE=1 SV=4		+						+	
Splicing factor, proline- and glutamine-rich OS=Homo sapiens GN=SFPQ PE=1 SV=2				+			+	+	
Staphylococcal nuclease domain-containing protein 1 OS=Homo sapiens GN=SND1 PE=1 SV=1							+		
SUMO-activating enzyme subunit 1 OS=Homo sapiens GN=SAE1 PE=1 SV=1		+	+		+	+			
SUMO-activating enzyme subunit 2 OS=Homo sapiens GN=UBA2 PE=1 SV=2	+	+	+		+	+			

SUMO-conjugating enzyme UBC9 OS=Homo sapiens GN=UBE2I PE=1 SV=1	+	+	+	+	+	+	+	+	+
SWI/SNF complex subunit SMARCC1 OS=Homo sapiens GN=SMARCC1 PE=1 SV=3	+								
Synaptotagmin-like protein 5 OS=Homo sapiens GN=SYTL5 PE=1 SV=1						+			+
TATA-binding protein-associated factor 2N OS=Homo sapiens GN=TAF15 PE=1 SV=1								+	
TBC1 domain family member 2A OS=Homo sapiens GN=TBC1D2 PE=1 SV=3			+						
T-complex protein 1 subunit alpha OS=Homo sapiens GN=TCP1 PE=1 SV=1					+			+	
T-complex protein 1 subunit beta OS=Homo sapiens GN=CCT2 PE=1 SV=4					+			+	
T-complex protein 1 subunit delta OS=Homo sapiens GN=CCT4 PE=1 SV=4		+			+			+	
T-complex protein 1 subunit epsilon OS=Homo sapiens GN=CCT5 PE=1 SV=1								+	
T-complex protein 1 subunit eta OS=Homo sapiens GN=CCT7 PE=1 SV=2		+			+			+	
T-complex protein 1 subunit gamma OS=Homo sapiens GN=CCT3 PE=1 SV=4					+			+	
T-complex protein 1 subunit theta OS=Homo sapiens GN=CCT8 PE=1 SV=4		+			+			+	
T-complex protein 1 subunit zeta OS=Homo sapiens GN=CCT6A PE=1 SV=3		+			+			+	
T-complex protein 1 subunit zeta-2 OS=Homo sapiens GN=CCT6B PE=1 SV=4								+	
THO complex subunit 4 OS=Homo sapiens GN=THOC4 PE=1 SV=3									+
Thyroid hormone receptor-associated protein 3 OS=Homo sapiens GN=THRAP3 PE=1 SV=2							+		
Transcription intermediary factor 1-beta OS=Homo sapiens GN=TRIM28 PE=1 SV=5							+		
Transitional endoplasmic reticulum ATPase OS=Homo sapiens GN=VCP PE=1 SV=4							+		
Transportin-1 OS=Homo sapiens GN=TNPO1 PE=1 SV=2				+					
Treacle protein OS=Homo sapiens GN=TCOF1 PE=1 SV=3							+		
tRNA (cytosine-5-)-methyltransferase NSUN2 OS=Homo sapiens GN=NSUN2 PE=1 SV=2							+		
Tropomyosin alpha-4 chain OS=Homo sapiens GN=TPM4 PE=1 SV=3									+

Tubulin alpha-1A chain OS=Homo sapiens GN=TUBA1A PE=1 SV=1	+			+				+	
Tubulin alpha-1B chain OS=Homo sapiens GN=TUBA1B PE=1 SV=1		+					+	+	
Tubulin beta chain OS=Homo sapiens GN=TUBB PE=1 SV=2	+	+			+		+	+	
Tubulin beta-2A chain OS=Homo sapiens GN=TUBB2A PE=1 SV=1		+			+			+	
Tubulin beta-2C chain OS=Homo sapiens GN=TUBB2C PE=1 SV=1		+			+		+	+	
Tubulin beta-3 chain OS=Homo sapiens GN=TUBB3 PE=1 SV=2		+			+			+	
Tubulin beta-6 chain OS=Homo sapiens GN=TUBB6 PE=1 SV=1		+			+			+	
U2 small nuclear ribonucleoprotein A' OS=Homo sapiens GN=SNRPA1 PE=1 SV=2									+
U4/U6.U5 tri-snRNP-associated protein 1 OS=Homo sapiens GN=SART1 PE=1 SV=1							+		
U5 small nuclear ribonucleoprotein 200 kDa helicase OS=Homo sapiens GN=SNRNP200 PE=1 SV=2							+		
Ubiquitin-40S ribosomal protein S27a OS=Homo sapiens GN=RPS27A PE=1 SV=2	+			+			+		+
Uncharacterized protein KIAA1107 OS=Homo sapiens GN=KIAA1107 PE=1 SV=2			+						
UPF0027 protein C22orf28 OS=Homo sapiens GN=C22orf28 PE=1 SV=1								+	
UPF0568 protein C14orf166 OS=Homo sapiens GN=C14orf166 PE=1 SV=1									+
Valyl-tRNA synthetase OS=Homo sapiens GN=VARS PE=1 SV=4				+			+		
Vigilin OS=Homo sapiens GN=HDLBP PE=1 SV=2							+		
Vimentin OS=Homo sapiens GN=VIM PE=1 SV=4		+			+			+	
X-ray repair cross-complementing protein 5 OS=Homo sapiens GN=XRCC5 PE=1 SV=3								+	
X-ray repair cross-complementing protein 6 OS=Homo sapiens GN=XRCC6 PE=1 SV=2			+					+	
Zinc finger RNA-binding protein OS=Homo sapiens GN=ZFR PE=1 SV=2							+		

Appendix C.1 List of Selected proteins from MS 1

Idendified Proteins	$p53_{WT}$ +S1	$p53_{K386R}$ +S1	$p53_{WT}$	Function
Bcl-2-associated transcription factor 1 OS=Homo sapiens GN=BCLAF1 PE=1 SV=2			+	Transcriptional Regulation
PC4 and SFRS1-interacting protein OS=Homo sapiens GN=PSIP1 PE=1 SV=1		+	+	
DNA-binding protein A OS=Homo sapiens GN=CSDA PE=1 SV=4		+		
Cullin-associated NEDD8-dissociated protein 1 OS=Homo sapiens GN=CAND1 PE=1 SV=2		+		Ubiquitylation
E3 ubiquitin/ISG15 ligase TRIM25 OS=Homo sapiens GN=TRIM25 PE=1 SV=1			+	
E3 ubiquitin-protein ligase HUWE1 OS=Homo sapiens GN=HUWE1 PE=1 SV=3		+		
Elongation factor 1-alpha 2 OS=Homo sapiens GN=EEF1A2 PE=1 SV=1			+	Translation
Elongation factor 1-delta OS=Homo sapiens GN=EEF1D PE=1 SV=5			+	
Elongation factor 1-gamma OS=Homo sapiens GN=EEF1G PE=1 SV=3		+	+	
Elongation factor 2 OS=Homo sapiens GN=EEF2 PE=1 SV=4			+	
Eukaryotic initiation factor 4A-II OS=Homo sapiens GN=EIF4A2 PE=1 SV=2		+	+	
Eukaryotic translation initiation factor 2 subunit 1 OS=Homo sapiens GN=EIF2S1 PE=1 SV=3		+	+	
Exportin-2 OS=Homo sapiens GN=CSE1L PE=1 SV=3	+	+		Nucleo-cytoplasmatic Transport
Importin subunit alpha-2 OS=Homo sapiens GN=KPNA2 PE=1 SV=1			+	
Importin subunit beta-1 OS=Homo sapiens GN=KPNB1 PE=1 SV=2		+	+	
Importin-5 OS=Homo sapiens GN=IPO5 PE=1 SV=4			+	
Transportin-1 OS=Homo sapiens GN=TNPO1 PE=1 SV=2		+		
General transcription factor II-I OS=Homo sapiens GN=GTF2I PE=1 SV=2			+	Transcription
General transcription factor II-I repeat domain-containing protein 2A OS=Homo sapiens GN=GTF2IRD2 PE=2 SV=2			+	
GTP-binding protein Di-Ras2 OS=Homo sapiens GN=DIRAS2 PE=1 SV=1		+		Signal Transduction
14-3-3 protein theta OS=Homo sapiens GN=YWHAQ PE=1 SV=1		+	+	
14-3-3 protein zeta/delta OS=Homo sapiens GN=YWHAZ PE=1 SV=1			+	
Coronin-1C OS=Homo sapiens GN=CORO1C PE=1 SV=1		+	+	
Prostaglandin E synthase 3 OS=Homo sapiens GN=PTGES3 PE=1 SV=1		+		Metabolism

Guanine nucleotide-binding protein subunit beta-2-like 1 OS=Homo sapiens GN=GNB2L1 PE=1 SV=3		+	+	
Nicotinate phosphoribosyltransferase OS=Homo sapiens GN=NAPRT1 PE=1 SV=2	+			
Heat shock 70 kDa protein 1A/1B OS=Homo sapiens GN=HSPA1A PE=1 SV=5			+	Chaperones
Heat shock 70 kDa protein 1-like OS=Homo sapiens GN=HSPA1L PE=1 SV=2			+	
Heat shock 70 kDa protein 6 OS=Homo sapiens GN=HSPA6 PE=1 SV=2			+	
Heat shock cognate 71 kDa protein OS=Homo sapiens GN=HSPA8 PE=1 SV=1		+	+	
Putative heat shock protein HSP 90-alpha A4 OS=Homo sapiens GN=HSP90AA4P PE=5 SV=1	+			
Heterochromatin protein 1-binding protein 3 OS=Homo sapiens GN=HP1BP3 PE=1 SV=1			+	Chromatin Remodeling
Poly [ADP-ribose] polymerase 1 OS=Homo sapiens GN=PARP1 PE=1 SV=4			+	DNA repair
Probable ATP-dependent RNA helicase DDX17 OS=Homo sapiens GN=DDX17 PE=1 SV=1		+	+	mRNA processing
Probable ATP-dependent RNA helicase DDX23 OS=Homo sapiens GN=DDX23 PE=1 SV=3			+	
Probable ATP-dependent RNA helicase DDX46 OS=Homo sapiens GN=DDX46 PE=1 SV=2			+	
Probable ATP-dependent RNA helicase DDX47 OS=Homo sapiens GN=DDX47 PE=1 SV=1			+	
Probable ATP-dependent RNA helicase DDX5 OS=Homo sapiens GN=DDX5 PE=1 SV=1	+	+	+	
Probable ATP-dependent RNA helicase DDX6 OS=Homo sapiens GN=DDX6 PE=1 SV=2			+	
Non-POU domain-containing octamer-binding protein OS=Homo sapiens GN=NONO PE=1 SV=4		+	+	
PHD and RING finger domain-containing protein 1 OS=Homo sapiens GN=PHRF1 PE=1 SV=3		+		
Proliferating cell nuclear antigen OS=Homo sapiens GN=PCNA PE=1 SV=1		+	+	Cell Proliferation
Proliferation-associated protein 2G4 OS=Homo sapiens GN=PA2G4 PE=1 SV=3		+	+	
Regulator of chromosome condensation OS=Homo sapiens GN=RCC1 PE=1 SV=1		+	+	Mitosis
Synaptotagmin-like protein 5 OS=Homo sapiens GN=SYTL5 PE=1 SV=1		+	+	Exocytosis
ATP-dependent DNA helicase Q1 OS=Homo sapiens GN=RECQL PE=1 SV=3		+	+	DNA helicases

X-ray repair cross-complementing protein 5 OS=Homo sapiens GN=XRCC5 PE=1 SV=3			+	
X-ray repair cross-complementing protein 6 OS=Homo sapiens GN=XRCC6 PE=1 SV=2	+		+	
Zinc finger RNA-binding protein OS=Homo sapiens GN=ZFR PE=1 SV=2			+	Development

Appendix D Complete list of proteins identified by MS 2

Experiment: UL01408DM

Scaffold: Version: Scaffold_4.4.1.1

Protein Grouping Strategy: Experiment-wide grouping with protein cluster analysis

Peptide Thresholds: 45.0% minimum

Protein Thresholds: 24.0% minimum and 2 peptides minimum

Peptide FDR: 0.2% (Decoy)

Protein FDR: 0.9% (Decoy)

Identified Proteins (997)	Accession Number	Molecular Weight	Total Unique Peptide Count								
			p53WT +SUMO-1			p53K386R +SUMO-1			p53WT		
			a)	b)	c)	a)	b)	c)	a)	b)	c)
116 kDa U5 small nuclear ribonucleoprotein component OS=Homo sapiens GN=EFTUD2 PE=2 SV=1	B4DK30 (+1)	105 kDa	9	0	0	7	0	0	11	0	0
14-3-3 protein beta/alpha OS=Homo sapiens GN=YWHAB PE=1 SV=3	P31946 (+1)	28 kDa	0	0	10	0	0	7	0	0	9
14-3-3 protein epsilon OS=Homo sapiens GN=YWHAE PE=1 SV=1	P62258	29 kDa	0	0	15	0	0	11	0	0	10
14-3-3 protein eta OS=Homo sapiens GN=YWHAH PE=1 SV=4	Q04917	28 kDa	0	0	11	0	0	6	0	0	7
14-3-3 protein gamma, N-terminally processed OS=Homo sapiens GN=YWHAG PE=2 SV=1	B4DHC4 (+1)	26 kDa	0	0	8	0	0	5	0	0	7
14-3-3 protein theta OS=Homo sapiens GN=YWHAQ PE=1 SV=1	P27348	28 kDa	0	0	16	0	0	17	0	0	17
14-3-3 protein zeta/delta OS=Homo sapiens GN=YWHAZ PE=1 SV=1	P63104 (+1)	28 kDa	0	0	14	0	0	13	0	0	13
2,4-dienoyl-CoA reductase, mitochondrial OS=Homo sapiens GN=DECR1 PE=2 SV=1	B7Z6B8 (+1)	35 kDa	0	0	3	0	0	2	0	0	3
26S protease regulatory subunit 10B OS=Homo sapiens GN=PSMC6 PE=1 SV=1	P62333	44 kDa	0	4	0	0	4	0	0	4	0
26S protease regulatory subunit 4 OS=Homo sapiens GN=PSMC1 PE=1 SV=1	P62191	49 kDa	0	8	0	0	5	0	0	7	0

26S protease regulatory subunit 6A OS=Homo sapiens GN=PSMC3 PE=1 SV=3	P17980	49 kDa	0	5	0	0	4	0	0	5	0
26S protease regulatory subunit 6B OS=Homo sapiens GN=PSMC4 PE=1 SV=2	P43686 (+1)	47 kDa	0	4	0	0	2	0	0	4	0
26S protease regulatory subunit 7 OS=Homo sapiens GN=PSMC2 PE=1 SV=3	P35998	49 kDa	0	8	0	0	7	0	0	3	0
26S protease regulatory subunit 8 OS=Homo sapiens GN=PSMC5 PE=2 SV=1	A8K3Z3 (+1)	45 kDa	0	5	0	0	4	0	0	7	0
26S proteasome non-ATPase regulatory subunit 1 OS=Homo sapiens GN=PSMD1 PE=1 SV=2	Q99460 (+1)	106 kDa	8	0	0	3	0	0	5	0	0
26S proteasome non-ATPase regulatory subunit 11 OS=Homo sapiens GN=PSMD11 PE=1 SV=3	O00231	47 kDa	0	7	0	0	4	0	0	8	0
26S proteasome non-ATPase regulatory subunit 12 OS=Homo sapiens GN=PSMD12 PE=1 SV=3	O00232 (+1)	53 kDa	0	9	0	0	7	0	0	7	0
26S proteasome non-ATPase regulatory subunit 13 OS=Homo sapiens GN=PSMD13 PE=1 SV=2	Q9UNM6	43 kDa	0	5	0	0	6	0	0	5	0
26S proteasome non-ATPase regulatory subunit 14 OS=Homo sapiens GN=PSMD14 PE=1 SV=1	O00487	35 kDa	0	0	3	0	2	2	0	3	0
26S proteasome non-ATPase regulatory subunit 2 OS=Homo sapiens GN=PSMD2 PE=4 SV=1	F5GZ16 (+1)	99 kDa	21	0	0	13	0	0	11	0	0
26S proteasome non-ATPase regulatory subunit 3 OS=Homo sapiens GN=PSMD3 PE=4 SV=1	F5H8K4 (+1)	60 kDa	0	5	0	0	3	0	0	2	0
26S proteasome non-ATPase regulatory subunit 4 (Fragment) OS=Homo sapiens GN=PSMD4 PE=4 SV=1	H0Y3Y9 (+2)	21 kDa	0	0	0	0	2	0	0	0	0
26S proteasome non-ATPase regulatory subunit 5 OS=Homo sapiens GN=PSMD5 PE=2 SV=1	B4DZM8 (+1)	51 kDa	0	7	0	0	7	0	0	9	0
26S proteasome non-ATPase regulatory subunit 6 OS=Homo sapiens GN=PSMD6 PE=4 SV=1	C9IZE4 (+1)	52 kDa	0	0	0	0	3	0	0	2	0
26S proteasome non-ATPase regulatory subunit 7 OS=Homo sapiens GN=PSMD7 PE=1 SV=2	P51665	37 kDa	0	0	0	0	2	0	0	0	0
26S proteasome non-ATPase regulatory subunit 8 OS=Homo sapiens GN=PSMD8 PE=1 SV=2	P48556	40 kDa	0	0	7	0	0	5	0	0	6
28 kDa heat- and acid-stable phosphoprotein OS=Homo sapiens GN=PDAP1 PE=1 SV=1	Q13442	21 kDa	0	0	0	0	0	0	0	0	3
4-trimethylaminobutyraldehyde dehydrogenase OS=Homo sapiens GN=ALDH9A1 PE=1 SV=3	P49189	54 kDa	0	4	0	0	3	0	0	6	0
40S ribosomal protein S10 OS=Homo sapiens GN=RPS10 PE=1 SV=1	P46783	19 kDa	0	0	4	0	0	4	0	0	5
40S ribosomal protein S11 OS=Homo sapiens GN=RPS11 PE=1 SV=3	P62280	18 kDa	0	0	6	0	0	6	0	0	11
40S ribosomal protein S12 OS=Homo sapiens GN=RPS12 PE=1 SV=3	P25398	15 kDa	0	0	5	0	0	4	0	0	6
40S ribosomal protein S13 OS=Homo sapiens GN=RPS13 PE=1 SV=2	P62277	17 kDa	0	0	7	0	0	7	0	0	7

40S ribosomal protein S14 OS=Homo sapiens GN=RPS14 PE=1 SV=3	P62263	16 kDa	0	0	4	0	0	6	0	0	6
40S ribosomal protein S15 OS=Homo sapiens GN=RPS15 PE=1 SV=2	P62841	17 kDa	0	0	2	0	0	0	0	0	2
40S ribosomal protein S15a OS=Homo sapiens GN=RPS15A PE=4 SV=1	I3L3P7 (+1)	11 kDa	0	0	4	0	0	4	0	0	8
40S ribosomal protein S16 OS=Homo sapiens GN=RPS16 PE=1 SV=2	P62249	16 kDa	0	0	3	0	0	7	0	0	11
40S ribosomal protein S17 OS=Homo sapiens GN=RPS17 PE=1 SV=2	P08708	16 kDa	0	0	4	0	0	5	0	0	8
40S ribosomal protein S18 OS=Homo sapiens GN=RPS18 PE=1 SV=3	P62269	18 kDa	0	0	7	0	0	7	0	0	10
40S ribosomal protein S19 OS=Homo sapiens GN=RPS19 PE=1 SV=2	P39019	16 kDa	0	0	4	0	0	4	0	0	8
40S ribosomal protein S2 OS=Homo sapiens GN=RPS2 PE=1 SV=2	P15880	31 kDa	0	0	6	0	0	5	0	0	11
40S ribosomal protein S20 OS=Homo sapiens GN=RPS20 PE=1 SV=1	P60866 (+1)	13 kDa	0	0	3	0	0	3	0	0	4
40S ribosomal protein S21 OS=Homo sapiens GN=RPS21 PE=2 SV=1	Q8WVC2 (+1)	9 kDa	0	0	0	0	0	2	0	0	3
40S ribosomal protein S23 OS=Homo sapiens GN=RPS23 PE=1 SV=3	P62266	16 kDa	0	0	3	0	0	3	0	0	4
40S ribosomal protein S24 OS=Homo sapiens GN=RPS24 PE=3 SV=1	E7EPK6 (+4)	32 kDa	0	0	0	0	0	0	0	0	3
40S ribosomal protein S25 OS=Homo sapiens GN=RPS25 PE=1 SV=1	P62851	14 kDa	0	0	2	0	0	2	0	0	4
40S ribosomal protein S26 OS=Homo sapiens GN=RPS26 PE=1 SV=3	P62854	13 kDa	0	0	2	0	0	2	0	0	4
40S ribosomal protein S27 OS=Homo sapiens GN=RPS27 PE=1 SV=3	P42677	9 kDa	0	0	2	0	0	2	0	0	4
40S ribosomal protein S27 OS=Homo sapiens GN=RPS27L PE=3 SV=1	H0YMV8 (+1)	11 kDa	0	0	2	0	0	2	0	0	3
Cluster of 40S ribosomal protein S3 OS=Homo sapiens GN=RPS3 PE=1 SV=2 (P23396)	P23396 [2]	27 kDa	0	0	16	0	0	16	0	0	21
40S ribosomal protein S3a (Fragment) OS=Homo sapiens GN=RPS3A PE=3 SV=1	D6RG13 (+1)	26 kDa	0	0	11	0	0	12	0	0	16
40S ribosomal protein S4, X isoform OS=Homo sapiens GN=RPS4X PE=1 SV=2	P62701	30 kDa	0	0	10	0	0	8	0	0	17
40S ribosomal protein S5 OS=Homo sapiens GN=RPS5 PE=1 SV=4	P46782	23 kDa	0	0	7	0	0	4	0	0	10
40S ribosomal protein S6 OS=Homo sapiens GN=RPS6 PE=1 SV=1	P62753	29 kDa	0	0	7	0	0	7	0	0	10
40S ribosomal protein S7 OS=Homo sapiens GN=RPS7 PE=1 SV=1	P62081	22 kDa	0	0	8	0	0	9	0	0	12

40S ribosomal protein S8 OS=Homo sapiens GN=RPS8 PE=1 SV=2	P62241 (+1)	24 kDa	0	0	7	0	0	5	0	0	10
40S ribosomal protein S9 OS=Homo sapiens GN=RPS9 PE=1 SV=3	P46781	23 kDa	0	0	5	0	0	6	0	0	12
40S ribosomal protein SA (Fragment) OS=Homo sapiens GN=RPSA PE=3 SV=1	C9J9K3 (+1)	30 kDa	0	9	0	0	10	0	0	11	0
5'-3' exoribonuclease 2 OS=Homo sapiens GN=XRN2 PE=2 SV=1	B4DZC3 (+2)	102 kDa	0	0	0	0	0	0	6	0	0
Cluster of 6-phosphofructokinase type C OS=Homo sapiens GN=PFKP PE=1 SV=2 (Q01813)	Q01813 [3]	86 kDa	15	0	0	11	0	0	16	0	0
6-phosphogluconate dehydrogenase, decarboxylating OS=Homo sapiens GN=PGD PE=2 SV=1	B4DQJ8 (+1)	52 kDa	0	18	0	0	17	0	0	16	0
6-phosphogluconolactonase OS=Homo sapiens GN=PGLS PE=1 SV=2	O95336	28 kDa	0	0	6	0	0	5	0	0	6
60 kDa heat shock protein, mitochondrial OS=Homo sapiens GN=HSPD1 PE=1 SV=2	P10809	61 kDa	0	16	0	0	10	0	0	12	0
60S acidic ribosomal protein P0 (Fragment) OS=Homo sapiens GN=RPLP0 PE=3 SV=1	F8VU65 (+1)	27 kDa	0	4	5	0	7	0	0	11	0
60S acidic ribosomal protein P2 (Fragment) OS=Homo sapiens GN=RPLP2 PE=4 SV=1	H0YDD8	9 kDa	0	0	0	0	0	0	0	0	2
60S acidic ribosomal protein P2 OS=Homo sapiens GN=RPLP2 PE=1 SV=1	P05387	12 kDa	0	0	2	0	0	2	0	0	5
60S ribosomal protein L10 OS=Homo sapiens GN=RPL10 PE=1 SV=4	P27635	25 kDa	0	0	4	0	0	5	0	0	9
60S ribosomal protein L10a OS=Homo sapiens GN=RPL10A PE=1 SV=2	P62906	25 kDa	0	0	8	0	0	7	0	0	10
60S ribosomal protein L11 OS=Homo sapiens GN=RPL11 PE=1 SV=2	P62913	20 kDa	0	0	3	0	0	2	0	0	6
60S ribosomal protein L12 OS=Homo sapiens GN=RPL12 PE=1 SV=1	P30050	18 kDa	0	0	5	0	0	5	0	0	10
60S ribosomal protein L13 OS=Homo sapiens GN=RPL13 PE=1 SV=4	P26373	24 kDa	0	0	6	0	0	6	0	0	8
60S ribosomal protein L13a OS=Homo sapiens GN=RPL13A PE=1 SV=2	P40429	24 kDa	0	0	4	0	0	4	0	0	7
60S ribosomal protein L14 OS=Homo sapiens GN=RPL14 PE=1 SV=4	P50914	23 kDa	0	0	4	0	0	5	0	0	7
60S ribosomal protein L15 OS=Homo sapiens GN=RPL15 PE=1 SV=2	P61313	24 kDa	0	0	4	0	0	2	0	0	4
60S ribosomal protein L17 OS=Homo sapiens GN=RPL17 PE=2 SV=1	B4E3C2 (+1)	17 kDa	0	0	0	0	0	0	0	0	3
60S ribosomal protein L18 OS=Homo sapiens GN=RPL18 PE=1 SV=2	Q07020	22 kDa	0	0	6	0	0	5	0	0	6
60S ribosomal protein L18a OS=Homo sapiens GN=RPL18A PE=2 SV=1	B4DM74 (+1)	18 kDa	0	0	0	0	0	0	0	0	4

60S ribosomal protein L19 OS=Homo sapiens GN=RPL19 PE=1 SV=1	P84098	23 kDa	0	0	3	0	0	0	0	0	2
60S ribosomal protein L21 OS=Homo sapiens GN=RPL21 PE=1 SV=2	P46778	19 kDa	0	0	4	0	0	3	0	0	6
60S ribosomal protein L22 OS=Homo sapiens GN=RPL22 PE=1 SV=2	P35268	15 kDa	0	0	3	0	0	3	0	0	2
60S ribosomal protein L23 OS=Homo sapiens GN=RPL23 PE=1 SV=1	P62829	15 kDa	0	0	4	0	0	6	0	0	7
60S ribosomal protein L23a OS=Homo sapiens GN=RPL23A PE=1 SV=1	P62750	18 kDa	0	0	2	0	0	3	0	0	5
60S ribosomal protein L24 OS=Homo sapiens GN=RPL24 PE=4 SV=1	C9JNW5 (+2)	18 kDa	0	0	2	0	0	2	0	0	2
60S ribosomal protein L26 OS=Homo sapiens GN=RPL26 PE=1 SV=1	P61254	17 kDa	0	0	4	0	0	5	0	0	11
60S ribosomal protein L27 OS=Homo sapiens GN=RPL27 PE=1 SV=2	P61353	16 kDa	0	0	5	0	0	5	0	0	7
60S ribosomal protein L27a OS=Homo sapiens GN=RPL27A PE=3 SV=1	E9PJD9 (+2)	10 kDa	0	0	0	0	0	0	0	0	2
60S ribosomal protein L28 OS=Homo sapiens GN=RPL28 PE=1 SV=3	P46779	16 kDa	0	0	2	0	0	2	0	0	5
60S ribosomal protein L29 OS=Homo sapiens GN=RPL29 PE=1 SV=2	P47914	18 kDa	0	0	0	0	0	0	0	0	3
60S ribosomal protein L3 OS=Homo sapiens GN=RPL3 PE=1 SV=2	P39023	46 kDa	0	9	0	0	10	0	0	15	0
60S ribosomal protein L30 (Fragment) OS=Homo sapiens GN=RPL30 PE=3 SV=1	E5RI99 (+1)	13 kDa	0	0	3	0	0	4	0	0	7
60S ribosomal protein L31 OS=Homo sapiens GN=RPL31 PE=2 SV=1	B7Z4C8 (+6)	15 kDa	0	0	3	0	0	3	0	0	5
60S ribosomal protein L32 (Fragment) OS=Homo sapiens GN=RPL32 PE=4 SV=1	D3YTB1 (+2)	16 kDa	0	0	0	0	0	2	0	0	5
60S ribosomal protein L34 OS=Homo sapiens GN=RPL34 PE=1 SV=3	P49207	13 kDa	0	0	3	0	0	2	0	0	4
60S ribosomal protein L35 OS=Homo sapiens GN=RPL35 PE=1 SV=2	P42766	15 kDa	0	0	3	0	0	2	0	0	4
60S ribosomal protein L35a OS=Homo sapiens GN=RPL35A PE=1 SV=2	P18077	13 kDa	0	0	0	0	0	0	0	0	4
60S ribosomal protein L36 OS=Homo sapiens GN=RPL36 PE=1 SV=3	Q9Y3U8	12 kDa	0	0	0	0	0	3	0	0	4
60S ribosomal protein L36a OS=Homo sapiens GN=RPL36A PE=1 SV=2	P83881	12 kDa	0	0	0	0	0	0	0	0	3
60S ribosomal protein L37a OS=Homo sapiens GN=RPL37A PE=1 SV=2	P61513	10 kDa	0	0	3	0	0	2	0	0	5
60S ribosomal protein L38 OS=Homo sapiens GN=RPL38 PE=1 SV=2	P63173	8 kDa	0	0	2	0	0	3	0	0	4

60S ribosomal protein L4 OS=Homo sapiens GN=RPL4 PE=4 SV=1	E7EWF1 (+1)	46 kDa	0	11	0	0	9	0	0	18	0
60S ribosomal protein L5 OS=Homo sapiens GN=RPL5 PE=1 SV=3	P46777	34 kDa	0	0	9	0	0	6	0	0	13
60S ribosomal protein L6 (Fragment) OS=Homo sapiens GN=RPL6 PE=3 SV=1	F8W181 (+1)	26 kDa	0	7	3	0	2	0	0	12	0
60S ribosomal protein L7 OS=Homo sapiens GN=RPL7 PE=1 SV=1	P18124	29 kDa	0	0	10	0	0	7	0	0	11
60S ribosomal protein L7a OS=Homo sapiens GN=RPL7A PE=1 SV=2	P62424	30 kDa	0	0	9	0	0	8	0	0	11
60S ribosomal protein L8 OS=Homo sapiens GN=RPL8 PE=1 SV=2	P62917	28 kDa	0	0	9	0	0	10	0	0	10
60S ribosomal protein L9 OS=Homo sapiens GN=RPL9 PE=1 SV=1	P32969	22 kDa	0	0	3	0	0	6	0	0	8
78 kDa glucose-regulated protein OS=Homo sapiens GN=HSPA5 PE=1 SV=2	P11021	72 kDa	0	6	0	0	2	0	0	11	0
A-kinase anchor protein 9 OS=Homo sapiens GN=AKAP9 PE=4 SV=1	F5H3X5 (+5)	450 kDa	0	0	0	0	0	2	0	0	2
Cluster of ADP-ribosylation factor 3 OS=Homo sapiens GN=ARF3 PE=3 SV=1 (F5H423)	F5H423 [5]	23 kDa	0	0	2	0	0	3	0	0	5
ADP-ribosylation factor 4 OS=Homo sapiens GN=ARF4 PE=1 SV=3	P18085	21 kDa	0	0	4	0	0	5	0	0	6
ADP-ribosylation factor-like protein 1 OS=Homo sapiens GN=ARL1 PE=2 SV=1	B4DWW1 (+2)	19 kDa	0	0	0	0	0	0	0	0	2
AN1-type zinc finger protein 1 OS=Homo sapiens GN=ZFAND1 PE=4 SV=1	E5RGE5 (+6)	13 kDa	0	0	2	0	0	0	0	0	0
Cluster of AP-1 complex subunit beta-1 OS=Homo sapiens GN=AP1B1 PE=4 SV=1 (F8WDL0)	F8WDL0 [6]	101 kDa	9	0	0	6	0	0	9	0	0
AP-1 complex subunit gamma-1 OS=Homo sapiens GN=AP1G1 PE=2 SV=1	B3KXW5 (+2)	94 kDa	7	0	0	7	0	0	10	0	0
AP-1 complex subunit mu-1 OS=Homo sapiens GN=AP1M1 PE=2 SV=1	B4DDG7 (+2)	40 kDa	0	2	0	0	3	0	0	5	0
AP-1 complex subunit sigma-1A (Fragment) OS=Homo sapiens GN=AP1S1 PE=4 SV=1	H7C1E4 (+1)	22 kDa	0	0	3	0	0	3	0	0	2
AP-2 complex subunit alpha-1 OS=Homo sapiens GN=AP2A1 PE=1 SV=3	O95782 (+1)	108 kDa	2	0	0	2	0	0	5	0	0
AP-2 complex subunit alpha-2 OS=Homo sapiens GN=AP2A2 PE=4 SV=2	C9J1S3 (+3)	73 kDa	2	0	0	2	0	0	3	0	0
AP-2 complex subunit mu (Fragment) OS=Homo sapiens GN=AP2M1 PE=4 SV=1	C9JGT8 (+5)	22 kDa	0	0	0	0	0	0	0	2	0
AP-3 complex subunit beta-1 OS=Homo sapiens GN=AP3B1 PE=4 SV=1	E5RJ68 (+1)	116 kDa	3	0	0	2	0	0	17	0	0
AP-3 complex subunit mu-1 OS=Homo sapiens GN=AP3M1 PE=1 SV=1	Q9Y2T2	47 kDa	0	0	0	0	0	0	0	4	0

ARD1 homolog A, N-acetyltransferase (S. cerevisiae), isoform CRA_b OS=Homo sapiens GN=NAA10 PE=4 SV=1	A6NM98 (+1)	25 kDa	0	0	6	0	0	4	0	0	3
ATP-binding cassette sub-family E member 1 OS=Homo sapiens GN=ABCE1 PE=1 SV=1	P61221	67 kDa	0	3	0	0	0	0	0	6	0
ATP-binding cassette sub-family F member 1 OS=Homo sapiens GN=ABCF1 PE=1 SV=2	Q8NE71 (+1)	96 kDa	4	0	0	0	0	0	8	0	0
ATP-citrate synthase OS=Homo sapiens GN=ACLY PE=4 SV=2	E7ENH9 (+2)	126 kDa	23	0	0	8	0	0	18	0	0
ATP-dependent DNA helicase Q1 OS=Homo sapiens GN=RECQL PE=1 SV=3	P46063	73 kDa	0	8	0	0	9	0	0	10	0
ATP-dependent RNA helicase A OS=Homo sapiens GN=DHX9 PE=1 SV=4	Q08211	141 kDa	18	0	0	14	0	0	26	0	0
ATP-dependent RNA helicase DDX1 OS=Homo sapiens GN=DDX1 PE=1 SV=2	Q92499 (+1)	82 kDa	3	0	0	4	0	0	9	0	0
ATP-dependent RNA helicase DDX19A OS=Homo sapiens GN=DDX19A PE=1 SV=1	Q9NUU7	54 kDa	0	9	0	0	6	0	0	8	0
ATP-dependent RNA helicase DDX3X OS=Homo sapiens GN=DDX3X PE=1 SV=3	O00571 (+1)	73 kDa	0	8	0	3	3	0	0	13	0
ATPase ASNA1 OS=Homo sapiens GN=ASNA1 PE=1 SV=2	O43681	39 kDa	0	3	0	0	5	0	0	4	0
Acetoacetyl-CoA synthetase OS=Homo sapiens GN=AACS PE=1 SV=1	Q86V21	75 kDa	0	0	0	0	2	0	0	0	0
Acetyl-CoA acetyltransferase, cytosolic OS=Homo sapiens GN=ACAT2 PE=1 SV=2	Q9BWD1	41 kDa	0	8	0	0	8	0	0	9	0
Acidic leucine-rich nuclear phosphoprotein 32 family member A OS=Homo sapiens GN=ANP32A PE=4 SV=2	F2Z3H3 (+2)	24 kDa	0	0	4	0	0	4	0	0	7
Acidic leucine-rich nuclear phosphoprotein 32 family member B OS=Homo sapiens GN=ANP32B PE=1 SV=1	Q92688 (+1)	29 kDa	0	0	6	0	0	4	0	0	7
Acidic leucine-rich nuclear phosphoprotein 32 family member E OS=Homo sapiens GN=ANP32E PE=1 SV=1	Q9BTT0	31 kDa	0	0	2	0	0	2	0	0	5
Cluster of Actin, cytoplasmic 2 OS=Homo sapiens GN=ACTG1 PE=1 SV=1 (P63261)	P63261 [5]	42 kDa	2	24	0	2	25	2	8	37	8
Actin-binding protein anillin OS=Homo sapiens GN=ANLN PE=1 SV=2	Q9NQW6 (+1)	124 kDa	2	0	0	0	0	0	0	0	0
Actin-related protein 2 OS=Homo sapiens GN=ACTR2 PE=1 SV=1	P61160	45 kDa	0	6	0	0	3	0	0	4	0
Actin-related protein 2/3 complex subunit 1B OS=Homo sapiens GN=ARPC1B PE=1 SV=3	O15143	41 kDa	0	5	0	0	3	0	0	5	0
Actin-related protein 2/3 complex subunit 2 OS=Homo sapiens GN=ARPC2 PE=1 SV=1	O15144	34 kDa	0	0	5	0	0	2	0	0	3

Actin-related protein 2/3 complex subunit 3 OS=Homo sapiens GN=ARPC3 PE=1 SV=3	O15145	21 kDa	0	0	6	0	0	4	0	0	7
Actin-related protein 2/3 complex subunit 4 OS=Homo sapiens GN=ARPC4 PE=4 SV=1	F8WCF6 (+1)	21 kDa	0	0	6	0	0	5	0	0	4
Actin-related protein 3 OS=Homo sapiens GN=ACTR3 PE=1 SV=3	P61158	47 kDa	0	11	0	0	11	0	0	9	0
Activator of 90 kDa heat shock protein ATPase homolog 1 OS=Homo sapiens GN=AHSA1 PE=2 SV=1	B4DUR9 (+2)	32 kDa	0	2	0	0	2	0	0	4	0
Acyl-protein thioesterase 1 (Fragment) OS=Homo sapiens GN=LYPLA1 PE=4 SV=1	E5RGR0 (+2)	21 kDa	0	0	2	0	0	2	0	0	3
Acyl-protein thioesterase 2 OS=Homo sapiens GN=LYPLA2 PE=4 SV=1	E9PH41 (+1)	23 kDa	0	0	2	0	0	0	0	0	4
Adenine phosphoribosyltransferase OS=Homo sapiens GN=APRT PE=4 SV=1	H3BQZ9 (+1)	17 kDa	0	0	3	0	0	3	0	0	5
Adenosylhomocysteinase OS=Homo sapiens GN=AHCY PE=1 SV=4	P23526	48 kDa	0	12	0	0	11	0	0	15	0
Adenylosuccinate lyase OS=Homo sapiens GN=ADSL PE=1 SV=2	P30566	55 kDa	0	5	0	0	7	0	0	4	0
Adenylyl cyclase-associated protein 1 OS=Homo sapiens GN=CAP1 PE=1 SV=5	Q01518 (+9)	52 kDa	0	2	0	0	0	0	0	0	0
Afadin OS=Homo sapiens GN=MLLT4 PE=4 SV=1	A8MQ02 (+9)	207 kDa	0	0	0	0	0	0	2	0	0
Alanine--tRNA ligase, cytoplasmic OS=Homo sapiens GN=AARS PE=1 SV=2	P49588	107 kDa	9	0	0	0	0	0	11	0	0
Alcohol dehydrogenase class-3 (Fragment) OS=Homo sapiens GN=ADH5 PE=3 SV=1	H0YAG8 (+1)	28 kDa	0	2	0	0	3	0	0	3	0
Aldose reductase OS=Homo sapiens GN=AKR1B1 PE=1 SV=3	P15121	36 kDa	0	3	0	0	0	0	0	2	0
Cluster of Alpha-actinin-4 OS=Homo sapiens GN=ACTN4 PE=1 SV=2 (O43707)	O43707 [4]	105 kDa	52	0	0	26	0	0	34	0	0
Alpha-aminoadipic semialdehyde dehydrogenase OS=Homo sapiens GN=ALDH7A1 PE=3 SV=1	E7EPT3 (+3)	54 kDa	0	2	0	0	3	0	0	0	0
Alpha-centractin OS=Homo sapiens GN=ACTR1A PE=1 SV=1	P61163	43 kDa	0	0	0	0	3	0	0	0	0
Cluster of Alpha-enolase OS=Homo sapiens GN=ENO1 PE=1 SV=2 (P06733)	P06733 [4]	47 kDa	0	23	0	0	19	0	0	20	0
Alpha-internexin OS=Homo sapiens GN=INA PE=1 SV=2	Q16352	55 kDa	0	0	0	0	2	0	0	0	0
Aminoacyl tRNA synthase complex-interacting multifunctional protein 1 OS=Homo sapiens GN=AIMP1 PE=1 SV=2	Q12904 (+1)	34 kDa	0	0	0	0	2	0	0	5	0
Aminoacyl tRNA synthase complex-interacting multifunctional protein 2 OS=Homo sapiens GN=AIMP2 PE=1 SV=2	Q13155	35 kDa	0	2	0	0	2	0	0	2	0

Ankyrin repeat domain-containing protein 32 OS=Homo sapiens GN=ANKRD32 PE=1 SV=2	Q9BQI6	121 kDa	0	0	0	0	2	0	0	0	0
Annexin A1 OS=Homo sapiens GN=ANXA1 PE=1 SV=2	P04083	39 kDa	0	9	0	0	5	0	0	3	0
Annexin A2 OS=Homo sapiens GN=ANXA2 PE=1 SV=2	P07355 (+1)	39 kDa	0	10	0	0	6	0	0	8	0
Annexin OS=Homo sapiens GN=ANXA5 PE=3 SV=1	D6RBL5 (+1)	29 kDa	0	0	5	0	0	2	0	0	2
Annexin OS=Homo sapiens GN=ANXA6 PE=3 SV=3	A6NN80 (+3)	75 kDa	0	3	0	0	0	0	0	0	0
Apoptosis inhibitor 5 OS=Homo sapiens GN=API5 PE=1 SV=3	Q9BZZ5 (+2)	59 kDa	0	15	0	0	14	0	0	13	0
Apoptotic chromatin condensation inducer in the nucleus OS=Homo sapiens GN=ACIN1 PE=4 SV=2	E7EQT4 (+1)	147 kDa	0	0	0	0	0	0	6	0	0
Archain 1, isoform CRA_a OS=Homo sapiens GN=ARCN1 PE=4 SV=1	B0YIW6 (+1)	62 kDa	0	12	0	0	9	0	0	13	0
Arginine--tRNA ligase, cytoplasmic OS=Homo sapiens GN=RARS PE=1 SV=2	P54136	75 kDa	0	17	0	0	19	0	0	23	0
Asparagine synthetase OS=Homo sapiens GN=ASNS PE=4 SV=1	E9PCI3 (+1)	62 kDa	0	13	0	0	10	0	0	12	0
Asparagine--tRNA ligase, cytoplasmic OS=Homo sapiens GN=NARS PE=1 SV=1	O43776	63 kDa	0	8	0	0	8	0	0	10	0
Aspartate--tRNA ligase, cytoplasmic OS=Homo sapiens GN=DARS PE=1 SV=2	P14868	57 kDa	0	22	0	0	16	0	0	21	0
Ataxin-10 OS=Homo sapiens GN=ATXN10 PE=4 SV=2	E7ESH8 (+2)	51 kDa	0	0	0	0	0	0	0	3	0
Ataxin-2-like protein OS=Homo sapiens GN=ATXN2L PE=2 SV=1	A8K1R6 (+8)	110 kDa	0	0	0	0	0	0	3	0	0
B-cell receptor-associated protein 31 OS=Homo sapiens GN=BCAP31 PE=1 SV=3	P51572 (+1)	28 kDa	0	0	0	0	0	0	0	0	2
BAG family molecular chaperone regulator 2 OS=Homo sapiens GN=BAG2 PE=1 SV=1	O95816	24 kDa	0	0	0	0	0	0	0	0	2
BRCA2 and CDKN1A-interacting protein OS=Homo sapiens GN=BCCIP PE=2 SV=1	B4E318 (+4)	30 kDa	0	3	0	0	3	0	0	2	0
Band 4.1-like protein 2 OS=Homo sapiens GN=EPB41L2 PE=4 SV=1	E9PHY5 (+6)	104 kDa	2	0	0	0	0	0	0	0	0
Basic leucine zipper and W2 domain-containing protein 1 OS=Homo sapiens GN=BZW1 PE=1 SV=1	Q7L1Q6 (+2)	48 kDa	0	14	0	0	11	0	0	14	0
Basic leucine zipper and W2 domain-containing protein 2 (Fragment) OS=Homo sapiens GN=BZW2 PE=4 SV=1	E7ETZ4 (+1)	47 kDa	0	9	0	0	7	0	0	11	0
Bcl-2-associated transcription factor 1 (Fragment) OS=Homo sapiens GN=BCLAF1 PE=4 SV=1	E9PK09 (+6)	83 kDa	0	0	0	0	0	0	4	0	0
Beta-catenin-like protein 1 OS=Homo sapiens GN=CTNNBL1 PE=1 SV=1	Q8WYA6	65 kDa	0	3	0	0	3	0	0	4	0

Bifunctional glutamate/proline--tRNA ligase OS=Homo sapiens GN=EPRS PE=1 SV=5	P07814	171 kDa	12	0	0	2	0	0	16	0	0
Biliverdin reductase A OS=Homo sapiens GN=BLVRA PE=1 SV=2	P53004	33 kDa	0	4	0	0	3	0	0	4	0
BolA-like protein 2 OS=Homo sapiens GN=BOLA2 PE=1 SV=1	Q9H3K6 (+1)	10 kDa	0	0	0	0	0	2	0	0	0
Bystin OS=Homo sapiens GN=BYSL PE=1 SV=3	Q13895	50 kDa	0	0	0	0	0	0	0	3	0
C-1-tetrahydrofolate synthase, cytoplasmic OS=Homo sapiens GN=MTHFD1 PE=1 SV=3	P11586	102 kDa	33	0	0	16	0	0	32	0	0
C-terminal-binding protein 2 OS=Homo sapiens GN=CTBP2 PE=1 SV=1	P56545 (+4)	49 kDa	0	0	0	0	0	0	0	3	0
C2orf4 protein OS=Homo sapiens GN=C2orf4 PE=2 SV=1	Q5R2V8 (+2)	34 kDa	0	0	0	0	0	0	0	0	3
CCR4-NOT transcription complex subunit 1 OS=Homo sapiens GN=CNOT1 PE=1 SV=2	A5YKK6	267 kDa	0	0	0	0	0	0	2	0	0
COMM domain-containing protein 3 OS=Homo sapiens GN=COMMD3 PE=1 SV=1	Q9UBI1	22 kDa	0	0	0	0	0	0	0	0	2
COP9 signalosome complex subunit 1 OS=Homo sapiens GN=GPS1 PE=1 SV=4	Q13098 (+2)	56 kDa	0	6	0	0	3	0	0	0	0
COP9 signalosome complex subunit 2 OS=Homo sapiens GN=COPS2 PE=2 SV=1	B4DIH5 (+2)	44 kDa	0	4	0	0	2	0	0	3	0
COP9 signalosome complex subunit 4 OS=Homo sapiens GN=COPS4 PE=4 SV=1	D6RAX7 (+1)	48 kDa	0	3	0	0	3	0	0	0	0
COP9 signalosome complex subunit 6 OS=Homo sapiens GN=COPS6 PE=4 SV=1	E7EM64 (+1)	36 kDa	0	3	0	0	2	0	0	4	0
Cluster of COP9 signalosome complex subunit 7a OS=Homo sapiens GN=COPS7A PE=1 SV=1 (Q9UBW8)	Q9UBW8 [2]	30 kDa	0	0	0	0	0	2	0	0	4
CTP synthase 1 OS=Homo sapiens GN=CTPS1 PE=1 SV=2	P17812	67 kDa	0	6	0	4	3	0	0	8	0
CUGBP Elav-like family member 1 OS=Homo sapiens GN=CELF1 PE=4 SV=1	F8W940 (+5)	52 kDa	0	6	0	0	4	0	0	4	0
Calcyclin-binding protein OS=Homo sapiens GN=CACYBP PE=1 SV=2	Q9HB71	26 kDa	0	0	5	0	0	2	0	0	5
Calnexin OS=Homo sapiens GN=CANX PE=2 SV=1	B4E2T8 (+1)	56 kDa	0	0	0	0	0	0	2	0	0
Calpain small subunit 1 OS=Homo sapiens GN=CAPNS1 PE=1 SV=1	P04632	28 kDa	0	0	4	0	0	3	0	0	5
Calpain-2 catalytic subunit OS=Homo sapiens GN=CAPN2 PE=4 SV=1	H0Y323 (+2)	83 kDa	0	2	0	0	0	0	0	3	0
Calpastatin OS=Homo sapiens GN=CAST PE=2 SV=1	B7Z468 (+17)	81 kDa	2	0	0	0	0	0	0	0	0
Calponin-2 (Fragment) OS=Homo sapiens GN=CNN2 PE=4 SV=1	H3BQH0	23 kDa	0	0	0	0	0	0	0	0	2

Calponin-2 OS=Homo sapiens GN=CNN2 PE=2 SV=1	B4DDF4 (+4)	33 kDa	0	0	2	0	0	2	0	0	2
Calreticulin OS=Homo sapiens GN=CALR PE=1 SV=1	P27797	48 kDa	0	2	0	0	0	0	0	0	0
Calumenin OS=Homo sapiens GN=CALU PE=1 SV=2	O43852 (+3)	37 kDa	0	2	0	0	2	0	0	4	0
Capping protein (Actin filament) muscle Z-line, beta OS=Homo sapiens GN=CAPZB PE=4 SV=1	B1AK87 (+3)	29 kDa	0	0	4	0	0	4	0	0	5
Caprin-1 OS=Homo sapiens GN=CAPRIN1 PE=1 SV=2	Q14444 (+1)	78 kDa	5	0	0	3	0	0	13	0	0
Carbonyl reductase [NADPH] 1 OS=Homo sapiens GN=CBR1 PE=1 SV=3	P16152	30 kDa	0	0	5	0	0	4	0	0	4
Carbonyl reductase [NADPH] 3 OS=Homo sapiens GN=CBR3 PE=1 SV=3	O75828	31 kDa	0	0	3	0	0	0	0	0	0
Casein kinase II subunit alpha OS=Homo sapiens GN=CSNK2A1 PE=4 SV=1	E7EU96 (+2)	45 kDa	0	2	0	0	0	0	0	5	0
Casein kinase II subunit beta OS=Homo sapiens GN=CSNK2B PE=1 SV=1	P67870 (+1)	25 kDa	0	0	0	0	0	0	0	0	2
Catenin alpha-1 OS=Homo sapiens GN=CTNNA1 PE=2 SV=1	B4E2G8 (+4)	98 kDa	2	0	0	0	0	0	2	0	0
Catenin alpha-2 OS=Homo sapiens GN=CTNNA2 PE=1 SV=5	P26232 (+3)	105 kDa	2	0	0	0	0	0	2	0	0
Cell differentiation protein RCD1 homolog OS=Homo sapiens GN=RQCD1 PE=4 SV=2	B5MDQ4 (+2)	29 kDa	0	0	0	0	0	0	0	0	2
Cell division control protein 42 homolog OS=Homo sapiens GN=CDC42 PE=1 SV=2	P60953 (+1)	21 kDa	0	0	0	0	0	0	0	0	2
Cell division cycle and apoptosis regulator protein 1 OS=Homo sapiens GN=CCAR1 PE=1 SV=2	Q8IX12 (+1)	133 kDa	0	0	0	0	0	0	2	0	0
Cell growth-regulating nucleolar protein OS=Homo sapiens GN=LYAR PE=1 SV=2	Q9NX58	44 kDa	0	0	0	0	0	0	0	4	0
Cellular nucleic acid-binding protein OS=Homo sapiens GN=CNBP PE=4 SV=1	E9PDR7 (+4)	20 kDa	0	0	2	0	0	3	0	0	3
Cluster of Cellular tumor antigen p53 OS=Homo sapiens GN=TP53 PE=1 SV=4 (P04637)	P04637 [3]	44 kDa	54	42	27	33	43	21	48	37	24
Chaperonin containing TCP1, subunit 8 (Theta), isoform CRA_a OS=Homo sapiens GN=CCT8 PE=3 SV=1	G5E9B2 (+1)	59 kDa	0	29	0	0	28	0	0	22	0
Chloride intracellular channel protein 1 OS=Homo sapiens GN=CLIC1 PE=1 SV=4	O00299	27 kDa	0	0	14	0	0	11	0	0	12
Chloride intracellular channel protein 4 OS=Homo sapiens GN=CLIC4 PE=4 SV=1	F5H1F8 (+1)	23 kDa	0	0	2	0	0	3	0	0	5
Chromatin target of PRMT1 protein OS=Homo sapiens GN=CHTOP PE=1 SV=2	Q9Y3Y2 (+2)	26 kDa	0	0	2	0	0	0	0	0	0
Chromodomain-helicase-DNA-binding protein 1 OS=Homo sapiens GN=CHD1 PE=1 SV=2	O14646 (+1)	197 kDa	0	0	0	0	0	0	2	0	0

Chromosome 20 open reading frame 43 (Fragment) OS=Homo sapiens GN=C20orf43 PE=4 SV=1	A2A2L5 (+3)	31 kDa	0	0	0	0	0	0	0	2	0
Chromosome-associated kinesin KIF4A OS=Homo sapiens GN=KIF4A PE=1 SV=3	O95239 (+1)	140 kDa	2	0	0	0	0	0	7	0	0
Clathrin heavy chain 1 OS=Homo sapiens GN=CLTC PE=1 SV=5	Q00610 (+1)	192 kDa	43	0	0	41	0	0	44	0	0
Clathrin light chain A OS=Homo sapiens GN=CLTA PE=1 SV=1	P09496 (+3)	27 kDa	0	0	3	0	0	4	0	0	3
Cleavage and polyadenylation specificity factor subunit 1 OS=Homo sapiens GN=CPSF1 PE=1 SV=2	Q10570	161 kDa	4	0	0	0	0	0	0	0	0
Cleavage and polyadenylation specificity factor subunit 5 OS=Homo sapiens GN=NUDT21 PE=1 SV=1	O43809	26 kDa	0	0	5	0	0	3	0	0	7
Cleavage and polyadenylation-specificity factor subunit 3 OS=Homo sapiens GN=CPSF3 PE=4 SV=2	E7ER23 (+2)	62 kDa	2	0	0	0	0	0	0	0	0
Cleavage and polyadenylation-specificity factor subunit 6 OS=Homo sapiens GN=CPSF6 PE=4 SV=1	F8WJN3 (+3)	52 kDa	0	0	0	0	2	0	0	0	0
Cleavage and polyadenylation-specificity factor subunit 7 (Fragment) OS=Homo sapiens GN=CPSF7 PE=4 SV=1	F5H669 (+3)	41 kDa	0	0	0	0	0	0	0	2	0
Cleavage stimulation factor subunit 1 OS=Homo sapiens GN=CSTF1 PE=1 SV=1	Q05048	48 kDa	0	0	0	0	0	0	0	3	0
Cleavage stimulation factor subunit 2 OS=Homo sapiens GN=CSTF2 PE=2 SV=1	B4DUD5 (+3)	59 kDa	0	2	0	0	2	0	0	0	0
Cleavage stimulation factor subunit 3 OS=Homo sapiens GN=CSTF3 PE=1 SV=1	Q12996	83 kDa	3	0	0	0	0	0	0	4	0
Coactosin-like protein OS=Homo sapiens GN=COTL1 PE=1 SV=3	Q14019	16 kDa	0	0	8	0	0	7	0	0	9
Coatomer protein complex, subunit beta 2 (Beta prime), isoform CRA_b OS=Homo sapiens GN=COPB2 PE=2 SV=1	B4DZI8 (+1)	99 kDa	5	0	0	2	0	0	3	0	0
Coatomer protein complex, subunit epsilon, isoform CRA_e OS=Homo sapiens GN=COPE PE=4 SV=1	A6NE29 (+2)	29 kDa	0	0	6	0	0	4	0	0	5
Coatomer subunit alpha OS=Homo sapiens GN=COPA PE=1 SV=2	P53621 (+1)	138 kDa	3	0	0	4	0	0	10	0	0
Coatomer subunit beta OS=Homo sapiens GN=COPB1 PE=1 SV=3	P53618	107 kDa	7	0	0	8	0	0	5	0	0
Coatomer subunit gamma-1 OS=Homo sapiens GN=COPG1 PE=1 SV=1	Q9Y678	98 kDa	6	0	0	3	0	0	8	0	0
Coatomer subunit gamma-2 OS=Homo sapiens GN=COPG2 PE=1 SV=1	Q9UBF2	98 kDa	3	0	0	0	0	0	3	0	0
Coatomer subunit zeta-1 OS=Homo sapiens GN=COPZ1 PE=4 SV=1	F8VVA7 (+3)	22 kDa	0	0	0	0	0	0	0	0	2
Cofilin-1 OS=Homo sapiens GN=CFL1 PE=1 SV=3	P23528	19 kDa	0	0	7	0	0	7	0	0	8

Cold shock domain-containing protein E1 OS=Homo sapiens GN=CSDE1 PE=4 SV=1	E9PGZ0 (+3)	91 kDa	6	0	0	2	0	0	7	0	0
Condensin complex subunit 1 OS=Homo sapiens GN=NCAPD2 PE=3 SV=1	F5GZJ1 (+1)	152 kDa	0	0	0	5	0	0	6	0	0
Condensin complex subunit 3 OS=Homo sapiens GN=NCAPG PE=1 SV=1	Q9BPX3	114 kDa	2	0	0	0	0	0	2	0	0
Copine I OS=Homo sapiens GN=CPNE1 PE=4 SV=1	A6PVH9 (+3)	53 kDa	0	2	0	0	2	0	0	4	0
Copine-3 OS=Homo sapiens GN=CPNE3 PE=1 SV=1	O75131	60 kDa	0	7	0	0	4	0	0	9	0
Copine-6 OS=Homo sapiens GN=CPNE6 PE=4 SV=1	F5GXN1 (+1)	68 kDa	0	2	0	0	2	0	0	0	0
Coronin-1B OS=Homo sapiens GN=CORO1B PE=1 SV=1	Q9BR76	54 kDa	0	7	0	0	7	0	0	4	0
Coronin-1C OS=Homo sapiens GN=CORO1C PE=2 SV=1	A7MAP0 (+1)	54 kDa	0	12	0	0	10	0	0	15	0
Cullin-1 OS=Homo sapiens GN=CUL1 PE=3 SV=1	E7EWR0 (+1)	81 kDa	5	0	0	3	0	0	6	0	0
Cullin-3 OS=Homo sapiens GN=CUL3 PE=1 SV=2	Q13618 (+1)	89 kDa	2	0	0	0	0	0	3	0	0
Cluster of Cullin-4B OS=Homo sapiens GN=CUL4B PE=1 SV=4 (Q13620)	Q13620 [4]	104 kDa	3	0	0	3	0	0	3	0	0
Cullin-associated NEDD8-dissociated protein 1 OS=Homo sapiens GN=CAND1 PE=1 SV=2	Q86VP6	136 kDa	30	0	0	26	0	0	29	0	0
Cluster of Cyclin-dependent kinase 1 OS=Homo sapiens GN=CDK1 PE=1 SV=3 (P06493)	P06493 [17]	34 kDa	0	0	10	0	0	13	0	0	13
Cyclin-dependent kinase 11B OS=Homo sapiens GN=CDK11B PE=1 SV=3	P21127 (+3)	93 kDa	0	0	0	0	0	0	9	0	0
Cystatin-B OS=Homo sapiens GN=CSTB PE=1 SV=2	P04080	11 kDa	0	0	3	0	0	0	0	0	3
Cysteine-rich protein 2 OS=Homo sapiens GN=CRIP2 PE=1 SV=1	P52943	22 kDa	0	0	5	0	0	4	0	0	5
Cytoplasmic FMR1-interacting protein 1 OS=Homo sapiens GN=CYFIP1 PE=4 SV=1	E7EQ04 (+1)	145 kDa	3	0	0	2	0	0	2	0	0
Cytoplasmic dynein 1 heavy chain 1 OS=Homo sapiens GN=DYNC1H1 PE=1 SV=5	Q14204	532 kDa	21	0	0	12	0	0	23	0	0
Cytosine-specific methyltransferase OS=Homo sapiens GN=DNMT1 PE=3 SV=1	F5GX68 (+2)	183 kDa	5	0	0	3	0	0	7	0	0
Cytoskeleton-associated protein 5 OS=Homo sapiens GN=CKAP5 PE=1 SV=3	Q14008 (+2)	226 kDa	0	0	0	0	0	0	8	0	0
Cytosol aminopeptidase OS=Homo sapiens GN=LAP3 PE=1 SV=3	P28838 (+1)	56 kDa	0	3	0	0	2	0	0	3	0
Cytosolic acyl coenzyme A thioester hydrolase OS=Homo sapiens GN=ACOT7 PE=1 SV=3	O00154 (+2)	42 kDa	0	8	0	0	9	0	0	10	0

D-3-phosphoglycerate dehydrogenase OS=Homo sapiens GN=PHGDH PE=1 SV=4	O43175	57 kDa	0	5	0	0	5	0	0	4	0
DAZ-associated protein 1 OS=Homo sapiens GN=DAZAP1 PE=1 SV=1	Q96EP5 (+1)	43 kDa	0	3	0	0	0	0	0	3	0
DBIRD complex subunit KIAA1967 OS=Homo sapiens GN=KIAA1967 PE=1 SV=2	Q8N163 (+1)	103 kDa	3	0	0	2	0	0	6	0	0
DCN1-like protein 5 OS=Homo sapiens GN=DCUN1D5 PE=4 SV=1	E9PM04 (+2)	18 kDa	0	0	2	0	0	0	0	0	0
DEAD (Asp-Glu-Ala-Asp) box polypeptide 46, isoform CRA_b OS=Homo sapiens GN=DDX46 PE=4 SV=1	D6RJA6 (+1)	54 kDa	0	0	0	0	0	0	2	0	0
DNA damage-binding protein 1 OS=Homo sapiens GN=DDB1 PE=1 SV=1	Q16531	127 kDa	8	0	0	2	0	0	4	0	0
DNA mismatch repair protein Msh2 OS=Homo sapiens GN=MSH2 PE=1 SV=1	P43246	105 kDa	5	0	0	5	0	0	9	0	0
DNA mismatch repair protein Msh6 OS=Homo sapiens GN=MSH6 PE=2 SV=1	B4DF41 (+2)	138 kDa	3	0	0	0	0	0	0	0	0
DNA primase large subunit OS=Homo sapiens GN=PRIM2 PE=1 SV=2	P49643	59 kDa	0	0	0	0	2	0	0	0	0
DNA replication licensing factor MCM2 OS=Homo sapiens GN=MCM2 PE=3 SV=1	F5H1E9 (+3)	107 kDa	9	0	0	4	0	0	7	0	0
DNA replication licensing factor MCM3 OS=Homo sapiens GN=MCM3 PE=1 SV=3	P25205	91 kDa	21	0	0	13	0	0	21	0	0
Cluster of DNA replication licensing factor MCM4 OS=Homo sapiens GN=MCM4 PE=3 SV=1 (E7EM48)	E7EM48 [3]	93 kDa	12	0	0	6	0	0	17	0	0
DNA replication licensing factor MCM5 OS=Homo sapiens GN=MCM5 PE=1 SV=5	P33992	82 kDa	16	0	0	14	0	0	21	0	0
DNA replication licensing factor MCM6 OS=Homo sapiens GN=MCM6 PE=1 SV=1	Q14566	93 kDa	17	0	0	9	0	0	16	0	0
DNA replication licensing factor MCM7 OS=Homo sapiens GN=MCM7 PE=1 SV=4	P33993	81 kDa	27	0	0	19	0	0	20	0	0
DNA topoisomerase 1 OS=Homo sapiens GN=TOP1 PE=1 SV=2	P11387	91 kDa	4	0	0	4	0	0	8	0	0
DNA-binding protein A OS=Homo sapiens GN=CSDA PE=1 SV=4	P16989 (+1)	40 kDa	0	5	0	0	2	0	0	2	0
DNA-dependent protein kinase catalytic subunit OS=Homo sapiens GN=PRKDC PE=1 SV=3	P78527	469 kDa	30	0	0	44	0	0	87	0	0
DNA-directed RNA polymerase I subunit RPA49 OS=Homo sapiens GN=POLR1E PE=1 SV=2	Q9GZS1 (+1)	54 kDa	0	0	0	0	0	0	0	2	0
DNA-directed RNA polymerases I, II, and III subunit RPABC1 OS=Homo sapiens GN=POLR2E PE=1 SV=4	P19388	25 kDa	0	0	0	0	0	0	0	0	2
DNAJC7 protein OS=Homo sapiens GN=DNAJC7 PE=2 SV=1	Q7Z784 (+1)	50 kDa	0	3	0	0	0	0	0	3	0
Deoxyuridine 5'-triphosphate nucleotidohydrolase, mitochondrial (Fragment) OS=Homo sapiens GN=DUT PE=4 SV=1	H0YKC5 (+3)	24 kDa	0	0	0	0	0	0	0	0	2

Dermcidin OS=Homo sapiens GN=DCD PE=1 SV=2	P81605 (+1)	11 kDa	0	0	0	0	2	2	0	0	0
Destrin OS=Homo sapiens GN=DSTN PE=4 SV=1	F6RFD5 (+1)	15 kDa	0	0	4	0	0	3	0	0	2
Deubiquitinating protein VCIP135 OS=Homo sapiens GN=VCPIP1 PE=1 SV=2	Q96JH7	134 kDa	0	0	0	2	0	0	0	0	0
Developmentally-regulated GTP-binding protein 1 OS=Homo sapiens GN=DRG1 PE=1 SV=1	Q9Y295	41 kDa	0	0	0	0	2	0	0	3	0
Dihydrofolate reductase OS=Homo sapiens GN=DHFR PE=2 SV=1	B4DDD2 (+4)	16 kDa	0	0	0	0	0	2	0	0	0
Dihydroorotase OS=Homo sapiens GN=CAD PE=3 SV=1	F8VPD4 (+1)	236 kDa	11	0	0	7	0	0	11	0	0
Cluster of Dihydropyrimidinase-related protein 2 OS=Homo sapiens GN=DPYSL2 PE=2 SV=1 (B4DR31)	B4DR31 [3]	58 kDa	0	11	0	0	3	0	0	10	0
Dipeptidyl peptidase 9 OS=Homo sapiens GN=DPP9 PE=4 SV=1	H7BYF3	95 kDa	2	0	0	0	0	0	0	0	0
DnaJ homolog subfamily A member 1 OS=Homo sapiens GN=DNAJA1 PE=1 SV=2	P31689	45 kDa	0	4	0	0	0	0	0	3	0
DnaJ homolog subfamily A member 2 OS=Homo sapiens GN=DNAJA2 PE=1 SV=1	O60884	46 kDa	0	2	0	0	0	0	0	2	0
DnaJ homolog subfamily B member 1 OS=Homo sapiens GN=DNAJB1 PE=2 SV=1	B4DX52 (+1)	27 kDa	0	2	0	0	2	0	0	2	0
Dolichyl-diphosphooligosaccharide--protein glycosyltransferase subunit 1 OS=Homo sapiens GN=RPN1 PE=1 SV=1	P04843	69 kDa	0	0	0	0	0	0	0	3	0
Double-strand break repair protein MRE11A OS=Homo sapiens GN=MRE11A PE=2 SV=1	B3KTC7 (+2)	81 kDa	0	0	0	0	0	0	2	0	0
Double-stranded RNA-specific adenosine deaminase OS=Homo sapiens GN=ADAR PE=4 SV=1	E7ENU4 (+6)	141 kDa	0	0	0	0	0	0	2	0	0
Dual-specificity mitogen-activated protein kinase kinase 3 (Fragment) OS=Homo sapiens GN=MAP2K3 PE=4 SV=1	E9PRZ0 (+4)	13 kDa	0	0	0	0	2	0	0	0	0
Dynamin-1-like protein OS=Homo sapiens GN=DNM1L PE=3 SV=1	F8W8D1 (+7)	88 kDa	4	0	0	3	0	0	0	5	0
Dynamin-2 OS=Homo sapiens GN=DNM2 PE=2 SV=1	A8K1B6 (+1)	98 kDa	6	0	0	0	0	0	4	0	0
Dynein heavy chain 9, axonemal OS=Homo sapiens GN=DNAH9 PE=1 SV=3	Q9NYC9	512 kDa	0	0	0	0	0	0	0	0	2
E3 ubiquitin-protein ligase LRSAM1 OS=Homo sapiens GN=LRSAM1 PE=1 SV=1	Q6UWE0 (+1)	84 kDa	2	0	0	0	0	0	0	0	0
E3 ubiquitin-protein ligase UHRF1 OS=Homo sapiens GN=UHRF1 PE=4 SV=1	F5GXG0 (+1)	90 kDa	0	0	0	2	0	0	2	0	0
E3 ubiquitin/ISG15 ligase TRIM25 OS=Homo sapiens GN=TRIM25 PE=1 SV=2	Q14258	71 kDa	0	3	0	0	2	0	0	7	0

EH domain-containing protein 1 (Fragment) OS=Homo sapiens GN=EHD1 PE=4 SV=1	C9J2Z4 (+2)	35 kDa	0	2	0	0	0	0	0	3	0
EH domain-containing protein 4 OS=Homo sapiens GN=EHD4 PE=1 SV=1	Q9H223	61 kDa	0	2	0	0	0	0	0	5	0
ELAV-like protein 1 OS=Homo sapiens GN=ELAVL1 PE=1 SV=2	Q15717	36 kDa	0	0	6	0	0	7	0	0	10
ElaC homolog 2 (E. coli), isoform CRA_a OS=Homo sapiens GN=ELAC2 PE=4 SV=1	G5E9D5 (+2)	90 kDa	2	0	0	2	0	0	0	0	0
Cluster of Elongation factor 1-alpha 1 OS=Homo sapiens GN=EEF1A1 PE=1 SV=1 (P68104)	P68104 [2]	50 kDa	11	24	8	8	26	5	9	28	8
Elongation factor 1-beta OS=Homo sapiens GN=EEF1B2 PE=1 SV=3	P24534	25 kDa	0	0	4	0	0	4	0	0	5
Elongation factor 1-delta (Fragment) OS=Homo sapiens GN=EEF1D PE=3 SV=1	E9PK01 (+1)	29 kDa	0	3	8	0	2	7	0	4	2
Elongation factor 1-gamma OS=Homo sapiens GN=EEF1G PE=1 SV=3	P26641	50 kDa	0	17	0	0	16	0	0	17	0
Elongation factor 2 OS=Homo sapiens GN=EEF2 PE=1 SV=4	P13639	95 kDa	43	0	0	33	0	0	37	2	0
Elongation factor Ts, mitochondrial OS=Homo sapiens GN=TSFM PE=3 SV=1	F8W6R3 (+1)	31 kDa	0	0	0	0	0	0	0	0	3
Elongation factor Tu, mitochondrial OS=Homo sapiens GN=TUFM PE=1 SV=2	P49411	50 kDa	0	4	0	0	6	0	0	5	0
Endophilin-A2 OS=Homo sapiens GN=SH3GL1 PE=1 SV=1	Q99961	41 kDa	0	0	0	0	0	0	0	2	0
Endophilin-B1 OS=Homo sapiens GN=SH3GLB1 PE=1 SV=1	Q9Y371 (+1)	41 kDa	0	2	0	0	2	0	0	0	0
Endoplasmic reticulum resident protein 44 OS=Homo sapiens GN=ERP44 PE=1 SV=1	Q9BS26	47 kDa	0	0	0	0	2	0	0	0	0
Endoplasmin OS=Homo sapiens GN=HSP90B1 PE=1 SV=1	P14625	92 kDa	11	0	0	5	0	0	9	0	0
Endothelial differentiation-related factor 1 OS=Homo sapiens GN=EDF1 PE=1 SV=1	O60869 (+1)	16 kDa	0	0	2	0	0	0	0	0	0
Cluster of Eukaryotic initiation factor 4A-I OS=Homo sapiens GN=EIF4A1 PE=1 SV=1 (P60842)	P60842 [3]	46 kDa	0	27	0	0	26	0	0	28	0
Eukaryotic initiation factor 4A-III OS=Homo sapiens GN=EIF4A3 PE=1 SV=4	P38919	47 kDa	0	4	0	0	2	0	0	14	0
Eukaryotic peptide chain release factor subunit 1 OS=Homo sapiens GN=ETF1 PE=2 SV=1	B7Z7P8 (+2)	47 kDa	0	0	0	0	0	0	0	2	0
Eukaryotic translation elongation factor 1 epsilon-1 OS=Homo sapiens GN=EEF1E1 PE=4 SV=2	C9J1V9 (+3)	17 kDa	0	0	0	0	0	0	0	0	3
Eukaryotic translation initiation factor 1A, X-chromosomal OS=Homo sapiens GN=EIF1AX PE=1 SV=2	P47813	16 kDa	0	0	2	0	0	0	0	0	0
Eukaryotic translation initiation factor 2 subunit 1 OS=Homo sapiens GN=EIF2S1 PE=1 SV=3	P05198	36 kDa	0	13	0	0	12	0	0	15	0

Eukaryotic translation initiation factor 2 subunit 2 OS=Homo sapiens GN=EIF2S2 PE=1 SV=2	P20042	38 kDa	0	4	0	0	0	0	0	8	0
Eukaryotic translation initiation factor 2 subunit 3 OS=Homo sapiens GN=EIF2S3 PE=1 SV=3	P41091	51 kDa	0	11	0	0	14	0	0	14	0
Eukaryotic translation initiation factor 2A OS=Homo sapiens GN=EIF2A PE=1 SV=3	Q9BY44 (+1)	65 kDa	0	0	0	0	2	0	0	5	0
Eukaryotic translation initiation factor 3 subunit A OS=Homo sapiens GN=EIF3A PE=1 SV=1	Q14152	167 kDa	16	0	0	8	0	0	34	0	0
Eukaryotic translation initiation factor 3 subunit B OS=Homo sapiens GN=EIF3B PE=2 SV=1	B4DV79 (+3)	85 kDa	9	0	0	6	0	0	14	0	0
Eukaryotic translation initiation factor 3 subunit D OS=Homo sapiens GN=EIF3D PE=2 SV=2	A8MWD3 (+2)	62 kDa	0	0	0	0	0	0	0	2	0
Eukaryotic translation initiation factor 3 subunit E OS=Homo sapiens GN=EIF3E PE=1 SV=1	P60228	52 kDa	0	8	0	0	9	0	0	11	0
Eukaryotic translation initiation factor 3 subunit F OS=Homo sapiens GN=EIF3F PE=2 SV=1	B3KSH1 (+2)	39 kDa	0	4	0	0	3	0	0	9	0
Eukaryotic translation initiation factor 3 subunit G OS=Homo sapiens GN=EIF3G PE=1 SV=2	O75821	36 kDa	0	2	0	0	4	0	0	6	0
Eukaryotic translation initiation factor 3 subunit H OS=Homo sapiens GN=EIF3H PE=1 SV=1	O15372	40 kDa	0	6	0	0	3	0	0	6	0
Eukaryotic translation initiation factor 3 subunit I OS=Homo sapiens GN=EIF3I PE=1 SV=1	Q13347	37 kDa	0	4	0	0	5	0	0	4	0
Eukaryotic translation initiation factor 3 subunit J OS=Homo sapiens GN=EIF3J PE=2 SV=1	B4DUI3 (+1)	23 kDa	0	0	0	0	0	0	0	4	0
Eukaryotic translation initiation factor 3 subunit K OS=Homo sapiens GN=EIF3K PE=2 SV=1	B7ZAM9 (+1)	24 kDa	0	0	4	0	0	4	0	0	4
Eukaryotic translation initiation factor 3 subunit L OS=Homo sapiens GN=EIF3EIP PE=4 SV=1	B0QY89 (+2)	71 kDa	0	3	0	0	4	0	0	8	0
Eukaryotic translation initiation factor 3 subunit M OS=Homo sapiens GN=EIF3M PE=1 SV=1	Q7L2H7	43 kDa	0	4	0	0	3	0	0	4	0
Cluster of Eukaryotic translation initiation factor 4 gamma 1 OS=Homo sapiens GN=EIF4G1 PE=4 SV=1 (E7EUU4)	E7EUU4 [10]	172 kDa	8	0	0	6	0	0	19	0	0
Eukaryotic translation initiation factor 4 gamma 2 OS=Homo sapiens GN=EIF4G2 PE=1 SV=1	P78344 (+1)	102 kDa	7	0	0	5	0	0	8	0	0
Eukaryotic translation initiation factor 4B OS=Homo sapiens GN=EIF4B PE=2 SV=1	B4DS13 (+3)	65 kDa	3	0	0	0	0	0	0	2	0
Eukaryotic translation initiation factor 4E OS=Homo sapiens GN=EIF4E PE=3 SV=1	D6RBW1 (+3)	29 kDa	0	0	2	0	0	2	0	0	2
Eukaryotic translation initiation factor 5 OS=Homo sapiens GN=EIF5 PE=1 SV=2	P55010	49 kDa	0	9	0	0	7	0	0	8	0
Eukaryotic translation initiation factor 5A-1 (Fragment) OS=Homo sapiens GN=EIF5A PE=4 SV=1	I3L397 (+3)	16 kDa	0	0	6	0	0	2	0	0	5
Eukaryotic translation initiation factor 5B OS=Homo sapiens GN=EIF5B PE=1 SV=4	O60841	139 kDa	2	0	0	0	0	0	5	0	0

Eukaryotic translation initiation factor 6 OS=Homo sapiens GN=EIF6 PE=1 SV=1	P56537	27 kDa	0	0	4	0	0	4	0	0	3
Exosomal core protein CSL4 OS=Homo sapiens GN=RP11-452K12.9 PE=4 SV=1	B1AMU3 (+1)	19 kDa	0	0	0	0	0	0	0	0	2
Exosome complex component MTR3 OS=Homo sapiens GN=EXOSC6 PE=1 SV=1	Q5RKV6	28 kDa	0	0	0	0	0	0	0	0	2
Exosome complex component RRP40 OS=Homo sapiens GN=EXOSC3 PE=1 SV=3	Q9NQT5	30 kDa	0	0	0	0	0	2	0	0	3
Exosome complex component RRP45 OS=Homo sapiens GN=EXOSC9 PE=4 SV=1	D6RIY6 (+2)	47 kDa	0	3	0	0	2	0	0	0	0
Exosome complex component RRP46 OS=Homo sapiens GN=EXOSC5 PE=1 SV=1	Q9NQT4	25 kDa	0	0	3	0	0	0	0	0	2
Exosome complex exonuclease RRP44 OS=Homo sapiens GN=DIS3 PE=1 SV=2	Q9Y2L1	109 kDa	3	0	0	3	0	0	0	0	0
Exosome component 10 OS=Homo sapiens GN=EXOSC10 PE=1 SV=2	Q01780	101 kDa	2	0	0	0	0	0	5	0	0
Exportin-1 OS=Homo sapiens GN=XPO1 PE=1 SV=1	O14980	123 kDa	15	0	0	13	0	0	15	0	0
Exportin-2 OS=Homo sapiens GN=CSE1L PE=1 SV=3	P55060 (+1)	110 kDa	27	0	0	29	0	0	30	0	0
Exportin-5 OS=Homo sapiens GN=XPO5 PE=1 SV=1	Q9HAV4	136 kDa	13	0	0	3	0	0	14	0	0
Exportin-7 OS=Homo sapiens GN=XPO7 PE=4 SV=1	E7ESC6 (+2)	124 kDa	2	0	0	0	0	0	0	0	0
Exportin-T OS=Homo sapiens GN=XPOT PE=1 SV=2	O43592	110 kDa	5	0	0	4	0	0	6	0	0
Extended synaptotagmin-1 OS=Homo sapiens GN=ESYT1 PE=2 SV=1	B3KY56 (+2)	117 kDa	0	0	0	2	0	0	5	0	0
Cluster of Ezrin OS=Homo sapiens GN=EZR PE=1 SV=4 (P15311)	P15311 [3]	69 kDa	18	19	0	4	2	0	0	13	0
F-actin-capping protein subunit alpha-1 OS=Homo sapiens GN=CAPZA1 PE=1 SV=3	P52907	33 kDa	0	0	0	0	2	0	0	0	0
F-box only protein 22 OS=Homo sapiens GN=FBXO22 PE=1 SV=1	Q8NEZ5	45 kDa	0	0	0	0	0	0	0	2	0
FACT complex subunit SPT16 OS=Homo sapiens GN=SUPT16H PE=1 SV=1	Q9Y5B9	120 kDa	11	0	0	5	0	0	25	0	0
FACT complex subunit SSRP1 OS=Homo sapiens GN=SSRP1 PE=1 SV=1	Q08945	81 kDa	6	0	0	3	0	0	12	0	0
Far upstream element-binding protein 1 OS=Homo sapiens GN=FUBP1 PE=2 SV=1	B4E0X8 (+4)	66 kDa	2	20	0	0	16	0	0	17	0
Far upstream element-binding protein 2 OS=Homo sapiens GN=KHSRP PE=1 SV=4	Q92945	73 kDa	31	2	0	17	0	0	23	5	0
Far upstream element-binding protein 3 OS=Homo sapiens GN=FUBP3 PE=1 SV=2	Q96I24	62 kDa	0	9	0	0	9	0	0	13	0

Farnesyl pyrophosphate synthase OS=Homo sapiens GN=FDPS PE=3 SV=1	E9PCI9 (+1)	41 kDa	0	4	0	0	5	0	0	6	0
Fascin OS=Homo sapiens GN=FSCN1 PE=1 SV=3	Q16658	55 kDa	0	17	0	0	14	0	0	12	0
Fatty acid synthase OS=Homo sapiens GN=FASN PE=1 SV=3	P49327	273 kDa	63	0	0	59	0	0	64	0	0
Fatty acid-binding protein, epidermal OS=Homo sapiens GN=FABP5 PE=1 SV=3	Q01469	15 kDa	0	0	7	0	0	5	0	0	8
Cluster of Filamin-C OS=Homo sapiens GN=FLNC PE=1 SV=3 (Q14315)	Q14315 [14]	291 kDa	24	0	0	9	0	0	30	0	0
Flap endonuclease 1 OS=Homo sapiens GN=FEN1 PE=1 SV=1	P39748	43 kDa	0	6	0	0	5	0	0	5	0
Flavin reductase (NADPH) OS=Homo sapiens GN=BLVRB PE=1 SV=3	P30043	22 kDa	0	0	2	0	0	0	0	0	0
Four and a half LIM domains protein 1 OS=Homo sapiens GN=FHL1 PE=2 SV=1	B7Z5V0 (+5)	31 kDa	0	0	2	0	0	0	0	0	0
Fragile X mental retardation syndrome-related protein 1 OS=Homo sapiens GN=FXR1 PE=2 SV=1	B4DXZ6 (+5)	68 kDa	0	0	0	0	0	0	2	4	0
Fragile X mental retardation syndrome-related protein 2 OS=Homo sapiens GN=FXR2 PE=1 SV=2	P51116	74 kDa	2	0	0	0	0	0	2	2	0
Fructose-bisphosphate aldolase A OS=Homo sapiens GN=ALDOA PE=1 SV=2	P04075	39 kDa	0	23	0	0	17	0	0	12	0
Fructose-bisphosphate aldolase OS=Homo sapiens GN=ALDOC PE=2 SV=1	B7Z1N6 (+1)	35 kDa	0	2	0	0	2	0	0	2	0
GMP synthase [glutamine-hydrolyzing] OS=Homo sapiens GN=GMPS PE=2 SV=1	B4DUT7 (+2)	71 kDa	0	12	0	0	12	0	0	10	0
GTP-binding nuclear protein Ran OS=Homo sapiens GN=RAN PE=4 SV=1	B5MDF5 (+1)	26 kDa	0	0	8	0	0	7	0	0	4
GTP-binding protein SAR1a OS=Homo sapiens GN=SAR1A PE=1 SV=1	Q9NR31	22 kDa	0	0	3	0	0	2	0	0	3
Galectin-1 OS=Homo sapiens GN=LGALS1 PE=1 SV=2	P09382	15 kDa	0	0	8	0	0	6	0	0	6
Gem-associated protein 5 OS=Homo sapiens GN=GEMIN5 PE=1 SV=3	Q8TEQ6	169 kDa	0	0	0	2	0	0	2	0	0
General transcription factor II-I OS=Homo sapiens GN=GTF2I PE=2 SV=1	B4DH52 (+4)	112 kDa	20	0	0	12	0	0	8	0	0
General vesicular transport factor p115 OS=Homo sapiens GN=USO1 PE=1 SV=2	O60763 (+1)	108 kDa	6	0	0	4	0	0	5	0	0
Glomulin OS=Homo sapiens GN=GLMN PE=1 SV=2	Q92990	68 kDa	0	0	0	0	4	0	0	4	0
Glucosamine--fructose-6-phosphate aminotransferase [isomerizing] 1 OS=Homo sapiens GN=GFPT1 PE=1 SV=3	Q06210 (+1)	79 kDa	6	0	0	0	0	0	0	0	0
Glucosamine-6-phosphate isomerase 1 OS=Homo sapiens GN=GNPDA1 PE=3 SV=1	D6R9P4 (+3)	31 kDa	0	0	2	0	0	0	0	0	0

Glucose-6-phosphate 1-dehydrogenase (Fragment) OS=Homo sapiens GN=G6PD PE=3 SV=1	E7EM57 (+5)	37 kDa	0	0	0	0	0	0	0	2	0
Glucose-6-phosphate isomerase OS=Homo sapiens GN=GPI PE=1 SV=4	P06744 (+1)	63 kDa	0	11	0	0	5	0	0	6	0
Glucosidase 2 subunit beta OS=Homo sapiens GN=PRKCSH PE=1 SV=2	P14314 (+1)	59 kDa	3	0	0	0	0	0	0	0	0
Glutamine--tRNA ligase OS=Homo sapiens GN=QARS PE=2 SV=1	B4DWJ2 (+1)	87 kDa	9	0	0	8	0	0	18	0	0
Glutathione S-transferase P OS=Homo sapiens GN=GSTP1 PE=1 SV=2	P09211	23 kDa	0	0	0	0	0	0	0	0	2
Glutathione S-transferase omega-1 OS=Homo sapiens GN=GSTO1 PE=1 SV=2	P78417	28 kDa	0	0	5	0	0	2	0	0	3
Cluster of Glyceraldehyde-3-phosphate dehydrogenase OS=Homo sapiens GN=GAPDH PE=1 SV=3 (P04406)	P04406 [2]	36 kDa	5	31	7	2	26	7	2	18	5
Glycine--tRNA ligase OS=Homo sapiens GN=GARS PE=1 SV=3	P41250	83 kDa	0	0	0	0	0	0	0	9	0
Glycogen phosphorylase, brain form OS=Homo sapiens GN=PYGB PE=1 SV=5	P11216	97 kDa	8	0	0	8	0	0	6	0	0
Glyoxalase domain-containing protein 4 (Fragment) OS=Homo sapiens GN=GLOD4 PE=4 SV=1	I3L3Q4	26 kDa	0	0	2	0	0	0	0	0	0
Glyoxylate reductase/hydroxypyruvate reductase OS=Homo sapiens GN=GRHPR PE=1 SV=1	Q9UBQ7	36 kDa	0	4	0	0	7	0	0	4	0
Golgi to ER traffic protein 4 homolog OS=Homo sapiens GN=GET4 PE=1 SV=1	Q7L5D6 (+1)	37 kDa	0	0	0	0	0	3	0	0	0
Grancalcin (Fragment) OS=Homo sapiens GN=GCA PE=4 SV=1	H7C2Z6	17 kDa	0	0	2	0	0	3	0	0	2
Guanine nucleotide-binding protein G(I)/G(S)/G(T) subunit beta-2 OS=Homo sapiens GN=GNB2 PE=4 SV=1	E7EP32 (+3)	32 kDa	0	0	2	0	0	0	0	0	0
Guanine nucleotide-binding protein subunit alpha-13 OS=Homo sapiens GN=GNA13 PE=4 SV=1	F8W818 (+1)	41 kDa	0	0	0	0	0	0	0	2	0
Guanine nucleotide-binding protein subunit beta-2-like 1 OS=Homo sapiens GN=GNB2L1 PE=1 SV=3	P63244	35 kDa	0	0	10	0	0	8	0	0	14
Guanine nucleotide-binding protein-like 1 OS=Homo sapiens GN=GNL1 PE=1 SV=2	P36915	69 kDa	6	0	0	2	0	0	0	2	0
H/ACA ribonucleoprotein complex subunit 1 OS=Homo sapiens GN=GAR1 PE=1 SV=1	Q9NY12 (+1)	22 kDa	0	0	0	0	0	2	0	0	0
H/ACA ribonucleoprotein complex subunit 4 OS=Homo sapiens GN=DKC1 PE=1 SV=3	O60832	58 kDa	0	0	0	0	2	0	0	3	0
HBS1-like protein OS=Homo sapiens GN=HBS1L PE=2 SV=1	B7Z1K2 (+4)	45 kDa	0	0	0	0	0	0	0	2	0
HCG2044781 OS=Homo sapiens GN=TMEM189 PE=4 SV=1	G3V2F7 (+4)	42 kDa	0	0	2	0	0	0	0	0	2

HCG27698, isoform CRA_c OS=Homo sapiens GN=DDX47 PE=3 SV=1	G5E955 (+1)	45 kDa	0	0	0	0	2	0	0	6	0
HEAT repeat-containing protein 2 OS=Homo sapiens GN=HEATR2 PE=1 SV=4	Q86Y56	94 kDa	5	0	0	4	0	0	7	0	0
HIV Tat-specific factor 1 OS=Homo sapiens GN=HTATSF1 PE=4 SV=2	E9PFP2 (+3)	82 kDa	0	0	0	0	0	0	2	0	0
HLA-B associated transcript 3 OS=Homo sapiens GN=BAT3 PE=4 SV=1	B0UX83 (+4)	119 kDa	3	0	0	4	0	0	5	0	0
Heat shock 70 kDa protein 1A/1B OS=Homo sapiens GN=HSPA1B PE=3 SV=1	H0YG33 (+1)	77 kDa	0	20	0	0	15	0	0	19	0
Heat shock 70 kDa protein 4 OS=Homo sapiens GN=HSPA4 PE=1 SV=4	P34932	94 kDa	13	0	0	3	0	0	4	0	0
Heat shock 70 kDa protein 4L OS=Homo sapiens GN=HSPA4L PE=3 SV=2	E7ES43 (+2)	98 kDa	5	0	0	0	0	0	0	0	0
Cluster of Heat shock cognate 71 kDa protein OS=Homo sapiens GN=HSPA8 PE=1 SV=1 (P11142)	P11142 [2]	71 kDa	0	31	0	0	26	0	0	32	0
Heat shock protein 105 kDa OS=Homo sapiens GN=HSPH1 PE=1 SV=1	Q92598 (+1)	97 kDa	12	0	0	3	0	0	7	0	0
Heat shock protein 75 kDa, mitochondrial OS=Homo sapiens GN=TRAP1 PE=3 SV=1	F5H897 (+3)	74 kDa	0	0	0	2	0	0	0	0	0
Cluster of Heat shock protein HSP 90-alpha OS=Homo sapiens GN=HSP90AA1 PE=1 SV=5 (P07900)	P07900 [6]	85 kDa	111	6	0	84	2	0	98	6	0
Heat shock protein beta-1 OS=Homo sapiens GN=HSPB1 PE=1 SV=2	P04792	23 kDa	0	0	8	0	0	7	0	0	10
Hepatocellular carcinoma-associated antigen 90 OS=Homo sapiens GN=HCA90 PE=2 SV=1	Q96RR5 (+1)	89 kDa	2	0	0	0	0	0	5	0	0
Hepatoma-derived growth factor-related protein 2 OS=Homo sapiens GN=HDGFRP2 PE=4 SV=1	I3L080 (+2)	75 kDa	0	0	0	0	0	0	3	0	0
Heterochromatin protein 1-binding protein 3 OS=Homo sapiens GN=HP1BP3 PE=1 SV=1	Q5SSJ5	61 kDa	0	0	0	0	0	0	0	3	0
Heterogeneous nuclear ribonucleoprotein A/B OS=Homo sapiens GN=HNRNPAB PE=4 SV=1	D6R9P3 (+4)	30 kDa	0	9	0	0	8	0	0	8	0
Heterogeneous nuclear ribonucleoprotein A0 OS=Homo sapiens GN=HNRNPA0 PE=1 SV=1	Q13151	31 kDa	0	3	7	0	3	8	0	5	8
Heterogeneous nuclear ribonucleoprotein A1 OS=Homo sapiens GN=HNRNPA1 PE=4 SV=1	F8VRQ1 (+4)	33 kDa	0	6	20	3	6	16	0	10	20
Heterogeneous nuclear ribonucleoprotein A3 OS=Homo sapiens GN=HNRNPA3 PE=1 SV=2	P51991	40 kDa	0	6	4	0	3	0	0	6	3
Heterogeneous nuclear ribonucleoprotein D-like OS=Homo sapiens GN=HNRPDL PE=1 SV=3	O14979 (+2)	46 kDa	0	5	4	0	6	2	0	6	0
Cluster of Heterogeneous nuclear ribonucleoprotein D0 OS=Homo sapiens GN=HNRNPD PE=1 SV=1 (Q14103)	Q14103 [3]	38 kDa	0	16	0	0	13	0	0	14	0
Heterogeneous nuclear ribonucleoprotein F OS=Homo sapiens GN=HNRNPF PE=2 SV=1	B4DKS8 (+1)	37 kDa	0	7	0	0	7	0	0	6	0

Heterogeneous nuclear ribonucleoprotein H, N-terminally processed OS=Homo sapiens GN=HNRNPH1 PE=4 SV=1	E9PCY7 (+2)	47 kDa	0	9	0	0	9	0	0	12	0
Heterogeneous nuclear ribonucleoprotein H3 OS=Homo sapiens GN=HNRNPH3 PE=1 SV=2	P31942 (+1)	37 kDa	0	6	3	0	7	3	0	5	2
Heterogeneous nuclear ribonucleoprotein L OS=Homo sapiens GN=HNRNPL PE=1 SV=2	P14866	64 kDa	0	15	0	0	12	0	0	16	0
Heterogeneous nuclear ribonucleoprotein M OS=Homo sapiens GN=HNRNPM PE=1 SV=3	P52272 (+1)	78 kDa	0	14	0	0	6	0	0	20	0
Heterogeneous nuclear ribonucleoprotein Q OS=Homo sapiens GN=SYNCRIP PE=1 SV=2	O60506 (+3)	70 kDa	5	18	0	5	18	0	0	18	0
Heterogeneous nuclear ribonucleoprotein R OS=Homo sapiens GN=HNRNPR PE=1 SV=1	O43390	71 kDa	11	11	0	5	7	0	2	10	0
Heterogeneous nuclear ribonucleoprotein U OS=Homo sapiens GN=HNRNPU PE=1 SV=6	Q00839	91 kDa	40	0	0	28	0	0	39	0	0
Heterogeneous nuclear ribonucleoprotein U-like protein 1 OS=Homo sapiens GN=HNRNPUL1 PE=2 SV=1	B7Z4B8 (+3)	86 kDa	17	0	0	9	0	0	8	0	0
Heterogeneous nuclear ribonucleoproteins A2/B1 OS=Homo sapiens GN=HNRNPA2B1 PE=1 SV=2	P22626	37 kDa	0	10	14	0	11	10	0	14	10
Cluster of Heterogeneous nuclear ribonucleoproteins C1/C2 OS=Homo sapiens GN=HNRNPC PE=2 SV=1 (B2R603)	B2R603 [8]	33 kDa	0	13	0	0	11	0	0	12	0
High mobility group protein 20A (Fragment) OS=Homo sapiens GN=HMG20A PE=4 SV=1	H0YKM5 (+2)	18 kDa	0	0	2	0	0	0	0	0	0
High mobility group protein B1 OS=Homo sapiens GN=HMGB1 PE=1 SV=3	P09429	25 kDa	0	0	10	0	0	6	0	0	5
High mobility group protein HMG-I/HMG-Y OS=Homo sapiens GN=HMGA1 PE=4 SV=1	H7BYM6 (+2)	34 kDa	0	0	0	0	0	0	0	0	2
Histone H1.4 OS=Homo sapiens GN=HIST1H1E PE=1 SV=2	P10412	22 kDa	0	0	4	0	0	2	0	0	7
Histone H1.5 OS=Homo sapiens GN=HIST1H1B PE=1 SV=3	P16401	23 kDa	0	0	3	0	0	3	0	0	5
Histone H1t OS=Homo sapiens GN=HIST1H1T PE=1 SV=4	P22492	22 kDa	0	0	0	0	0	0	0	0	3
Cluster of Histone H2A type 1 OS=Homo sapiens GN=HIST1H2AG PE=1 SV=2 (P0C0S8)	P0C0S8 [11]	14 kDa	0	0	4	0	0	4	0	0	5
Histone H2B OS=Homo sapiens GN=HIST2H2BF PE=2 SV=1	B4DR52 (+10)	18 kDa	0	0	4	0	0	3	0	0	4
Histone H3.1 OS=Homo sapiens GN=HIST1H3A PE=1 SV=2	P68431 (+3)	15 kDa	0	0	3	0	0	3	0	0	5
Histone H4 OS=Homo sapiens GN=HIST1H4A PE=1 SV=2	P62805	11 kDa	0	0	5	0	0	5	0	0	6
Histone acetyltransferase type B catalytic subunit OS=Homo sapiens GN=HAT1 PE=1 SV=1	O14929	50 kDa	0	4	0	0	0	0	0	0	0

Histone deacetylase OS=Homo sapiens GN=HDAC2 PE=2 SV=1	B3KRS5 (+2)	52 kDa	0	2	0	0	0	0	0	2	0
Histone-arginine methyltransferase CARM1 OS=Homo sapiens GN=CARM1 PE=1 SV=3	Q86X55 (+1)	66 kDa	0	2	0	0	0	0	0	2	0
Histone-binding protein RBBP4 OS=Homo sapiens GN=RBBP4 PE=1 SV=3	Q09028 (+1)	48 kDa	0	3	0	0	0	0	0	4	0
Hsc70-interacting protein OS=Homo sapiens GN=ST13 PE=1 SV=2	P50502	41 kDa	0	5	0	0	4	0	0	4	0
Hsp90 co-chaperone Cdc37 OS=Homo sapiens GN=CDC37 PE=1 SV=1	Q16543	44 kDa	0	11	0	0	8	0	0	5	0
Hypoxanthine-guanine phosphoribosyltransferase OS=Homo sapiens GN=HPRT1 PE=1 SV=2	P00492	25 kDa	0	0	4	0	0	6	0	0	6
IST1 homolog OS=Homo sapiens GN=IST1 PE=2 SV=1	A8KAH5 (+6)	42 kDa	0	2	0	0	0	0	0	2	0
Importin subunit alpha-1 (Fragment) OS=Homo sapiens GN=KPNA1 PE=4 SV=1	C9J352 (+5)	19 kDa	0	0	0	0	0	0	0	3	0
Importin subunit alpha-2 OS=Homo sapiens GN=KPNA2 PE=1 SV=1	P52292	58 kDa	0	8	0	0	7	0	0	9	0
Importin subunit alpha-3 OS=Homo sapiens GN=KPNA3 PE=1 SV=2	O00505	58 kDa	0	0	0	0	4	0	0	4	0
Importin subunit alpha-4 OS=Homo sapiens GN=KPNA4 PE=1 SV=1	O00629	58 kDa	0	2	0	0	5	0	0	3	0
Importin subunit beta-1 OS=Homo sapiens GN=KPNB1 PE=1 SV=2	Q14974	97 kDa	16	0	0	17	0	0	18	0	0
Importin-4 OS=Homo sapiens GN=IPO4 PE=1 SV=2	Q8TEX9 (+1)	119 kDa	8	0	0	8	0	0	12	0	0
Importin-5 OS=Homo sapiens GN=IPO5 PE=1 SV=4	O00410 (+1)	124 kDa	26	0	0	22	0	0	25	0	0
Importin-7 OS=Homo sapiens GN=IPO7 PE=1 SV=1	O95373	120 kDa	5	0	0	6	0	0	4	0	0
Importin-8 OS=Homo sapiens GN=IPO8 PE=1 SV=2	O15397	120 kDa	0	0	0	5	0	0	0	0	0
Inorganic pyrophosphatase OS=Homo sapiens GN=PPA1 PE=1 SV=2	Q15181 (+1)	33 kDa	0	0	0	0	0	0	0	0	2
Inosine triphosphate pyrophosphatase OS=Homo sapiens GN=ITPA PE=1 SV=2	Q9BY32	21 kDa	0	0	3	0	0	4	0	0	3
Inosine-5'-monophosphate dehydrogenase 2 (Fragment) OS=Homo sapiens GN=IMPDH2 PE=3 SV=1	H0Y4R1 (+1)	51 kDa	0	3	0	0	4	0	0	6	0
Inositol monophosphatase 1 (Fragment) OS=Homo sapiens GN=IMPA1 PE=4 SV=1	H0YBL1 (+1)	29 kDa	0	0	0	0	0	0	0	0	4
Inositol-3-phosphate synthase 1 OS=Homo sapiens GN=ISYNA1 PE=4 SV=1	G3V1R9 (+3)	45 kDa	0	2	0	0	0	0	0	0	0
Cluster of Insulin-like growth factor 2 mRNA-binding protein 1 OS=Homo sapiens GN=IGF2BP1 PE=1 SV=2 (Q9NZI8)	Q9NZI8 [2]	63 kDa	0	11	0	0	12	0	0	17	0

Insulin-like growth factor 2 mRNA-binding protein 2 OS=Homo sapiens GN=IGF2BP2 PE=4 SV=1	F8W930 (+6)	67 kDa	0	3	0	0	4	0	0	4	0
Integrin-linked kinase-associated serine/threonine phosphatase 2C OS=Homo sapiens GN=ILKAP PE=1 SV=1	Q9H0C8	43 kDa	0	0	0	0	0	0	0	3	0
Interleukin enhancer-binding factor 2 OS=Homo sapiens GN=ILF2 PE=1 SV=2	Q12905	43 kDa	0	16	0	0	12	0	0	13	0
Interleukin enhancer-binding factor 3 OS=Homo sapiens GN=ILF3 PE=4 SV=1	C9JFV5 (+7)	83 kDa	13	0	0	9	0	0	22	0	0
Intron-binding protein aquarius OS=Homo sapiens GN=AQR PE=1 SV=4	O60306	171 kDa	0	0	0	0	0	0	2	0	0
Isocitrate dehydrogenase [NADP] cytoplasmic OS=Homo sapiens GN=IDH1 PE=1 SV=2	O75874	47 kDa	0	2	0	0	5	0	0	4	0
Isoform 2 of COP9 signalosome complex subunit 2 OS=Homo sapiens GN=COPS2	P61201-2-DECOY	?	0	2	0	0	0	0	0	0	0
Isoform 2 of DNA (cytosine-5)-methyltransferase 1 OS=Homo sapiens GN=DNMT1	P26358-2-DECOY	?	0	0	0	0	0	0	0	2	0
Isoform 2 of Eukaryotic peptide chain release factor GTP-binding subunit ERF3A OS=Homo sapiens GN=GSPT1	P15170-2	69 kDa	4	0	0	0	0	0	0	0	0
Isoform 2 of Histone-binding protein RBBP7 OS=Homo sapiens GN=RBBP7	Q16576-2 (+2)	52 kDa	0	4	0	0	0	0	0	4	0
Isoform 2 of Methylthioribose-1-phosphate isomerase OS=Homo sapiens GN=MRI1	Q9BV20-2 (+1)	35 kDa	0	3	0	0	0	0	0	0	0
Isoform 2 of Septin-2 OS=Homo sapiens GN=SEPT2	Q15019-2	45 kDa	0	3	0	0	2	0	0	2	0
Isoform 2 of Signal recognition particle 54 kDa protein OS=Homo sapiens GN=SRP54	P61011-2	50 kDa	0	0	0	0	0	0	0	5	0
Isoform 2 of Titin OS=Homo sapiens GN=TTN	Q8WZ42-2-DECOY	?	0	0	0	2	0	4	0	0	0
Cluster of Isoform 2 of Tropomyosin alpha-3 chain OS=Homo sapiens GN=TPM3 (P06753-2)	P06753-2 [10]	29 kDa	0	0	19	0	0	15	0	0	16
Isoform 2 of mRNA cap guanine-N7 methyltransferase OS=Homo sapiens GN=RNMT	O43148-2	58 kDa	0	2	0	0	2	0	0	5	0
Isoform 3 of Heterogeneous nuclear ribonucleoprotein K OS=Homo sapiens GN=HNRNPK	P61978-3	49 kDa	0	23	0	0	22	0	0	21	0
Cluster of Isoform 3 of Nucleoside diphosphate kinase B OS=Homo sapiens GN=NME2 (P22392-2)	P22392-2 [4]	30 kDa	0	0	9	0	0	8	0	0	9
Isoform 3 of Titin OS=Homo sapiens GN=TTN	Q8WZ42-3-	?	2	0	0	0	0	0	0	0	0

	DECOY										
Isoform 3 of Unconventional myosin-XVIIIa OS=Homo sapiens GN=MYO18A	Q92614-3	227 kDa	0	0	0	0	0	2	0	0	0
Isoform 7 of Titin OS=Homo sapiens GN=TTN	Q8WZ42-7	3734 kDa	3	2	3	4	0	0	0	0	0
Isoform 7 of Titin OS=Homo sapiens GN=TTN	Q8WZ42-7-DECOY	?	0	0	2	2	0	0	0	0	0
Isoform 8 of Fibronectin OS=Homo sapiens GN=FN1	P02751-8-DECOY	?	0	0	0	0	0	0	2	0	0
Isoform 8 of Titin OS=Homo sapiens GN=TTN	Q8WZ42-8-DECOY	?	0	0	4	0	0	3	0	0	0
Isoform 9 of Titin OS=Homo sapiens GN=TTN	Q8WZ42-9-DECOY	?	0	0	3	0	0	0	0	0	0
Cluster of Isoform M1 of Pyruvate kinase isozymes M1/M2 OS=Homo sapiens GN=PKM (P14618-2)	P14618-2 [2]	58 kDa	8	47	2	7	46	2	3	43	2
Isoform Short of Eukaryotic translation initiation factor 4H OS=Homo sapiens GN=EIF4H	Q15056-2	25 kDa	0	0	6	0	0	7	0	0	4
Isoleucine--tRNA ligase, cytoplasmic OS=Homo sapiens GN=IARS PE=1 SV=2	P41252	145 kDa	7	0	0	5	0	0	11	0	0
Isopentenyl-diphosphate Delta-isomerase 1 OS=Homo sapiens GN=IDI1 PE=1 SV=2	Q13907 (+1)	26 kDa	0	0	2	0	0	2	0	0	2
KH domain-containing, RNA-binding, signal transduction-associated protein 1 OS=Homo sapiens GN=KHDRBS1 PE=1 SV=1	Q07666	48 kDa	0	8	0	0	6	0	0	6	0
Keratin, type I cytoskeletal 10 OS=Homo sapiens GN=KRT10 PE=1 SV=6	P13645	59 kDa	22	24	22	13	20	15	16	23	20
Keratin, type I cytoskeletal 14 OS=Homo sapiens GN=KRT14 PE=1 SV=4	P02533	52 kDa	6	6	6	5	5	4	4	6	7
Keratin, type I cytoskeletal 18 OS=Homo sapiens GN=KRT18 PE=3 SV=1	F8VZY9 (+1)	44 kDa	0	0	0	0	0	0	0	2	0
Keratin, type I cytoskeletal 9 OS=Homo sapiens GN=KRT9 PE=1 SV=3	P35527	62 kDa	13	15	12	8	15	4	8	16	13
Cluster of Keratin, type II cytoskeletal 1 OS=Homo sapiens GN=KRT1 PE=1 SV=6 (P04264)	P04264 [10]	66 kDa	46	59	48	41	51	21	35	42	41
Kinesin-1 heavy chain OS=Homo sapiens GN=KIF5B PE=1 SV=1	P33176	110 kDa	3	0	0	0	0	0	0	0	0
Kinesin-like protein KIF2A OS=Homo sapiens GN=KIF2A PE=3 SV=1	E9PB70 (+4)	78 kDa	0	0	0	0	0	0	2	0	0

Kinesin-like protein KIF2C OS=Homo sapiens GN=KIF2C PE=2 SV=1	B7Z6Q6 (+3)	77 kDa	0	0	0	0	0	0	2	0	0
L-lactate dehydrogenase A chain OS=Homo sapiens GN=LDHA PE=1 SV=2	P00338	37 kDa	0	0	19	0	4	16	0	9	13
L-lactate dehydrogenase B chain OS=Homo sapiens GN=LDHB PE=1 SV=2	P07195	37 kDa	0	5	15	0	8	15	0	13	15
LUC7-like (S. cerevisiae) OS=Homo sapiens GN=LUC7L PE=4 SV=1	A8MYV2 (+8)	32 kDa	0	2	0	0	0	0	0	2	0
La-related protein 1 OS=Homo sapiens GN=LARP1 PE=1 SV=2	Q6PKG0	124 kDa	0	0	0	0	0	0	6	0	0
Lactoylglutathione lyase OS=Homo sapiens GN=GLO1 PE=1 SV=4	Q04760 (+1)	21 kDa	0	0	4	0	0	0	0	0	0
Leucine--tRNA ligase, cytoplasmic OS=Homo sapiens GN=LARS PE=2 SV=1	B4DER1 (+2)	131 kDa	16	0	0	14	0	0	17	0	0
Leucine-rich PPR motif-containing protein, mitochondrial OS=Homo sapiens GN=LRPPRC PE=1 SV=3	P42704	158 kDa	5	0	0	0	0	0	4	0	0
Leucine-rich repeat-containing protein 47 OS=Homo sapiens GN=LRRC47 PE=1 SV=1	Q8N1G4	63 kDa	0	9	0	0	5	0	0	10	0
Leucine-rich repeat-containing protein 59 OS=Homo sapiens GN=LRRC59 PE=1 SV=1	Q96AG4	35 kDa	0	0	0	0	0	0	0	0	3
Leukotriene A-4 hydrolase OS=Homo sapiens GN=LTA4H PE=1 SV=2	P09960 (+1)	69 kDa	0	0	0	0	3	0	0	0	0
Luc7-like protein 3 OS=Homo sapiens GN=LUC7L3 PE=2 SV=1	B4DJ96 (+2)	43 kDa	0	2	0	0	0	0	0	2	0
Lysine--tRNA ligase OS=Homo sapiens GN=KARS PE=1 SV=3	Q15046	68 kDa	0	16	0	0	12	0	0	15	0
Lysine-specific histone demethylase 1A OS=Homo sapiens GN=KDM1A PE=4 SV=1	F6S0T5 (+2)	95 kDa	2	0	0	0	0	0	0	0	0
MAP1S heavy chain OS=Homo sapiens GN=MAP1S PE=2 SV=1	B4DH53 (+1)	110 kDa	0	0	0	0	0	0	2	0	0
Macrophage migration inhibitory factor OS=Homo sapiens GN=MIF PE=1 SV=4	P14174	12 kDa	0	0	2	0	0	2	0	0	2
Major vault protein OS=Homo sapiens GN=MVP PE=1 SV=4	Q14764	99 kDa	2	0	0	0	0	0	0	0	0
Malate dehydrogenase OS=Homo sapiens GN=MDH2 PE=3 SV=1	G3XAL0 (+1)	25 kDa	0	0	2	0	0	0	0	0	0
Malate dehydrogenase, cytoplasmic OS=Homo sapiens GN=MDH1 PE=4 SV=1	B9A041 (+3)	23 kDa	0	0	2	0	0	0	0	0	0
Malignant T-cell-amplified sequence 1 OS=Homo sapiens GN=MCTS1 PE=1 SV=1	Q9ULC4 (+2)	21 kDa	0	0	2	0	0	0	0	0	3
Matrin-3 OS=Homo sapiens GN=MATR3 PE=4 SV=1	A8MXP9 (+1)	100 kDa	11	0	0	6	0	0	8	0	0
Mediator of DNA damage checkpoint protein 1 OS=Homo sapiens GN=MDC1 PE=4 SV=1	E7EVA7 (+3)	196 kDa	0	0	0	0	0	0	2	0	0

Cluster of Melanoma-associated antigen 4 OS=Homo sapiens GN=MAGEA4 PE=1 SV=2 (P43358)	P43358	35 kDa	0	8	0	0	7	0	0	8	0
Methionine--tRNA ligase, cytoplasmic OS=Homo sapiens GN=MARS PE=1 SV=2	P56192	101 kDa	15	0	0	11	0	0	15	0	0
Cluster of Microtubule-associated protein OS=Homo sapiens GN=MAP4 PE=4 SV=1 (E7EVA0)	E7EVA0 [4]	245 kDa	5	0	0	4	0	0	16	0	0
Microtubule-associated protein RP/EB family member 1 OS=Homo sapiens GN=MAPRE1 PE=1 SV=3	Q15691	30 kDa	0	0	8	0	0	7	0	0	6
Mini-chromosome maintenance complex-binding protein OS=Homo sapiens GN=MCMBP PE=1 SV=2	Q9BTE3 (+2)	73 kDa	0	2	0	0	0	0	0	2	0
Mitochondrial import receptor subunit TOM34 OS=Homo sapiens GN=TOMM34 PE=1 SV=2	Q15785	35 kDa	0	0	3	0	0	2	0	2	0
Mitotic checkpoint protein BUB3 OS=Homo sapiens GN=BUB3 PE=1 SV=1	O43684 (+1)	37 kDa	0	4	0	0	3	0	0	5	0
Cluster of Mothers against decapentaplegic homolog 3 (Fragment) OS=Homo sapiens GN=SMAD3 PE=4 SV=1 (H3BVD1)	H3BVD1 [4]	24 kDa	0	0	0	0	3	0	0	2	0
Mucin-16 OS=Homo sapiens GN=MUC16 PE=1 SV=2	Q8WXI7 (+1)	2353 kDa	0	0	0	2	0	0	0	0	0
Myb-binding protein 1A OS=Homo sapiens GN=MYBBP1A PE=1 SV=2	Q9BQG0 (+1)	149 kDa	2	0	0	0	0	0	9	0	0
Myosin light polypeptide 6 OS=Homo sapiens GN=MYL6 PE=2 SV=1	B7Z6Z4 (+6)	27 kDa	0	0	0	0	0	2	0	0	3
Myosin-9 OS=Homo sapiens GN=MYH9 PE=1 SV=4	P35579	227 kDa	6	0	0	2	0	0	5	0	0
N-acetylglucosamine-1-phosphotransferase subunits alpha/beta OS=Homo sapiens GN=GNPTAB PE=1 SV=1	Q3T906	144 kDa	0	0	0	0	0	2	0	0	0
N-alpha-acetyltransferase 15, NatA auxiliary subunit OS=Homo sapiens GN=NAA15 PE=1 SV=1	Q9BXJ9	101 kDa	10	0	0	7	0	0	8	0	0
N-alpha-acetyltransferase 50 OS=Homo sapiens GN=NAA50 PE=4 SV=1	C9J5D1 (+2)	15 kDa	0	0	2	0	0	2	0	0	5
NEDD8-conjugating enzyme Ubc12 OS=Homo sapiens GN=UBE2M PE=1 SV=1	P61081	21 kDa	0	0	3	0	0	4	0	0	2
Nascent polypeptide-associated complex subunit alpha OS=Homo sapiens GN=NACA PE=4 SV=1	E9PAV3 (+7)	205 kDa	0	0	3	0	0	2	0	2	0
Nebulin OS=Homo sapiens GN=NEB PE=1 SV=4	P20929	773 kDa	0	0	0	0	0	0	0	0	2
Negative elongation factor B OS=Homo sapiens GN=COBRA1 PE=1 SV=1	Q8WX92	66 kDa	0	0	0	0	2	0	0	2	0
Negative elongation factor C/D OS=Homo sapiens GN=TH1L PE=1 SV=2	Q8IXH7 (+1)	66 kDa	0	0	0	0	0	0	0	2	0
Nesprin-1 OS=Homo sapiens GN=SYNE1 PE=1 SV=3	Q8NF91 (+3)	1011	0	0	0	2	0	0	0	0	0

		kDa									
Nesprin-2 OS=Homo sapiens GN=SYNE2 PE=4 SV=1	F8WAA3 (+3)	788 kDa	2	0	0	0	0	0	0	0	0
Neurofilament light polypeptide OS=Homo sapiens GN=NEFL PE=1 SV=3	P07196	62 kDa	0	0	0	0	2	0	0	0	0
Neutral alpha-glucosidase AB OS=Homo sapiens GN=GANAB PE=4 SV=1	F5H6X6 (+1)	96 kDa	8	0	0	3	0	0	3	0	0
Niban-like protein 1 OS=Homo sapiens GN=FAM129B PE=1 SV=3	Q96TA1	84 kDa	3	0	0	2	0	0	0	0	0
Nicotinamide mononucleotide adenylyltransferase 1 OS=Homo sapiens GN=NMNAT1 PE=1 SV=1	Q9HAN9	32 kDa	0	0	0	0	0	0	0	0	3
Nicotinamide phosphoribosyltransferase OS=Homo sapiens GN=NAMPT PE=1 SV=1	P43490	56 kDa	0	4	0	0	5	0	0	4	0
Nitric oxide synthase-interacting protein OS=Homo sapiens GN=NOSIP PE=1 SV=1	Q9Y314	33 kDa	0	0	0	0	0	0	0	0	2
Non-POU domain-containing octamer-binding protein OS=Homo sapiens GN=NONO PE=1 SV=4	Q15233	54 kDa	2	16	0	2	14	0	2	21	0
Non-erythrocytic beta-spectrin 4 OS=Homo sapiens GN=SPTBN4 PE=2 SV=2	E9PDB1 (+1)	289 kDa	0	0	0	2	0	0	2	0	0
Nuclear autoantigenic sperm protein OS=Homo sapiens GN=NASP PE=1 SV=2	P49321 (+2)	85 kDa	3	7	0	0	4	0	2	6	0
Nuclear cap-binding protein subunit 1 OS=Homo sapiens GN=NCBP1 PE=1 SV=1	Q09161	92 kDa	4	0	0	2	0	0	4	0	0
Nuclear migration protein nudC OS=Homo sapiens GN=NUDC PE=1 SV=1	Q9Y266	38 kDa	0	4	0	0	3	0	0	5	0
Nuclear pore complex protein Nup155 OS=Homo sapiens GN=NUP155 PE=2 SV=1	B4DLT2 (+3)	151 kDa	0	0	0	3	0	0	0	0	0
Nuclear pore complex protein Nup93 OS=Homo sapiens GN=NUP93 PE=4 SV=1	H3BVG0 (+1)	100 kDa	2	0	0	2	0	0	2	0	0
Nuclear protein localization protein 4 homolog OS=Homo sapiens GN=NPLOC4 PE=1 SV=3	Q8TAT6 (+1)	68 kDa	0	0	0	0	0	0	0	3	0
Nuclease-sensitive element-binding protein 1 OS=Homo sapiens GN=YBX1 PE=4 SV=1	E7ETA0 (+2)	34 kDa	0	7	0	0	5	0	0	4	0
Nucleolar RNA helicase 2 OS=Homo sapiens GN=DDX21 PE=1 SV=5	Q9NR30 (+1)	87 kDa	0	0	0	2	0	0	6	0	0
Nucleolar transcription factor 1 OS=Homo sapiens GN=UBTF PE=4 SV=1	E9PKP7 (+2)	87 kDa	0	0	0	0	0	0	4	0	0
Nucleolin OS=Homo sapiens GN=NCL PE=1 SV=3	P19338	77 kDa	25	0	0	14	0	0	32	5	0
Nucleolysin TIAR OS=Homo sapiens GN=TIAL1 PE=1 SV=1	Q01085 (+1)	42 kDa	0	2	0	0	2	0	0	4	0
Nucleophosmin OS=Homo sapiens GN=NPM1 PE=1 SV=2	P06748	33 kDa	0	10	2	0	12	2	0	13	2
Nucleosome assembly protein 1-like 1 OS=Homo sapiens GN=NAP1L1 PE=3 SV=1	F5H4R6	45 kDa	0	9	0	0	5	0	0	5	0

Nucleosome assembly protein 1-like 4 OS=Homo sapiens GN=NAP1L4 PE=3 SV=3	A8MZ22 (+7)	44 kDa	0	3	0	0	0	0	0	2	0
NudC domain-containing protein 2 OS=Homo sapiens GN=NUDCD2 PE=1 SV=1	Q8WVJ2	18 kDa	0	0	0	2	0	0	2	0	0
Obscurin OS=Homo sapiens GN=OBSCN PE=4 SV=1	H3BPX2	946 kDa	0	0	0	0	2	0	0	0	0
PC4 and SFRS1-interacting protein OS=Homo sapiens GN=PSIP1 PE=1 SV=1	O75475	60 kDa	0	2	0	0	0	0	0	6	0
PDZ and LIM domain protein 7 OS=Homo sapiens GN=PDLIM7 PE=1 SV=1	Q9NR12	50 kDa	0	4	0	0	3	0	0	4	0
Pachytene checkpoint protein 2 homolog OS=Homo sapiens GN=TRIP13 PE=1 SV=2	Q15645	49 kDa	0	4	0	0	4	0	0	7	0
Parafibromin OS=Homo sapiens GN=CDC73 PE=1 SV=1	Q6P1J9	61 kDa	0	0	0	0	2	0	0	8	0
Paraspeckle component 1 OS=Homo sapiens GN=PSPC1 PE=4 SV=1	F5H656 (+2)	53 kDa	0	5	0	0	3	0	0	8	0
Peflin OS=Homo sapiens GN=PEF1 PE=1 SV=1	Q9UBV8	30 kDa	0	0	0	0	0	0	0	0	2
Peptidyl-prolyl cis-trans isomerase A OS=Homo sapiens GN=PPIA PE=1 SV=2	P62937	18 kDa	0	0	9	0	0	10	0	0	10
Peptidyl-prolyl cis-trans isomerase B OS=Homo sapiens GN=PPIB PE=1 SV=2	P23284	24 kDa	0	0	5	0	0	3	0	0	4
Peptidyl-prolyl cis-trans isomerase D OS=Homo sapiens GN=PPID PE=1 SV=3	Q08752	41 kDa	0	4	0	0	4	0	0	6	0
Peptidyl-prolyl cis-trans isomerase FKBP4 OS=Homo sapiens GN=FKBP4 PE=1 SV=3	Q02790	52 kDa	0	20	0	0	13	0	0	20	0
Perilipin-3 OS=Homo sapiens GN=PLIN3 PE=1 SV=3	O60664 (+1)	47 kDa	0	6	0	0	5	0	0	5	0
Peroxiredoxin-1 OS=Homo sapiens GN=PRDX1 PE=1 SV=1	Q06830	22 kDa	0	0	14	0	0	13	0	0	12
Peroxiredoxin-4 OS=Homo sapiens GN=PRDX4 PE=1 SV=1	Q13162	31 kDa	0	0	4	0	0	4	0	0	2
Peroxiredoxin-5, mitochondrial OS=Homo sapiens GN=PRDX5 PE=4 SV=1	A6NG06 (+2)	17 kDa	0	0	0	0	0	0	0	0	2
Peroxiredoxin-6 OS=Homo sapiens GN=PRDX6 PE=1 SV=3	P30041	25 kDa	0	0	8	0	0	4	0	0	4
Phenylalanine--tRNA ligase alpha subunit OS=Homo sapiens GN=FARSA PE=2 SV=1	B4E363 (+1)	54 kDa	0	0	0	0	2	0	0	3	0
Phenylalanine--tRNA ligase beta subunit OS=Homo sapiens GN=FARSB PE=1 SV=3	Q9NSD9	66 kDa	0	8	0	0	8	0	0	11	0
Phosphatidylinositol transfer protein beta isoform OS=Homo sapiens GN=PITPNB PE=2 SV=1	B7Z7Q0 (+2)	32 kDa	0	0	2	0	0	3	0	0	2
Phosphoacetylglucosamine mutase OS=Homo sapiens GN=PGM3 PE=3 SV=1	D6RF12 (+2)	62 kDa	0	2	0	0	2	0	0	0	0

Cluster of Phosphoglycerate kinase 1 OS=Homo sapiens GN=PGK1 PE=1 SV=3 (P00558)	P00558 [2]	45 kDa	0	34	0	0	36	0	0	33	0
Phosphoglycerate mutase 1 OS=Homo sapiens GN=PGAM1 PE=1 SV=2	P18669	29 kDa	0	0	3	0	0	4	0	0	3
Phospholipase A-2-activating protein OS=Homo sapiens GN=PLAA PE=1 SV=2	Q9Y263	87 kDa	0	0	0	0	0	0	2	0	0
Phospholipase D3 OS=Homo sapiens GN=PLD3 PE=1 SV=1	Q8IV08	55 kDa	0	2	0	0	0	0	0	0	0
Phosphomannomutase 2 (Fragment) OS=Homo sapiens GN=PMM2 PE=4 SV=1	H3BPH4 (+2)	16 kDa	0	0	2	0	0	0	0	0	2
Phosphoribosyl pyrophosphate synthase-associated protein 2 OS=Homo sapiens GN=PRPSAP2 PE=1 SV=1	O60256	41 kDa	0	3	0	0	5	0	0	2	0
Phosphoribosyl pyrophosphate synthase-associated protein 2 OS=Homo sapiens GN=PRPSAP2 PE=4 SV=1	C9JLZ5	5 kDa	0	0	2	0	0	2	0	0	0
Phosphoribosylaminoimidazole-succinocarboxamide synthase (Fragment) OS=Homo sapiens GN=PAICS PE=4 SV=1	E9PBS1 (+2)	46 kDa	0	2	0	0	0	0	0	0	0
Phosphoribosylaminoimidazolecarboxamide formyltransferase OS=Homo sapiens GN=ATIC PE=4 SV=1	E9PBU3 (+2)	65 kDa	0	10	0	0	5	0	0	4	0
Phosphoribosylformylglycinamidine synthase OS=Homo sapiens GN=PFAS PE=1 SV=4	O15067	145 kDa	8	0	0	4	0	0	3	0	0
Phosphorylase OS=Homo sapiens GN=PYGL PE=3 SV=1	E9PK47 (+2)	94 kDa	3	0	0	4	0	0	4	0	0
Phosphoserine aminotransferase OS=Homo sapiens GN=PSAT1 PE=1 SV=2	Q9Y617 (+1)	40 kDa	0	3	0	0	2	0	0	0	0
Plasminogen activator inhibitor 1 RNA-binding protein OS=Homo sapiens GN=SERBP1 PE=1 SV=2	Q8NC51 (+3)	45 kDa	0	4	0	0	5	0	0	11	0
Plastin-3 OS=Homo sapiens GN=PLS3 PE=2 SV=1	B4DGB4 (+3)	69 kDa	0	3	0	0	0	0	0	3	0
Platelet-activating factor acetylhydrolase IB subunit alpha OS=Homo sapiens GN=PAFAH1B1 PE=1 SV=2	P43034	47 kDa	0	4	0	0	5	0	0	5	0
Platelet-activating factor acetylhydrolase IB subunit beta OS=Homo sapiens GN=PAFAH1B2 PE=1 SV=1	P68402	26 kDa	0	0	2	0	0	0	0	0	0
Platelet-activating factor acetylhydrolase IB subunit gamma OS=Homo sapiens GN=PAFAH1B3 PE=1 SV=1	Q15102	26 kDa	0	0	3	0	0	0	0	0	0
Poly [ADP-ribose] polymerase 1 OS=Homo sapiens GN=PARP1 PE=1 SV=4	P09874	113 kDa	0	0	0	2	0	0	8	0	0
Poly(A) polymerase alpha OS=Homo sapiens GN=PAPOLA PE=4 SV=1	F5H5I8 (+2)	82 kDa	2	0	0	0	0	0	0	0	0
Poly(U)-binding-splicing factor PUF60 OS=Homo sapiens GN=PUF60 PE=1 SV=1	Q9UHX1 (+5)	60 kDa	0	0	0	0	2	0	0	5	0
Poly(rC)-binding protein 1 OS=Homo sapiens GN=PCBP1 PE=1 SV=2	Q15365	37 kDa	0	9	0	0	9	0	0	8	0
Cluster of Poly(rC)-binding protein 2 OS=Homo sapiens GN=PCBP2 PE=4 SV=1 (I6L8F9)	I6L8F9 [3]	38 kDa	0	9	0	0	8	0	0	9	0

Cluster of Polyadenylate-binding protein 1 OS=Homo sapiens GN=PABPC1 PE=1 SV=2 (P11940)	P11940 [5]	71 kDa	0	12	0	0	9	0	0	20	0
Polypyrimidine tract-binding protein 1 OS=Homo sapiens GN=PTBP1 PE=1 SV=1	P26599 (+2)	57 kDa	0	10	0	0	11	0	0	14	0
Pre-mRNA-processing factor 19 OS=Homo sapiens GN=PRPF19 PE=1 SV=1	Q9UMS4	55 kDa	0	4	0	0	4	0	0	7	0
Pre-mRNA-processing factor 6 OS=Homo sapiens GN=PRPF6 PE=1 SV=1	O94906 (+1)	107 kDa	0	0	0	0	0	0	4	0	0
Pre-mRNA-processing-splicing factor 8 OS=Homo sapiens GN=PRPF8 PE=1 SV=2	Q6P2Q9	274 kDa	4	0	0	5	0	0	7	0	0
Pre-mRNA-splicing factor ATP-dependent RNA helicase PRP16 OS=Homo sapiens GN=DHX38 PE=1 SV=2	Q92620	141 kDa	2	0	0	0	0	0	0	0	0
Pre-rRNA-processing protein TSR1 homolog OS=Homo sapiens GN=TSR1 PE=1 SV=1	Q2NL82	92 kDa	0	0	0	0	0	0	2	0	0
Prelamin-A/C OS=Homo sapiens GN=LMNA PE=1 SV=1	P02545 (+2)	74 kDa	0	15	0	0	10	0	0	18	0
Cluster of Probable ATP-dependent RNA helicase DDX17 OS=Homo sapiens GN=DDX17 PE=3 SV=1 (H3BLZ8)	H3BLZ8 [4]	80 kDa	9	9	0	6	9	0	0	18	0
Probable ATP-dependent RNA helicase DDX23 OS=Homo sapiens GN=DDX23 PE=1 SV=3	Q9BUQ8	96 kDa	6	0	0	0	0	0	3	0	0
Probable ATP-dependent RNA helicase DDX5 OS=Homo sapiens GN=DDX5 PE=1 SV=1	P17844	69 kDa	2	18	0	2	15	0	0	19	0
Probable ATP-dependent RNA helicase DDX6 OS=Homo sapiens GN=DDX6 PE=1 SV=2	P26196	54 kDa	0	0	0	0	3	0	0	3	0
Probable ATP-dependent RNA helicase DHX40 OS=Homo sapiens GN=DHX40 PE=4 SV=2	C9JEW8 (+1)	83 kDa	0	0	0	0	0	0	2	0	0
Probable global transcription activator SNF2L1 (Fragment) OS=Homo sapiens GN=SMARCA1 PE=4 SV=1	F6TQG2 (+2)	117 kDa	0	0	0	2	0	0	4	0	0
Profilin-1 OS=Homo sapiens GN=PFN1 PE=1 SV=2	P07737	15 kDa	0	0	13	0	0	13	0	0	12
Programmed cell death 6-interacting protein OS=Homo sapiens GN=PDCD6IP PE=4 SV=1	E9PFU1 (+1)	97 kDa	13	0	0	2	0	0	10	0	0
Programmed cell death protein 10 OS=Homo sapiens GN=PDCD10 PE=1 SV=1	Q9BUL8	25 kDa	0	0	0	0	0	0	0	0	2
Programmed cell death protein 6 OS=Homo sapiens GN=PDCD6 PE=1 SV=1	O75340 (+1)	22 kDa	0	0	2	0	0	3	0	0	3
Proliferating cell nuclear antigen OS=Homo sapiens GN=PCNA PE=1 SV=1	P12004	29 kDa	0	0	14	0	0	14	0	0	13
Cluster of Proliferation-associated protein 2G4 OS=Homo sapiens GN=PA2G4 PE=4 SV=1 (H0Y3X3)	H0Y3X3 [3]	45 kDa	0	15	0	0	14	0	0	17	0
Prostaglandin E synthase 3 OS=Homo sapiens GN=PTGES3 PE=2 SV=1	B4DP11 (+2)	16 kDa	0	0	3	0	0	4	0	0	3
Proteasome activator complex subunit 2 OS=Homo sapiens GN=PSME2 PE=4 SV=1	H0YM70 (+1)	26 kDa	0	0	2	0	0	0	0	0	4

Proteasome assembly chaperone 1 OS=Homo sapiens GN=PSMG1 PE=1 SV=1	O95456 (+1)	33 kDa	0	0	0	0	0	0	0	0	2
Proteasome assembly chaperone 2 OS=Homo sapiens GN=PSMG2 PE=1 SV=1	Q969U7	29 kDa	0	0	3	0	0	4	0	0	2
Proteasome subunit alpha type OS=Homo sapiens GN=PSMA6 PE=3 SV=1	G3V295 (+4)	23 kDa	0	0	3	0	0	2	0	0	2
Proteasome subunit alpha type-1 OS=Homo sapiens GN=PSMA1 PE=4 SV=1	F5GX11 (+2)	27 kDa	0	0	2	0	0	4	0	0	5
Proteasome subunit alpha type-3 OS=Homo sapiens GN=PSMA3 PE=1 SV=2	P25788 (+1)	28 kDa	0	0	3	0	0	3	0	0	0
Proteasome subunit alpha type-4 OS=Homo sapiens GN=PSMA4 PE=1 SV=1	P25789	29 kDa	0	0	3	0	0	3	0	0	5
Proteasome subunit alpha type-5 OS=Homo sapiens GN=PSMA5 PE=1 SV=3	P28066	26 kDa	0	0	4	0	0	4	0	0	5
Proteasome subunit alpha type-7 OS=Homo sapiens GN=PSMA7 PE=1 SV=1	O14818 (+1)	28 kDa	0	0	4	0	0	4	0	0	2
Proteasome subunit beta type-1 OS=Homo sapiens GN=PSMB1 PE=1 SV=2	P20618	26 kDa	0	0	4	0	0	0	0	0	0
Proteasome subunit beta type-5 (Fragment) OS=Homo sapiens GN=PSMB5 PE=3 SV=1	H0YJM8 (+2)	13 kDa	0	0	3	0	0	0	0	0	0
Proteasome-associated protein ECM29 homolog OS=Homo sapiens GN=ECM29 PE=1 SV=2	Q5VYK3	204 kDa	4	0	0	3	0	0	4	0	0
Protein DEK OS=Homo sapiens GN=DEK PE=1 SV=1	P35659	43 kDa	0	12	0	0	12	0	0	13	0
Protein DJ-1 OS=Homo sapiens GN=PARK7 PE=1 SV=2	Q99497	20 kDa	0	0	8	0	0	5	0	0	6
Protein FAM49B OS=Homo sapiens GN=FAM49B PE=1 SV=1	Q9NUQ9	37 kDa	0	0	6	0	0	7	0	0	6
Protein IWS1 homolog OS=Homo sapiens GN=IWS1 PE=4 SV=2	E7EX51 (+3)	87 kDa	0	0	0	0	0	0	7	0	0
Protein KIAA0664 OS=Homo sapiens GN=KIAA0664 PE=1 SV=2	O75153	147 kDa	4	0	0	3	0	0	0	0	0
Protein O-GlcNAcase OS=Homo sapiens GN=MGEA5 PE=4 SV=1	E9PGF9 (+3)	97 kDa	3	0	0	0	0	0	0	0	0
Protein RCC2 OS=Homo sapiens GN=RCC2 PE=1 SV=2	Q9P258	56 kDa	0	3	0	0	3	0	0	7	0
Protein SET OS=Homo sapiens GN=SET PE=2 SV=2	A6NGV1 (+4)	31 kDa	0	5	0	0	4	0	0	4	0
Protein arginine N-methyltransferase 1 OS=Homo sapiens GN=PRMT1 PE=4 SV=1	E9PKG1 (+5)	38 kDa	0	6	0	0	4	0	0	6	0
Protein disulfide-isomerase A3 OS=Homo sapiens GN=PDIA3 PE=2 SV=1	B3KQT9 (+2)	54 kDa	0	4	0	0	2	0	0	3	0
Protein disulfide-isomerase A6 OS=Homo sapiens GN=PDIA6 PE=3 SV=1	B5MCQ5 (+4)	53 kDa	0	2	0	0	3	0	0	3	0

Protein flightless-1 homolog OS=Homo sapiens GN=FLII PE=4 SV=1	E7EPM0 (+2)	135 kDa	0	0	0	0	0	0	2	0	0
Protein mago nashi homolog OS=Homo sapiens GN=MAGOH PE=1 SV=1	P61326 (+1)	17 kDa	0	0	0	0	0	0	0	0	2
Protein phosphatase 1G OS=Homo sapiens GN=PPM1G PE=3 SV=1	F5H7G7 (+1)	57 kDa	0	0	0	0	0	0	0	2	0
Protein transport protein Sec23A OS=Homo sapiens GN=SEC23A PE=4 SV=1	F5H365 (+1)	83 kDa	2	0	0	0	0	0	2	0	0
Protein transport protein Sec24C OS=Homo sapiens GN=SEC24C PE=4 SV=2	E7EP00 (+1)	107 kDa	0	0	0	3	0	0	4	0	0
Protein transport protein Sec31A OS=Homo sapiens GN=SEC31A PE=2 SV=1	B7ZL00 (+8)	128 kDa	5	0	0	2	0	0	0	0	0
Protein unc-45 homolog A OS=Homo sapiens GN=UNC45A PE=1 SV=1	Q9H3U1 (+1)	103 kDa	4	0	0	0	0	0	7	0	0
Protein-L-isoaspartate O-methyltransferase OS=Homo sapiens GN=PCMT1 PE=3 SV=1	H7BY58 (+2)	30 kDa	0	0	2	0	0	2	0	0	4
Puromycin-sensitive aminopeptidase OS=Homo sapiens GN=NPEPPS PE=4 SV=1	E9PLK3 (+1)	103 kDa	11	0	0	4	0	0	5	0	0
Putative RNA-binding protein 3 OS=Homo sapiens GN=RBM3 PE=1 SV=1	P98179	17 kDa	0	0	0	0	0	0	0	0	2
Putative deoxyribose-phosphate aldolase OS=Homo sapiens GN=DERA PE=4 SV=1	E9PPM8 (+1)	31 kDa	0	0	0	0	0	2	0	0	0
Putative pre-mRNA-splicing factor ATP-dependent RNA helicase DHX15 OS=Homo sapiens GN=DHX15 PE=4 SV=1	F5H6K0 (+1)	90 kDa	12	0	0	3	0	0	8	0	0
Putative pre-mRNA-splicing factor ATP-dependent RNA helicase DHX16 OS=Homo sapiens GN=DHX16 PE=1 SV=2	O60231	119 kDa	5	0	0	0	0	0	6	0	0
Putative ribosomal RNA methyltransferase NOP2 OS=Homo sapiens GN=NOP2 PE=1 SV=2	P46087 (+1)	89 kDa	4	0	0	0	0	0	9	0	0
RAP1, GTP-GDP dissociation stimulator 1, isoform CRA_b OS=Homo sapiens GN=RAP1GDS1 PE=4 SV=1	G5E9P9 (+1)	66 kDa	0	3	0	0	4	0	0	6	0
RNA 3'-terminal phosphate cyclase OS=Homo sapiens GN=RTCA PE=1 SV=1	O00442 (+1)	39 kDa	0	0	0	0	0	0	0	2	0
RNA binding protein, autoantigenic (HnRNP-associated with lethal yellow homolog (Mouse)) (Fragment) OS=Homo sapiens GN=RALY PE=2 SV=1	Q5QPM0	19 kDa	0	2	0	0	4	0	0	5	0
RNA polymerase II subunit A C-terminal domain phosphatase SSU72 OS=Homo sapiens GN=SSU72 PE=1 SV=1	Q9NP77	23 kDa	0	0	4	0	0	0	0	0	0
RNA polymerase II-associated factor 1 homolog OS=Homo sapiens GN=PAF1 PE=4 SV=1	F8W9Q2 (+2)	53 kDa	0	0	0	0	0	0	0	5	0
RNA polymerase-associated protein CTR9 homolog OS=Homo sapiens GN=CTR9 PE=1 SV=1	Q6PD62	134 kDa	0	0	0	0	0	0	11	0	0

RNA polymerase-associated protein RTF1 homolog OS=Homo sapiens GN=RTF1 PE=1 SV=4	Q92541	80 kDa	0	0	0	0	0	0	2	0	0
RNA-binding motif protein, X chromosome OS=Homo sapiens GN=RBMX PE=1 SV=3	P38159	42 kDa	0	10	0	0	10	0	0	7	0
RNA-binding motif protein, X-linked-like-3 OS=Homo sapiens GN=RBMXL3 PE=2 SV=2	Q8N7X1	115 kDa	0	0	0	0	0	0	0	2	0
RNA-binding protein 25 OS=Homo sapiens GN=RBM25 PE=1 SV=3	P49756 (+2)	100 kDa	2	0	0	0	0	0	2	0	0
RNA-binding protein 39 OS=Homo sapiens GN=RBM39 PE=4 SV=1	E1P5S2 (+5)	41 kDa	0	0	0	0	0	0	0	3	0
RNA-binding protein 4 OS=Homo sapiens GN=RBM4 PE=4 SV=1	D6R9K7 (+8)	17 kDa	0	0	0	0	0	0	0	3	0
RNA-binding protein 42 OS=Homo sapiens GN=RBM42 PE=1 SV=1	Q9BTD8 (+3)	50 kDa	0	3	0	0	3	0	0	5	0
RNA-binding protein FUS OS=Homo sapiens GN=FUS PE=2 SV=1	B4DR70 (+3)	45 kDa	0	3	0	0	0	0	0	6	0
RNA-binding protein PNO1 OS=Homo sapiens GN=PNO1 PE=1 SV=1	Q9NRX1	28 kDa	0	0	0	0	0	0	0	0	2
Rab GDP dissociation inhibitor beta OS=Homo sapiens GN=GDI2 PE=4 SV=1	E7EU23 (+2)	51 kDa	0	4	0	0	0	0	0	0	0
Rab3 GTPase-activating protein non-catalytic subunit OS=Homo sapiens GN=RAB3GAP2 PE=1 SV=1	Q9H2M9	156 kDa	0	0	0	2	0	0	0	0	0
Ran GTPase-activating protein 1 OS=Homo sapiens GN=RANGAP1 PE=1 SV=1	P46060	64 kDa	10	0	0	8	0	0	2	12	0
Ran-specific GTPase-activating protein OS=Homo sapiens GN=RANBP1 PE=1 SV=1	P43487	23 kDa	0	0	3	0	0	0	0	0	2
Ras GTPase-activating protein 1 OS=Homo sapiens GN=RASA1 PE=2 SV=1	B4DTL2 (+3)	102 kDa	0	0	0	0	0	0	2	0	0
Ras GTPase-activating protein-binding protein 1 OS=Homo sapiens GN=G3BP1 PE=1 SV=1	Q13283	52 kDa	0	3	0	0	3	0	0	6	0
Ras GTPase-activating protein-binding protein 2 OS=Homo sapiens GN=G3BP2 PE=1 SV=2	Q9UN86 (+1)	54 kDa	0	0	0	0	0	0	0	4	0
Ras GTPase-activating-like protein IQGAP1 OS=Homo sapiens GN=IQGAP1 PE=1 SV=1	P46940	189 kDa	28	0	0	16	0	0	27	0	0
Ras-related C3 botulinum toxin substrate 2 OS=Homo sapiens GN=RAC2 PE=3 SV=1	B1AH77 (+4)	17 kDa	0	0	0	0	0	0	0	0	2
Cluster of Ras-related protein Rab-10 OS=Homo sapiens GN=RAB10 PE=1 SV=1 (P61026)	P61026 [3]	23 kDa	0	0	5	0	0	7	0	0	10
Ras-related protein Rab-11B OS=Homo sapiens GN=RAB11B PE=1 SV=4	Q15907	24 kDa	0	0	3	0	0	4	0	0	3
Ras-related protein Rab-14 OS=Homo sapiens GN=RAB14 PE=1 SV=4	P61106	24 kDa	0	0	2	0	0	0	0	0	0
Ras-related protein Rab-21 OS=Homo sapiens GN=RAB21 PE=1 SV=3	Q9UL25	24 kDa	0	0	0	0	0	0	0	0	3

Ras-related protein Rab-2A OS=Homo sapiens GN=RAB2A PE=1 SV=1	P61019	24 kDa	0	0	3	0	0	2	0	0	3
Ras-related protein Rab-5C OS=Homo sapiens GN=RAB5C PE=3 SV=1	F8W1H5 (+1)	27 kDa	0	0	0	0	0	0	0	0	2
Ras-related protein Rab-6A (Fragment) OS=Homo sapiens GN=RAB6A PE=3 SV=1	F5GZB1 (+4)	16 kDa	0	0	0	0	0	2	0	0	2
Ras-related protein Rab-7a OS=Homo sapiens GN=RAB7A PE=1 SV=1	P51149	23 kDa	0	0	4	0	0	5	0	0	3
Regulator of chromosome condensation OS=Homo sapiens GN=RCC1 PE=1 SV=1	P18754 (+1)	45 kDa	0	8	0	0	8	0	0	9	0
Regulator of microtubule dynamics protein 1 (Fragment) OS=Homo sapiens GN=FAM82B PE=4 SV=1	H0YC27	13 kDa	0	0	3	0	0	4	0	0	2
Regulator of microtubule dynamics protein 1 OS=Homo sapiens GN=FAM82B PE=2 SV=1	B4DZW6 (+1)	32 kDa	0	0	3	0	0	5	0	0	3
Regulator of nonsense transcripts 1 OS=Homo sapiens GN=UPF1 PE=1 SV=2	Q92900 (+1)	124 kDa	5	0	0	3	0	0	6	0	0
Replication factor C subunit 4 OS=Homo sapiens GN=RFC4 PE=1 SV=2	P35249	40 kDa	0	0	0	0	0	0	0	5	0
Replication protein A 70 kDa DNA-binding subunit OS=Homo sapiens GN=RPA1 PE=1 SV=2	P27694	68 kDa	0	8	0	0	10	0	0	8	0
Reticulon-4 OS=Homo sapiens GN=RTN4 PE=4 SV=1	F8W914 (+3)	37 kDa	0	2	0	0	2	0	0	0	0
Rho GDP-dissociation inhibitor 1 OS=Homo sapiens GN=ARHGDIA PE=1 SV=3	P52565	23 kDa	0	0	4	0	0	2	0	0	0
Ribonuclease P protein subunit p30 OS=Homo sapiens GN=RPP30 PE=4 SV=1	E9PB02 (+1)	36 kDa	0	0	0	0	0	0	0	0	5
Ribonuclease inhibitor OS=Homo sapiens GN=RNH1 PE=1 SV=2	P13489	50 kDa	0	3	0	0	3	0	0	7	0
Cluster of Ribose-phosphate pyrophosphokinase 2 OS=Homo sapiens GN=PRPS2 PE=1 SV=2 (P11908)	P11908 [3]	35 kDa	0	0	8	0	4	4	0	5	2
Ribosomal RNA small subunit methyltransferase NEP1 OS=Homo sapiens GN=EMG1 PE=1 SV=4	Q92979	27 kDa	0	0	0	0	0	2	0	0	5
Ribosome biogenesis protein BRX1 homolog OS=Homo sapiens GN=BRIX1 PE=1 SV=2	Q8TDN6	41 kDa	0	0	0	0	0	0	0	2	0
Ribosome maturation protein SBDS OS=Homo sapiens GN=SBDS PE=1 SV=4	Q9Y3A5	29 kDa	0	0	12	0	0	10	0	0	12
Rotatin OS=Homo sapiens GN=RTTN PE=4 SV=1	C9JTR3 (+4)	179 kDa	0	0	2	0	0	0	0	0	0
RuvB-like 1 OS=Homo sapiens GN=RUVBL1 PE=1 SV=1	Q9Y265	50 kDa	0	9	0	0	8	0	0	10	0
RuvB-like 2 OS=Homo sapiens GN=RUVBL2 PE=1 SV=3	Q9Y230	51 kDa	0	13	0	0	10	0	0	13	0
S-adenosylmethionine synthase isoform type-2 OS=Homo sapiens GN=MAT2A PE=1 SV=1	P31153	44 kDa	0	2	0	0	0	0	0	0	0

S-formylglutathione hydrolase OS=Homo sapiens GN=ESD PE=1 SV=2	P10768	31 kDa	0	0	0	0	0	0	0	0	2
SAM domain and HD domain-containing protein 1 OS=Homo sapiens GN=SAMHD1 PE=1 SV=2	Q9Y3Z3	72 kDa	0	0	0	0	3	0	0	0	0
SAP domain-containing ribonucleoprotein OS=Homo sapiens GN=SARNP PE=4 SV=1	F8VZQ9 (+2)	24 kDa	0	0	2	0	0	2	0	0	3
SCY1-like protein 2 OS=Homo sapiens GN=SCYL2 PE=4 SV=2	E7EMM7 (+2)	38 kDa	0	0	0	2	0	0	0	0	0
SUMO-activating enzyme subunit 1 OS=Homo sapiens GN=SAE1 PE=1 SV=1	Q9UBE0	38 kDa	6	29	21	3	27	17	0	9	0
SUMO-activating enzyme subunit 2 OS=Homo sapiens GN=UBA2 PE=1 SV=2	Q9UBT2	71 kDa	42	52	41	31	42	36	8	0	5
SUMO-conjugating enzyme UBC9 OS=Homo sapiens GN=UBE2I PE=1 SV=1	P63279	18 kDa	14	6	4	5	5	4	9	5	5
SWI/SNF complex subunit SMARCC1 OS=Homo sapiens GN=SMARCC1 PE=1 SV=3	Q92922	123 kDa	2	0	0	0	0	0	2	0	0
SWI/SNF complex subunit SMARCC2 OS=Homo sapiens GN=SMARCC2 PE=1 SV=1	Q8TAQ2	133 kDa	2	0	0	0	0	0	5	0	0
Scaffold attachment factor B1 OS=Homo sapiens GN=SAFB PE=2 SV=1	B7Z2F6 (+4)	86 kDa	0	0	0	2	0	0	3	0	0
Septin 10, isoform CRA_c OS=Homo sapiens GN=SEPT10 PE=3 SV=2	B5ME97 (+6)	63 kDa	0	0	0	0	2	0	0	0	0
Septin-7 OS=Homo sapiens GN=SEPT7 PE=2 SV=1	B4DNE4 (+5)	45 kDa	0	2	0	0	0	0	0	2	0
Septin-9 OS=Homo sapiens GN=SEPT9 PE=1 SV=2	Q9UHD8 (+3)	65 kDa	0	0	0	0	0	0	0	2	0
Sequestosome-1 OS=Homo sapiens GN=SQSTM1 PE=4 SV=1	E7ERP8	32 kDa	0	2	0	0	0	0	0	0	0
Serine--tRNA ligase, cytoplasmic OS=Homo sapiens GN=SARS PE=1 SV=3	P49591 (+1)	59 kDa	0	3	0	0	3	0	0	3	0
Serine-threonine kinase receptor-associated protein OS=Homo sapiens GN=STRAP PE=2 SV=1	B4DNJ6 (+1)	40 kDa	0	3	0	0	2	0	0	2	0
Serine/arginine-rich splicing factor 1 OS=Homo sapiens GN=SRSF1 PE=1 SV=2	Q07955	28 kDa	0	0	4	0	0	5	0	0	8
Serine/arginine-rich splicing factor 5 OS=Homo sapiens GN=SRSF5 PE=1 SV=1	Q13243 (+1)	31 kDa	0	0	0	0	0	0	0	2	0
Serine/arginine-rich splicing factor 6 OS=Homo sapiens GN=SRSF6 PE=1 SV=2	Q13247 (+1)	40 kDa	0	3	0	0	3	0	0	3	0
Serine/arginine-rich splicing factor 9 OS=Homo sapiens GN=SRSF9 PE=1 SV=1	Q13242	26 kDa	0	0	3	0	0	0	0	0	4
Serine/arginine-rich-splicing factor 2 OS=Homo sapiens GN=SRSF2 PE=4 SV=1	H0YG49 (+2)	25 kDa	0	0	2	0	0	2	0	0	4
Serine/arginine-rich-splicing factor 3 OS=Homo sapiens GN=SRSF3 PE=2 SV=1	B4E241 (+1)	14 kDa	0	0	3	0	0	2	0	0	4

Serine/arginine-rich-splicing factor 7 OS=Homo sapiens GN=SRSF7 PE=4 SV=1	C9JAB2 (+4)	27 kDa	0	0	4	0	0	2	0	0	4
Serine/threonine-protein kinase D1 OS=Homo sapiens GN=PRKD1 PE=4 SV=1	F8WBA3-DECOY	?	0	0	0	0	0	0	0	0	2
Serine/threonine-protein kinase N1 OS=Homo sapiens GN=PKN1 PE=1 SV=2	Q16512 (+1)	104 kDa	0	0	0	2	0	0	0	0	0
Serine/threonine-protein kinase N2 OS=Homo sapiens GN=PKN2 PE=1 SV=1	Q16513 (+4)	112 kDa	0	0	0	0	0	0	2	0	0
Serine/threonine-protein kinase SMG1 OS=Homo sapiens GN=SMG1 PE=4 SV=1	I3L0C1 (+4)	411 kDa	0	2	0	0	2	0	0	0	0
Serine/threonine-protein kinase VRK1 (Fragment) OS=Homo sapiens GN=VRK1 PE=4 SV=1	H0YJ50 (+1)	27 kDa	0	0	0	0	0	0	0	2	0
Serine/threonine-protein phosphatase 1 regulatory subunit 10 OS=Homo sapiens GN=PPP1R10 PE=1 SV=1	Q96QC0	99 kDa	0	0	0	0	0	0	4	0	0
Serine/threonine-protein phosphatase 2A 56 kDa regulatory subunit delta isoform OS=Homo sapiens GN=PPP2R5D PE=4 SV=1	E9PFR3 (+5)	69 kDa	0	0	0	0	2	0	0	2	0
Cluster of Serine/threonine-protein phosphatase 2A 65 kDa regulatory subunit A alpha isoform OS=Homo sapiens GN=PPP2R1A PE=1 SV=4 (P30153)	P30153 [4]	65 kDa	0	13	0	0	17	0	0	15	0
Cluster of Serine/threonine-protein phosphatase PP1-alpha catalytic subunit OS=Homo sapiens GN=PPP1CA PE=1 SV=1 (P62136)	P62136 [6]	38 kDa	0	9	0	0	9	0	0	9	0
Serpin B6 OS=Homo sapiens GN=SERPINB6 PE=1 SV=3	P35237	43 kDa	0	10	0	0	8	0	0	5	0
Serpin H1 OS=Homo sapiens GN=SERPINH1 PE=2 SV=1	B4DN87 (+2)	44 kDa	0	2	0	0	0	0	0	2	0
Serrate RNA effector molecule homolog OS=Homo sapiens GN=SRRT PE=1 SV=1	Q9BXP5 (+4)	101 kDa	14	0	0	4	0	0	7	0	0
Serum albumin OS=Homo sapiens GN=ALB PE=4 SV=2	E7ESU5 (+2)	70 kDa	4	2	2	3	3	2	3	2	2
Sialic acid synthase OS=Homo sapiens GN=NANS PE=1 SV=2	Q9NR45	40 kDa	0	3	0	0	0	0	0	0	0
Signal recognition particle 14 kDa protein OS=Homo sapiens GN=SRP14 PE=1 SV=2	P37108	15 kDa	0	0	4	0	0	5	0	0	5
Signal recognition particle 68 kDa protein OS=Homo sapiens GN=SRP68 PE=4 SV=1	E7ETK6 (+5)	67 kDa	0	0	0	0	0	0	0	2	0
Signal transducer and activator of transcription 1-alpha/beta OS=Homo sapiens GN=STAT1 PE=1 SV=2	P42224 (+1)	87 kDa	3	0	0	0	0	0	0	0	0
Signal transducer and activator of transcription 3 OS=Homo sapiens GN=STAT3 PE=1 SV=2	P40763 (+1)	88 kDa	2	0	0	0	0	0	2	0	0

Sister chromatid cohesion protein PDS5 homolog A OS=Homo sapiens GN=PDS5A PE=1 SV=1	Q29RF7	151 kDa	3	0	0	2	0	0	8	0	0
Small glutamine-rich tetratricopeptide repeat-containing protein alpha OS=Homo sapiens GN=SGTA PE=1 SV=1	O43765	34 kDa	0	5	0	0	4	0	0	4	0
Small nuclear ribonucleoprotein Sm D2 OS=Homo sapiens GN=SNRPD2 PE=1 SV=1	P62316	14 kDa	0	0	2	0	0	4	0	0	7
Small nuclear ribonucleoprotein Sm D3 OS=Homo sapiens GN=SNRPD3 PE=2 SV=1	B4DJP7 (+1)	13 kDa	0	0	2	0	0	2	0	0	3
Small nuclear ribonucleoprotein-associated protein OS=Homo sapiens GN=SNRPN PE=2 SV=1	B3KVR1 (+5)	25 kDa	0	0	6	0	0	4	0	0	6
Small ubiquitin-related modifier 1 OS=Homo sapiens GN=SUMO1 PE=1 SV=1	P63165 (+1)	12 kDa	17	8	8	10	5	6	0	0	2
Sorbitol dehydrogenase OS=Homo sapiens GN=SORD PE=1 SV=4	Q00796	38 kDa	0	4	0	0	4	0	0	3	0
Sorcin OS=Homo sapiens GN=SRI PE=4 SV=2	A8MTH6 (+3)	20 kDa	0	0	8	0	0	8	0	0	7
Sorting nexin 1, isoform CRA_d OS=Homo sapiens GN=SNX1 PE=4 SV=2	A6NKH4 (+4)	53 kDa	0	2	0	0	0	0	0	0	0
Sorting nexin-3 OS=Homo sapiens GN=SNX3 PE=1 SV=3	O60493 (+1)	19 kDa	0	0	2	0	0	0	0	0	0
Spermidine synthase OS=Homo sapiens GN=SRM PE=1 SV=1	P19623	34 kDa	0	0	8	0	0	7	0	0	5
Spermine synthase OS=Homo sapiens GN=SMS PE=1 SV=2	P52788	41 kDa	0	4	0	0	5	0	0	4	0
Cluster of Spliceosome RNA helicase DDX39B OS=Homo sapiens GN=DDX39B PE=4 SV=1 (F8VQ10)	F8VQ10 [4]	51 kDa	0	14	0	0	11	0	0	14	0
Splicing factor 1 OS=Homo sapiens GN=SF1 PE=2 SV=1	B4DX42 (+7)	46 kDa	0	0	0	0	0	0	0	2	0
Splicing factor 3A subunit 1 OS=Homo sapiens GN=SF3A1 PE=4 SV=1	F5H048 (+1)	77 kDa	4	0	0	0	0	0	5	0	0
Splicing factor 3A subunit 3 OS=Homo sapiens GN=SF3A3 PE=4 SV=1	E7EUT8 (+1)	52 kDa	0	0	0	0	2	0	0	3	0
Splicing factor 3B subunit 1 OS=Homo sapiens GN=SF3B1 PE=1 SV=3	O75533	146 kDa	10	0	0	7	0	0	12	0	0
Splicing factor 3B subunit 2 OS=Homo sapiens GN=SF3B2 PE=1 SV=2	Q13435 (+1)	100 kDa	9	0	0	3	0	0	11	0	0
Splicing factor 3B subunit 3 OS=Homo sapiens GN=SF3B3 PE=1 SV=4	Q15393	136 kDa	11	0	0	7	0	0	10	0	0
Splicing factor U2AF 35 kDa subunit OS=Homo sapiens GN=U2AF1 PE=1 SV=3	Q01081	28 kDa	0	0	2	0	0	2	0	0	2
Splicing factor U2AF 65 kDa subunit OS=Homo sapiens GN=U2AF2 PE=1 SV=4	P26368 (+1)	54 kDa	0	3	0	0	2	0	0	3	0
Splicing factor, proline- and glutamine-rich OS=Homo sapiens GN=SFPQ PE=1 SV=2	P23246	76 kDa	12	0	0	11	0	0	22	3	0

Squamous cell carcinoma antigen recognized by T-cells 3 OS=Homo sapiens GN=SART3 PE=1 SV=1	Q15020 (+1)	110 kDa	0	0	0	0	0	0	5	0	0
Src substrate cortactin OS=Homo sapiens GN=CTTN PE=1 SV=2	Q14247 (+2)	62 kDa	2	0	0	0	0	0	0	0	0
Staphylococcal nuclease domain-containing protein 1 OS=Homo sapiens GN=SND1 PE=4 SV=2	E7ESM6 (+1)	101 kDa	12	0	0	8	0	0	19	0	0
Stathmin OS=Homo sapiens GN=STMN1 PE=1 SV=3	P16949	17 kDa	0	0	5	0	0	0	0	0	3
Stress-70 protein, mitochondrial OS=Homo sapiens GN=HSPA9 PE=2 SV=1	B7Z4V2 (+2)	72 kDa	0	0	0	0	0	0	0	2	0
Stress-induced-phosphoprotein 1 OS=Homo sapiens GN=STIP1 PE=1 SV=1	P31948	63 kDa	0	25	0	0	18	0	0	28	0
Structural maintenance of chromosomes flexible hinge domain-containing protein 1 OS=Homo sapiens GN=SMCHD1 PE=1 SV=2	A6NHR9 (+2)	226 kDa	0	0	0	0	0	0	2	0	0
Structural maintenance of chromosomes protein 1A OS=Homo sapiens GN=SMC1A PE=1 SV=2	Q14683	143 kDa	4	0	0	0	0	0	5	2	0
Structural maintenance of chromosomes protein 2 OS=Homo sapiens GN=SMC2 PE=1 SV=2	O95347 (+1)	136 kDa	3	0	0	2	0	0	6	0	0
Structural maintenance of chromosomes protein OS=Homo sapiens GN=SMC4 PE=3 SV=1	E9PD53 (+2)	144 kDa	6	0	0	0	0	0	3	0	0
Superkiller viralicidic activity 2-like 2 OS=Homo sapiens GN=SKIV2L2 PE=1 SV=3	P42285	118 kDa	8	0	0	8	0	0	12	0	0
Suppressor of G2 allele of SKP1 homolog OS=Homo sapiens GN=SUGT1 PE=1 SV=3	Q9Y2Z0 (+1)	41 kDa	0	5	0	0	5	0	0	3	0
Symplekin OS=Homo sapiens GN=SYMPK PE=1 SV=2	Q92797	141 kDa	0	0	0	0	0	0	2	0	0
T-complex protein 1 subunit alpha OS=Homo sapiens GN=TCP1 PE=1 SV=1	P17987	60 kDa	0	19	0	0	19	0	0	23	0
T-complex protein 1 subunit beta OS=Homo sapiens GN=CCT2 PE=1 SV=4	P78371	57 kDa	0	25	0	0	23	0	0	27	0
T-complex protein 1 subunit delta OS=Homo sapiens GN=CCT4 PE=1 SV=4	P50991	58 kDa	0	25	0	0	22	0	0	24	0
T-complex protein 1 subunit epsilon OS=Homo sapiens GN=CCT5 PE=1 SV=1	P48643	60 kDa	0	28	0	0	23	0	0	23	0
T-complex protein 1 subunit eta OS=Homo sapiens GN=CCT7 PE=1 SV=2	Q99832	59 kDa	0	19	0	0	19	0	0	16	0
Cluster of T-complex protein 1 subunit gamma OS=Homo sapiens GN=CCT3 PE=1 SV=4 (P49368)	P49368 [2]	61 kDa	0	25	0	0	24	0	0	23	0
T-complex protein 1 subunit zeta OS=Homo sapiens GN=CCT6A PE=1 SV=3	P40227	58 kDa	0	20	0	0	19	0	0	19	0
TAR DNA-binding protein 43 OS=Homo sapiens GN=TARDBP PE=1 SV=1	Q13148 (+1)	45 kDa	0	5	0	0	4	0	0	6	0
THO complex subunit 4 OS=Homo sapiens GN=ALYREF PE=1 SV=3	Q86V81	27 kDa	0	0	6	0	0	6	0	0	7

THO complex subunit 4 OS=Homo sapiens GN=ALYREF PE=4 SV=1	E9PB61	28 kDa	0	0	5	0	0	6	0	0	7
THO complex subunit 6 homolog OS=Homo sapiens GN=THOC6 PE=1 SV=1	Q86W42	38 kDa	0	0	0	0	0	0	0	3	0
TOX high mobility group box family member 4 OS=Homo sapiens GN=TOX4 PE=2 SV=1	B4DPY8 (+2)	64 kDa	0	0	0	0	0	0	2	0	0
Talin-1 OS=Homo sapiens GN=TLN1 PE=1 SV=3	Q9Y490	270 kDa	21	0	0	35	0	0	47	0	0
Tetratricopeptide repeat protein 1 (Fragment) OS=Homo sapiens GN=TTC1 PE=4 SV=1	H0YB37 (+1)	19 kDa	0	0	0	0	0	0	0	2	0
Thioredoxin OS=Homo sapiens GN=TXN PE=1 SV=3	P10599	12 kDa	0	0	3	0	0	2	0	0	4
Thioredoxin domain-containing protein 17 OS=Homo sapiens GN=TXNDC17 PE=1 SV=1	Q9BRA2	14 kDa	0	0	0	0	0	2	0	0	2
Thioredoxin domain-containing protein 9 OS=Homo sapiens GN=TXNDC9 PE=2 SV=1	B7Z7A4 (+2)	25 kDa	0	0	0	0	0	3	0	0	3
Thioredoxin-like protein 1 OS=Homo sapiens GN=TXNL1 PE=1 SV=3	O43396	32 kDa	0	0	4	0	0	2	0	2	2
Threonine--tRNA ligase, cytoplasmic OS=Homo sapiens GN=TARS PE=2 SV=1	B4DEG8 (+1)	87 kDa	19	0	0	13	0	0	13	0	0
Thyroid hormone receptor-associated protein 3 OS=Homo sapiens GN=THRAP3 PE=1 SV=2	Q9Y2W1	109 kDa	0	0	0	0	0	0	3	0	0
Trafficking protein particle complex 3, isoform CRA_a OS=Homo sapiens GN=TRAPPC3 PE=4 SV=1	A6NDN0 (+1)	15 kDa	0	0	3	0	0	3	0	0	3
Trafficking protein particle complex subunit 5 OS=Homo sapiens GN=TRAPPC5 PE=1 SV=1	Q8IUR0	21 kDa	0	0	0	0	0	0	0	0	2
Transcription elongation factor A protein 1 OS=Homo sapiens GN=TCEA1 PE=4 SV=1	E5RIS7 (+2)	13 kDa	0	0	0	0	0	0	0	3	0
Transcription elongation factor B (SIII), polypeptide 2 (18kDa, elongin B), isoform CRA_a OS=Homo sapiens GN=TCEB2 PE=4 SV=1	B7WPD3 (+1)	18 kDa	0	0	3	0	0	2	0	0	5
Transcription elongation factor B polypeptide 1 OS=Homo sapiens GN=TCEB1 PE=4 SV=1	E5RGD9 (+2)	11 kDa	0	0	0	0	0	0	0	0	4
Transcription elongation factor SPT5 OS=Homo sapiens GN=SUPT5H PE=1 SV=1	O00267 (+1)	121 kDa	2	0	0	0	0	0	0	0	0
Transcription elongation regulator 1 OS=Homo sapiens GN=TCERG1 PE=4 SV=1	G3V220 (+2)	116 kDa	0	0	0	0	0	0	3	0	0
Transcription intermediary factor 1-beta OS=Homo sapiens GN=TRIM28 PE=1 SV=5	Q13263 (+1)	89 kDa	11	0	0	9	0	0	8	0	0
Transcriptional repressor protein YY1 OS=Homo sapiens GN=YY1 PE=1 SV=2	P25490	45 kDa	0	2	0	0	0	0	0	0	0
Transformer-2 protein homolog beta (Fragment) OS=Homo sapiens GN=TRA2B PE=4 SV=1	H7BXF3 (+2)	15 kDa	0	0	0	0	0	0	0	2	0
Transforming protein RhoA OS=Homo sapiens GN=RHOA PE=1 SV=1	P61586	22 kDa	0	0	6	0	0	3	0	0	3

Transgelin-2 OS=Homo sapiens GN=TAGLN2 PE=1 SV=3	P37802	22 kDa	0	0	10	0	0	10	0	0	9
Transitional endoplasmic reticulum ATPase OS=Homo sapiens GN=VCP PE=1 SV=4	P55072	89 kDa	25	0	0	15	0	0	18	0	0
Translation initiation factor eIF-2B subunit alpha OS=Homo sapiens GN=EIF2B1 PE=2 SV=1	B4DGX0 (+1)	25 kDa	0	0	0	0	0	0	0	0	3
Translation initiation factor eIF-2B subunit epsilon OS=Homo sapiens GN=EIF2B5 PE=4 SV=1	E9PC74 (+1)	78 kDa	0	0	0	0	0	0	2	0	0
Translation initiation factor eIF-2B subunit gamma (Fragment) OS=Homo sapiens GN=EIF2B3 PE=4 SV=1	H0Y580 (+3)	25 kDa	0	0	0	0	0	0	0	2	0
Translational activator GCN1 OS=Homo sapiens GN=GCN1L1 PE=1 SV=6	Q92616	293 kDa	8	0	0	15	0	0	20	0	0
Translationally-controlled tumor protein (Fragment) OS=Homo sapiens GN=TPT1 PE=4 SV=1	E9PJF7 (+2)	18 kDa	0	0	4	0	0	2	0	0	2
Cluster of Transportin-1 OS=Homo sapiens GN=TNPO1 PE=1 SV=2 (Q92973)	Q92973 [4]	102 kDa	18	0	0	17	0	0	19	0	0
Treacle protein OS=Homo sapiens GN=TCOF1 PE=4 SV=1	E9PHK9 (+3)	156 kDa	0	0	0	0	0	0	12	0	0
Trifunctional purine biosynthetic protein adenosine-3 OS=Homo sapiens GN=GART PE=1 SV=1	P22102	108 kDa	13	0	0	9	0	0	10	0	0
Triosephosphate isomerase OS=Homo sapiens GN=TPI1 PE=1 SV=3	P60174	31 kDa	0	0	12	0	0	7	0	0	6
Tripeptidyl-peptidase 2 OS=Homo sapiens GN=TPP2 PE=1 SV=4	P29144 (+1)	138 kDa	4	0	0	3	0	0	0	0	0
Trypsin-3 OS=Homo sapiens GN=PRSS3 PE=1 SV=2	P35030	33 kDa	0	0	0	0	0	0	0	2	0
Cluster of Tryptophan--tRNA ligase, cytoplasmic OS=Homo sapiens GN=WARS PE=1 SV=2 (P23381)	P23381 [2]	53 kDa	0	12	0	0	7	0	0	10	0
Cluster of Tubulin alpha-1B chain OS=Homo sapiens GN=TUBA1B PE=1 SV=1 (P68363)	P68363 [3]	50 kDa	8	18	0	7	18	2	8	21	2
Cluster of Tubulin beta chain OS=Homo sapiens GN=TUBB PE=3 SV=1 (F8VUJ7)	F8VUJ7 [7]	47 kDa	14	51	0	14	49	0	13	45	2
Tubulin-folding cofactor B OS=Homo sapiens GN=TBCB PE=1 SV=2	Q99426	27 kDa	0	0	7	0	0	3	0	0	5
Tubulin-specific chaperone D OS=Homo sapiens GN=TBCD PE=4 SV=1	F8WC00 (+2)	110 kDa	3	0	0	5	0	0	5	0	0
Tyrosine--tRNA ligase, cytoplasmic OS=Homo sapiens GN=YARS PE=1 SV=4	P54577	59 kDa	0	5	0	0	0	0	0	0	0
Cluster of Tyrosine-protein kinase Fgr OS=Homo sapiens GN=FGR PE=4 SV=1 (F5H3M4)	F5H3M4 [26]	52 kDa	0	0	0	0	0	3	0	0	2
U1 small nuclear ribonucleoprotein A OS=Homo sapiens GN=SNRPA PE=1 SV=3	P09012	31 kDa	0	0	6	0	0	3	0	0	6
U2 small nuclear ribonucleoprotein A' OS=Homo sapiens GN=SNRPA1 PE=1 SV=2	P09661	28 kDa	0	0	0	0	0	2	0	0	4

U2 small nuclear ribonucleoprotein B'' OS=Homo sapiens GN=SNRPB2 PE=1 SV=1	P08579	25 kDa	0	0	0	0	0	0	0	0	3
U4/U6 small nuclear ribonucleoprotein Prp3 OS=Homo sapiens GN=PRPF3 PE=4 SV=1	E7EVD1 (+1)	72 kDa	0	0	0	0	0	0	3	0	0
U4/U6 small nuclear ribonucleoprotein Prp31 OS=Homo sapiens GN=PRPF31 PE=4 SV=1	E7EVX8 (+1)	55 kDa	0	3	0	0	0	0	0	3	0
U4/U6 small nuclear ribonucleoprotein Prp4 OS=Homo sapiens GN=PRPF4 PE=1 SV=2	O43172 (+1)	58 kDa	0	0	0	0	2	0	0	2	0
U4/U6.U5 tri-snRNP-associated protein 1 OS=Homo sapiens GN=SART1 PE=1 SV=1	O43290	90 kDa	2	0	0	0	0	0	6	0	0
U4/U6.U5 tri-snRNP-associated protein 2 OS=Homo sapiens GN=USP39 PE=4 SV=1	B8ZZD1 (+2)	58 kDa	0	0	0	0	2	0	0	4	0
U5 small nuclear ribonucleoprotein 200 kDa helicase OS=Homo sapiens GN=SNRNP200 PE=1 SV=2	O75643	245 kDa	9	0	0	9	0	0	16	0	0
U6 snRNA-associated Sm-like protein LSm4 OS=Homo sapiens GN=LSM4 PE=1 SV=1	Q9Y4Z0	15 kDa	0	0	0	0	0	0	0	0	2
UDP-N-acetylhexosamine pyrophosphorylase OS=Homo sapiens GN=UAP1 PE=1 SV=3	Q16222 (+2)	59 kDa	0	4	0	0	0	0	0	0	0
UDP-glucose 6-dehydrogenase OS=Homo sapiens GN=UGDH PE=1 SV=1	O60701	55 kDa	0	11	0	0	9	0	0	10	0
UPF0568 protein C14orf166 OS=Homo sapiens GN=C14orf166 PE=1 SV=1	Q9Y224	28 kDa	0	0	0	0	0	0	0	0	6
Ubiquilin-1 OS=Homo sapiens GN=UBQLN1 PE=1 SV=2	Q9UMX0 (+1)	63 kDa	0	6	0	0	7	0	0	3	0
Ubiquilin-2 OS=Homo sapiens GN=UBQLN2 PE=4 SV=1	F5H2G2 (+1)	53 kDa	0	5	0	0	5	0	0	3	0
Ubiquilin-4 OS=Homo sapiens GN=UBQLN4 PE=1 SV=2	Q9NRR5	64 kDa	0	2	0	0	2	0	0	0	0
Ubiquitin carboxyl-terminal hydrolase 5 OS=Homo sapiens GN=USP5 PE=1 SV=2	P45974 (+1)	96 kDa	23	0	0	9	0	0	17	0	0
Ubiquitin carboxyl-terminal hydrolase 7 OS=Homo sapiens GN=USP7 PE=2 SV=1	B7Z7T5 (+4)	93 kDa	0	0	0	0	0	0	2	0	0
Ubiquitin carboxyl-terminal hydrolase OS=Homo sapiens GN=USP14 PE=3 SV=1	A6NJA2 (+2)	52 kDa	0	11	0	0	9	0	0	9	0
Ubiquitin carboxyl-terminal hydrolase isozyme L1 OS=Homo sapiens GN=UCHL1 PE=1 SV=2	P09936	25 kDa	0	0	7	0	0	4	0	0	4
Ubiquitin thioesterase OTUB1 OS=Homo sapiens GN=OTUB1 PE=4 SV=1	F5GYN4 (+1)	28 kDa	0	0	5	0	0	4	0	0	5
Ubiquitin-40S ribosomal protein S27a OS=Homo sapiens GN=RPS27A PE=1 SV=2	P62979	18 kDa	4	2	5	3	4	5	5	4	6
Ubiquitin-associated protein 2-like OS=Homo sapiens GN=UBAP2L PE=4 SV=1	F8W726 (+5)	113 kDa	3	0	0	0	0	0	0	0	0
Ubiquitin-conjugating enzyme E2 Z OS=Homo sapiens GN=UBE2Z PE=4 SV=1	F8WBS1 (+1)	33 kDa	0	0	0	0	3	0	0	4	0

Ubiquitin-conjugating enzyme E2 variant 2 OS=Homo sapiens GN=UBE2V2 PE=1 SV=4	Q15819	16 kDa	0	0	0	0	0	0	0	0	2
Ubiquitin-like modifier-activating enzyme 1 OS=Homo sapiens GN=UBA1 PE=1 SV=3	P22314	118 kDa	14	0	0	7	0	0	8	0	0
Uncharacterized methyltransferase WBSCR22 OS=Homo sapiens GN=WBSCR22 PE=4 SV=1	C9K060 (+1)	34 kDa	0	0	0	0	0	0	0	0	2
Uncharacterized protein OS=Homo sapiens GN=EIF3C PE=2 SV=1	B4DDN4 (+7)	92 kDa	7	0	0	6	0	0	19	0	0
Uncharacterized protein OS=Homo sapiens GN=P4HB PE=2 SV=1	B4DUA5 (+4)	51 kDa	0	7	0	0	2	0	0	4	0
Uncharacterized protein OS=Homo sapiens GN=TKT PE=2 SV=1	B3KSI4 (+3)	59 kDa	0	10	0	0	4	0	0	3	0
Uncharacterized protein OS=Homo sapiens GN=ZNF207 PE=4 SV=1	E1P660 (+3)	53 kDa	0	0	0	0	0	0	0	3	0
Uridine 5'-monophosphate synthase OS=Homo sapiens GN=UMPS PE=3 SV=1	E9PFD2 (+1)	38 kDa	0	3	0	0	0	0	0	4	0
Uridine-cytidine kinase 2 OS=Homo sapiens GN=UCK2 PE=1 SV=1	Q9BZX2	29 kDa	0	0	2	0	0	0	0	0	3
Uroporphyrinogen decarboxylase (Fragment) OS=Homo sapiens GN=UROD PE=4 SV=1	H0Y5R6 (+2)	25 kDa	0	4	0	0	4	0	0	4	0
V-type proton ATPase catalytic subunit A OS=Homo sapiens GN=ATP6V1A PE=2 SV=1	B7Z1R5 (+1)	65 kDa	0	5	0	0	3	0	0	4	0
Vacuolar protein sorting-associated protein 26A OS=Homo sapiens GN=VPS26A PE=4 SV=1	F5H4L7 (+1)	37 kDa	0	3	0	0	2	0	0	5	0
Vacuolar protein sorting-associated protein 26B OS=Homo sapiens GN=VPS26B PE=4 SV=1	E9PRT4 (+1)	38 kDa	0	0	0	0	0	0	0	2	0
Vacuolar protein sorting-associated protein 35 OS=Homo sapiens GN=VPS35 PE=1 SV=2	Q96QK1	92 kDa	11	0	0	8	0	0	8	0	0
Vacuolar protein sorting-associated protein VTA1 homolog OS=Homo sapiens GN=VTA1 PE=1 SV=1	Q9NP79	34 kDa	0	2	0	0	0	0	0	4	0
Cluster of Valine--tRNA ligase OS=Homo sapiens GN=VARS PE=3 SV=1 (B0V043)	B0V043 [2]	140 kDa	24	0	0	13	0	0	18	0	0
Vigilin OS=Homo sapiens GN=HDLBP PE=1 SV=2	Q00341	141 kDa	6	0	0	5	0	0	19	0	0
Vimentin OS=Homo sapiens GN=VIM PE=1 SV=4	P08670	54 kDa	2	37	0	0	39	0	0	36	0
Vinculin OS=Homo sapiens GN=VCL PE=4 SV=1	F5H7T3 (+2)	110 kDa	16	0	0	6	0	0	5	0	0
WD repeat-containing protein 1 OS=Homo sapiens GN=WDR1 PE=1 SV=4	O75083	66 kDa	0	15	0	0	14	0	0	16	0
WD repeat-containing protein 61 (Fragment) OS=Homo sapiens GN=WDR61 PE=4 SV=1	H0YN81 (+1)	32 kDa	0	0	0	0	0	0	0	0	3
WD repeat-containing protein 82 OS=Homo sapiens GN=WDR82 PE=1 SV=1	Q6UXN9	35 kDa	0	0	0	0	0	2	0	0	0

WD40 repeat-containing protein SMU1 OS=Homo sapiens GN=SMU1 PE=1 SV=2	Q2TAY7	58 kDa	0	0	0	0	2	0	0	3	0
X-ray repair cross-complementing protein 5 OS=Homo sapiens GN=XRCC5 PE=1 SV=3	P13010	83 kDa	30	0	0	19	0	0	23	0	0
X-ray repair cross-complementing protein 6 OS=Homo sapiens GN=XRCC6 PE=1 SV=2	P12956	70 kDa	0	17	0	0	14	0	0	21	0
YTH domain family protein 3 OS=Homo sapiens GN=YTHDF3 PE=1 SV=1	Q7Z739	64 kDa	0	2	0	0	0	0	0	4	0
Zinc finger CCCH domain-containing protein 15 OS=Homo sapiens GN=ZC3H15 PE=4 SV=1	F5H0F5 (+1)	45 kDa	0	0	0	0	0	0	0	5	0
Zinc finger RNA-binding protein OS=Homo sapiens GN=ZFR PE=4 SV=1	B5MEH6 (+1)	115 kDa	4	0	0	0	0	0	5	0	0
Zyxin (Fragment) OS=Homo sapiens GN=ZYX PE=4 SV=1	H0Y2Y8 (+1)	58 kDa	7	0	0	0	0	0	0	0	0
mRNA turnover protein 4 homolog OS=Homo sapiens GN=MRTO4 PE=1 SV=2	Q9UKD2	28 kDa	0	0	4	0	0	3	0	0	8
rRNA 2'-O-methyltransferase fibrillarin OS=Homo sapiens GN=FBL PE=1 SV=2	P22087	34 kDa	0	3	0	0	4	0	0	6	0
tRNA (cytosine(34)-C(5))-methyltransferase OS=Homo sapiens GN=NSUN2 PE=1 SV=2	Q08J23 (+1)	86 kDa	5	0	0	0	0	0	3	0	0
tRNA methyltransferase 112 homolog OS=Homo sapiens GN=TRMT112 PE=4 SV=1	F5GX77 (+1)	12 kDa	0	0	2	0	0	2	0	0	3
tRNA-splicing ligase RtcB homolog OS=Homo sapiens GN=C22orf28 PE=1 SV=1	Q9Y3I0	55 kDa	0	7	0	0	7	0	0	11	0

Appendix D.1 List of Selected proteins from MS 2

Protein Identified	$p53_{WT}$ +S1	$p53_{K386R}$ +S1	$p53_{WT}$	Function
SWI/SNF complex subunit SMARCC1 (BAF155)	+			Chromatin remodelling
SWI/SNF complex subunit SMARCC2	+			
Chromodomain-helicase-DNA-binding protein 1			+	
High mobility group protein 20A	+			
Histone Acetyltransferase HAT1	+			
Histone-binding protein RBBP4	+		+	
Histone-arginine methyltransferase CARM1	+		+	
Heterochromatin protein 1-binding protein 3			+	
WD repeat-containing protein 61			+	
WD repeat-containing protein 82		+		
Lysine-specific demethylase KDM1A (LSD1)	+			Transcriptional Regulation
Transcriptional Repressor YY1	+			
Global Transcription Activator SMARCA1		+	+	
Histone Deacetylase HDAC2	+			
Bcl-2-associated transcription factor 1			+	
DNA-directed RNA polymerase I subunit RPA49			+	Transcription
DNA-directed RNA polymerases I, II, and III subunit RPABC1			+	
Negative elongation factor B		+	+	
Negative elongation factor C/D			+	
RNA polymerase II subunit A C-terminal domain phosphatase SSU72	+			
RNA polymerase II-associated factor 1 homolog			+	
RNA-binding protein 25			+	
RNA-binding protein 39			+	
RNA-binding protein 4			+	
RNA-binding protein PNO1			+	
Nucleolar RNA helicase 2 DDX21		+	+	
UPF0568 protein C14orf166				
Exportin-7	+			Nucleo-cytoplasmatic Transport
Importin alpha-1			+	
Importin alpha-3		+	+	
Importin-8		+		
Nuclear pore complex protein Nup155		+		
Eukaryotic translation initiation factor 2a eIF2a		+	+	Translation

Eukaryotic translation elongation factor 1 epsilon-1			+	
Eukaryotic translation initiation factor 1A, X-chromosomal	+			
Eukaryotic translation initiation factor 3 subunit D			+	
Eukaryotic translation initiation factor 3 subunit J			+	
Eukaryotic translation initiation factor 4B	+		+	
Eukaryotic translation initiation factor 5B	+		+	
HBS1-like protein			+	
DNA mismatch repair protein Msh6	+			DNA Repair
Poly [ADP-ribose] polymerase 1		+	+	
Double-strand break repair protein MRE11A			+	
Cell division control protein 42 homolog			+	Mitosis
Cell division cycle and apoptosis regulator protein 1			+	
Cyclin-dependent kinase 11B			+	
Cullin-3	+		+	Ubiquitylation
Deubiquitinating protein VCIP135		+		
E3 ubiquitin-protein ligase LRSAM1	+			
E3 ubiquitin-protein ligase UHRF1		+	+	
Ubiquitin carboxyl-terminal hydrolase 7			+	
Ubiquitin-associated protein 2-like	+			
Ubiquitin-conjugating enzyme E2 Z		+	+	
Cleavage and polyadenylation specificity factor subunit 1	+			mRNA processing
Cleavage and polyadenylation-specificity factor subunit 3	+			
Cleavage and polyadenylation-specificity factor subunit 6		+		
Cleavage and polyadenylation-specificity factor subunit 7			+	
Cleavage stimulation factor subunit 1			+	
Cleavage stimulation factor subunit 2	+	+		
Poly(A) polymerase alpha	+			
Poly(U)-binding-splicing factor PUF60		+	+	
Probable ATP-dependent RNA helicase DDX6		+	+	
Probable ATP-dependent RNA helicase DDX47		+	+	
Probable ATP-dependent RNA helicase DHX40			+	
Gem-associated protein 5		+	+	Splicing
Probable ATP-dependent RNA helicase DDX46			+	
U2 small nuclear ribonucleoprotein A'		+	+	
U4/U6 small nuclear ribonucleoprotein Prp3			+	
U4/U6 small nuclear ribonucleoprotein Prp31	+		+	
U4/U6 small nuclear ribonucleoprotein Prp4		+	+	

U4/U6.U5 tri-snRNP-associated protein 1				
U4/U6.U5 tri-snRNP-associated protein 2		+	+	
U6 snRNA-associated Sm-like protein LSm4			+	
Glucosamine--fructose-6-phosphate aminotransferase [isomerizing] 1	+			Metabolism
Glucosamine-6-phosphate isomerase 1	+			
Glycine--tRNA ligase			+	
Inositol-3-phosphate synthase 1	+			
Malate dehydrogenase	+			
Malate dehydrogenase, cytoplasmic	+			
Dihydrofolate reductase		+		
Guanine nucleotide-binding protein G(I)/G(S)/G(T) subunit beta-2	+			
40S ribosomal protein S21		+	+	Ribosomal Proteins
40S ribosomal protein S24			+	
60S ribosomal protein L17			+	
60S ribosomal protein L18a			+	
60S ribosomal protein L19	+		+	
60S ribosomal protein L27a			+	
60S ribosomal protein L29			+	
60S ribosomal protein L32 (Fragment)		+	+	
60S ribosomal protein L35a			+	
60S ribosomal protein L36		+	+	
60S ribosomal protein L36a			+	
H/ACA ribonucleoprotein complex subunit 1		+		Ribosome biogenesis
H/ACA ribonucleoprotein complex subunit 4		+	+	
Nuclear protein localization protein 4 homolog			+	Proteosomal Degradation
26S proteasome non-ATPase regulatory subunit 4 (Fragment)		+		
26S proteasome non-ATPase regulatory subunit 6		+	+	
26S proteasome non-ATPase regulatory subunit 7		+		
B-cell receptor-associated protein 31			+	Chaperone
Heat shock 70 kDa protein 4L	+			
Heat shock protein 75 kDa, mitochondrial		+		
BAG family molecular chaperone regulator 2			+	
Developmentally-regulated GTP-binding protein 1		+	+	Differentiation